ESD-TR-91-061

Technical Report
916

Volume 1: Principal Results

Multifrequency Measurements of Radar Ground Clutter at 42 Sites

Volume 2 contains Appendices A through D.
Volume 3 contains Appendix E.

J.B. Billingsley
J.F. Larrabee

15 November 1991

Lincoln Laboratory
MASSACHUSETTS INSTITUTE OF TECHNOLOGY
LEXINGTON, MASSACHUSETTS

Prepared for the Department of the Air Force
under Contract F19628-90-C-0002.

This report is based on studies performed at Lincoln Laboratory, a center for research operated by Massachusetts Institute of Technology. The work was sponsored by the Department of the Air Force under Contract F19628-90-C-0002.

The ESD Public Affairs Office has reviewed this report, and it is releasable to the National Technical Information Service, where it will be available to the general public, including foreign nationals.

This technical report has been reviewed and is approved for publication.

FOR THE COMMANDER

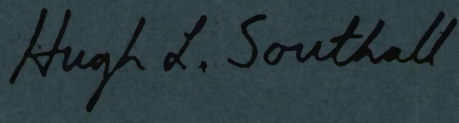

Hugh L. Southall, Lt. Col., USAF
Chief, ESD Lincoln Laboratory Project Office

MASSACHUSETTS INSTITUTE OF TECHNOLOGY
LINCOLN LABORATORY

MULTIFREQUENCY MEASUREMENTS OF RADAR GROUND CLUTTER AT 42 SITES

J.B. BILLINGSLEY
Group 45
J.F. LARRABEE
Loral Aerospace

TECHNICAL REPORT 916
VOLUME 1: PRINCIPAL RESULTS

15 NOVEMBER 1991

LEXINGTON MASSACHUSETTS

ABSTRACT

This report determines how ground clutter strength varies with RF frequency from VHF to X-band in ground-sited radar. This determination is accomplished by providing extensive empirical results from multifrequency clutter measurements conducted at 42 different sites widely dispersed over the North American continent. These results indicate that the frequency dependence of ground clutter strength depends upon terrain type and can vary, for example, from a strongly decreasing function of frequency in forest to a strongly increasing function of frequency in farmland. Five major terrain categories are defined that encompass this dependence, namely, urban, mountains, forest, farmland, and desert. Within each terrain category, results are also shown to be dependent upon the relief or roughness of the terrain and upon the depression angle at which the terrain is illuminated. The depression angle dependence is important, even for the very low angles (typically within a degree of grazing incidence) and small (typical fractional) variations in angle that occur in ground-sited radar. This report presents specific clutter strength results at each of five frequencies (VHF, UHF, L-, S-, and X-band) from each of the 42 sites at which measurements were conducted. The report then combines results from similar sites to obtain the general dependence of clutter strength versus frequency for each terrain category. Clutter strengths are described in terms of moments (including the mean) and percentile levels (including the median) in measured clutter amplitude distributions resulting from cell-by-cell spatial variation over a selected large kilometer-sized macroregion of terrain at each site called the repeat sector. Measurements over the repeat sector at each site were repeated a number of times to increase the reliability of the results. In addition to determining the frequency dependence of ground clutter strength in various terrain types, this report determines dependencies of clutter strength with radar polarization and resolution and specifies long-term temporal variability of clutter strength with weather and season. The report includes descriptions of the clutter measurement equipment and measurement procedures, provides calibration results, and describes the resultant multifrequency ground clutter measurement data bases that are now maintained at Lincoln Laboratory.

PREFACE

The radar ground clutter measurements program at MIT Lincoln Laboratory has provided two major results. The first result is the dependence of low-angle ground clutter spatial amplitude distributions on depression angle, such that the mean strengths of these distributions increase, and their spreads decrease with increasing depression angle. These depression angle effects are largely the result of shadowing at low angles in a sea of patchy visibility and discrete or localized scattering sources.

The second major result is the dependence of clutter strength on RF frequency, VHF to X-band, in various types of terrain. For example, in steep forest terrain mean clutter strengths decrease strongly with increasing frequency; whereas, in level farmland terrain mean clutter strengths increase strongly with increasing frequency. This result is expanded upon at length in this report.

These two results have led us to a model for ground clutter spatial amplitude distributions. In the model, the mean strengths of these clutter amplitude distributions vary with frequency, and the spreads of these distributions vary with spatial resolution, depending on terrain type. For a given terrain type, mean strengths increase and spreads decrease with increasing depression angle. This clutter model is described in detail elsewhere.

This report is based upon the repeat sector measurements that represent an important subset of the total data base of measurements. The repeat sector at each site is a narrow azimuth sector in which clutter measurements were repeated a number of times to increase the depth of understanding and the reliability of the results. What remains is to obtain the statistical benefit of analyzing and subsuming within the clutter model the much more voluminous 360-deg spatially comprehensive survey data at each site. At the time of writing (October 1990), we have generated and stored the approximately 100,000 clutter patch amplitude histograms upon which this survey analysis will be based. This reduces the 3600 calibrated clutter tapes and associated terrain descriptions and ground truth onto five clutter patch tapes. The many stored patch histograms on these five tapes represent a final distillate of all the measurement data into a highly dense medium rich in modeling information. Analysis of these data, which is currently well advanced, will allow an increase in the prediction accuracy of our clutter model by vastly increasing the number of terrain samples upon which it is based.

ACKNOWLEDGMENTS

The results of this report are due to dedicated efforts by many people in measuring, reducing, and analyzing our ground clutter data. Many of our measurements were made in Canada within a joint program in which support was provided by the Canadian Department of National Defence. The Phase One measurement equipment was fabricated and operated by the General Electric Company. The principal Phase One operations crew members from GE were Harry Dence, crew chief; Joe Miller, computer operator; and Guy Burnett. Other crew members were Jerry Anderson of Intera Environmental Consultants and Captain Ken Lockhart of the Canadian Forces. The success of our program is directly due to the efforts of this operations crew, who put in 60-hour work weeks over three years under rather trying circumstances and who had to assume tower rigging and tractor-trailer operating responsibilities as well as maintaining and operating our five-frequency radar. At Lincoln Laboratory, the principal people involved in the management and technical interface with GE during fabrication and operation of the Phase One equipment were David Kettner and John Hartt. People who have had major involvement in data reduction and computer programming activities include Ken Gregson, Sharon Kelsey, Charlotte Schell, Bill Dustin, Leo Demers, and Bob Graham-Munn. George McDowell and Seichoong Chang played important consultant roles during calibration and reduction of the data. The Phase One program was originally conceived at Lincoln Laboratory by William P. Delaney, and was subsequently guided and managed by Carl E. Nielsen, Jr., David L. Briggs, and Lewis A. Thurman. It is a pleasure to acknowledge the skillful efforts of Pat DeCuir, Lois Masoner, Marilyn Kushmerek, and Jean O'Hare in preparing the manuscript.

TABLE OF CONTENTS

VOLUME 1

TABLE OF CONTENTS (Continued)

LIST OF ILLUSTRATIONS

LIST OF ILLUSTRATIONS (Continued)

LIST OF ILLUSTRATIONS (Continued)

LIST OF ILLUSTRATIONS (Continued)

LIST OF ILLUSTRATIONS (CONTINUED)

LIST OF TABLES

LIST OF TABLES (Continued)

1. INTRODUCTION

During the three-year period from October 1981 to October 1984, MIT Lincoln Laboratory conducted a multifrequency radar ground clutter measurement program at 42 different sites widely dispersed geographically across the North American continent. Many of the sites were in western Canada. This multifrequency measurement program is referred to as Phase One, in contrast to our earlier, X-band only, measurement program, which is referred to as Phase Zero. The Phase One clutter measurement equipment was self-contained and mobile, principally housed within three sixteen-wheeler tractor-trailer combination trucks, and manned by a five-man crew. The equipment included a transportable antenna tower expandable in six sections to a maximum height of 100 ft. A photograph of the Phase One equipment erected at our Lethbridge West site in Alberta, Canada, is shown in Figure 1. At each site, we measured all of the discernible ground clutter within the field-of-view through 360 deg in azimuth and from 1 to 25 or 50 km or more in range at each of five frequencies: VHF, UHF, L-, S-, and X-bands. The duration of time that our equipment spent at each site making these measurements was typically two to three weeks. The amount of raw, digitally recorded, pulse-by-pulse measurement data collected at each site usually filled about 25 to 30 high-density magnetic tapes. Within the measurement program we included seven repeated data collection visits to a few sites at different times of the year to provide seasonal variations in our clutter measurement data base. Altogether we maintained our Phase One measurement equipment almost continuously in the field for three years conducting this 49-site-visit measurement program.

Our objective in conducting this extensive new measurement program was to develop a capability for predicting ground clutter spatial amplitude distributions in ground-sited radars, as these distributions typically arise at grazing incidence from large kilometer-sized spatial regions of visible terrain. Data from each of the 49 site visits have now been analyzed. From these data a multifrequency clutter model has been developed. The purpose of this report is to provide detailed and comprehensive documentation of the multifrequency measurement results upon which the model is based. In particular, we wish to show how ground clutter strength varies with RF frequency, VHF to X-band, in various types of terrain.

The particular clutter spatial amplitude distributions analyzed in this report were measured in what is called the repeat sector at each site. That is, at each site a narrow azimuth sector was selected as a sector of concentration in which measurements were repeated a number of times during the time on site. Typically, the repeat sector is about 20 deg in azimuth extent and exists at ranges beginning a few kilometers from the radar and extending 5 or 10 km. The principal multifrequency clutter data we so far have under analysis and upon which this report is based are from the repeat sector measurements conducted during each of the 49 site visits.

1.1 SCOPE

A ground-based radar often experiences ground clutter interference to ranges of many kilometers. Most of the relatively significant clutter comes from geometrically visible terrain. From most places on the surface of the earth, geometric visibility is spatially patchy; looking out from a site, high regions of terrain are visible, and intervening low regions of terrain are masked. Thus, clutter occurs within kilometer-sized macroregions of general geometric visibility, each containing hundreds or thousands of

spatial resolution cells. The spatial patterns of occurrence of ground clutter can be predicted geometrically with reasonable accuracy using available digital terrain elevation data bases. Predicting, in this manner, the existence of some macroregion of ground clutter, we then need to be able to predict the amplitude statistics of the clutter as they exist within that region in order to estimate average signal-to-clutter ratios for the radar operating in that clutter. Thus, our general objective is the prediction of ground clutter amplitude statistics for distribution over spatial macroregions of visible terrain. A fundamental requirement in this prediction is knowledge of how the mean strengths of clutter spatial amplitude distributions vary with RF frequency in various types of terrain. Provision of this information is a specific major objective of this report.

Dominant clutter sources within macroregions of general geometric visibility are often spatially localized or discrete, such that groups of cells providing strong returns are often separated by cells providing weak or noise-level returns. We have previously shown that a fundamental parametric dependence in low-angle clutter amplitude statistics is that of depression angle as it affects microshadowing in a sea (i.e., macroregion) of discrete clutter sources, such that mean strengths increase and cell-to-cell fluctuations decrease with increasing angle. Depression angle is the angle below the horizontal at which a clutter patch is observed at the radar. This fundamental dependence of ground clutter statistics on depression angle exists even for the very low angles, typically < 1 deg, and small fractional variations in angle that occur in ground-based radar. In this report, the major influence of depression angle at all Phase One frequencies shall be seen.

The means and other measures (e.g., higher moments and percentiles) of clutter amplitude statistics that are presented in this report are absolute measures not dependent on radar sensitivity. The Phase One measurement radar was almost always sensitive enough to measure discernible returns from the dominant discrete clutter sources that occurred within the visible repeat sector macroregions, regardless of range. Increasing sensitivity merely acts to reduce the relative proportion of cells at radar noise level (i.e., microshadowed cells) within such regions. The measured clutter amplitude distributions and their means presented in this report cover all of the cells within the repeat sector macroregion, including those at noise level in the measurements.

The subject of this report is ground clutter from visible regions of terrain. Ground clutter from regions well beyond the horizon is usually much weaker than that from directly illuminated regions. Although weak, such interference is not necessarily inconsequential to radars operating against targets beyond the horizon. We are investigating long-range diffraction-illuminated ground clutter using instrumentation other than that described here. However, we understand these weak signals fundamentally as clutter returns reduced by large propagation losses due to the indirect illumination, and we do not further consider them here.

Figure 1. Phase One equipment at Lethbridge West, Alberta. Antenna tower erected to 60 ft. May 1983.

1.2 GUIDE TO REPORT

In this section, a brief guide is provided to the contents of this report.

1.2.1 Ground Clutter Strength Versus Frequency

The major purpose of this report is to show how ground clutter strength varies with RF frequency, VHF to X-band, in various types of terrain. Our best high-level answer to this question is given by the data in Figure 98 and Table 11. These data provide mean clutter strength versus frequency for 12 different terrain categories, generalized (i.e., medianized) across a number of similar measurement sites in each category. The remainder of this report, in large measure, seeks to explain, enlarge upon, and provide background about the data in Figure 98 and Table 11. Thus, much of the central body of this report (i.e., Section 4) is given over to the specific interpretation of our multifrequency measurements of mean clutter strength at each of the 42 sites, organized within broad terrain groups of urban, mountains, forest, farmland, and desert. Appendix E shows a plot of measured values of mean clutter strength versus frequency for the repeat sector at each Phase One site.

1.2.2 Means and Medians

There is more to ground clutter than mean strength. Every value of mean clutter strength provided in this report comes from a clutter amplitude distribution measured over a repeat sector spatial macroregion. Appendix E shows one or more sample clutter amplitude histograms for each repeat sector. These distributions are brought under more complete statistical description by tabulation of their higher moments and several percentile levels, including the median in Section 6. All of these statistical attributes are generalized across a number of similar measurement scenarios within the same terrain categories as were the means in Figure 98 and Table 11.

1.2.3 Polarization and Resolution

The mean clutter strength versus frequency results of Figure 98 and Table 11 are averaged across measurements of both vertical and horizontal polarization, using both 150-m and 15/36-m pulse lengths. Variations of mean clutter strength with resolution and polarization are generally small, typically on the order of 1 or 2 dB. Discussion of average differences in clutter strength with polarization and resolution as well as the one-sigma range of variations and the maximum variation encountered with these parameters is presented in Section 5.

1.2.4 Weather and Season

Because low-angle clutter is dominated by discrete scattering sources, effects with weather and season are also small, usually less than 1.5 dB and 3.0 dB, respectively. Discussion of variability of mean clutter strength with weather and season is given in Section 7.

1.2.5 Multipath Propagation

At low angles in open terrain, clutter measurements are dominated by multipath propagation that causes lobing on the free-space antenna pattern and hence introduces strong variations in effective antenna gain on the measured clutter. These propagation-induced variations are not removed in our assessments of clutter strength. In other words, what we measure as clutter strength $\sigma^\circ F^4$ is the product of the intrinsic backscattering coefficient σ° that would be theoretically measured under free-space illumination and the propagation factor F raised to the fourth power, which includes all propagation effects, both reflective and diffractive. Thus, in attempting to interpret many of the measurement results in this report, we are faced with having to estimate the effects of propagation, particularly multipath, in the data. To do so requires knowledge of terrain elevation variations over the measurement interval. How we proceed to estimate effects of multipath in these circumstances is discussed in Appendix B, particularly Section B.2.

1.2.6 Antenna Tower Height

Multifrequency Phase One clutter measurements were obtained with multiple antenna tower heights at four different sites. Results from Corinne for three different antenna heights are first shown in Section 3.2.1 and then further discussed in Section 4.1.4.3. Also briefly discussed in Section 4.1.4.3 are two-tower-height results at each of the other three multiple tower height sites, namely, Shilo, Suffield, and Lethbridge West. In addition, Section 4.1.4.3 provides a comparison at X-band between Phase Zero and Phase One across many sites in two regimes of antenna height — one where Phase One had similar heights to Phase Zero, and another where the Phase One antenna height was twice as high as Phase Zero.

1.2.7 Long-Range Mountain Clutter

When a ground-sited radar experiences strong ground clutter from visible terrain at very long ranges, such as 100 km or more, it has been our experience that such clutter comes from mountains because only mountains rise high enough to be within geometric line-of-sight at such long ranges. Even so, the mountains at such long ranges are barely within line-of-sight, just rising above a distant horizon. When observed from open agricultural terrain, one might expect a significant multipath propagation loss at VHF, and as a result weaker effective clutter strength from the mountains at VHF compared to microwave bands. Our measurements show the opposite; long-range mountain clutter at VHF is significantly stronger than in the microwave bands, whether observed over forested or agricultural surfaces. A fact contributing to this effect in agricultural terrain is that the agricultural surfaces supporting multipath are usually slightly inclined rather than level. In all bands, the long-range mountain clutter is substantially weaker than mountain clutter observed at shorter ranges due to diffraction over the intervening terrain. This interesting aside from the general thrust of our studies of looking at clutter from much closer ranges is discussed in Section B.3 of Appendix B.

1.2.8 Coherency of Clutter Returns

The Phase One measurements were coherent; that is, the phase* of the clutter return signal was recorded as well as its amplitude. Clutter may be regarded as partially correlated noise in which the degree of correlation depends on the type of clutter. Pulse-by-pulse coherent integration can increase clutter-to-noise ratios; however, care must be taken not to integrate beyond a correlation period, or the quasi-noiselike clutter returns will also be unintentionally reduced. These important matters concerning data reduction are discussed, and examples are given in Appendix C.

1.2.9 Data Documentation

Our multifrequency clutter model predicts clutter amplitude distributions within a context of Weibull statistics, where each Weibull distribution is characterized by two parameters, a mean strength, and a spread parameter. The mean strength carries the dependence on RF frequency, and the spread parameter carries the dependence on radar spatial resolution. The frequency dependence in the model is based on the Phase One repeat sector measurements. As is amply illustrated in this report, site-to-site variations in the frequency dependence of mean clutter strength are complex and specific. The model irons out many of these detailed variations in order to be generally representative. A major purpose of this report is to show the detailed results at each site and how we ironed them out. Appendix D provides a measurement-by-measurement documentation of the data behind our model by providing the mean and standard deviation of each of the nominally 960 different measured clutter amplitude distributions (i.e., 48 repeat sectors, each at five frequencies, two polarizations, and two resolutions).

1.2.10 Phase One Program Documentation

Another important purpose of this report is to provide a summary documentation of the overall Phase One clutter measurement program. The report in total and the site-by-site accounts in Section 4 in particular contribute towards this purpose. Appendix E provides photographs of the Phase One equipment on site and sample clutter measurement results from most of the Phase One sites as a companion volume to Section 4. Section 6.1 provides a short historical summary of how our analyses of the data have proceeded. However, Appendix A provides a separate, stand-alone account of the Phase One history, measurement procedures, and resulting data base structure across the complete project. Thus, Appendix A provides a first point-of-entry for any new user into our overall program, taking this user from initial introduction to the point where he or she can knowledgeably request individual experiments from the clutter data base.

---

* Actually, in-phase and quadrature samples from 13-bit A/D converters at rates of 1 to 10 MHz.

2. MULTIFREQUENCY CLUTTER MEASUREMENTS

The overall ground clutter measurement activities went forward in two phases: Phase Zero, a pilot phase that was noncoherent and at X-band only, followed by Phase One, the full-scale program that was coherent and multifrequency in five frequency bands (VHF, UHF, L-, S-, and X-bands). The Phase Zero program has been described previously. This current report describes the results obtained so far from the multifrequency Phase One measurement program. Results from both measurement programs have been used as the basis of development of our multifrequency clutter model, which is described elsewhere.

The remainder of Section 2 is organized as follows. Section 2.1 provides overview information describing Phase One schedule and equipment. More detailed information on these subjects is provided in Appendix A. Section 2.2 discusses the different kinds of Phase One clutter measurement experiments recorded at each site. First, Section 2.2.1 discusses the five-frequency 360-deg survey measurements and briefly illustrates them as measured at the Gull Lake West site in Manitoba. In this discussion the mainline measurement objectives and the approaches to meeting them are discussed. Section 2.2.2 provides more information about the actual repeat sector measurements upon which this report is based. Section 2.2.2.1 provides a more lengthy discussion of repeat sector data at Gull Lake West, in which we consider many of the underlying aspects of the ground clutter phenomenon and illustrate what lies behind the values of mean clutter strength, which this report subsequently emphasizes. Section 2.3 defines the approaches for describing and classifying the terrain from which the backscatter is measured.

2.1 PHASE ONE SCHEDULE AND EQUIPMENT

The Phase One measurement program consisted of setting up and acquiring clutter measurement data 49 times at 42 different sites. These 49 site visits are listed chronologically in Table 1. Their locations are shown by setup number in the map of Figure 2. Site locations by latitude and longitude are given in Table A-2 of Appendix A. Figure 3 shows photographs of the Phase One equipment at two of these sites: Puskwaskau, a forested site, and Orion, a farmland site, both in Alberta. Previously, we have discussed how, at X-band, variations in clutter amplitude statistics with land cover (for example, between forest and farmland terrains of similar relief and observed at similar viewing angles) are not extreme, and how we have made good modeling headway by combining them as rural/low-relief terrain. In this report, we shall show that as frequency decreases from X-band to VHF, mean clutter strengths of forested terrain viewed at high angle strongly increase; whereas, mean clutter strengths of level farmland terrain viewed at grazing incidence strongly decrease. As a result, forested terrain as is shown in Figure 3(a) provides mean clutter strengths at VHF 10 or 15 dB stronger than in the microwave bands (a result that was initially quite surprising); whereas farmland terrain as is shown in Figure 3(b) provides mean clutter strengths at VHF 20 or 30 dB weaker than in the microwave bands (a more expected result). A plot comparing mean clutter strength versus frequency for these two terrain types is shown in Figure 21. The purpose of this report is to expand upon and explain these and other similar variations of mean clutter strength with frequency.

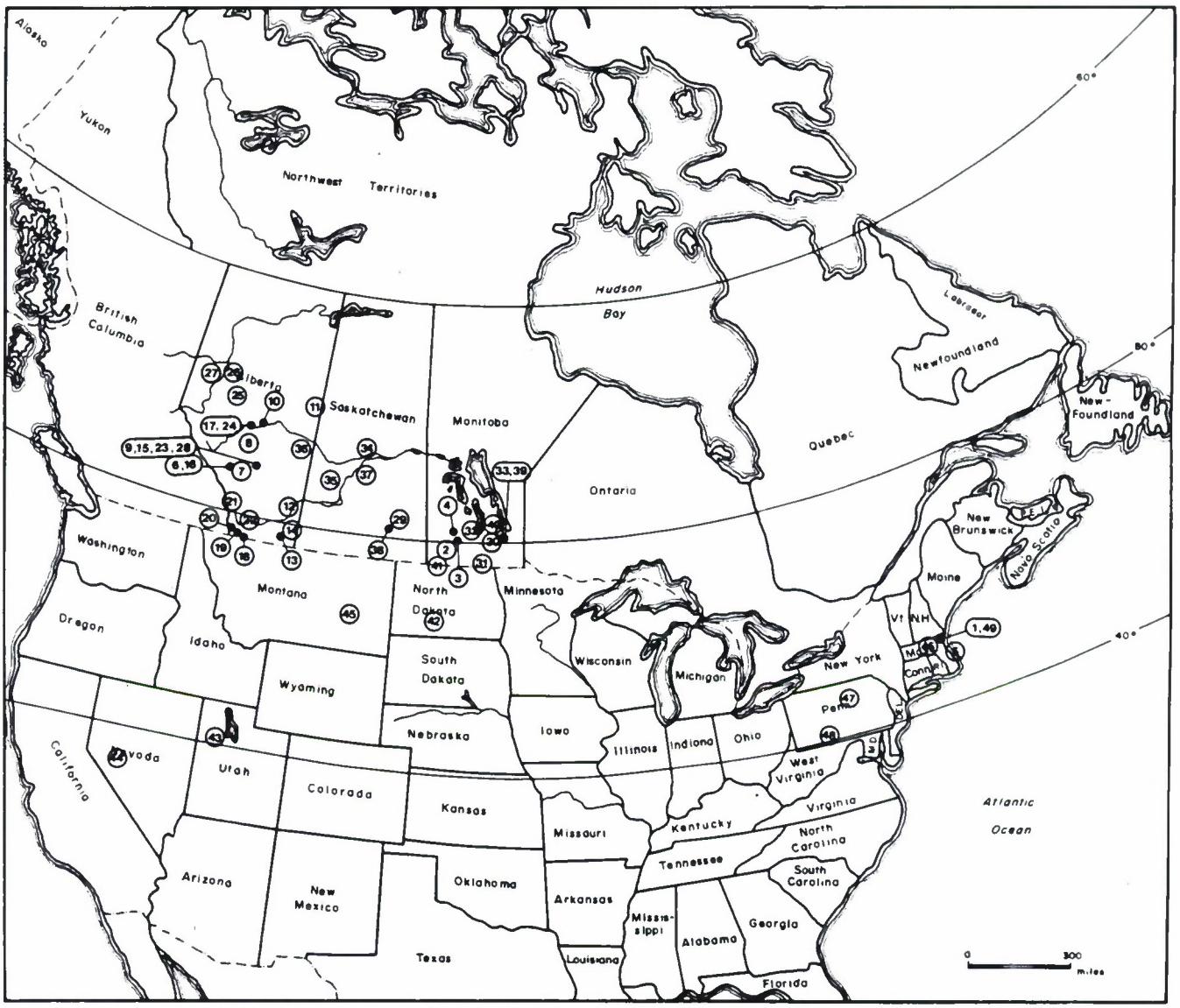

Figure 2. Location of 42 Phase One radar ground clutter measurement sites. Shown by setup numbers 1 through 49; see Table 1.

Figure 3. Phase One measurements in forest and farmland. (a) Forest at Puskwaskau, Alberta. View SW into repeat sector.

Figure 3. Phase One measurements in forest and farmland. (b) Farmland at Orion, Alberta. View SSW past equipment into repeat sector beyond.

TABLE 1
Summary Schedule of Phase One Ground Clutter Measurements

Setup Number	Site Name	Dates Visited	Days on Site
1.	Katahdin Hill, Mass.	2 Oct – 17 Dec 1981	77
2.	Shilo, Man.	1 Feb – 2 Mar 1982	30
3.	Neepawa, Man.	3 Mar – 18 Mar 1982	16
4.	Polonia, Man.	19 Mar – 30 Mar 1982	12
5.	North Truro, Mass.	23 Jun – 21 Jul 1982	29
6.	Cochrane, Alta.	11 Aug – 31 Aug 1982	21
7.	Strathcona, Alta.	1 Sep – 25 Sep 1982	25
8.	Penhold II, Alta.	27 Sep – 16 Oct 1982	20
9.	Beiseker, Alta.	18 Oct – 13 Nov 1982	27
10.	Westlock, Alta.	15 Nov – 25 Nov 1982	11
11.	Cold Lake, Alta.	27 Nov – 9 Dec 1982	13
12.	Suffield, Alta.	11 Dec 1982 – 21 Jan 1983	42
13.	Pakowki Lake, Alta.	22 Jan – 2 Feb 1983	12
14.	Orion, Alta.	2 Feb – 11 Feb 1983	10
15.	Beiseker (2), Alta.	12 Feb – 24 Feb 1983	13
16.	Cochrane (2), Alta.	24 Feb – 18 Mar 1983	23
17.	Brazeau, Alta.	26 Mar – 13 Apr 1983	19
18.	Lethbridge West, Alta.	29 Apr – 17 May 1983	19
19.	Magrath, Alta.	17 May – 6 Jun 1983	21
20.	Waterton, Alta.	6 Jun – 16 Jun 1983	11
21.	Plateau Mountain, Alta.	17 Jun – 24 Jun 1983	08
22.	Picture Butte II, Alta.	20 Jul – 6 Aug 1983	18
23.	Beiseker (3), Alta.	6 Aug – 24 Aug 1983	19
24.	Brazeau (2), Alta.	25 Aug – 13 Sep 1983	20
25.	Puskwaskau, Alta.	28 Sep – 11 Oct 1983	14
26.	Peace River South II, Alta.	12 Oct – 3 Nov 1983	23
27.	Woking, Alta.	5 Nov – 14 Nov 1983	10
28.	Beiseker (4), Alta.	16 Nov – 26 Nov 1983	11
29.	Wolseley, Sask.	29 Nov – 5 Dec 1983	07
30.	Headingley, Man.	7 Dec – 21 Dec 1983	15
31.	Altona II, Man.	5 Jan – 31 Jan 1984	27

TABLE 1 (Continued)
Summary Schedule of Phase One Ground Clutter Measurements

Setup Number	Site Name	Dates Visited	Days on Site
32.	Big Grass Marsh, Man.	1 Feb – 14 Feb 1984	14
33.	Gull Lake West, Man.	15 Feb – 25 Feb 1984	11
34.	Spruce Home, Sask.	27 Feb – 10 Mar 1984	13
35.	Rosetown Hill, Sask.	12 Mar – 21 Mar 1984	10
36.	Wainwright, Alta.	23 Mar – 2 Apr 1984	11
37.	Dundurn, Sask.	3 Apr – 13 Apr 1984	11
38.	Corinne, Sask.	13 Apr – 30 Apr 1984	18
39.	Gull Lake West (2), Man.	2 May – 12 May 1984	11
40.	Sandridge, Man.	12 May – 21 May 1984	10
41.	Turtle Mountain, Man.	22 May – 4 Jun 1984	14
42.	Beulah, N. Dak.	5 Jun – 15 Jun 1984	11
43.	Knolls, Utah	18 Jun – 25 Jun 1984	08
44.	Booker Mountain, Nev.	17 Jul – 27 Jul 1984	11
45.	Vananda East, Mont.	30 Jul – 4 Aug 1984	06
46.	Wachusett Mountain, Mass.	15 Aug – 25 Aug 1984	11
47.	Scranton, Penn.	27 Aug – 11 Sep 1984	16
48.	Blue Knob, Penn.	12 Sep – 22 Sep 1984	11
49.	Katahdin Hill (2), Mass.	25 Sep – 19 Oct 1984	25

NOTE: (n) n-th repeated visit to a site to establish seasonal variations.

The Phase One multifrequency ground clutter measurement instrument was self-contained and mobile in a three tractor-trailer configuration. Important Phase One system parameters are shown in Table 2. Phase One operated in five frequency bands: VHF, UHF, L-, S-, and X-bands. These five bands shared three antenna reflectors. The large 10 ft by 30 ft reflector was a shared dual-frequency antenna between VHF and UHF with each band having its own set of crossed-dipole feeds. The intermediate-sized reflector was also a similar shared reflector between L- and S-bands, with a crossed-dipole feed at L-band and a dual-polarized waveguide feed at S-band. The L- and S-band feeds were protected by a radome. The small reflector was dedicated to X-band, which was fed with a dual-polarized horn. The antenna tower upon which these three reflectors were mounted was expandable in six sections to a nominal maximum height of 100 ft. The weight on top of this tower due to the five antenna systems and associated equipment was 3000 lbs. The tower was guyed with 28 cables, each tensioned to 1000 or 2000 lbs. Eight guy anchors were emplaced at each site, and each was tested to 20,000 lbs withholding capacity. Motion at the center of mass on top of the tower, critical to system stability and phase coherence, was tested to within a specified tolerance, (viz., 0.1035 in/sec) using a vertically

directed laser. The antenna beams were relatively wide in elevation and were fixed with boresight horizontal at 0-deg depression angle. That is, no control was provided on the position of the elevation beam. For most sites and landscapes, the terrain at all ranges from 1 to many kilometers was usually illuminated within the 3-dB points of the fixed elevation beamwidth. The measured clutter statistics are corrected for gain variations on the elevation beam both within and beyond the 3-dB points, depending on the depression angle to the backscattering terrain point.

TABLE 2
Phase One System Parameters

a) Frequency-Dependent Parameters

	Frequency Band				
	VHF	**UHF**	**L-Band**	**S-Band**	**X-Band**
MHz	**167**	**435**	**1230**	**3240**	**9200**
Range Resolution	36 or 150 m	36 or 150 m	15 or 150 m	15 or 150 m	15 or 150 m
Azimuth Beamwidth (deg)	13	5	3	1	1
Elevation Beamwidth (deg)	42	15	10	4	3
Antenna Gain (dBi)	13	25	28.5	35.5	38.5
Peak Power (kW)	10	10	10	10	50

b) Parameters Not Dependent on Frequency

Polarization	Either VV or HH
10-km Sensitivity	$\sigma^\circ F^4 \cong$ -60 dB
A/D Sampling Rate	1, 2, 5, or 10 MHz
A/D Number of Bits	13
Data Recording Rate	625K bytes/sec
Output Data	I and Q
RCS Accuracy	2 dB rms
Minimum Range	1 km
Dynamic Range	
Instantaneous	60 dB
Attenuator Controlled	40 dB
Data Collection Modes	Beam Scan
	Parked Beam
	Beam Step
Azimuth Scan Rate	0 to 3 deg/sec
Tower Height	30, 60, 100 ft

The Phase One radar was a computer-controlled, instrumentation radar with high data rate recording capability (i.e., linear receiver with 13-bit analog-to-digital converters in in-phase and quadrature channels) and maintained coherence and stability sufficient for 60-dB two-pulse-canceller clutter attenuation in postprocessing. The instrument had uncoded, pulsed waveforms with two pulse lengths available in each band to provide high- and low-range resolution, as is shown in Table 2. Polarization was selectable as vertical or horizontal with transmit and receive antennas always co-polarized (i.e., the cross-polarized component in the radar return signal could not be received). The Phase One system activated one combination of frequency, polarization, and pulse length at a time for any particular clutter experiment. These three major radar parameters as well as other parameters (e.g., spatial extent in range and azimuth, number of pulses, and pulse repetition rate, see Table A-18) were selectable at the on-board computer console for each clutter experiment recorded. Internal calibration was provided for every clutter measurement. External calibration was provided at most sites (see Table A-1) through use of standard gain antennas and corner reflectors mounted on portable towers. Occasional Doppler measurements involving a moving sphere sliding down a 45-deg line were performed to corroborate the standard Phase One external tests. More information describing the Phase One system and its calibration is provided in Appendix A.

2.2 PHASE ONE DATA COLLECTION

Phase One collected most of its clutter measurement data within three different kinds of experiments, namely, survey experiments, repeat sector experiments, and long time dwell experiments. Our spatially comprehensive survey data are discussed in Section 2.2.1. More in-depth repeat sector data are discussed in Section 2.2.2. The third major type of Phase One clutter experiment is the long time dwell experiment. Reported elsewhere [1] are temporal and spectral characteristics of ground clutter returns based on the long time dwell experiments. See Appendix A for more detailed information on these types of experiments.

2.2.1 360-Deg Survey Data

One important aspect in Phase One data collection was to record in survey mode all of the discernible clutter within the field-of-view through 360 deg in azimuth and to 25 or 50 km or more in range. The primary purpose of this comprehensive spatial survey data was to develop an understanding of multifrequency clutter spatial amplitude statistics as they typically occur in ground-based air defense radar. Figure 4 shows ground clutter maps measured in survey mode at all five Phase One frequencies at Gull Lake West in Manitoba. These maps are at high-range resolution and horizontal polarization. They are thresholded such that cells in which clutter strength* is greater than or equal to -35 dB are shown as black. Maximum range in these maps is 15 km. North is zenith. At Gull Lake West the Phase One site is on a 100-ft-high ridge running north-south. This ridge provides good visibility to the west and southwest down onto level composite terrain. The shoreline of Lake Winnipeg is observable in the northwest quadrant with some lake clutter evident at X-band.

---

* Clutter strength = $\sigma^{\circ}F^4$, where σ° is the clutter backscatter coefficient, and F is the propagation factor. See Section 3.1.

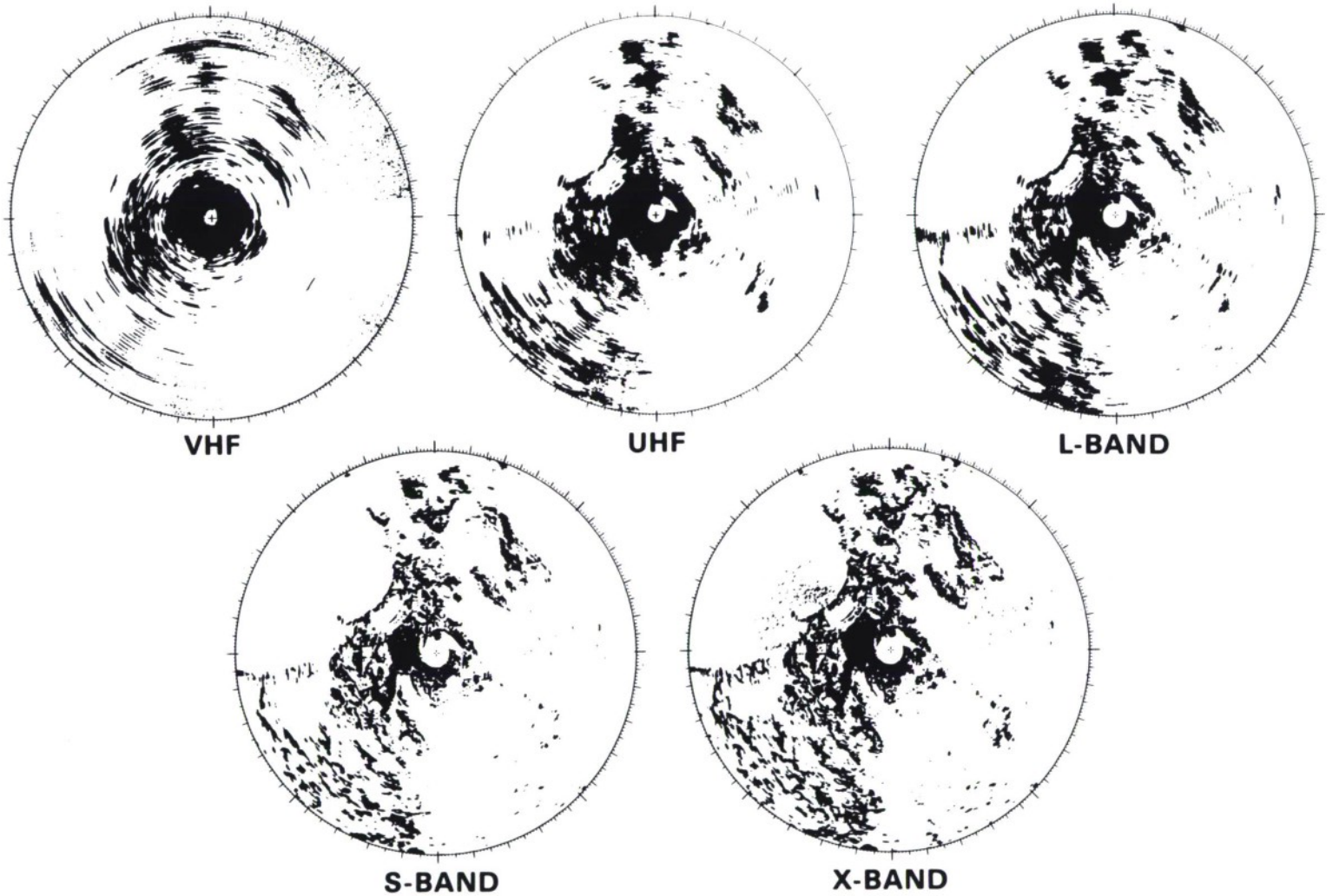

Figure 4. Measured multifrequency ground clutter maps at Gull Lake West, Manitoba. Phase One data, 15-km maximum range, $\sigma^{\circ}F^{4} \geq -35$ dB.

The first and most obvious thing we draw notice to in the clutter maps of Figure 4 is that, as patterns of spatial occurrence of ground clutter, in overall gross measure they are quite similar. The reason for this similarity is that the relatively significant or strong clutter being shown here comes from visible terrain. Such patterns of spatial occurrence of ground clutter can, in gross measure, be approximately and deterministically predicted at a given site simply as geometric visibility using Defense Mapping Agency digital terrain elevation data.

The second thing we draw notice to in the clutter maps of Figure 4 is the patchy, granular, on-again, off-again nature of the clutter. That is, clutter comes from discrete sources distributed over geometrically visible surfaces and separated by microshadowed cells where the radar is often at its noise floor. As a result, depression angle* is of fundamental parametric importance in the modeling investigations as it influences shadowing in a sea of patchy visibility and discrete scattering sources. Depression angle will be seen to be of principal influence in the multifrequency measurements of this report, where mean strengths of clutter amplitude distributions will increase, and cell-to-cell variations in these distributions will decrease with increasing angle.

The final thing we draw notice to in the clutter maps of Figure 4 is the effect of increasing azimuth beamwidth (see Table 2) with decreasing frequency to smear out the clutter. This illustrates that the role of spatial resolution of the radar is important as it influences spreads in clutter amplitude distributions. Our multifrequency clutter model directly implements this important dependency. In this report, we comprehensively document spreads in all of the measured spatial amplitude distributions as ratios of standard deviation to mean in these distributions (see Figures 105 and 106, Tables 17 and 18, and Tables D-2 through D-6). The trend of spread versus resolution is illustrated over a number of measurements at three sites in Figure 104. Beyond this, however, the primary emphasis in this report is to comprehensively discuss and document important trends we have observed in mean strength versus frequency, not spreads versus resolution.

2.2.2 Repeat Sector Data

One limitation in the Phase One survey data is that, due to limitations in acquisition time and data volume, we were not able to establish a very complete time record for each spatial clutter cell that was measured in this mode. In much of the survey data, we recorded only about 125 pulses on each cell for each of the 20 data acquisition experiments in the 20-element radar parameter matrix (i.e., five frequencies, two polarizations, two pulse lengths). To help overcome this limitation, we established a second mode of data acquisition whereby, at each Phase One site, a series of ground clutter measurements were repeatedly conducted over a specially selected narrow azimuth sector. In total these measurements are referred to as repeat sector measurements. In each repeat sector measurement, we recorded many more pulses (e.g., 1024) per spatial cell than we recorded in our survey data, and, in addition, we repeated each measurement in the repeat sector a number of times (often four) for each set of radar parameters during the Phase One stay at each site.

---

* Depression angle is the angle below the horizontal at which a clutter patch is observed at the radar.

The approximately 80 repeat sector measurements at each site (i.e., four repeated measurements for each combination of parameters in our 20-element radar parameter matrix) also encompassed variations of other underlying parameters, such as data rate of recording, pulse repetition frequency, number of pulses recorded, scan and step antenna modes, fixed and variable RF attenuation schedules, and, occasionally, different antenna mast heights. The objectives in collecting the repeat sector data were (1) to allow an assessment of quality of data to be made based on comparison of similar measurements, (2) to provide a data base with substantially more depth in terms of parameter variations than our mainline survey measurements, and (3) to allow determination of day-to-day temporal clutter variations caused by weather and other natural and cultural processes of change occurring on the landscape.

In the initial analyses of Phase One measurements, special attention was given to the repeat sector measurements. These data provide a manageable subset of the overall data acquired at each site. Almost all of the clutter data following in this report are repeat sector data. A brief account of how the Phase One analysis activities evolved, particularly the repeat sector analyses, is given in Section 6.1. Descriptions of the terrain within all of our 42 repeat sectors are provided in Table D-1. Across all these repeat sectors, the median azimuth extent is 20 deg, the median start range is 4 km, the median range extent is 6 km, and the median area is 12 km^2. Altogether, we made 4465 measurements of pulse-by-pulse clutter backscatter from repeat sector spatial macroregions in 49 setups of the Phase One equipment.

2.2.2.1 Gull Lake West. We now show repeat sector data in several formats at Gull Lake West as a background to what lies behind the mean clutter strengths emphasized through the body of this report. Figure 5 shows a larger picture of an X-band PPI clutter map at Gull Lake West at a reduced maximum range of 7 km in which the spatial nature of the clutter is apparent. This clutter map clearly shows that ground clutter has many different kinds and degrees of spatial correlation and texture, both man-made and natural. That is, clutter does not occur as random salt and pepper. Theoretical studies that attempt to get at the texture in clutter by treating clutter as correlated noise show that correlated clutter leads to much higher false alarm rates in detection statistics than uncorrelated clutter with the same amplitude distribution [6]. The boundaries of the repeat sector are shown overlaid in Figure 5 with heavy black lines. A photograph of the Phase One equipment and a Phase One tower-top photograph looking into the repeat sector at Gull Lake West are shown in Figure 6. We are looking out from a 100-ft-high ridge, initially over level forested wetland to 3.5-km range, then across a swampy open pond area from 3.5 to 5 km, then to a higher sand dune area along the shoreline of Lake Winnipeg between 5 and 6 km, and finally to the open water of Lake Winnipeg itself. Figure 7 shows mean clutter strength versus range through the Gull Lake West repeat sector at all five Phase One frequencies. These data are shown range gate by range gate, averaged over the 20-deg azimuth sector in each range gate. We refer to such A-scope traces as sector displays. These Gull Lake West sector displays in Figure 7 graphically depict not only the varying spatial nature of the clutter, as does the PPI clutter map, but also the extreme variation in mean clutter strength (i.e., 40 dB in Figure 7) that can occur in a given repeat sector. As is indicated in Figure 7, we visited Gull Lake West twice, in winter (February) and late spring (May). Sector displays for both visits are shown together in Figure 7 to indicate seasonal variability. Day-to-day and seasonal changes are another aspect of the complex ground clutter phenomenon that we need to come to grips with. We will discuss the detailed seasonal variation shown in Figure 7 in Section 4.1.3.4.

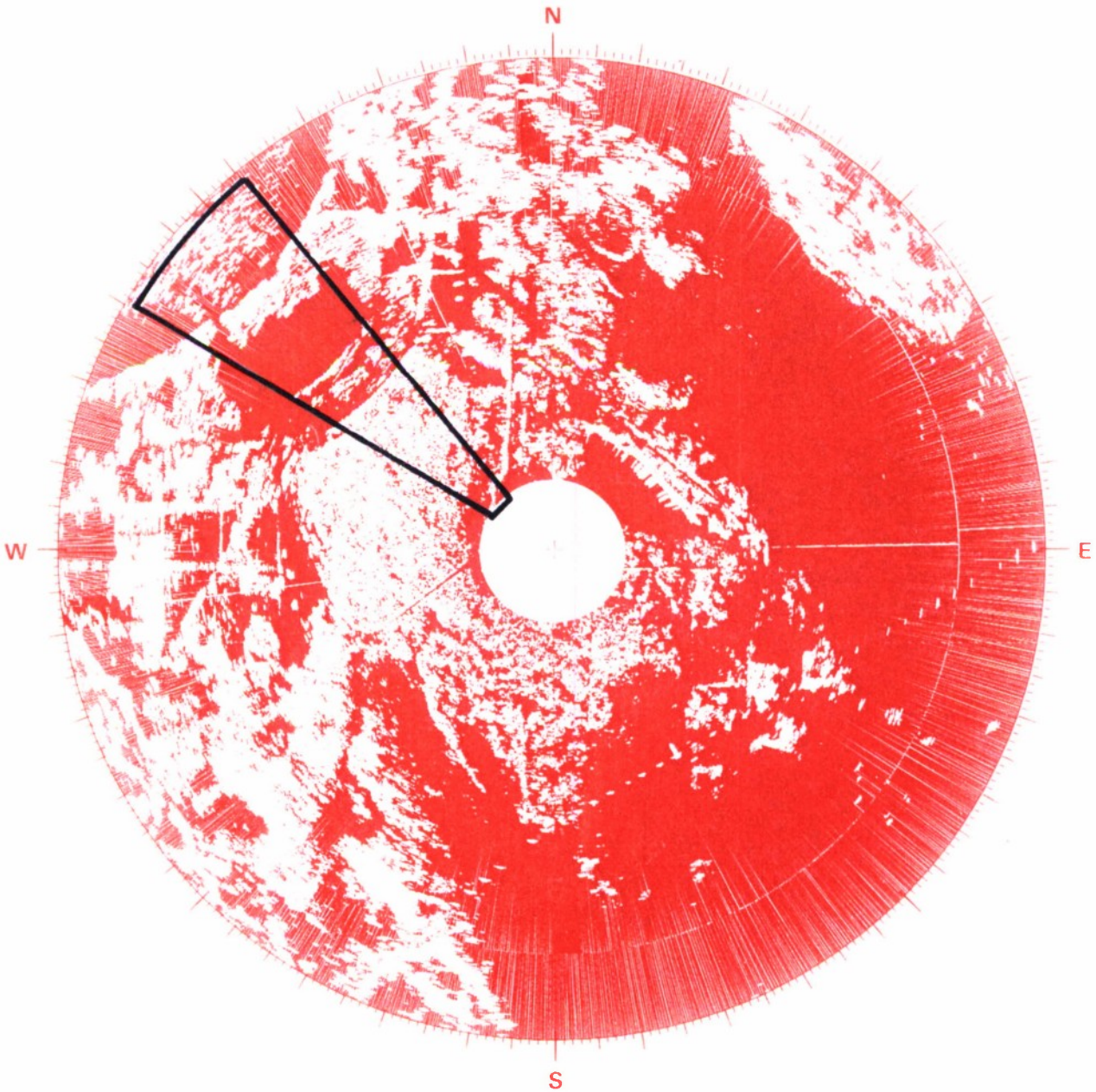

Figure 5. PPI clutter map and repeat sector at Gull Lake West. Repeat sector is outlined in black. Max range = 7 km; X-band, 15-m pulse, horizontal polarization; cells with $\sigma^{\circ}F^{4} \geq -40$ dB are white. Second visit (May 1984). Setup number 39, Table 7.

(a)

(b)

Figure 6. Phase One at Gull Lake West. February 1984. (a) Looking NW to equipment on site and (b) tower-top view NW into repeat sector.

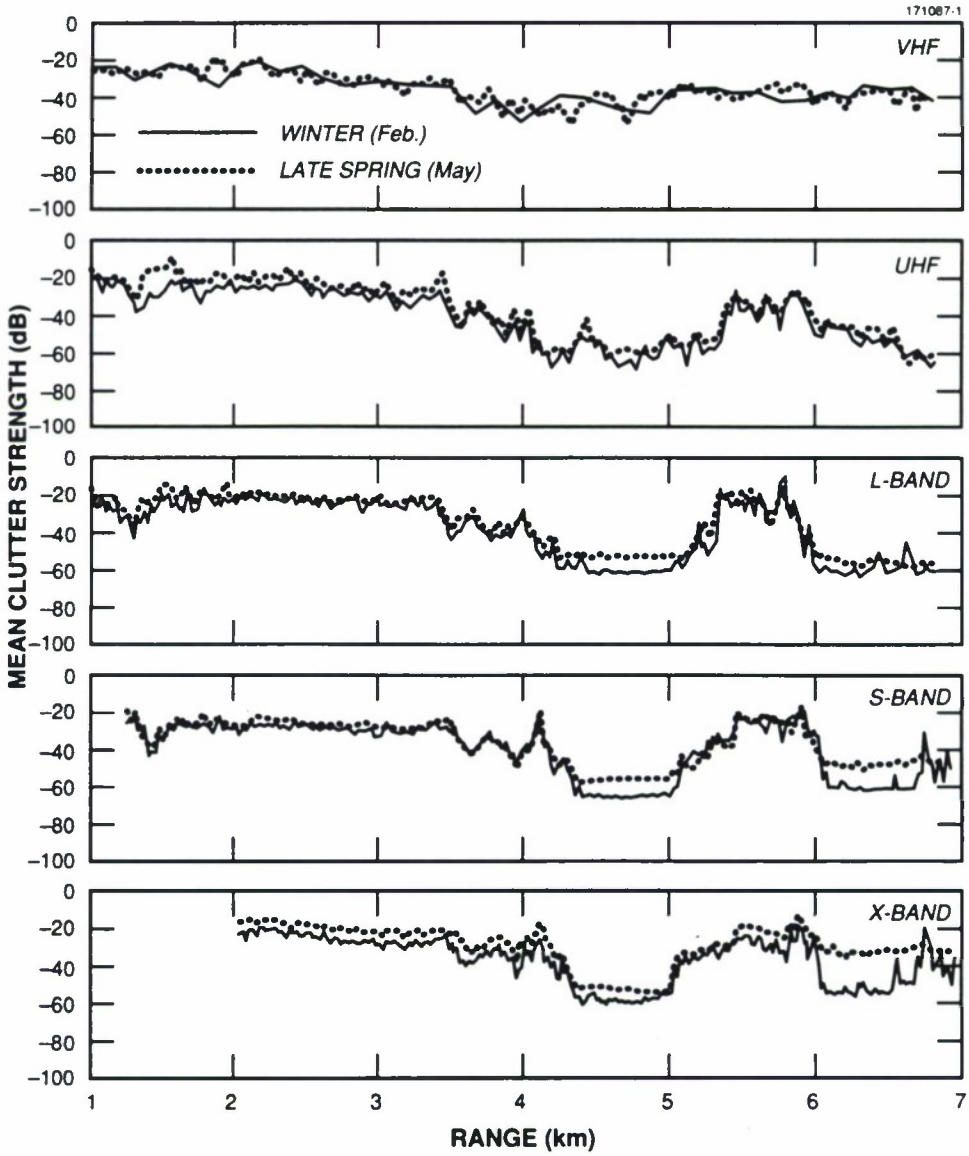

Figure 7. Seasonal variation in mean clutter strength versus range for five frequency bands at Gull Lake West, Manitoba. Repeat sector data; level forest and forested wetland with lake edges; winter visit in February 1984 (solid lines), spring visit in May 1984 (dotted lines); vertical polarization, high range resolution data, except VHF winter visit where low range resolution data are shown.

Next, we consider mean clutter strength over the complete Gull Lake West repeat sector. First, Figure 8 shows histograms of clutter amplitude statistics at X-band over the Gull Lake West repeat sector at 15-m range resolution or pulse length in Figure 8(a), as in Figure 5, and at 150-m range resolution in Figure 8(b). The high resolution histogram is smoother because it has more samples.* In both of these histograms, the range of amplitudes is extreme, covering many orders of magnitude. The numbers in the tables at the tops of these histograms are as follows. The second line in the table is terrain classification information (see Section 2.3 and Appendix E). Below that, the first three columns of numbers on the left are the moments of the distribution, i.e., mean, standard deviation, and coefficients of skewness and kurtosis (see Appendices C and E). The moments are shown computed three ways in the first three columns, as shadowed upper bounds (black noise samples get the measured noise-level values), shadowed lower bounds (black noise samples get zero power values), and shadowless (black noise samples are left out of the computation). The next two columns of numbers show goodness-of-fit coefficients to Weibull and lognormal distributions. The last column of numbers on the right shows the maximum and minimum values of clutter strength in the histogram, as well as the maximum and minimum values of saturated samples (if any, default = 999) and noise samples in the histogram.† Below that are percentile levels in the histogram, 50 (or median), 70, 90, and 99. These appear first in the shadowed histogram including noise samples, and second in the shadowless histogram excluding noise samples. These matters are discussed in more detail in Appendices C and E. Many additional examples of such histograms are included in Appendix E.

Some observations about the two histograms of Figures 8(a) and (b) may be made. The most important attribute of these histograms is the shadowed upper bound mean level, equal to -31.30 dB at 15-m resolution in Figure 8(a) and equal to -32.15 dB at 150-m resolution in Figure 8(b). It is shadowed upper bound mean strength numbers like these from many (i.e., 4465) repeat sector histograms that this report dwells upon. We know these two numbers are accurate in Figure 8(a) and (b) because the shadowed upper and lower bound mean strengths are identical to two decimal places (i.e., we have very tight bounds for mean strength; the black noise samples do not affect these mean strengths except beyond the second decimal place). Shadowless mean strengths are disregarded in this report because they are dependent on radar sensitivity. A radar of theoretically infinite sensitivity would give a single value of mean strength somewhere between our shadowed upper and lower bounds.

The next observation has to do with the wide spread in each of the two histograms of Figure 8. There may not appear to be much to choose between them in this regard, but let us examine them more closely. A measure of spread is the ratio of standard deviation to mean. This ratio is equal to 7.36 dB for the 15-m pulse in Figure 8(a) and is equal to 5.78 dB for the 150-m pulse in Figure 8(b). Thus, the moments of these histograms do indicate what we would expect, increasing spread with increasing

---

* The number of samples in these histograms is the number of range-azimuth cells times the number of pulse groups per cell, 32 pulses per group, from our partially integrated data base (see Appendix A).

† In addition, bins containing noise samples are indicated with a double underline, and bins containing saturated samples are indicated with a triple underline. For example, there is one saturated sample in Figure 18(a) in the -23-dB bin.

SITE • GULL LAKE WEST RDF • RXTH1B.RDF;1

LC • 61 52 43 LF • 1 0 TC • 2 DA • 1.07 DAC • 3.60 PN • R99 DATE • 20-FEB-84

	SHDWUB	SHDWLB	SHDLSS		SHDW	SHDLSS			
MEAN	-31.30	-31.30	-29.43	WEIB0	0.125E+01	0.149E+01	SIG(MAX)		-7
SD	-23.94	-23.94	-23.05	WEIB1	0.306E-01	0.433E-01	NOI(MAX)		-51
COS	14.01	14.01	13.14	WEIR2	0.981E+00	0.997E+00	SAT(MAX)		-23
CDK	29.82	29.82	28.06	WEISS	0.636E-01	0.226E-01	SIG(MIN)		-85
SPDL	-999.00	-999.00	-999.00	LDGB0	0.280E+01	0.298E+01	NOI(MIN)		-85
SPDR	8.09	8.09	7.28	LDGB1	0.623E-01	0.762E-01	SAT(MIN)		-23
DBME	-47.41		-38.97	LOGR2	0.953E+00	0.977E+00	50	-48.0	-37.0
DBSD	14.97		11.12	LDGSS	0.684E+00	0.477E+00	70	-36.0	-32.0
DBCOS	0.481E-02		-0.52				90	-28.0	-26.0
DBCOK	1.85		2.82				99	-20.0	-18.0

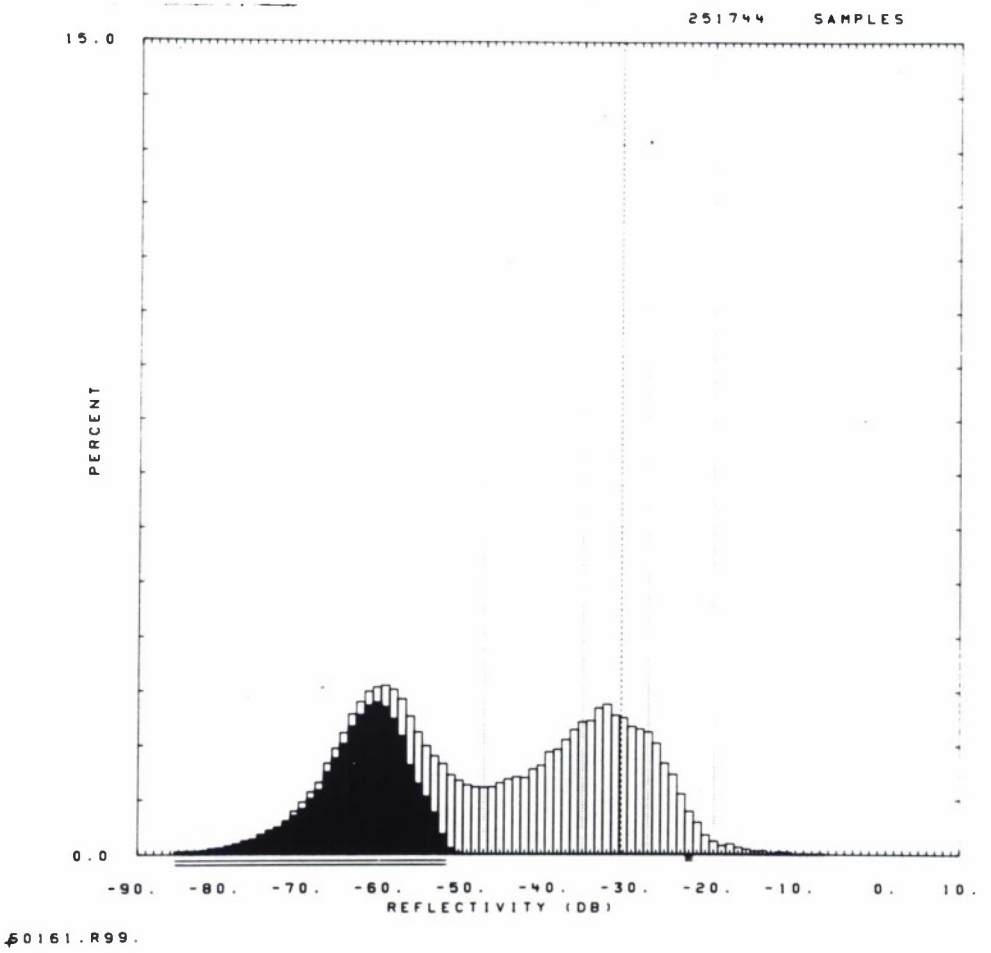

Figure 8. Histograms of clutter amplitude statistics at X-band over the Gull Lake West repeat sector. (a) 15-m range resolution, horizontal polarization, measured 20 February 1984.

SITE • GULL LAKE WEST RDF • RXFH20.RDF;1

LC • 61 52 43 LF • 1 0 TC • 2 DA • 1.06 DAC • 3.55 PN • R99 DATE • 20-FEB-

	SHDWUB	SHDWLB	SHDLSS		SHDW	SHDLSS			
MEAN	-32.15	-32.15	-31.92	WEIB0	0.129E+01	0.135E+01	SIG(MAX)		-14
SD	-26.37	-26.37	-26.26	WEIB1	0.321E-01	0.345E-01	NDI(MAX)		-64
COS	10.41	10.41	10.30	WEIR2	0.983E+00	0.986E+00	SAT(MAX)		999
COK	21.96	21.96	21.74	WEISS	0.146E+00	0.141E+00	SIG(MIN)		-73
SPDL	-999.00	-999.00	-999.00	LOGB0	0.256E+01	0.261E+01	NDI(MIN)		-85
SPOR	6.80	6.80	6.70	LOGB1	0.548E-01	0.571E-01	SAT(MIN)		999
DBME	-45.51		-44.01	LOGR2	0.939E+00	0.947E+00	50	-42.0	-41.0
DBSD	14.27		13.04	LOGSS	0.157E+01	0.147E+01	70	-35.0	-35.0
DBCOS	-0.31		-0.23				90	-29.0	-29.0
DBCOK	2.02		1.84				99	-21.0	-21.0

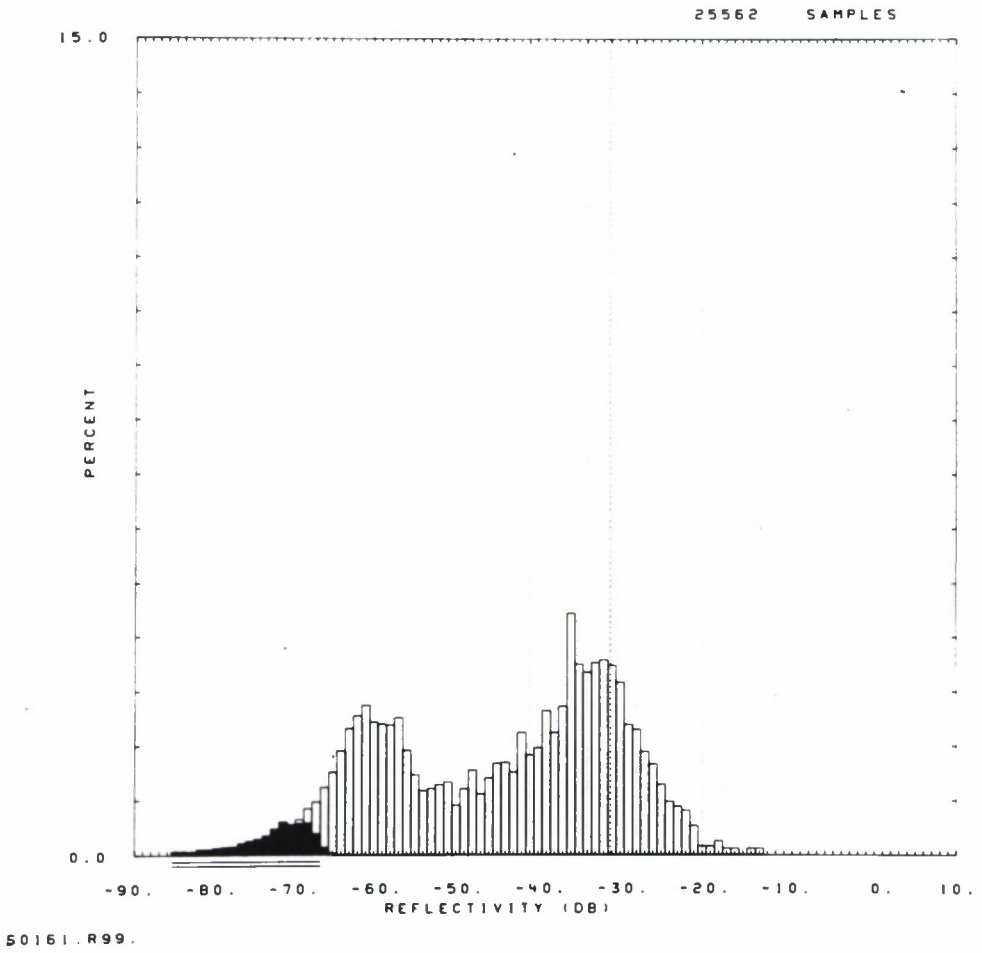

Figure 8. Histograms of clutter amplitude statistics at X-band over the Gull Lake West repeat sector. (b) 150-m range resolution, horizontal polarization, measured 20 February 1984.

resolution. This dependency with resolution is a major element in our clutter model. Ratios of standard deviation to mean are provided for all repeat sector measurements in this report. Note that increased spread at higher resolution is also observable in Figure 8 in terms of ratios of percentiles and in ratio of maximum to minimum clutter strength measured. Finally, note that the higher resolution histogram also has higher coefficients of skewness (i.e., asymmetry) and kurtosis (i.e., concentration about the mean).

Multifrequency mean clutter strengths over the Gull Lake West repeat sector are shown in Figure 9. Results from both winter and spring visits are included in Figure 9. At first consideration, it seems difficult to draw any conclusions from these mean strengths, presented by themselves in Figure 9. There does not seem to be a strong clear-cut dependence of mean strength with frequency in Figure 9, except that the S-band data seem lower. In terms of seasonal variations in mean clutter strength between winter (snow and ice, deciduous foliage off trees) and spring (no snow or ice, deciduous foliage beginning to emerge) visits as Figure 9, spring results tend to be a few decibels stronger than winter results, although there is a fair amount of overlap within bands, band by band, with the exception of X-band where a more clear-cut 5-dB seasonal difference is indicated. The results of Figure 9 will be discussed in more detail in Section 4.1.3.4, including the S-band dip and seasonal variations. The format of Figure 9 showing repeat sector mean clutter strength versus frequency will be the standard format for displaying the Phase One results, site by site, in this report (although most repeat sectors are not so markedly variable in terrain type through the repeat sector as is the Gull Lake West repeat sector).

Making generalizations from the mean clutter strength results of Figure 9 is difficult, as was pointed out in the preceding paragraph. That is, isolated single-point measurements or even multipoint measurements at a single site are not easily extrapolable to other sites. Looking back through the Gull Lake results in Figures 5 through 9, we can certainly do more detailed analyses of clutter from forest versus clutter from sand dunes, but an analytic model of backscatter from homogeneous forest does not provide the answers needed describing clutter statistics from large extents of composite landscape. We need to include characterization of the strong returns from the discontinuities between homogeneous terrain features as they actually occur in ground-based radar. On the other hand, averaging all the returns in a single mean number is, by itself, also insufficient.

Our solution to this dilemma, and the main thrust of this report, is to obtain results like those of Figure 9 at many sites, to combine them within similar terrain categories, to separate them between grossly different terrain categories, and by this means to provide the missing connecting tissue between dissimilar single-point results that leads to generality and predictability. Thus, as the report proceeds, we provide results like Figure 9 for repeat sectors at all of our measurement sites and look for important similarities among them and differences between them.

2.3 TERRAIN DESCRIPTION

The prediction of radar ground clutter and its effects requires a methodology for describing terrain. Clutter attributes are extremely variable from one kind of terrain to another. The terrain description system used needs to be universally applicable and consistently applied. It needs to find important threads of commonality among sites but not over-emphasize unimportant detail. For example, as will be shown, it matters a great deal in terms of mean clutter strength whether agricultural terrain is of very low relief

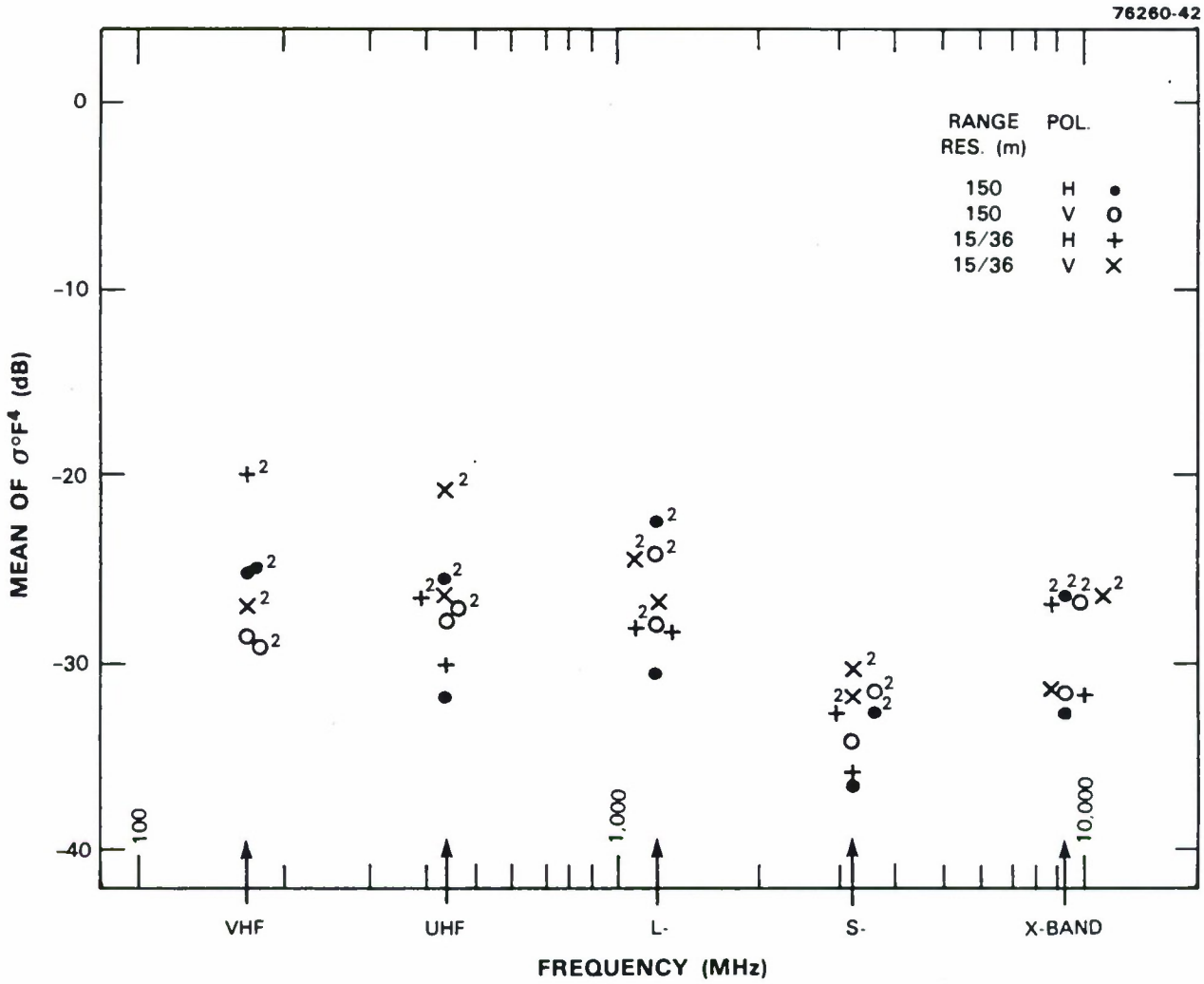

Figure 9. Mean clutter strength versus frequency at Gull Lake West. Repeat sector data. Two seasonal visits, February 1984 (winter) and May 1984 (spring). Data from the May visit are indicated with superscript 2's to the upper right of the plot symbol.

or just moderately low-relief. Also, as will be shown, it matters whether generally open terrain has small secondary occurrences of trees. Thus, any attempt to investigate and predict ground clutter can only be as successful as its terrain description methodology permits.

This report is based on clutter measurements in 42 repeat sectors. As an indication of the variability of the terrain in these repeat sectors, Figures 10(a) and (b) show terrain elevation profiles and masking in five Phase One repeat sectors. Figure 10(a) shows them on an adaptive ordinate that varies from site to site; Figure 10(b) shows them on a common ordinate. These profiles include the sphericity of a 4/3 radius spherical earth to account for nominal atmospheric refraction; that is, at a completely level site, the elevation drops by 23.55 m at 20-km range due to earth sphericity. These profiles indicate that terrain visibility and hence clutter is patchy at low angles. Visibility is shown at two antenna heights, 50 ft in Figure 10(a) and 100 ft in Figure 10(b), to show that it is usually not very sensitive to antenna height. The terrain elevation data of Figure 10 were obtained manually from 1:50,000 scale topographic maps. Subsequently, in Section 4 we show repeat sector terrain profiles based on Defense Mapping Agency digital terrain elevation data (DTED) for which the source material was 1:250,000 scale maps. The accuracy of these DTED profiles is significantly less than the accuracy of the profiles in Figure 10 because of this fivefold decrease in scale of the source material. The DTED profiles in Section 4 show terrain elevation above mean sea level (MSL). Thus, unlike the profiles of Figure 10, the DTED profiles do not incorporate earth curvature and do not show terrain masking.

An important parameter affecting clutter statistics is the depression angle below the local horizontal at which the antenna illuminates the clutter patch. Depression angle is strongly dependent on the height of the site above the clutter patch. Figures 10(a) and (b) illustrate that there is a large range of variation in the Phase One site heights. Table 3 provides height of site above repeat sector midpoint elevation for all of the Phase One sites, in decreasing order of site height.

The terrain in each repeat sector is classified both in terms of its land cover or land use characteristics and in terms of its land-surface form or relief or roughness. The classes of landform and land cover we use are shown in Tables 4 and 5, respectively. Both of these systems of classification are slight modifications by us of general classification systems used by the earth resources community. These terrain classification systems are universally applicable. Note the important footnote in Table 4. That is, although we make use of nine specific landform classes, it is helpful to separate them into two overview classes, namely, high-relief with terrain slopes generally greater than 2 deg and relief generally greater than 100 ft, and low-relief with slopes generally less than 2 deg and relief generally less than 100 ft. Also note that the landform class numbers in Table 4 do not strictly progress in order of increasing steepness and/or roughness of terrain. This is a fact that, if not understood, could be confusing in subsequent detailed discussions of results in this report. If we do attempt to arrange the landform classes in increasing order of steepness and/or roughness (a somewhat subjective undertaking, depending on criteria), that order would be something like the following: 1, 3, 2, 9, 5, 4, 6, 7, 8.

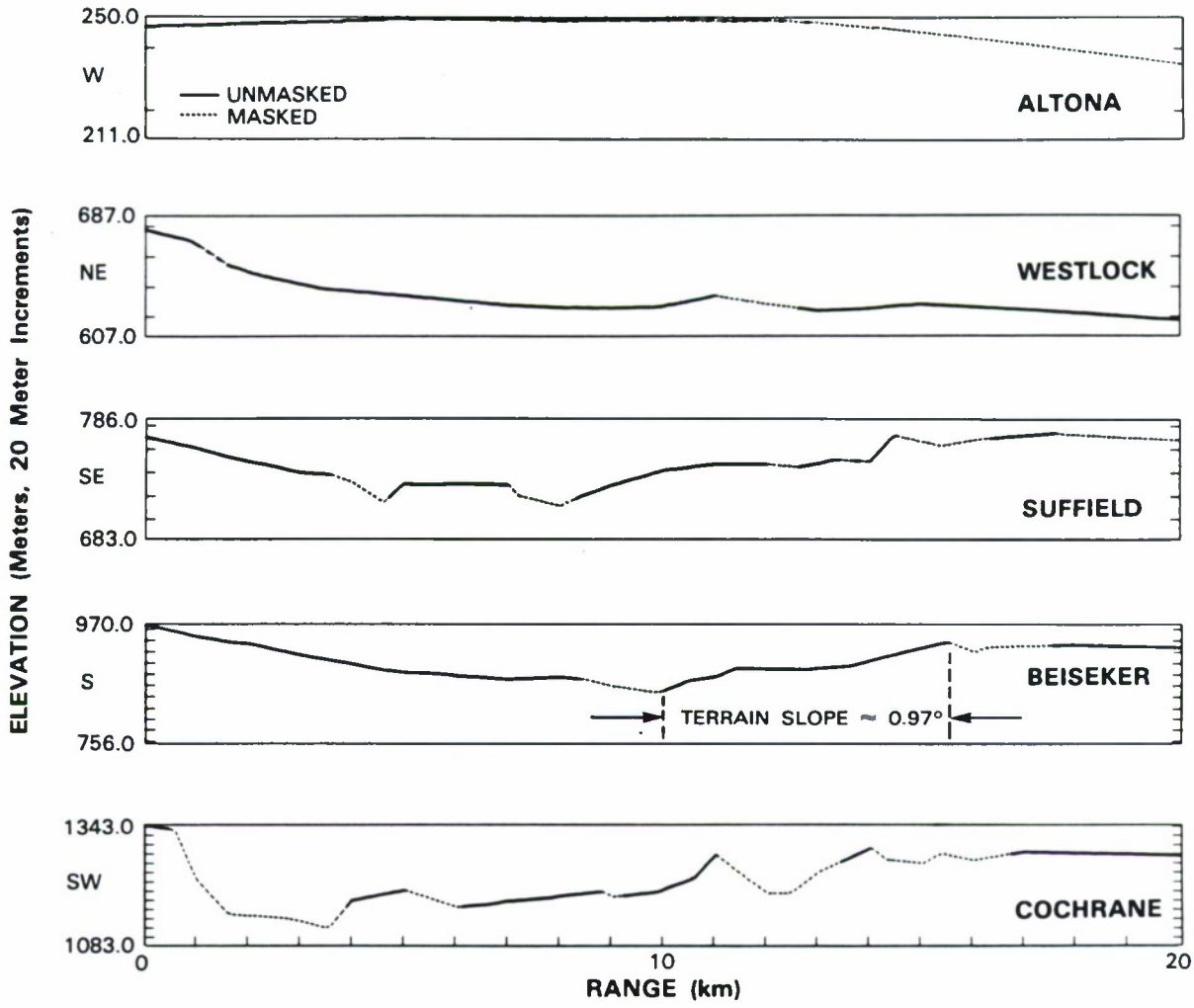

Figure 10. Terrain elevations and masking in five Phase One repeat sectors. (a) Antenna mast height = 50 ft; adaptive ordinate. Data from 1:50,000 scale topographic maps.

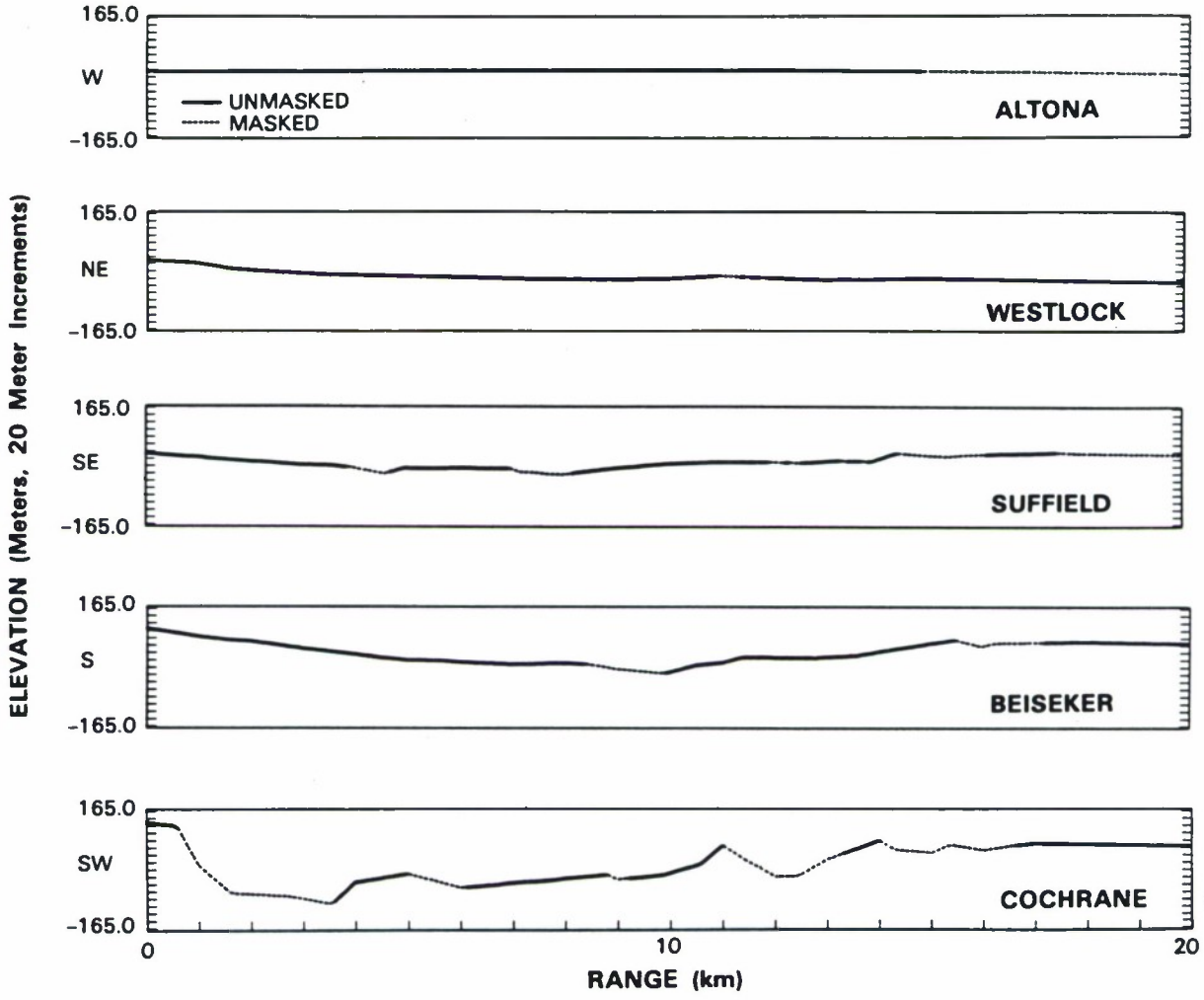

Figure 10. Terrain elevations and masking in five Phase One repeat sectors. (b) Antenna mast height = 100 ft; common ordinate. Data from 1:50,000 scale topographic maps.

TABLE 3
Phase One Site Heights

Site	Site Height Above Repeat Sector (ft)	Site	Site Height Above Repeat Sector (ft)
Plateau Mt. (a)	4021	Lethbridge West	105
Blue Knob	1710	Wainwright	102
Booker Mt.	1570	Rosetown Hill	98
Wachusett Mt.	1259	Penhold II	68
Plateau Mt. (b)	921	Spruce Home	63
Polonia	576	Pakowki Lake	50
Scranton	555	Turtle Mountain	49
Cochrane	509	Headingley	38
Strathcona	425	Knolls	25
Brazeau	392	Woking	25
Puskwaskau	382	Shilo	20
Vananda East	342	Sandridge	10
Orion	335	Katahdin Hill	5
Magrath	300	Cold Lake	0
Beiseker	255	Big Grass Marsh	-3
Beulah	214	Corinne	-10
Picture Butte II	210	Dundurn	-12
Wolseley	180	Altona II	-22
Westlock	150	Peace River South II	-150
Gull Lake West	147	Neepawa	-340
Suffield	125	Waterton	-1250

Note: Site elevation minus repeat sector midpoint elevation, in feet. In order of decreasing site height.

TABLE 4
Landform Classes and Descriptions

Landform Class	Terrain Relief (ft)	Terrain Slope (deg)	
1 Level	<25	<1	
2 Inclined	>50	1 – 2;	Unidirectional
3 Undulating	25 – 100	<1;	Regular sequences of gentle slopes; wavelike
*4 Rolling	>150	2 – 5;	Regular to irregular sequences of moderate slopes
5 Hummocky	25 – 150	<2;	Complex sequences of slopes
*6 Ridged	50 – 500	2 – 10;	Sharp breaks in slope at tops and bottoms of terrain features
*7 Moderately Steep	>100	2 – 10;	Undirectional
*8 Steep	>100	10 – 35;	Frequently unidirectional
9 Broken	>50	1 – 5;	Short dissected slopes

* Classes so indicated are "high-relief;" classes not so indicated are "low-relief."

TABLE 5
Land Cover Classes

1	Urban or Built-up Land
11	Residential
12	Commercial
2	Agricultural Land
21	Cropland
22	Pasture
3	Rangeland
31	Herbaceous
32	Shrub
33	Mixed
4	Forest
41	Deciduous
42	Coniferous
43	Mixed
5	Water
51	Rivers, Streams, Canals
52	Lakes, Ponds
6	Wetland
61	Forested
62	Nonforested
7	Barren Land

The terrain within each of the 42 repeat sectors is classified both in terms of landform and land cover, according to the classification systems shown in Tables 4 and 5. We performed this classification principally through use of topographic maps and preexisting available stereo aerial photos, usually at 1:50,000 scale. A typical aerial photo at 1:50,000 scale showing some of the terrain within the Peace River South II repeat sector is shown in Figure 11. This Peace River terrain is briefly discussed in Section 4.1.3.2. The repeat sectors are large, ranging in area from 4 km^2 (Puskwaskau) to 105 km^2 [Plateau Mountain (a)]. Over such areas, terrain is usually to some extent composite, heterogeneous, or nonuniform. Thus, a single classifier either for landform or land cover is usually not sufficient to completely describe the terrain. We usually use more than one classifier and arrange them in order of decreasing percent area of occurrence within the repeat sector (i.e., most area first, least area last). Terrain classifications for all of our repeat sectors are shown in Tables 7 and 10 in the body of this report, and in Table D-1 in Appendix D.

Figure 11. Aerial photo of repeat sector at Peace River South II. Scale = 1:50,000. North is up. Repeat sector range extent is from 12 to 17.9 km; azimuth extent is from 348 to 358 deg; see Table 7.

Recently, as part of studies (coordinated with us) being undertaken elsewhere* of our Phase One measurements, in which an emphasis is on a more fine-grained approach to analyzing the data, special aerial photography missions were commissioned and flown over many of our repeat sectors to provide new color infrared (CIR) stereo aerial photographs of repeat sector terrain at 1:10,000 scale. One of the new Peace River South II CIR aerial photography frames is shown in Figure 12. There is obviously much more detailed information available in the photograph of Figure 12 at 1:10,000 scale than in the photograph of Figure 11, in which much of the same terrain is included at 1:50,000 scale. In Figure 12, we see the Peace River at the bottom of the photograph and the steep 800-ft drop to the river down forested slopes from low-relief agricultural terrain above. We illuminate this terrain from 12 km south across the river, and the repeat sector starts near the top of the high bluffs and extends out north across the agricultural terrain there (see Table 7).

In the studies making use of these new CIR aerial photos, the terrain is classified cell by cell in cells 1 deg wide in azimuth and of 150-m range extent. The results of these cell-by-cell classifications for the Cochrane repeat sector are shown in Figures 13 and 14.† Such results are available for the repeat sectors at all Phase One measurement sites in Canada and have been used to iterate upon, refine, and improve the repeat sector terrain classifications used in this report. In addition, occasional subsequent field visits have been required to resolve ambiguities in clutter results.

Finally, we refer to additional ground truth information collected during Phase One data acquisition. This is described in more detail in Section A.1 of Appendix A. Thus, to keep track of wind, weather, and seasonal conditions during the measurements, we maintained and updated a ground truth file consisting of 60 parameters that was written on the raw clutter data tapes in front of each clutter experiment recorded. We maintained weather stations on site and in the repeat sector to provide information for this file. We recorded TV video in a 360-deg azimuth scan from an antenna bore-sighted TV camera atop the tower. Finally, at each site many field photographs were taken of the terrain being measured, where the photography position and direction is keyed to points on maps. Often these photographs included a 360-deg pan from the top of the Phase One tower. Examples of these photographs are provided in this report for every site.

Terrain descriptive detail can be overwhelming. The approach in this report is to funnel all of this information down to key macroclassifiers that cause the clutter statistics to cluster within class and separate between classes.

---

* At the Defence Research Establishment Ottawa.

† Figures 13 and 14 were provided through courtesy of Dr. Chan, DREO.

Figure 12. CIR aerial photo of repeat sector at Peace River South II. Scale = 1:10,000. North is up.

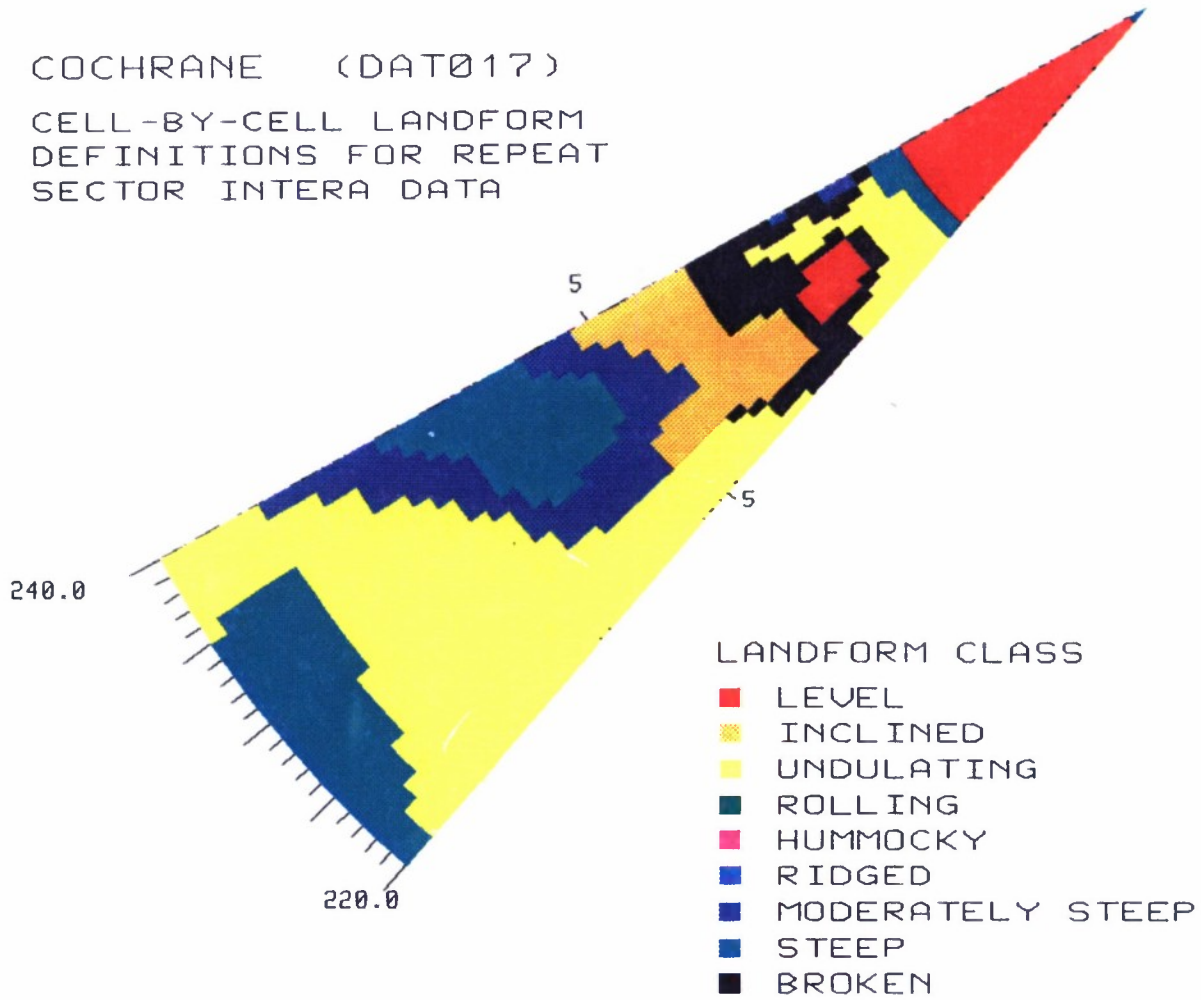

Figure 13. Cell-by-cell landform classification of the Cochrane repeat sector. From 1:10,000 scale CIR aerial photos. Courtesy of Dr. Chan, DREO.

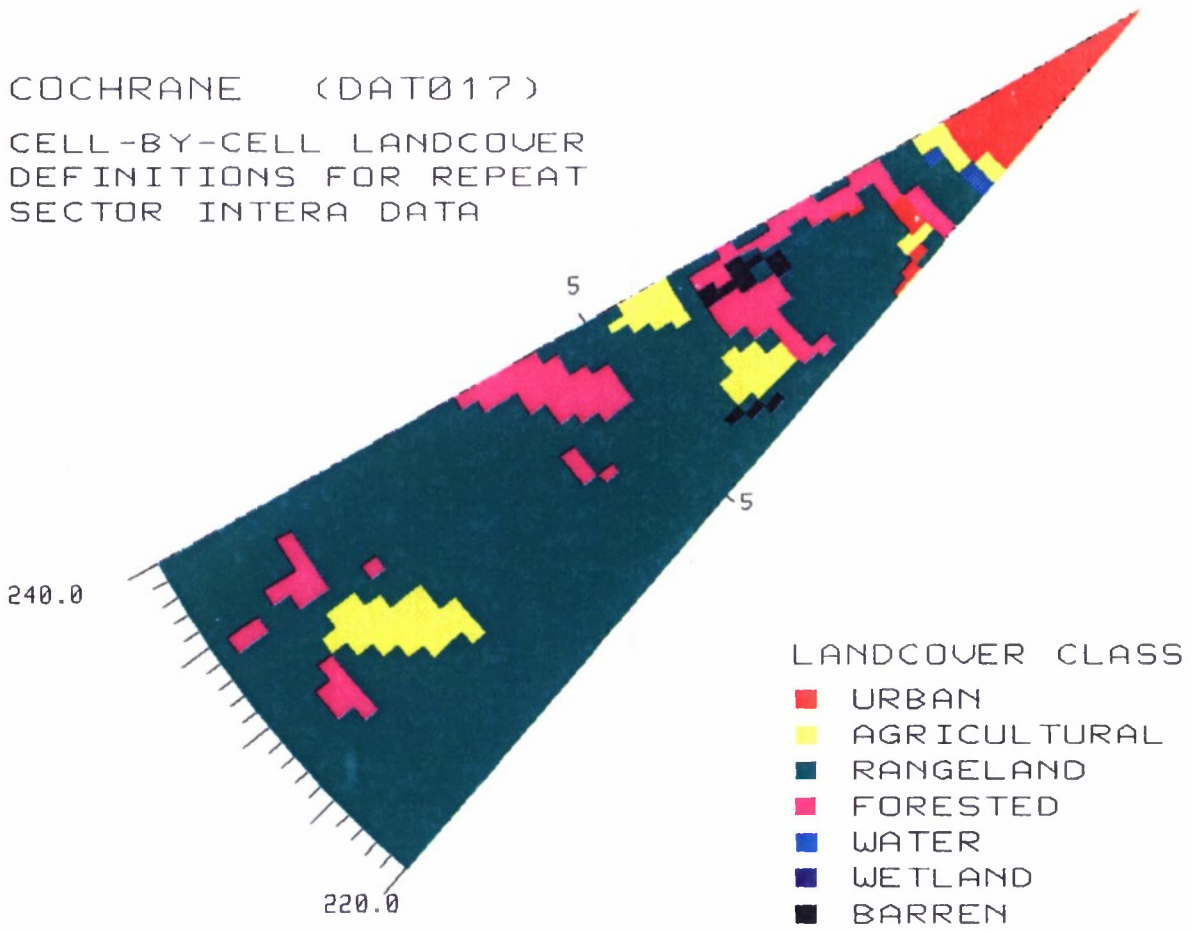

Figure 14. Cell-by-cell land cover classification of the Cochrane repeat sector. From 1:10,000 scale CIR aerial photos. Courtesy of Dr. Chan, DREO.

3. FUNDAMENTAL EFFECTS IN LOW-ANGLE GROUND CLUTTER

In Section 4, we provide measured results showing how clutter strength varies with frequency across the Phase One frequency regime. Before we begin detailed interpretation of these results, we first briefly review here in Section 3 the basic mechanisms at work in low-angle ground clutter, following the examples of measured clutter discussed in Section 2.2. In reviewing these mechanisms, we want to establish what might cause major parametric trends in the Phase One repeat sector results as RF frequency ranges from VHF to X-band.

3.1 CLUTTER PHYSICS

The major elements that are involved in low-angle clutter are shown in Figure 15. Attention is focused on directly illuminated clutter from large regions of visible terrain such as our repeat sector patches. Within such regions, at the low angles of ground-based radars, the clutter sources are all of the vertical features on the landscape, either objects associated with the land cover (such as trees or buildings) or just the high points of the terrain itself. Such sources are usually spatially localized or discrete in nature with microshadowed resolution cells occurring between them where the receiver is at its noise floor. As the angle of illumination increases, the amount of microshadowing decreases. As a result, mean clutter strengths measured over repeat sectors will increase, and cell-to-cell fluctuations (and hence ratios of standard deviation to mean) within repeat sectors will decrease with increasing angle. These effects with angle constitute a major parametric dependence in low-angle clutter at all Phase One measurement frequencies.

The terrain between the radar and the clutter patch influences the illumination of the clutter patch. For example, multipath reflections can interfere with the direct illumination and cause lobing on the free-space antenna pattern. As shown in Figure 15, such lobing can act to significantly increase or decrease the effective gain at which the patch is measured. All such propagation effects are included within the propagation factor F, which is defined to be the ratio of the incident field that actually exists at the clutter cell being measured to the incident field that would exist there if the clutter cell existed by itself in free space. What we measure as clutter strength $\sigma^\circ F^4$ is the product of the clutter coefficient itself, σ°, defined to be radar cross section (RCS) per unit ground area in the resolution cell and the fourth power of the propagation factor. Thus, throughout this report, clutter strength is given by $\sigma^\circ F^4$, which is computed in units of m^2/m^2 but is shown subsequently converted to decibels with respect to 1 m^2/m^2. Occasionally we refer to the product $\sigma^\circ F^4$ as "effective clutter strength" to emphasize that it is this product including propagation effects, not just the backscattering coefficient σ° that is important to radar system performance. How we compute clutter strength is defined in more detail in Appendix C.

In Section 4 we attempt to observe general variations of clutter strength $\sigma^\circ F^4$ through terrain-specific dispersive influences entering via the propagation factor F. This often requires multiple independent measurements of similar terrain from different sites to find underlying parametric trends. The important, often poorly predictable role of propagation in low-angle clutter can be confusing at first consideration. In Appendix B we provide further discussion of propagation and how we deal with it in clutter analysis and modeling.

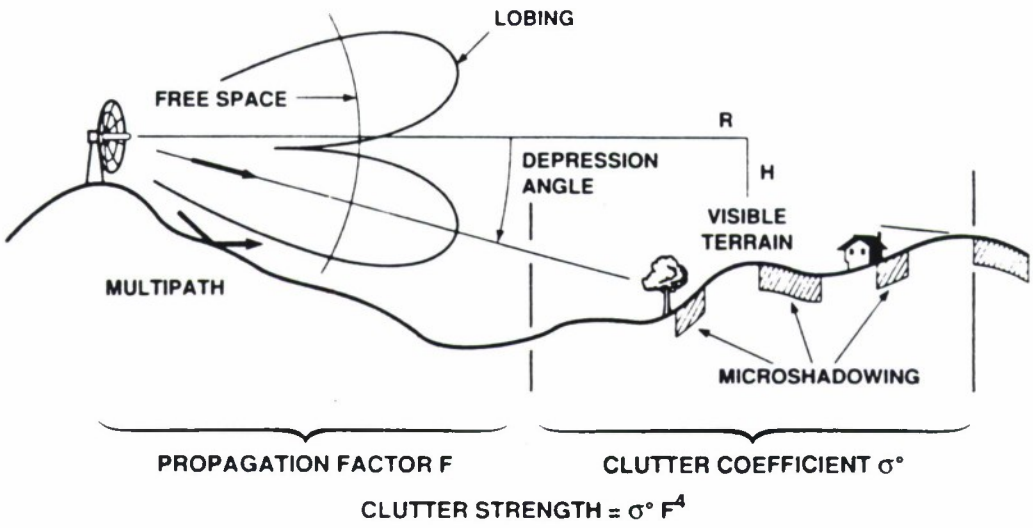

Figure 15. Clutter physics.

Within the low-angle clutter phenomenon thus characterized by granularity of sources and specific propagation influences, how may we expect clutter strengths to be affected by the spatial resolution of the radar? Theoretically, the mean clutter strength from a spatial region such as a repeat sector is independent of the spatial resolution of the measurement radar in situations involving many randomly phased clutter returns per resolution cell. This matter is discussed at greater length in Section 5.3, including discussion of occasional examples where resolution does affect mean clutter strength significantly. However, as shown in Section 4, the theoretical expectation of little dependence of mean strength on resolution is largely borne out in the Phase One results (i.e., on the average, less than 1-dB dependence of mean strength with resolution, see Figures 102 and 103). Little dependence of mean strength on resolution is also illustrated in the histograms of Figures 8(a) and (b). Although spatial resolution does not usually affect mean clutter strength very much, because of the heterogeneous nature of low-angle clutter (wherein cells providing strong returns are often separated by cells providing weak or noise-level returns) the spatial resolution of the radar does play a fundamental role in the amount of spread in clutter amplitude distributions from large spatial regions. Increasing resolution results in less averaging within a cell, more variability from cell-to-cell, and hence, increased spread in the distributions [again, see Figures 8(a) and (b)]. Thus, in Tables 17 and 18 and in Tables D-2 through D-6 in Appendix D, ratios of standard deviation to mean for all of the repeat sectors may be observed to generally increase both with decreasing pulse length at all Phase One frequencies and with decreasing azimuth beamwidth as Phase One frequency increases.

Polarization has very little effect on clutter amplitude statistics. In Section 5.2, we shall see that the distribution of differences of vertically polarized mean clutter strength minus horizontally polarized mean

clutter strength across all of the multifrequency repeat sector clutter measurement data base results in a median difference of only +1.48 dB (see Figures 100 and 101). However, occasional specific measurements can show more significant variation with polarization. For example, measurements from both of the steep mountainous sites, Plateau Mountain and Waterton, indicate that at VHF, vertically polarized backscatter can be 7 to 8 dB stronger than horizontally polarized backscatter (see Figure 29 and Table D-2).

3.2 EXPECTED TRENDS WITH FREQUENCY

Within the context of the above mechanisms, frequency does not generally play as fundamental a role as do depression angle and resolution. Averaged across all of our multifrequency measured data, independent of terrain type, we shall see in Section 5.1 that mean clutter strength shows no significant trend of variation with frequency (see Table 12). One reason for this behavior is that at low angles, clutter sources tend to be vertical objects and edges of vertical features (e.g., tree lines), which are large with respect to RF wavelength from VHF through X-band.

However, two strong trends with frequency occur in particular circumstances. One of these trends is directly the result of the intrinsic backscattering coefficient itself, σ°, having an inherent frequency-dependent characteristic. Thus, at high illumination angles in forested terrain, we have shown through our propagation measurements that forward reflections are minimal (e.g., $F \approx 1$), and in such terrain we shall observe that σ° decreases strongly with increasing frequency (e.g., see Figure 39). This result is due to the RF absorption characteristic of forest increasing with frequency, and hence, the diffusely radiative characteristic of forest (including the backscatter direction) decreasing with frequency [4].

The other trend with frequency is the result of a general propagation effect entering clutter strength $\sigma^\circ F^4$ through the propagation factor F. Thus, at low depression angles in level open terrain, strong forward reflections cause multipath lobing on the free-space antenna pattern. At low frequencies such as VHF, these lobes tend to be broad for typical antenna heights. As a result, at such low frequencies, returns from most clutter sources are received well on the underside of the first multipath lobe, and effective clutter strengths are much reduced. As frequency increases for a given antenna height, say from VHF to UHF to L-band, the multipath lobes become narrower, and the first lobe is increasingly squeezed closer and closer to the ground (see Figures B-4 and B-5). As a result, the effective gain on the underside of this lobe at which backscatter from clutter sources is received increases, and hence, clutter strengths rise with increasing frequency. Eventually, as frequency increases further to S- and X-band, the multipath lobes become still narrower, and typical clutter sources such as buildings or trees tend to subtend multiple lobes. The result is that at higher frequencies the overall multipath effect on illumination tends to average out and have less dominating influence on the effective clutter strength. Thus, at low angles on level open terrain, we shall observe a strongly increasing characteristic of mean clutter strength with frequency introduced through the propagation factor (see Figure 72). Because this characteristic is caused by the interference between the direct ray and the multipath ray, it depends on geometric factors such as antenna mast height (54 to 59 ft in many of our measurements in open terrain, see Tables A-1 and A-5) and range to the clutter patch. In inclined or rolling open terrain of increased relief, multipath is as likely to reinforce as to cancel clutter returns even at low frequencies (see Figure 30).

3.2.1 Blue Knob and Corinne

We now illustrate by measurement example the preceding remarks concerning frequency dependence of ground clutter in steep forest and level farmland. We choose to emphasize forest data from Blue Knob, Pennsylvania, and farmland data from Corinne, Saskatchewan. Photos looking into the repeat sectors at these two sites from the top of the Phase One antenna tower are shown in Figure 16. Figure 3 shows another pair of forest and farmland sites. Distinguishing between different classes of forest and farmland terrain is a major theme of this report.

Figures 17 and 18 show measured ground clutter from Blue Knob and Corinne at X-band and VHF, respectively. The repeat sector patch at Blue Knob is from 16 to 21.9 km in range and is from 80 to 100 deg in azimuth. That is, the Blue Knob repeat sector patch is the patch of black clutter at the extreme right side of the PPI in Figures 17 and 18. The repeat sector patch at Corinne is from 1 to 8.9 km in range and from 330 to 30 deg (CW) in azimuth in these two figures. First consider the X-band clutter in Figure 17. Although the shapes of the forest and farmland histograms are quite different, the mean strengths in these two histograms are nearly the same, namely, -24 dB in forest and -23 dB in farmland. We take into account the differences in histogram shape in Figure 17 in our clutter model by means of the Weibull spread (or shape) parameter, which may be directly related to the ratio of standard deviation to mean or to the mean-to-median ratio in the histogram, which are both measures of spread (see Appendix C). Reading the ratios of mean to median directly in the histograms of Figure 17, we see 8-dB mean-to-median ratio at X-band in steep forest versus a very large value of 33-dB mean-to-median ratio at X-band in level farmland; this latter large value reflects the extreme spread evident in the Corinne farmland histogram of Figure 17.

Now consider the VHF clutter from the same two sites, Blue Knob and Corinne, as shown in Figure 18. Note that, in the steep forest histogram from Blue Knob, mean clutter strength at VHF has increased by 13 dB from its X-band value to -11 dB; whereas, in the level farmland histogram from Corinne, mean clutter strength at VHF has decreased by 32 dB from its X-band value to -55 dB. In both VHF histograms in Figure 18, the mean-to-median ratios indicating spread in the histograms have decreased considerably, from an X-band value of 8 dB to a VHF value of 4 dB in forest and from an X-band value of 33 dB to a VHF value of 15 dB in farmland. This is the result of the decreased spatial resolution of Phase One at VHF due to its increased azimuth beamwidth (i.e., 13 deg at VHF versus 1 deg at X-band, see Table A-6).

Thus, there are many influences at work in these histograms of Figures 17 and 18 that must be sorted out as our studies proceed in this report. These influences include effects of (1) landform (steep versus level), (2) land cover (forest versus farmland), (3) depression angle (not overtly mentioned here but contributing to the differences observed; depression angle at Blue Knob was 1.6 deg, at Corinne was 0.15 deg), (4) RF frequency, and (5) spatial resolution. Our clutter model takes all of these effects into account. Looking ahead to Table 11 one sees how to sort through these influences as they affect mean clutter strength in the 42 repeat sectors.

We now go on to show similar forest and farmland histograms as were shown in Figures 17 and 18 at VHF and X-band, but now in all five Phase One frequency bands. Such five-frequency histograms

(a)

(b)

Figure 16. Phase One tower-top views into repeat sectors at Corinne and Blue Knob. (a) Looking north at Corinne and (b) looking east at Blue Knob.

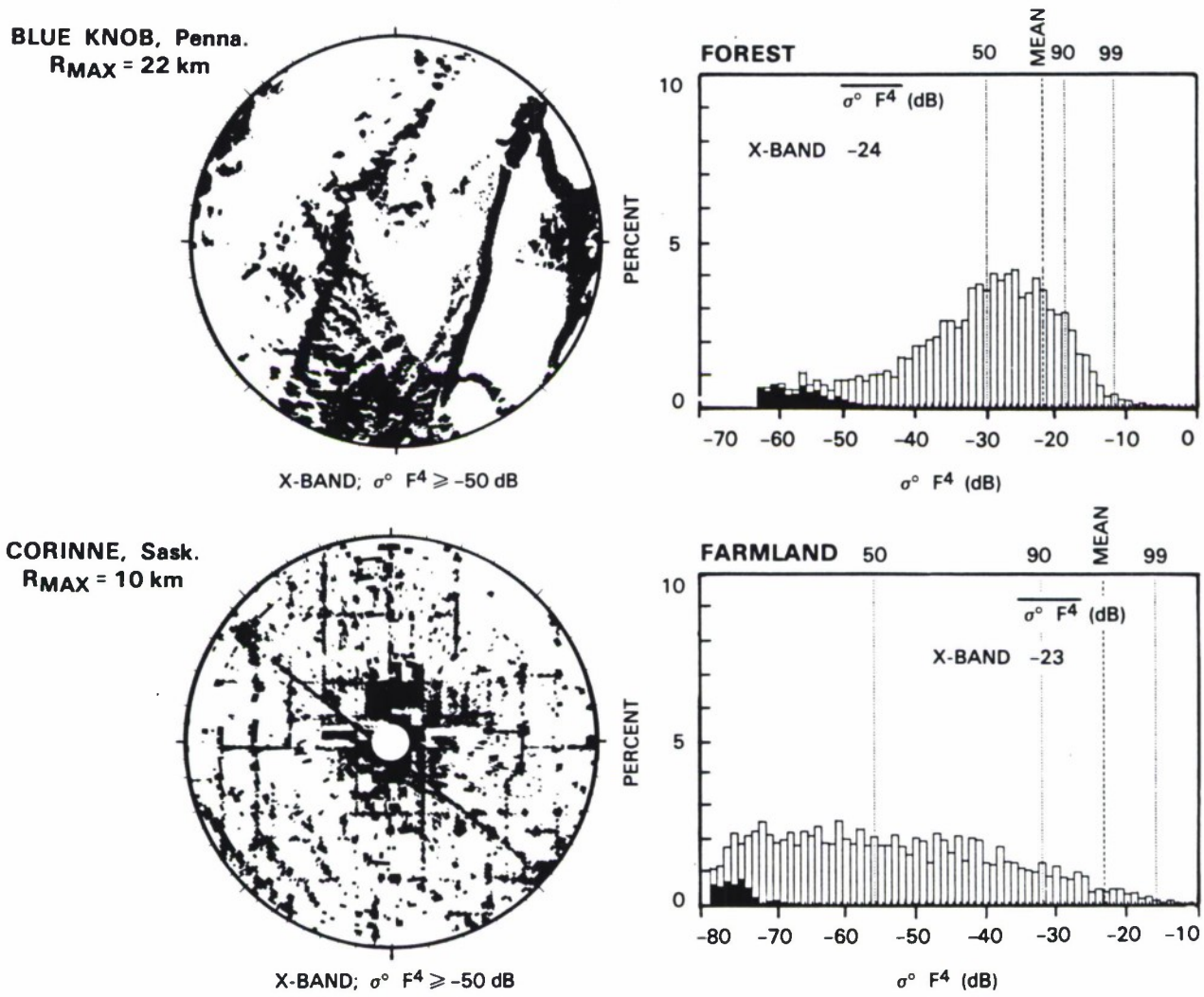

Figure 17. X-band ground clutter in steep forest and level farmland. Histograms show repeat sector data. In the PPI clutter maps, cells with $\sigma^\circ F^4 \geq -50$ dB are shown as black.

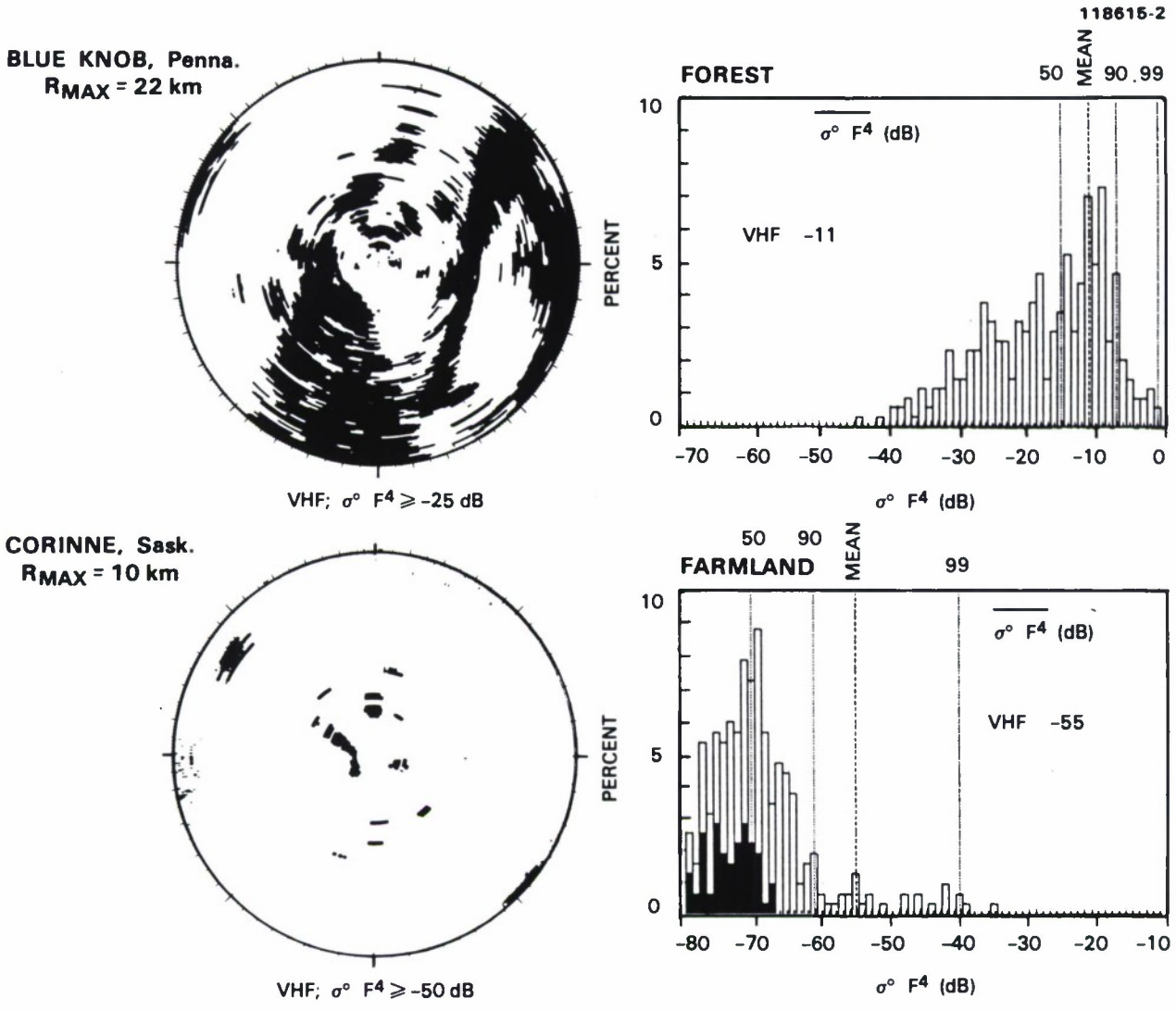

Figure 18. VHF ground clutter in steep forest and level farmland. Histograms show repeat sector data. In the PPI clutter maps, cells containing clutter stronger than the indicated threshold are shown as black.

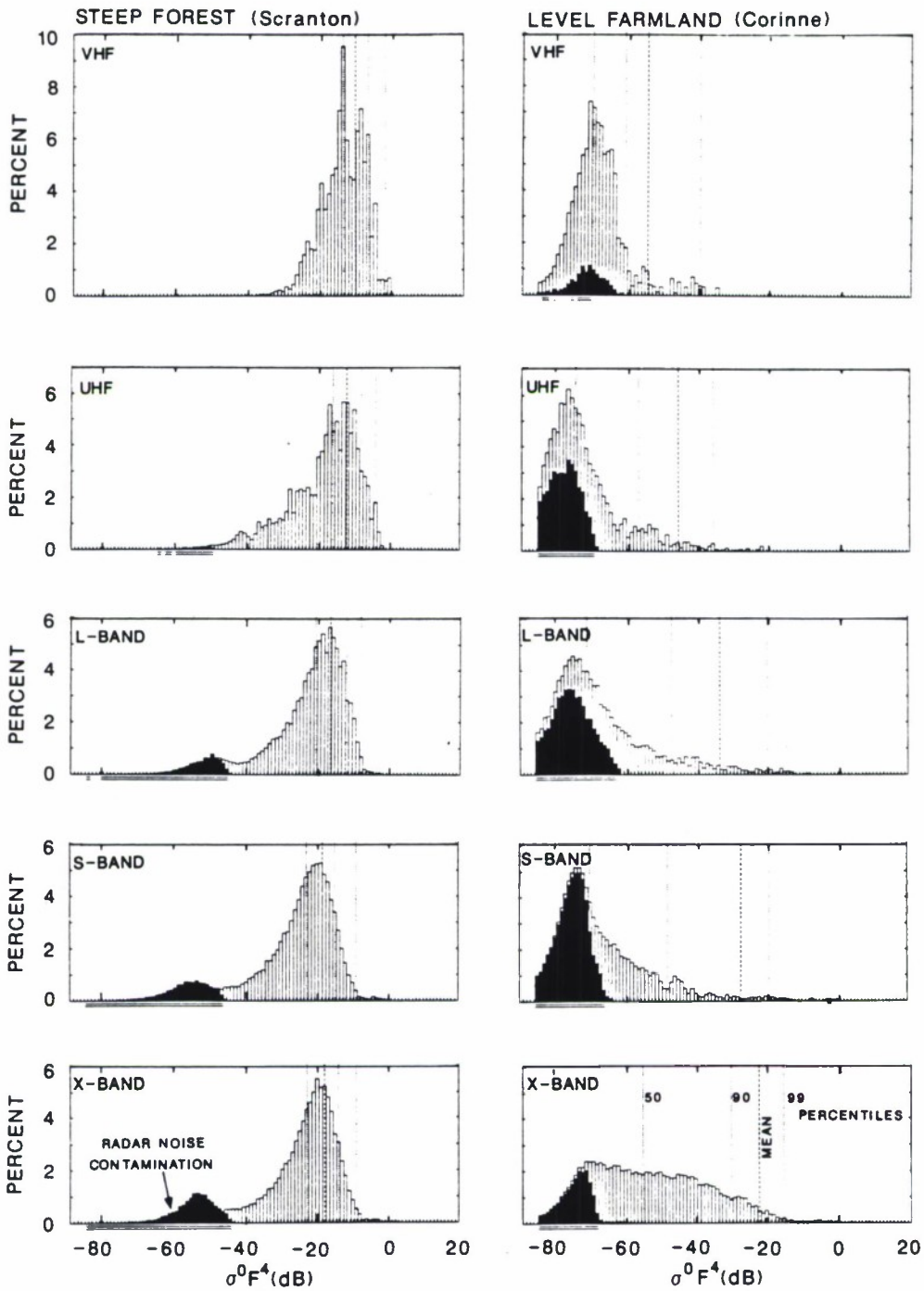

Figure 19. Five frequency histograms of clutter strength from steep forest at Scranton, Pennsylvania, and level farmland at Corinne, Saskatchewan. Repeat sector data; 15-m range resolution (36 m at VHF and UHF), vertical polarization at Scranton; 150-m range resolution, horizontal polarization at Corinne. Partially integrated data. See Table 6.

are shown in Figure 19. Here, we remain with level farmland at Corinne but now switch to steep forest as measured at Scranton* rather than at Blue Knob.† Table 6 shows means and ratios of standard deviation to mean for the histograms of Figure 19. It is clear from Table 6 that in steep forest, mean clutter strengths decrease strongly with increasing frequency; whereas, in level farmland, mean clutter strengths increase strongly with increasing frequency. We also observe in Table 6 that spreads (i.e., ratios of standard deviation to mean) in clutter amplitude statistics are much greater in level farmland terrain than in steep forest terrain, but that in both terrain types spreads decrease with decreasing spatial resolution as the azimuth beamwidth increases from 1 deg at X-band to 13 deg at VHF. The physical mechanisms causing these observed effects were previously discussed in Section 3.2. Thus, the data of Figure 19 and Table 6 provide examples from five-frequency Phase One measurements for the general remarks of the preceding section.

TABLE 6
Clutter Strengths for Steep Forest at Scranton and Level Farmland at Corinne

	Mean (dB)		SD/Mean (dB)	Percent of Samples Above Noise Floor
	Upper Bound	Lower Bound		
SCRANTON				
VHF	−10.62	−10.62	1.2	99.8
UHF	−12.25	−12.25	1.8	99.4
L-Band	−16.74	−16.74	2.0	92.9
S-Band	−18.46	−18.46	4.6	89.7
X-Band	−17.88	−17.88	5.2	86.2
CORINNE				
VHF	−54.80	−54.82	8.1	89.3
UHF	−45.75	−45.75	11.0	60.8
L-Band	−33.58	−33.58	10.4	52.8
S-Band	−26.94	−26.94	12.5	44.6
X-Band	−22.37	−22.37	13.9	80.9

Note: Repeat sector data; 15/36-m pulse length, vertical polarization at Scranton; 150-m pulse length, horizontal polarization at Corinne. Partially integrated data. See Figure 19.

* Scranton results in Figure 19 and Table 6 apply to a reduced repeat sector range interval from 10.5 to 12.9 km containing a steep forested ridge.

† Looking ahead to Figure 32, it may be seen that clutter statistics at Scranton and Blue Knob are very similar, and the repeat sectors at these two sites are grouped in the same terrain category.

The reason mean clutter strength rises with increasing frequency in level farmland is due to multipath propagation loss entering clutter strength $\sigma^{\circ}F^4$ through the propagation factor F. As pointed out previously in Section 3, the propagation factor is a function of geometric factors including antenna height and range. At Corinne, the level farmland site, we made a full series of Phase One repeat sector measurements at each of three different antenna heights to provide a data base with which we could investigate antenna height effects on clutter in a multipath environment on very level terrain. Thus, we made measurements with one, two, and three antenna tower sections raised, giving us nominal antenna tower heights of about 30, 44, and 57 ft, respectively (see Table A-5 for actual feed heights by frequency band). Sector displays showing mean clutter strength versus range in the Corinne repeat sector at these three antenna tower heights are shown in Figures 20(a), (b), and (c), respectively. Data at three frequencies, UHF, L-, and X-band are shown. Only the UHF noise floor is shown; the noise floors in the other bands are in the same neighborhood but are omitted to avoid complicating the figures. Data are reduced only over the first 20 deg of the 60-deg-wide Corinne repeat sector because of data limitations in processing (i.e., data within the very wide Corinne azimuth interval had to be calibrated and reduced in three separate azimuth subintervals). Over the 1- to 4-km range shown, variations of mean clutter strength are complex as discrete sources drop in or out of range gates. We see the expected dependency with frequency band due to the more extreme multipath effects at lower frequencies. If these three curves are overlaid and compared range gate by range gate within bands (we leave it to the interested reader to do so), the higher antenna usually but not invariably measures higher mean clutter strengths by several decibels or so. We do not dwell further on these antenna height effects here. We have presented them to illustrate with measured data the effects alluded to in the previous section. These three figures give some sense of what lies behind mean clutter strength over geometrically visible regions of farmland terrain and how the geometric factor of antenna height affects such results. Later in Section 4.1.4.3 we return to this discussion of antenna height effects at Corinne and provide mean strengths at all bands and waveforms over the complete Corinne repeat sector at each of the three antenna heights.

Before leaving Blue Knob and Corinne, we show in Figure 21 mean clutter strength versus frequency for the repeat sectors at both sites, at all combinations of polarization and pulse length on one common set of coordinate axes, for the purpose of comparison. The data of Figure 21 dramatically illustrate that the frequency dependency of mean clutter strength at high angles in steep forest terrain is very different from that at grazing incidence in level farmland terrain. In the following sections we do include dramatic variations in mean clutter strength such as are shown in Figure 21, but within an overall scheme involving finer variations with terrain type and depression angle so as to provide a continuous matrix of information across all of the terrain types and measurement scenarios.

3.3 DEPRESSION ANGLE AND TERRAIN SLOPE

Illumination angle is of major importance in its effects on both strength and spread in low-angle ground clutter spatial amplitude statistics. We use depression angle as our measure of the angle at which terrain is illuminated. As is shown in Figure 15, depression angle is the angle below the horizontal at which a clutter patch is observed at the radar. More specifically, we define depression angle to be the complement of incidence angle at the backscattering terrain point under consideration. Incidence angle

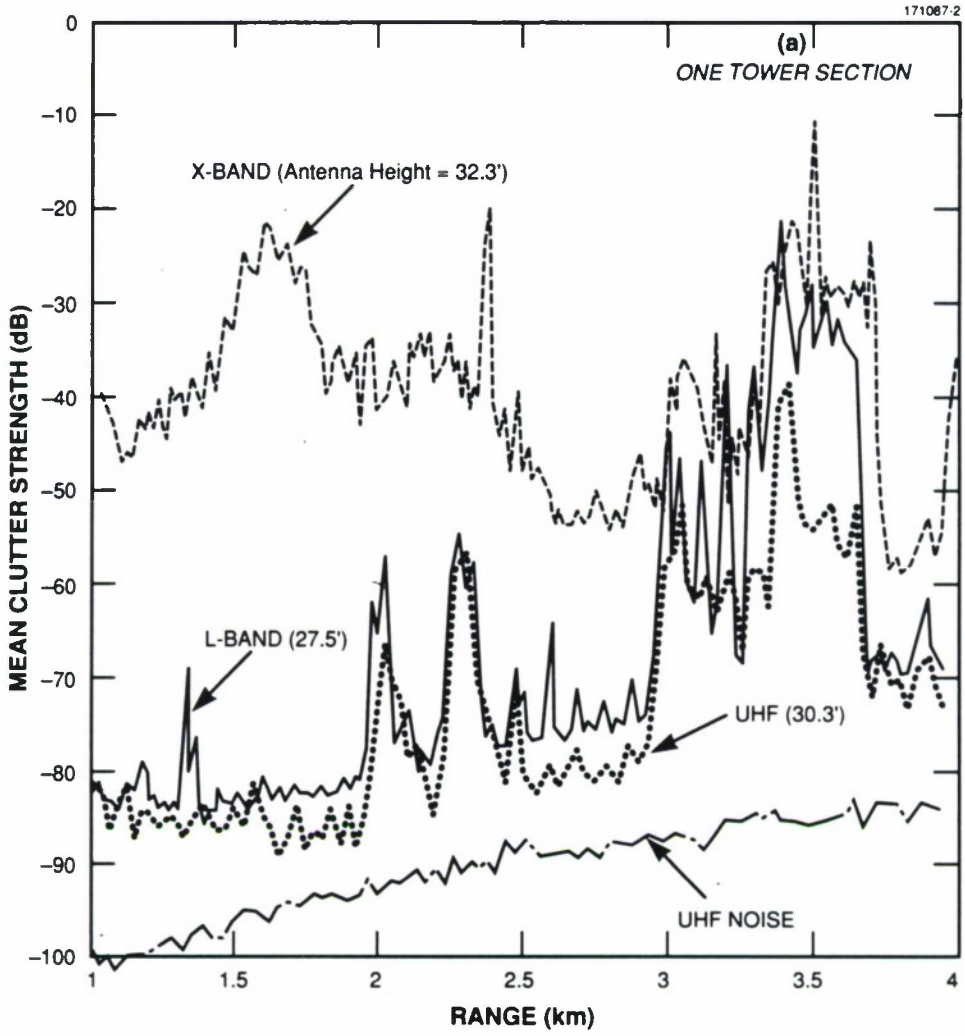

Figure 20. Mean clutter strength versus range as a function of antenna height at Corinne. (a) One antenna tower section raised. Subregion within repeat sector, 330 to 350 deg azimuth, 1- to 4-km range. UHF, L-, X-band. Vertical polarization, 15/36-m pulse length. Data shown range gate by range gate averaged in azimuth over 20 deg.

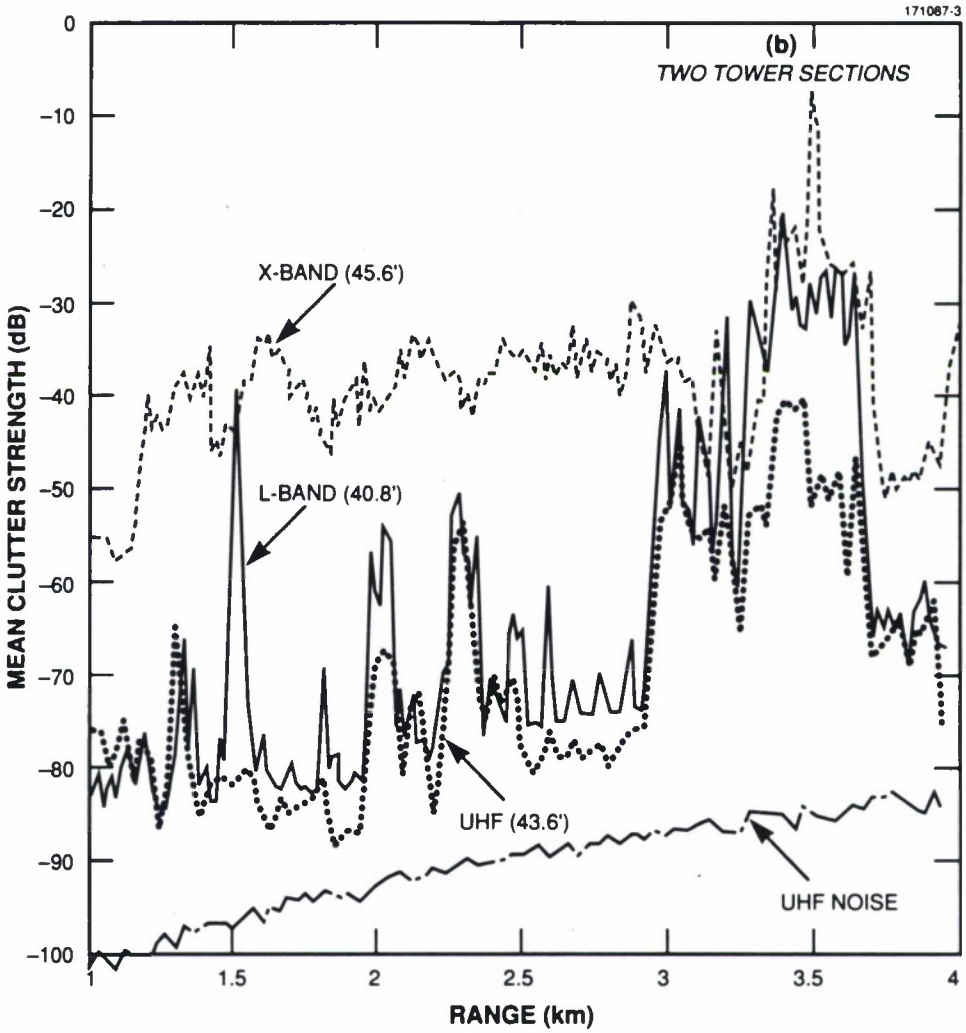

Figure 20. Mean clutter strength versus range as a function of antenna height at Corinne. (b) Two antenna tower sections raised. Subregion within repeat sector, 330 to 350 deg azimuth, 1- to 4-km range. UHF, L-, X-band. Vertical polarization, 15/36-m pulse length. Data shown range gate by range gate and averaged in azimuth over 20 deg.

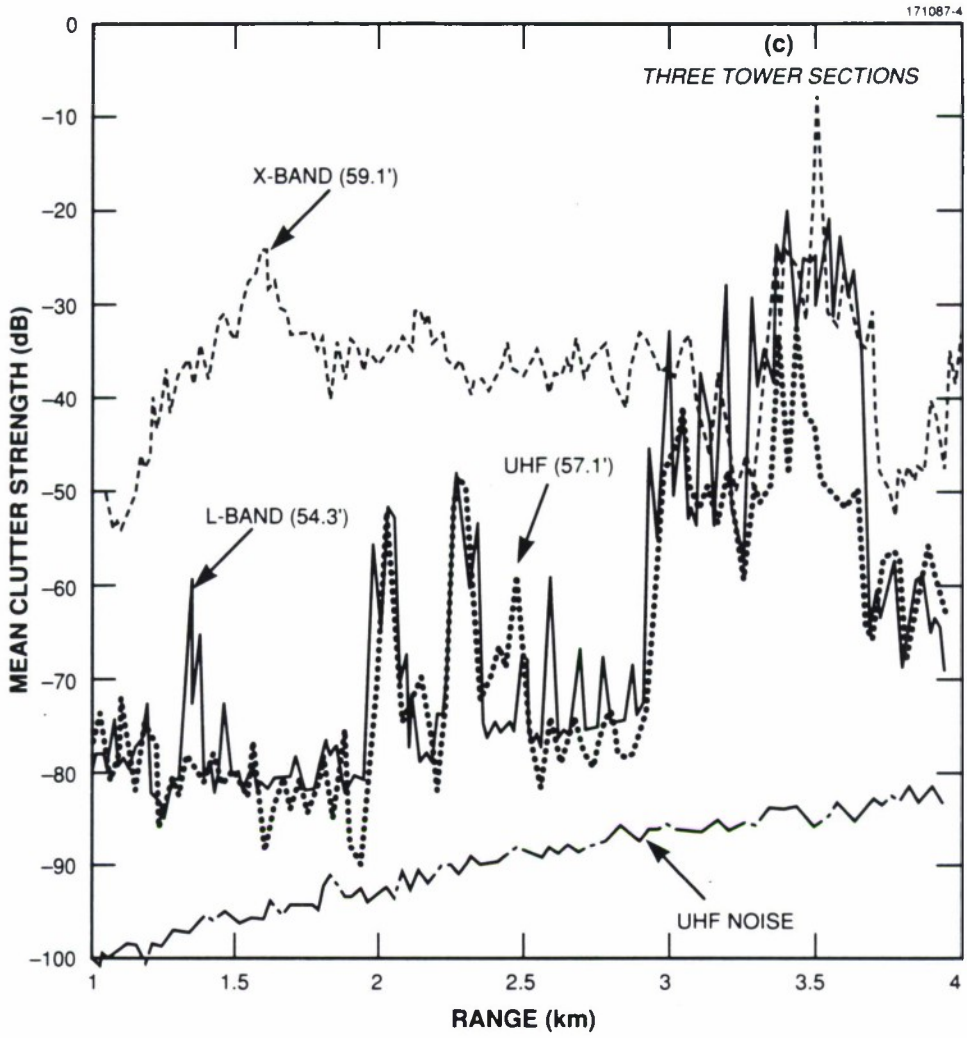

Figure 20. Mean clutter strength versus range as a function of antenna height at Corinne. (c) Three antenna tower sections raised. Subregion within repeat section, 330 to 350 deg azimuth, 1- to 4-km range. UHF, L-, X-band. Vertical polarization, 15/36-m pulse length. Data shown range gate by range gate and averaged in azimuth over 20 deg.

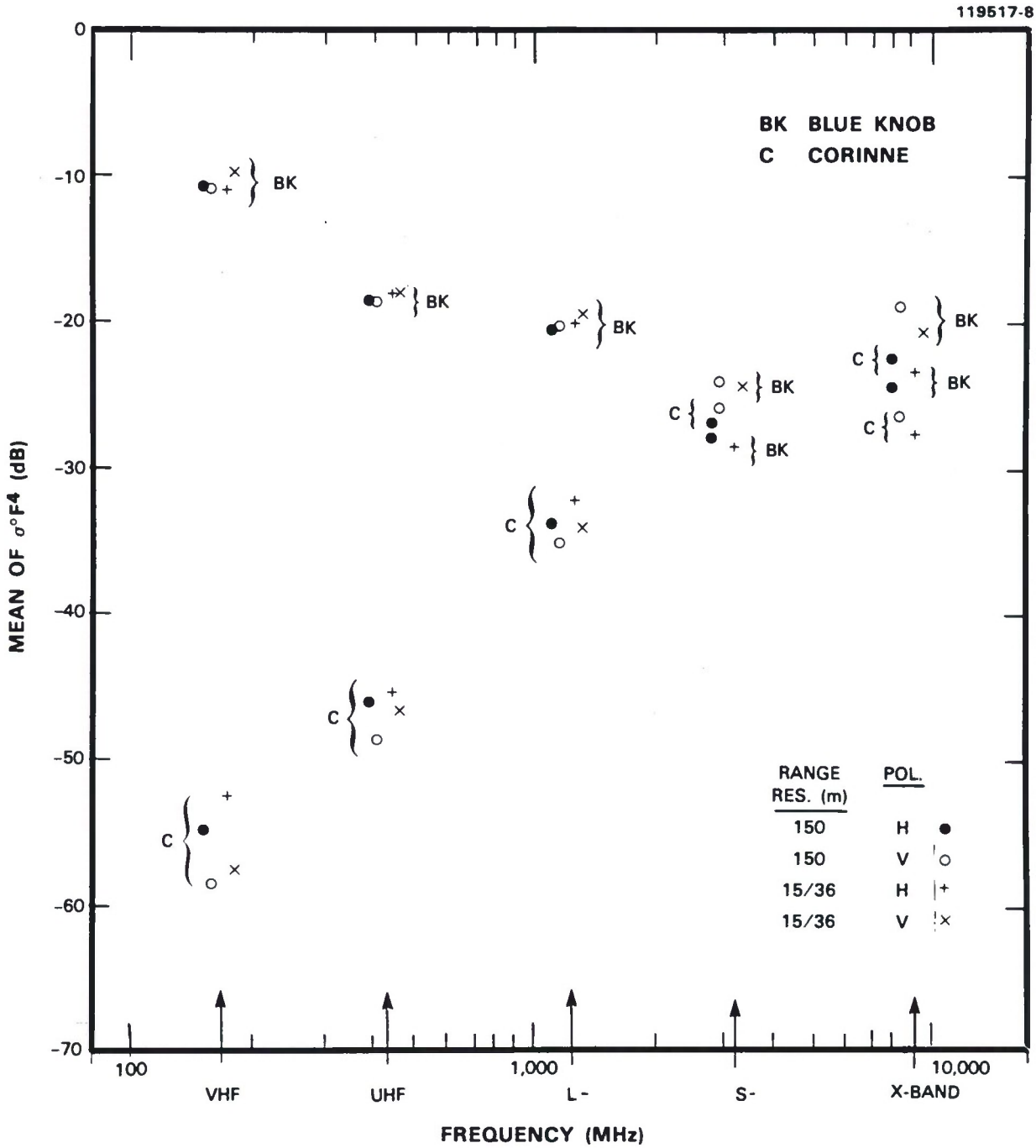

Figure 21. Mean ground clutter strengths in steep forest and level farmland. Repeat sector data from steep forest at Blue Knob and level farmland at Corinne.

equals the angle between the outward projection of the earth's radius at the terrain point and the direction of illumination at that point, assuming a 4/3 earth radius to account for nominal atmospheric refraction. Thus, our rigorous definition of depression angle is in a reference frame centered at the terrain point, not at the antenna. This definition of depression angle includes the effect of earth curvature on the angle of illumination but does not include any effect of the local terrain slope. Grazing angle is the angle between the tangent to the local terrain surface at the backscattering terrain point and the direction of illumination. Thus, grazing angle does take into account the local terrain slope. At short enough ranges that earth curvature is insignificant, depression angle simplifies to be the angle below the horizontal at which the terrain point is viewed from the antenna.

We do not use grazing angle as our measure of the angle at which terrain is illuminated. That is, we do not attempt to incorporate a quantitative measure of local terrain slope at the backscattering terrain point in our definition of illumination angle. One reason for this is that slopes exist at many physical scales in landscape, and it is difficult to formulate a useful definition of terrain slope using available terrain elevation data that actually correlates significantly with clutter returns from terrain cells at the scale of radar resolution.* Rather than attempting to assign a single numerical value of terrain slope to each resolution cell, we describe the whole distribution of terrain slopes presented to the radar over each large repeat sector of terrain as being bounded within limits defining terrain relief classes (see Table 4). As with Phase Zero, in most terrains we capture much of the statistical significance in the dependency of clutter strength on terrain slope in the Phase One results by using just two classes of relief, namely, "high-relief" terrain (terrain slopes are greater than 2 deg) and "low-relief" terrain (terrain slopes are less than 2 deg).

However, the Phase One results do require one important modification to this basic two-class terrain relief descriptive scheme. In low-relief open agricultural terrain supportive of multipath, the general effect of increasing effective clutter strength with increasing frequency requires the terrain to be very level, so low-frequency clutter returns are always received on the underside of the first multipath lobe but with increasing gain with increasing frequency. Even relatively low inclinations of terrain at between 1 and 2 deg of terrain slope are enough to prevent this general illumination effect by directing the multipath lobes more randomly with respect to the clutter sources in the repeat sector. That is, in such terrain, even at low frequencies, clutter returns are received well up on the multipath lobing pattern, not just on the extreme underside of the first lobe, at increased or decreased gain over free space depending on the particular terrain involved.

Therefore, in low-relief agricultural terrain, we further classify terrain relief into two subcategories, namely, "moderately low-relief" (terrain slopes lie between 1 and 2 deg), and "very low-relief" (terrain slopes are less than 1 deg). This refinement in classification is sufficient to distinguish between terrain that is level enough so that multipath results in generally increasing strength of illumination of clutter sources with increasing frequency and terrain in which multipath effects on illumination are more specific.

---

* Ongoing research of our Phase One data at Defence Research Establishment Ottawa indicates that if large discretes are first removed, we can begin to show correlation of clutter strength versus grazing angle as defined by DTED.

4. MEAN GROUND CLUTTER STRENGTH VERSUS FREQUENCY BY TERRAIN TYPE

In this section we show how mean ground clutter strength varies with frequency as measured within Phase One repeat sectors. These results depend on three different categories of descriptive parameter. First, there are parameters descriptive of the radar, namely, frequency, resolution, and polarization. Our basic format of data presentation is to show mean strength (ordinate) versus frequency (abscissa) across the five Phase One frequency bands for each of four combinations of pulse length and polarization. Second, there are parameters descriptive of the geometry of illumination. We use depression angle, a quantity relatively simple and unambiguous to determine, which depends on range and relative elevation difference (see Table 3) between the radar antenna and the centroid of the repeat sector clutter patch. Third, there are parameters descriptive of the terrain within the repeat sector clutter patch. We classify the terrain within each repeat sector both in terms of its landform (i.e., its roughness or relief, see Table 4) and its land cover (e.g., forest, farmland, urban, etc., see Table 5). These terrain classifications were obtained by overlaying and registering measured clutter maps onto stereo aerial photos and topographic maps, originally at about 1:50,000 scale, but more recently at 1:10,000 scale. We have previously introduced all of these parameters. Their effects in our Phase One repeat sector ground clutter data base will now be illustrated.

Table 7 describes the repeat sectors at 38 different Phase One measurement sites in terms of range and azimuth extent from the radar, depression angle, and terrain type by landform and land cover. When multiple landform or land cover terrain classes are indicated in Table 7, they are in decreasing order by percent area within the repeat sector clutter patch. In reviewing the specific information describing repeat sectors in Table 7, it may be observed that every repeat sector is different. This illustrates the essentially infinite variability of terrain. As a result of this variability, the set of 20 multifrequency mean clutter strengths (i.e., five frequencies, two polarizations, two range resolutions) plotted for each site in Appendix E is different, at least in detail, for every site. Our objective is to move beyond this abundance of detail to determine useful, simple generalizations in the measurement results. Our approach for achieving this objective requires statistically combining measurements that are reasonably similar within broad classes of terrain type and depression angle, such that the results satisfactorily cluster within each class and significantly separate between different classes.

The repeat sectors in Table 7 are grouped within the best broad classes that have been developed in the repeat sector data base. Thus, based on the multifrequency characteristics of mean clutter strength that they produce, five broadly different terrain classes are observed in Table 7, namely, urban, mountains, forest, agricultural, and desert, marsh, or grassland. Observe that, except for mountains, these groups are basically distinguished by major land cover type; mountains are distinguished more by landform. Within each of these five broadly different terrain classes, when terrain relief can vary enough within class to require further subclassification, two subcategories of terrain relief are usually enough, namely, low-relief with terrain slopes < 2 deg and high-relief with terrain slopes > 2 deg. An exception is agricultural terrain, which requires additional subclassification of low-relief terrain into categories of moderately low-relief with terrain slopes between 1 and 2 deg and very low-relief with terrain slopes < 1 deg. For each terrain type/relief category (eight altogether), when depression angle can vary enough within class to be important, Table 7 indicates that usually three categories of depression angle (low, intermediate, and high) are enough to separate effects.

TABLE 7

Terrain Descriptions of 38 Repeat Sectors Within 12 Groups by Terrain Type and Depression Angle

	Dep Ang (deg)	Land-form	Land Cover	Range (km)	Azimuth (deg)	Setup Number
URBAN						
Strathcona, Alta.	1.5	3-2	11-12-51	1-10	62-82	7
Lethbridge West, Alta.	0.3	3-8	11-12-21	6-11.9	92-102	18
Altona II, Man.	0.2	1	21-11-14	2.5-8.4	262-272	31
Picture Butte II, Alta.	0.1	3-8	11-12	22-27.9	172-182	22
Headingley, Man.	0.04	1	11-12-41	14-19.9	82-92	30
MOUNTAINS						
Plateau Mountain, Alta.	1.2	8	42-7	11-16.7	255-265	21(b)
Waterton, Alta.	–1.8	8-7	42-7-41	9-14.9	175-185	20
FOREST/HIGH-RELIEF (Terrain Slopes > 2°)						
High Depression Angle						
Blue Knob, Pa.	1.6	4	21-43-11	16-21.9	80-100	48
Scranton, Pa.	1.0	7-4-3	43-12-11	8-13.9	300-320	47
Low Depression Angle						
Cold Lake, Alta.	0.2	3-7	43-21	5-10.9	120-130	11
Woking, Alta.	0.2	2-7	43	4-9.9	118-136	27
Penhold II, Alta.	0.1	4-2	21-41-11	15-24	54-74	8
Peace River South II, Alta.	–0.1	2-7	21-41	12-17.9	348-358	26
FOREST/LOW-RELIEF (Terrain Slopes < 2°)						
High Depression Angle						
Puskwaskau, Alta.	2.1	2	43	1-6.9	230-240	25
Brazeau, Alta.	1.2	3	42-62-41	4-9.9	170-180	17,24
Intermediate Depression Angle						
Gull Lake West, Man.	1.0	1	61-52-43	1-6.9	300-320	33,39
Wainwright, Alta.	0.6	5-3	41-32-31	1-6.9	120-150	36
Turtle Mountain, Man.	0.5	5	41-52	2-7.9	102-122	41
Katahdin Hill, Mass.	0.4	5-4	43-21-52	1-6.9	220-250	49
Westlock, Alta.	0.4	3	43-21-62	8-13.9	42-52	10

TABLE 7 (Continued)

Terrain Descriptions of 38 Repeat Sectors Within 12 Groups by Terrain Type and Depression Angle

	Dep Ang (deg)	Land-form	Land Cover	Range (km)	Azimuth (deg)	Setup Number
Low Depression Angle						
Sandridge, Man.	0.3	1	41-62-22	1-6.9	298-318	40
Dundurn, Sask.	0.2	5	32-41-31	1-6.9	295-325	37
AGRICULTURAL/HIGH-RELIEF (Terrain Slopes >2°)						
Plateau Mountain, Alta.	2.3	4	31-32-21	20-40	40-50	21(a)
Polonia, Man.	2.0	7-2	21-41	1-10	107-127	4
Neepawa, Man.	-0.9	7-2	21-41	1-10	287-307	3
AGRICULTURAL/LOW-RELIEF						
Moderately Low-Relief (1° < Terrain Slopes < 2°)						
Beulah, N.D.	1.2	2	21	1-6.9	50-70	42
Magrath, Alta.	0.7	3-2	21-33	5-10.9	125-135	19
Beiseker, Alta.	0.4	3-2	21-31	8-17	150-170	9,15 23,28
Very Low-Relief (Terrain Slopes < 1°)						
Orion, Alta.	1.2	3-1	21-31	1-10	186-196	14
Wolseley, Sask.	0.5	3-1	21	6-10	301-311	29
Rosetown Hill, Sask.	0.4	1	21	4-9	45-65	35
Pakowki Lake, Alta.	0.3	1-3	21-31	1-10	6-16	13
Shilo, Man.	0.2	1-3	21-31	1-10	228-258	2
Corinne, Sask.	0.15	1	21	1-8.9	330-30	38
DESERT, MARSH, OR GRASSLAND (Few Discretes)						
High Depression Angle						
Booker Mountain, Nev.	1.8	3	7-33	12-17.9	125-145	44
Vananda East, Mont.	1.0	3-5	31-32	3.6-9.5	40-60	45
Low Depression Angle						
Knolls, Utah	0.3	1	7-33	3.0-6.5	290-307	43
Big Grass Marsh, Man.	0.2	1	62-22	1-6.9	350-10	32

In total we observe in Table 7 that separating the five broadly different terrain types into subclasses by relief and depression angle leads to a manageable set of 12 categories. In following subsections, we illustrate how measured mean clutter strength varies with frequency in each category.

As we discuss these Phase One results, we occasionally compare them at X-band with the earlier Phase Zero results. These comparisons help to put the Phase One results in somewhat broader perspective because the Phase Zero results, although at X-band only (and horizontal polarization and usually 75-m pulse length), involve many more terrain samples (viz., 2177 clutter patches) than do the Phase One results of this report (viz., 42 repeat sectors). Unless specified otherwise, when we compare Phase Zero results with Phase One, we select the horizontal polarization, 150-m pulse length waveform in the Phase One results as the closest radar parameter match to Phase Zero. In comparing Phase Zero and Phase One results, note that Phase Zero made most of its measurements several years before Phase One, often with minor variations in site location and elevation and not always with similar antenna mast heights. In particular, the different X-band vertical beamwidths of Phase Zero and Phase One (3-dB elevation beamwidths equal to 23 and 3 deg, respectively; see Table A-6) could cause large differences in F^4 even if σ° was the same.

We carry range resolution and polarization as parameters in the Phase One results presented in the following subsections. As discussed in Section 3, we expect that general effects of polarization and resolution on mean clutter strength will be small. Thus, later in Section 4.3, we provide general results for mean clutter strength versus frequency in each of the 12 terrain type/relief/depression angle categories, obtained as median averages within each category independent of polarization and resolution. These general results are shown in Table 11. Discussions throughout Section 4, when citing numerical values to quantify observed trends, often implicitly draw upon the medianized mean clutter strength data of Table 11. We return to more extensive discussion of polarization and resolution effects in Section 5.

4.1 DETAILED DISCUSSION OF MEASUREMENTS IN URBAN, MOUNTAIN, FOREST, FARMLAND, AND DESERT TERRAIN

In following subsections, multifrequency measurements of mean clutter strength within the 12 terrain type/relief/depression angle categories of Table 7 are discussed. In addition to providing resultant general trends, which is the main purpose of this report, each subsection also discusses the specific measurement situation at each site. The reason for this is that every site is different; and to have a proper appreciation for what is drawn out of these data as generalities and the extrapolation of these generalities to other sites and scenes, it helps to be familiar with the terrain specifics involved in the measurements. Also included are site-specific descriptions of the seasonal state of terrain and weather during the measurement period and occasional remarks concerning problems and/or special activities of the Phase One equipment.

With 42 different Phase One sites to describe, we cannot take space in Section 4 to provide all the descriptive information available on each site. We do provide terrain elevation profiles along the center azimuth of many of the repeat sectors as a first indication of the terrain in the measurement zone. These terrain profiles are generated from Defense Mapping Agency digital terrain elevation data (DTED) for which the original source material was usually small scale 1:250,000 maps with, typically, 100-ft contour intervals,

although occasionally greater. Thus, at the scale of the repeat sectors (e.g., a 10-km repeat sector covers 1-1/2 in on the original map), there is extensive interpolation in the DTED.* As a result, 10-m errors in the terrain profiles shown are common, and much fine detail in terrain elevation is omitted. Therefore, these DTED profiles should be regarded only as relatively rough approximations, sometimes even misleading approximations in places, and where they differ in detail from other information provided in this report, either verbal or quantitative, we need to quickly defer to the other information as more accurate. Unlike the profiles shown earlier in Figure 10 for which the data were generated from 1:50,000 scale maps with 25-ft contour intervals, the DTED profiles in Section 4 are neither adjusted to include earth curvature (i.e., these DTED profiles merely show height above mean sea level) nor do these DTED profiles show terrain masked to the Phase One antenna. Also, when considering these profiles we need to remember that we are only showing elevations along the central radial through the repeat sector and that significant variations can occur along other radials even within a 10-deg repeat sector.

In Appendix E, we provide considerably more information about each site, including terrain photos, a PPI clutter map, a clutter amplitude histogram, and a plot of multifrequency mean clutter strengths. Five-frequency sector displays showing clutter strength versus range are also provided in Appendix E for a selected site from each terrain group. These site-specific packages of information in Appendix E are arranged in the same site-by-site order as the discussions that follow in Section 4.1; thus, Appendix E may be regarded as expansionary visual reference material accompanying the following discussions.

In the limited site-descriptive words provided here in Section 4.1, we only attempt to give the essence of the site in a few thumbnail notes. We include what the terrain is like and our first impressions about each site as to its importance, its uniqueness, how it compares and contrasts with other sites, and its overall context within the group of 42 sites. These discussions of data from individual sites are also used as opportunities to discourse on various topics concerning the Phase One measurement program (e.g., calibration, seasonal variation, tower height effects, and propagation), using examples of data as a springboard to provide increased depth of understanding of our program and its results. In these discussions, we occasionally allude to individual site data presented in Appendix E without explicit reference.

4.1.1 Urban

A photograph of the city center of Calgary, which is located in the Strathcona repeat sector, is shown in Figure 22. We took this photograph at the time of the Phase One measurements there (viz., September 1982). Multifrequency measurements of mean ground clutter strength from the five urban repeat sector patches are shown in Figure 23. DTED terrain elevation profiles through these urban repeat sectors are shown in Figure 24. All five of the sites with urban repeat sectors are located on open low-relief terrain of the Canadian prairies supportive of multipath. At X- and S-bands and even L-band, the angle to the first maximum on the Phase One multipath lobing pattern is usually small enough (viz., 0.03, 0.07, and 0.20 deg) that typical urban clutter sources such as buildings at typical repeat sector ranges usually reach well up

---

* The DTED values at about a 100-m sampling interval are interpolated values at a sampling interval of about every 0.015 in on the source map.

on the lobing pattern even on very level terrain. As a result, multipath effects on illumination, although still acting to introduce considerable statistical fluctuation from measurement to measurement in these bands, do not usually introduce any strong dependence of mean clutter strength with frequency. Thus, in these bands we see very strong, relatively frequency independent mean clutter strength from the group of urban patches as a whole at or near the -10-dB level in the data of Figure 23.

Altona II and Headingley. At VHF and UHF, multipath effects in the urban data of Figure 23 are more complex. At these lower frequencies, multipath lobes are broader and can more significantly increase or decrease the effective gain of the measurement over the whole repeat sector. Consider first Altona II and Headingley. At both of these sites, mean clutter strengths decrease by more than 20 dB with decreasing frequency, from maximum mean levels of greater than -10 dB at X- or S-band to minimum mean levels of less than -30 dB at VHF. At both of these sites, the terrain is very level (i.e., landform class = 1, see Table 7). Neither site has any terrain elevation advantage over surrounding terrain, so that the depression angles at which the urban clutter patches are illuminated are low. Therefore, at both sites the effect of decreasing mean clutter strength with decreasing frequency is due to strongly decreasing intensity of illumination caused by multipath. That is, the VHF clutter returns are received deep in the first, relatively wide, horizon plane multipath null (see Figure B-4). Otherwise, these two urban repeat sector clutter patches are physically quite different. At Headingley, the repeat patch is centered on the downtown high-rise city center of Winnipeg (population 300,000) at relatively long range. At Altona II, the repeat patch is centered on the tiny village of Plum Coulee (population 510) at relatively short range. Furthermore, at Headingley we extended three antenna tower sections for a nominal tower height of 60 ft; whereas, at Altona II we extended six antenna tower sections for a nominal tower height of 100 ft (see Tables A-1 and A-5). Thus, there exist considerable differences in antenna tower height, range, and distribution of clutter source heights in these two propagation-dominated urban clutter measurement situations. Of course, antenna height, range, and clutter source height all strongly affect the amplitudes of received clutter returns in a multipath-dominated situation. As a result, in detailed band-by-band comparison, we observe Headingley clutter significantly stronger than Altona II clutter at X-band and UHF, Altona II stronger than Headingley at S-band and VHF, and rough equality at L-band (see Figures E-17 and E-26). It would clearly require very detailed, terrain-specific information to predict such complex variations. Nevertheless, the two sites taken together do appear to belong to the same overall class and provide bounds on what we might expect for urban mean clutter strengths on level open terrain.

Strathcona. Now consider Strathcona. In contrast to the level situations at Headingley and Altona II, the Strathcona site is situated on a grassy hill on the outskirts of Calgary. The repeat sector clutter patch at Strathcona is centered on the downtown high-rise city center of Calgary (population 600,000). The slope of the hill at Strathcona, 5 deg, was so situated as to direct the peak of the second VHF multipath lobe at the city center clutter patch. As a result, the urban mean clutter strengths measured at Strathcona are 10 to 12 dB stronger at VHF than at UHF and L-band. This situation is illustrated in Figure 25. Thus, at Strathcona multipath propagation augments rather than cancels VHF clutter.

Lethbridge West and Picture Butte II. Finally, consider the urban clutter measurements at Lethbridge West and Picture Butte II. At both sites, we measured urban clutter from the city of Lethbridge (population 55,000) as viewed from across the Oldman River valley. An aerial photo of Lethbridge is shown in Figure 26. The secondary landform class of "moderately steep" (landform = 8) at both sites applies to the illuminated

Figure 22. High-rise city center of Calgary. Urban clutter, Strathcona repeat sector. 13 September 1982.

steep banks on the far side of the river just before the urban clutter was encountered, which were included in the repeat patch. These steep banks are visible at the bottom of Figure 26. From Lethbridge West, we viewed the city from the west over relatively low-relief terrain. As a result, from Lethbridge West a VHF multipath propagation loss of more than 20 dB occurred in the mean clutter strength measured from the city. However, from Picture Butte II, we viewed the city at longer range from the north over an initial long gradual downslope in terrain elevation of about 0.5 deg. This initial incline rotated the multipath lobing pattern downwards by about 0.5 deg with respect to the clutter sources distributed on the more level terrain farther out (see Section B.2) and substantially reduced the VHF propagation loss to less than 10 dB (i.e., the angle to the peak of the first VHF multipath lobe was effectively reduced from 1.5 deg to 1.0 deg). Thus, VHF mean clutter strength measured from the city of Lethbridge was 12 dB stronger (i.e., higher on the underside of the first multipath lobe) measured from the north than from the west over

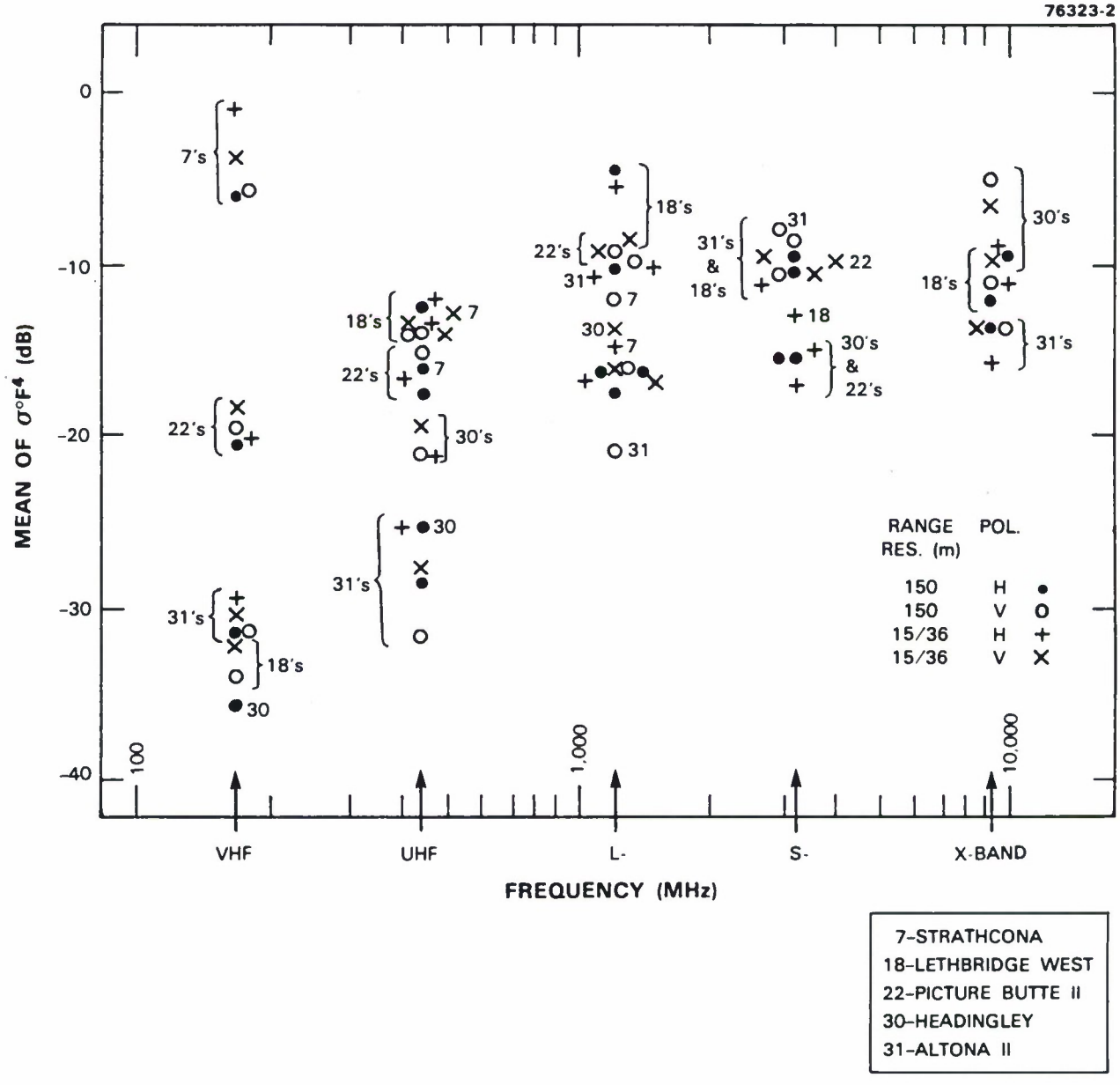

Figure 23. Mean clutter strength versus frequency for urban terrain. See Table 7.

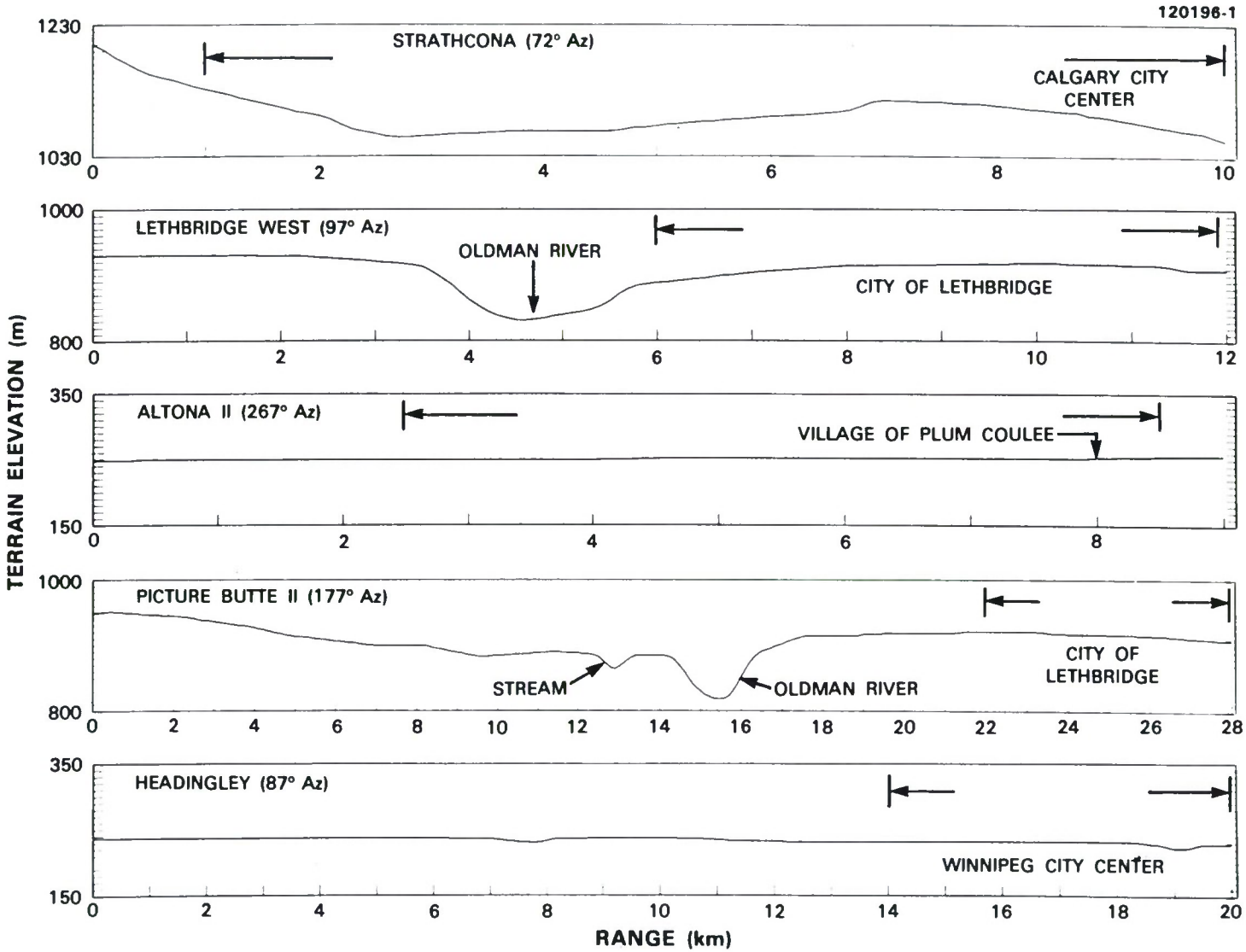

Figure 24. DTED terrain profiles at Strathcona, Lethbridge West, Altona II, Picture Butte II, and Headingley. Elevation in meters above sea level, 10 m between tick marks. Range extent of repeat sectors is indicated by horizontal arrows.

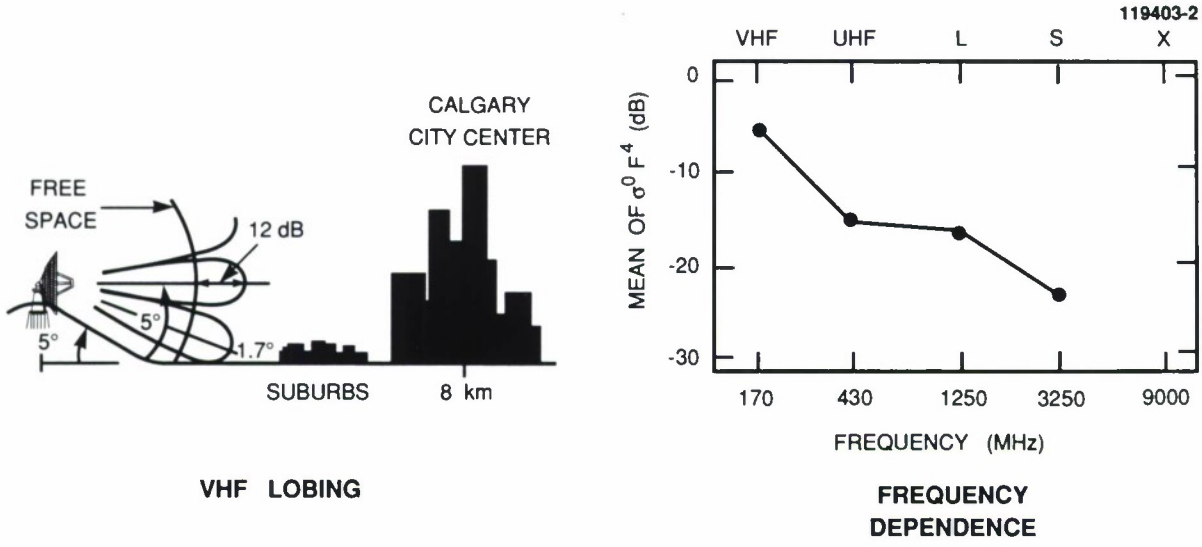

Figure 25. Strong VHF clutter induced by multipath at Strathcona.

relatively similar agricultural terrain. Such specific propagation-induced variations occur in many of our measurements in open terrain. Note that the city of Lethbridge measurements from the north (Picture Butte II) and the west (Lethbridge West) are very similar in other bands (see Figures E-21 and E-11).

In the preceding paragraphs, we have indicated how the urban mean clutter strengths in Figure 23 begin to separate by angle of illumination, including effects of both depression angle and terrain slope. In following subsections involving other terrain types, we will continue to see the importance of angle of illumination, and as a result, will explicitly separate the data into different categories of depression angle and relief.

Phase Zero. We now briefly compare the Phase One urban data of Figure 23 at X-band with earlier, X-band only, Phase Zero results that included measurements of 122 urban clutter patches. Of these patches, the single strongest Phase Zero mean clutter strength measured was -4.6 dB for the small town of Rosetown, Saskatchewan. The strongest Phase One X-band urban mean clutter strength in Figure 23 is -4.8 dB for downtown Winnipeg (at 150-m pulse length and vertical polarization) measured from the Headingley site, a comparable value. As another example, the Phase Zero measurement of mean clutter strength in the Phase One repeat sector at Lethbridge West was -10.2 dB, which may be compared with the Phase One value (at 150-m pulse length and horizontal polarization) of -11.9 dB. On the other hand, the median value of mean clutter strength over all 122 Phase Zero urban clutter patches was -23.2 dB, which is considerably less (viz., 12.4 dB) than the median of the Phase One X-band urban data in Figure 23. This would suggest that the five Phase One urban patches in Figure 23, all of which are open prairie results and thus multipath augmented at X-band, may be thought of as close to upper bound or worst-case situations involving stronger than average urban clutter at X-band.

Figure 26. Aerial photo of the city of Lethbridge showing the Picture Butte II repeat sector. Scale = 1:50,000. North is to the left.

The multifrequency data set of urban mean clutter strength shown in Figure 23 illustrates how many specific effects in individual measurements statistically combine so that the group as a whole provides useful bounds for urban clutter. This data set is representative of our approach of using measurements from multiple sites to define low-angle clutter within broad terrain classes. In following subsections we similarly show multisite data in other terrain classes.

4.1.2 Mountains

The steepest, roughest terrain from which we measured ground clutter was that of the Canadian Rocky Mountains in southern Alberta. One of the sites, Plateau Mountain, was a flat-topped mountain site high in the Rockies (8121 ft above sea level), which provided road access for our truck-borne clutter measurement equipment. From Plateau Mountain, the view in repeat sector (b) to the west was of steep barren rock faces from some of the highest peaks in the Rockies.* A photograph of Plateau Mountain and the view looking west into repeat sector (b) is given in Figure 27. The lower part of this photograph shows how the terrain drops off precipitously on the east side of Plateau Mountain. The other Rocky Mountain site was at Waterton, Alberta. At Waterton, we set up on the high prairie in southern Alberta just a few kilometers from steep mountain terrain. The area around Waterton is characterized by an abrupt transition from prairie to mountains without much of an intermediate forested foothills region, as is generally the case farther north. Terrain elevation profiles for repeat sectors at Plateau Mountain (b) and Waterton are given in Figure 28. From Waterton, the view in the repeat sector to the south beyond the intervening rangeland (landform = 3, land cover = 33) also included some regions of steep exposed bedrock. At both Plateau Mountain and Waterton, the lower slopes of the mountains visible at near ranges in the repeat sector patches were densely forested with the trees gradually thinning out at higher elevations. At far ranges in both repeat sectors, but particularly at Plateau Mountain, there were substantial areas where the clutter originated only from rocky peaks. Nevertheless, on a percent-area basis over the complete repeat sector patch at both sites, there was more steep forest (land cover = 42) than barren rock (land cover = 7). At both sites, there were many patches of snow and ice at the upper elevations at the time of the measurements in June 1983 (see Table 1).†

Multifrequency measurements of mean ground clutter strength from these two mountain sites are shown in Figure 29. First, we observe that mean clutter strength decreases strongly with increasing frequency, VHF to X-band, by about 14 dB. We attribute much of this observed effect (as much as 10 dB [4]) to the increasing RF absorption by the forest vegetation within the repeat sector with increasing frequency.

Multipath. Second, we observe in Figure 29 that Waterton mean strengths are greater than Plateau Mountain mean strengths in all bands and waveforms. We attribute this effect to multipath from the intervening rangeland in the Waterton measurements. Let us consider this effect in more detail. At Waterton, the highest peaks in the repeat sector subtend a positive elevation angle of 3.8 deg at the Phase

---

* Plateau Mountain had two repeat sectors: repeat sector (a) to the northeast, providing an airbornelike view of the prairie below, see Section 4.1.4.1, and repeat sector (b) to the west, containing mountains.

† While Phase One was on Plateau Mountain, in June 1983, there occurred heavy snowfall, high winds, and daytime temperature highs below freezing.

One antenna. This angle is large enough to subtend multiple multipath lobes, certainly at the higher Phase One frequencies. Even at VHF, depending on details in assumptions concerning terrain profiles and Fresnel zones, at least between one and two lobes and probably between two and three lobes are subtended by 3.8 deg (see Figure B-5). For the theoretical situation of interference between a direct ray and a multipath ray reflected from a perfectly conducting infinite planar surface, the mean value of F^4 averaged over one or more complete interference lobes is 7.8 dB. Thus, at Waterton we would expect mountain values of σ° to be augmented by multipath by as much as 7.8 dB in the measurements of $\sigma^\circ F^4$. At Plateau Mountain, on the other hand, the terrain falls off from the site steeply enough to prevent any multipath. Thus, at Plateau Mountain we would expect that we would be measuring essentially intrinsic values of σ° from mountain terrain under free-space illumination (i.e., $F = 1$). Indeed, measured values of mean clutter strength $\sigma^\circ F^4$ at Waterton at VHF and S-band are observed in Figure 29 to be 6 or 7 dB stronger than at Plateau Mountain (viz., in order of wide pulse, horizontal and vertical polarization, then thin pulse, horizontal and vertical, at VHF the differences are 6.5, 6.9, 8.0, and 4.4 dB, and at S-band the differences are 6.6, 6.1, 5.8, and 5.7 dB, respectively). This difference would appear to suggest similar values of intrinsic σ° from mountains at both sites at VHF and S-band with multipath augmentation close to that theoretically expected from a flat plane with unity reflection coefficient. In contrast, at UHF and L-band, mean clutter strengths at Waterton are observed in Figure 29 to be only 2 or 3 dB stronger than at Plateau Mountain, although in every individual measurement by frequency and waveform the Waterton value remains greater than the Plateau Mountain value. This effect could be the result of differing values of intrinsic σ° at the two sites in these two bands or more complicated propagation effects. Certainly, although both repeat sectors contain mountains, they are dramatically different in specific physical detail. And, although the intervening terrain at Waterton is low-relief rangeland generally supportive of multipath, it is far from a theoretical level reflecting surface. Rather, it is undulating and broken in places, dissected by streams, and with many patches of brush, low trees, and shrub vegetation (see Figure E-31).

Polarization. Third, we observe in Figure 29 (and Figures E-30 and E-35) that at both mountain sites, mean clutter strengths at VHF are usually 7 to 8 dB stronger at vertical polarization than at horizontal polarization (viz., in order of wide pulse, then thin pulse, at Waterton the differences are 7.6 and 4.1 dB, and at Plateau Mountain the differences are 7.2 and 7.7 dB). At UHF the polarization differences have dropped to the 2- to 3-dB range, although vertical is still always stronger than horizontal, respectively, by pulse length at both sites. In the higher bands, the polarization differences are still smaller, usually less than 1 dB, with neither vertical nor horizontal predominating. Why VHF mountain clutter is 7 or 8 dB stronger at vertical polarization than at horizontal polarization is not well understood but may be a general effect* based on its existence in multiple measurements at two different mountain sites.

Bare Rock Faces. Our first observation was that mountain clutter strength decreases with increasing frequency due to vegetation absorption. We attempted to isolate the bare rock faces dominant in the far range portions of the Plateau Mountain (b) repeat sector to determine whether "pure rock" clutter amplitudes are frequency independent. Measurement data from Plateau Mountain were reduced at vertical polarization and 15/36-m pulse length over a pure rock region in repeat sector (b) from 14.7 to 16.7 km. Resultant mean clutter strengths from these pure rocks at VHF, UHF, L-, and S-bands were -14.3, -19.6, -19.2, and -20.1 dB, respectively. (No X-band data were collected at Plateau Mountain because of a high-altitude transmitter failure.)

---

* We have subsequently observed this effect in many more mountain clutter patches in our Phase One survey data at these two sites.

Figure 27. Plateau Mountain. Airborne view looking west into repeat sector (b). Level terrain in foreground is top of Plateau Mountain.

These results indicate essential frequency invariance of mean clutter strength from pure rocks, UHF through S-band, at about the -19- or -20-dB level; however, there is a 5-dB increase of mean strength from this level at VHF.

Phase Zero. The Phase Zero measurements included measurements of 90 mountain clutter patches. The strongest of these, a small Plateau Mountain patch containing near vertical rock faces at a mountain summit, provided a mean clutter strength of -9.6 dB. However, the Phase Zero measurement of the Phase One repeat sector at Waterton resulted in a mean strength of -20.9 dB, close to the Phase One wide

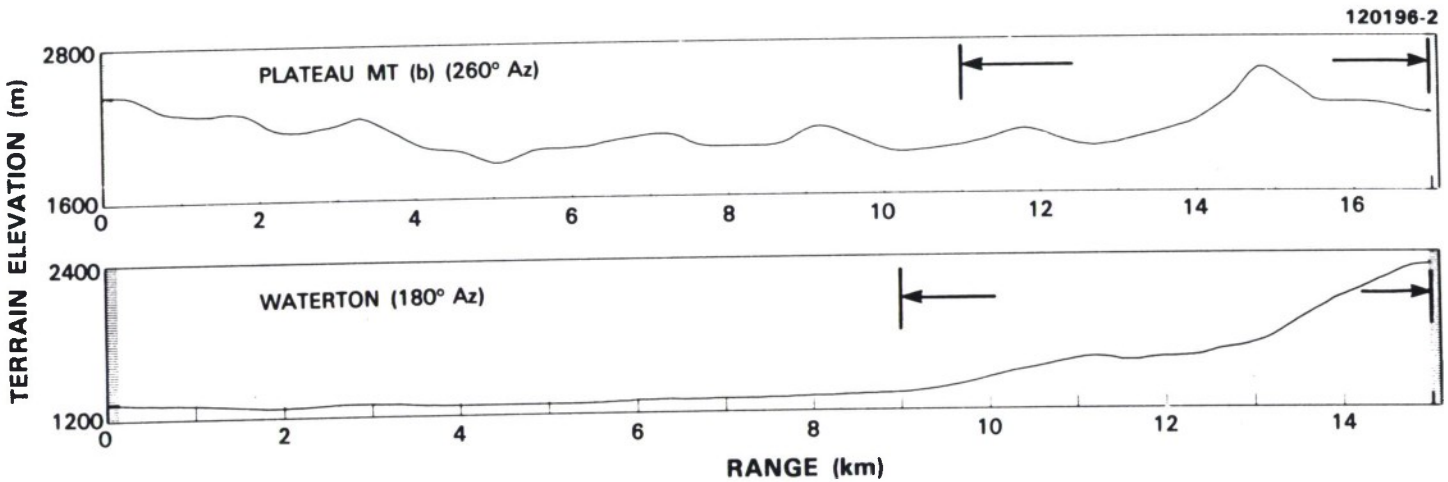

Figure 28. DTED terrain profiles at Plateau Mountain (b) and Waterton. Elevation in meters above mean sea level, 20 m between tick marks. Range extent of repeat sectors is indicated by horizontal arrows.

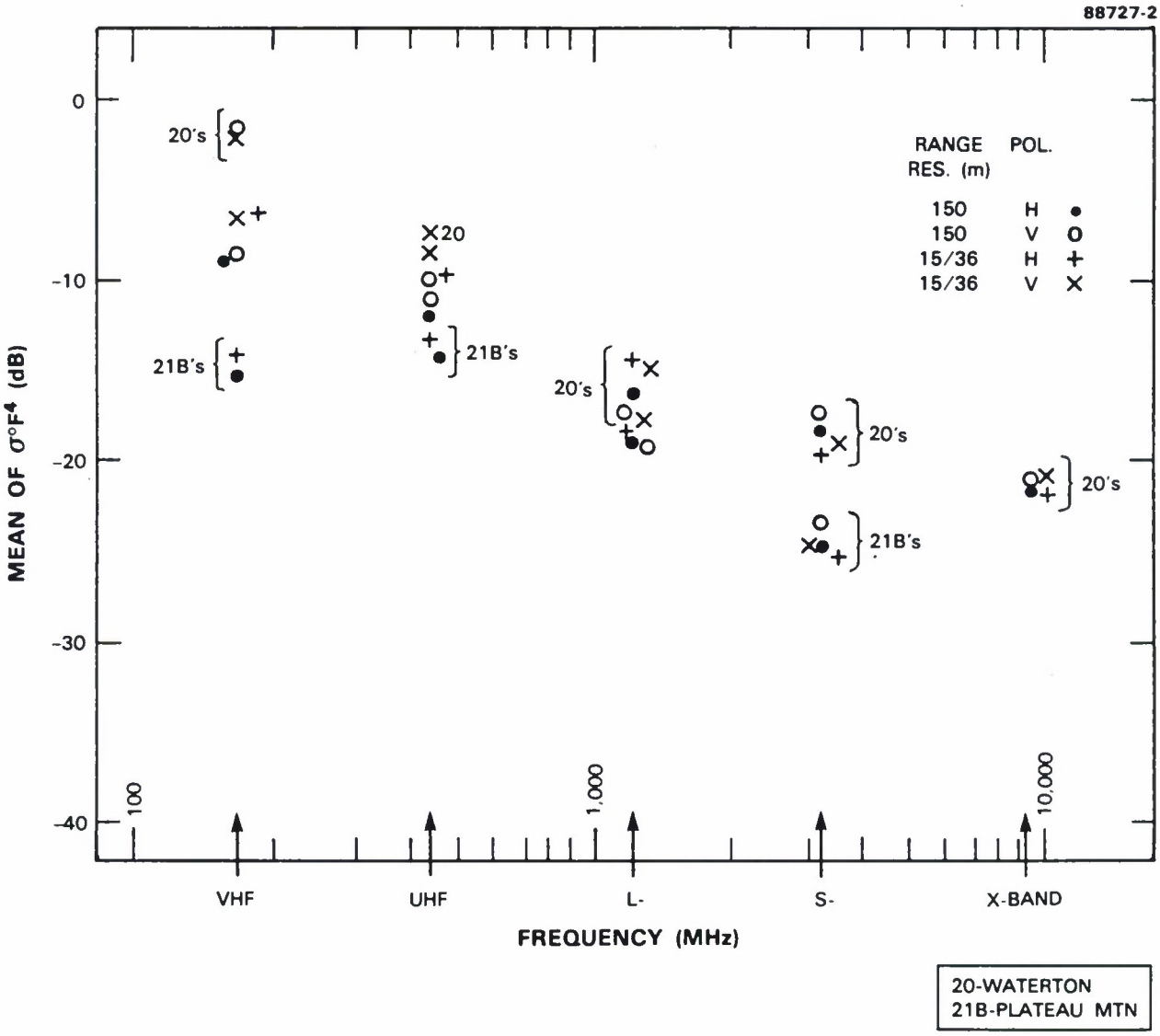

Figure 29. Mean clutter strength versus frequency for mountain terrain. See Table 7.

pulse, horizontal polarization value of -21.9 dB. The median value of mean clutter strength over all 90 Phase Zero mountain clutter patches was -22.9 dB, very close to the median of the Phase One X-band Waterton mountain data in Figure 29 (Waterton data only; no X-band data at Plateau Mountain) of -21.6 dB.

4.1.3 Forest

In following subsections we present multifrequency mean clutter strengths from forest in five regimes of relief and depression angle, as shown in Table 7. Because forest is much less supportive of multipath than is open terrain, particularly at high illumination angles, many of these forest measurements are much more measurements of relatively pure intrinsic σ^o and are much less contaminated by dispersive propagation influences than are measurements in open terrain. To the extent that this is true, fewer measurements can establish trends in forest terrain than in farmland terrain. However, VHF multipath propagation loss may occasionally appear in these forest results at low angles of illumination.

4.1.3.1 Forest/High-Relief/High Depression Angle. There are two sites, Scranton and Blue Knob, which fall into the category of forest/high-relief/high depression angle. A photograph of the Blue Knob terrain along with a PPI clutter map is shown in Figure 30. Both sites are located in the steeply ridged, generally forested terrain of the Appalachian Mountains in Pennsylvania. Terrain profiles of the repeat sectors at these two sites are shown in Figure 31. Multifrequency mean clutter strengths measured over the repeat sectors at these two sites are shown in Figure 32. The results from these two sites, for which there is considerable commonality in classification by terrain type and depression angle (see Table 7), are quite similar. Again, we observe in Figure 32 a trend of decreasing mean strength with increasing frequency, extending from VHF to S-band; whereas, in the mountain data of Figure 29 a similar trend extended from VHF to X-band. As in the mountain data, as much as 10 dB of this 12.8-dB effect in Figure 32 can be attributed to increasing vegetative absorption of the RF energy by the forest with increasing frequency. Later in this section we discuss further the high X-band values in Figure 32, many of which are 4 or 5 dB higher than the respective measurements by polarization and pulse length at S-band.

Next, we observe in Figure 32 that mean strengths measured from the steeper terrain at Scranton (i.e., landform = 7, moderately steep) are 3 or 4 dB stronger than those measured from the less steep terrain at Blue Knob (i.e., landform = 4, rolling) in most bands and waveforms but less so at VHF. At both sites, the four measurements at each combination of polarization and pulse length in each of the lower three bands cluster remarkably tightly, which may be indicative of relatively little propagation influence, and hence, relatively little statistical dispersion caused by specific propagation effects at these sites. In the upper two bands, we observe that the vertical polarization result is usually several decibels stronger than the horizontal at both sites, but more so at Blue Knob.

Scranton. There is much commonality in illumination angle, terrain type, and measurement results at Scranton and Blue Knob. However, in detailed physical characteristics, these two sites are quite different. At Scranton the site is located high on the east side of the Lackawanna River on Scrub Oak Mountain fire tower lookout at 2070-ft elevation, and the view into the repeat sector is west across the river valley and the city of Scranton at elevations in the range of 700 to 900 ft and up the steeply rising

forested slopes of West Mountain to a peak elevation of 2160 ft on the far side of the river valley. Much of the near-in terrain in this sector is masked to the radar. The repeat sector patch for which we provide measurement results in Figure 32 is of geometrically visible terrain on the far side of the river valley at 8- to 14-km range. From 8 to 10 km, our repeat sector patch contains heavily settled urban terrain (commercial, industrial, and residential) on the west side of the city of Scranton, although with a substantial incidence of trees among the buildings. Beyond this, at ranges from 10 to 14 km, the terrain rises steeply up the heavily forested side of West Mountain at slopes as great as 9.5 deg. Roads and power transmission lines and other man-made clearings occur on the lower and middle slopes of this rising terrain, and this area also contains revegetated spoil heaps from strip mine operations.

Blue Knob. Blue Knob is located in high-relief forested terrain in the Allegheny Range south of Altoona. From Blue Knob, at an elevation of 3110 ft, the view into the repeat sector is east across an intervening sharp forested ridge at 2000-ft elevation and 10-km range to a farmland valley beyond at elevations of 1400 to 1500 ft. The repeat sector patch is of geometrically visible terrain within this distant agricultural valley at ranges from 16 to 22 km and 1.6-deg depression angle. A photograph of this terrain is shown in Figure 33. The terrain on this valley floor is hilly (not picked up in the DTED of Figure 31). Typical relief is in the range of 100 to 150 ft and occasionally greater. Typical terrain slopes presented to the radar are 2.5 deg. The town of Martinsburg (population 1800) occupies the northeast corner of the patch. Most of the terrain within the patch is agricultural. However, there are many trees scattered throughout the patch, such as in woodlots and orchards, along roads and railway rights-of-way, between fields, and around farmsteads. A 20-m tree throws a 716-m geometrical shadow at the Blue Knob depression angle of 1.6 deg. The percent of visual area occupied by trees in a plane normal to a 1.6-deg line-of-sight would have to be determined by oblique aerial photography, which we have not done. However, the multifrequency clutter characteristic from this patch in Figure 32 shows the clear trend of decreasing strength with increasing frequency that we obtain from forest at high angles of illumination. In contrast, clutter returns from treeless farmland (e.g., Beulah) or rangeland [e.g., Plateau Mountain, sector (a)] at similar high depression angles show a multifrequency characteristic that is essentially invariant with frequency at a mean level of about -30 dB (e.g., see Figures E-113 and E-100, respectively). Hence, we believe that it is the secondary component of trees (i.e., land cover = 43) in the rolling agricultural valley at Blue Knob that dominates its clutter characteristics. Similar results were obtained at Cochrane (see Section 4.2) and, at lower depression angle, at Penhold II. (Blue Knob and Penhold II are compared and contrasted in the following section; note the similarity in Table 7 of landform, land cover, and even range and azimuth extent for Blue Knob and Penhold II.) We have discussed elsewhere (and from another point of view, namely, X-band clutter amplitude distributions versus percent tree cover) how small percent incidences of trees on agricultural landscapes dominate low-angle terrain backscatter characteristics.

Phase Zero. The Phase Zero X-band measurements in the Phase One repeat sectors at Scranton and Blue Knob were -17.9 and -24.4 dB, respectively, which in these multipath-free measurement situations are close to the Phase One X-band values of -20.0 and -24.5 dB, respectively. However, across all 65 Phase Zero measurements of high-relief forested clutter patches at depression angles between 1 and 2 deg, the median value of mean clutter strength was -27.1 dB. Even across the subset of 20 of these measurements for which the primary landform classification was, like Scranton, moderately steep, the median value of mean clutter strength was -24.5 dB. These Phase Zero results suggest that the Phase One

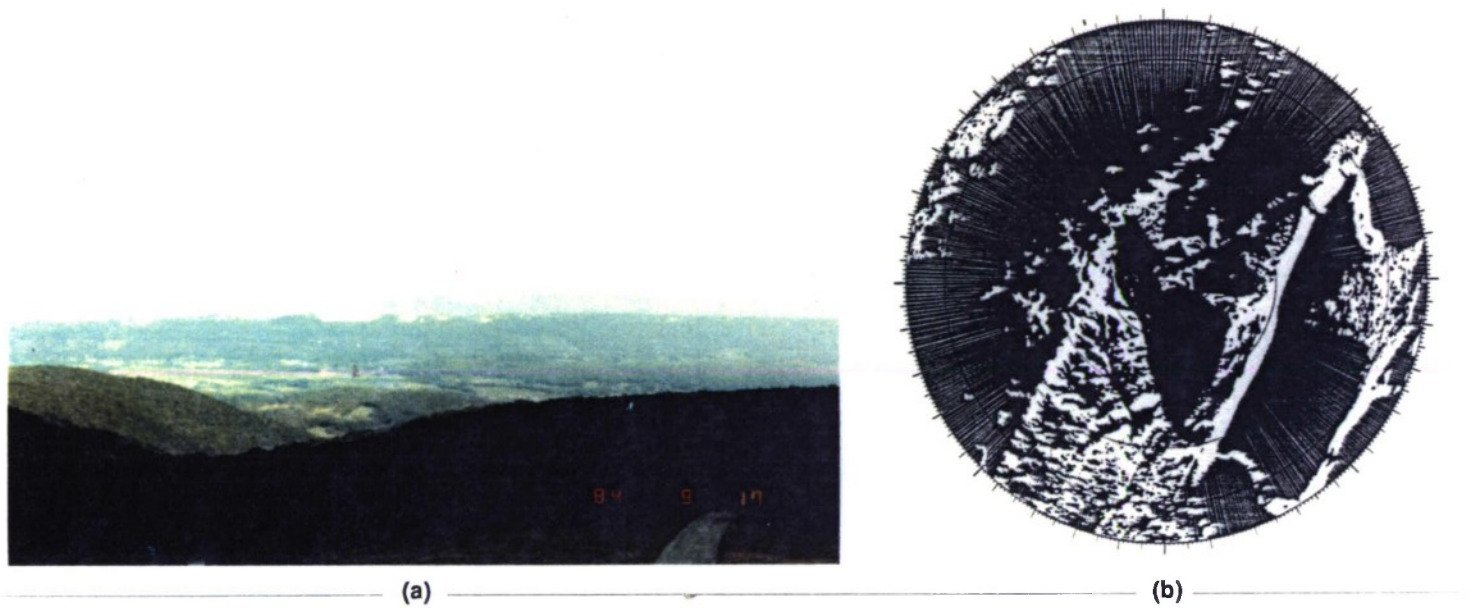

Figure 30. Forested terrain at Blue Knob. (a) Tower-top view looking east into repeat sector and (b) X-band PPI clutter map. North is zenith. Maximum range = 24 km.

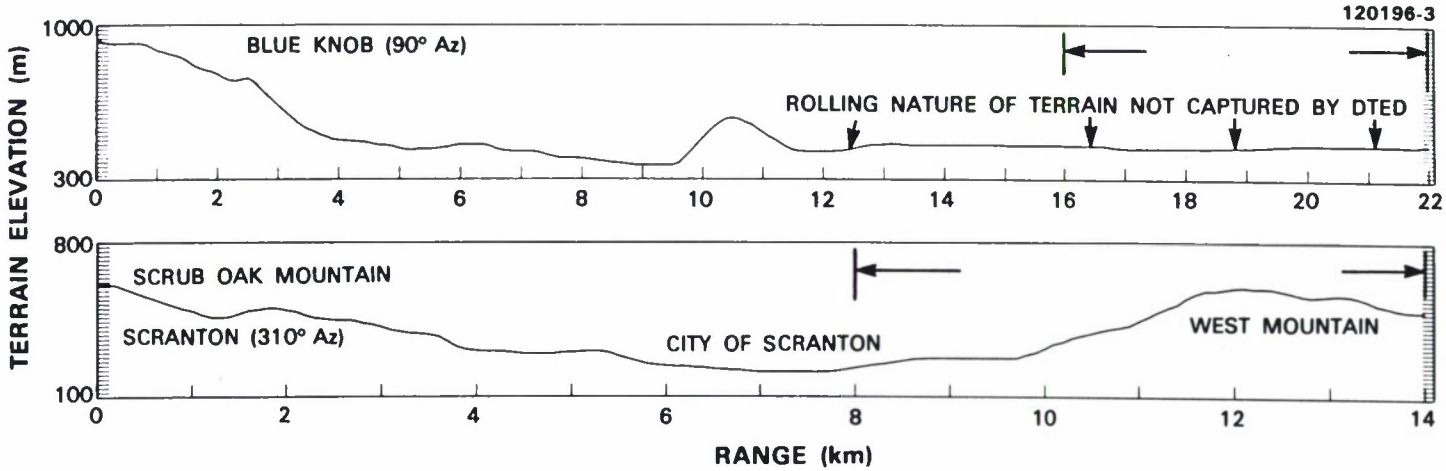

Figure 31. DTED terrain profiles at Blue Knob and Scranton. Elevation in meters above mean sea level, 20 m between tick marks. Range extent of repeat sectors is indicated by horizontal arrows.

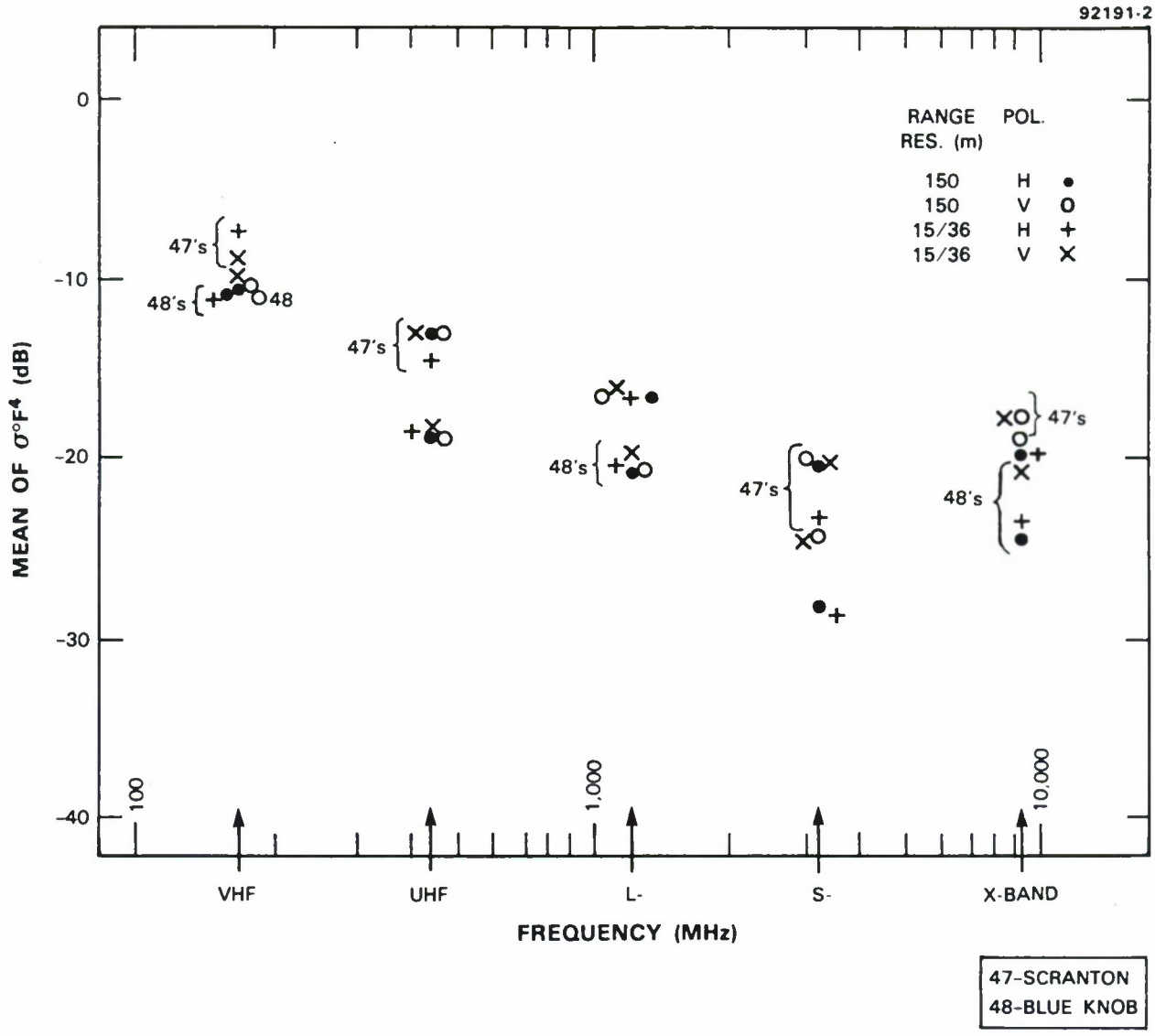

Figure 32. Mean clutter strength versus frequency for forest/high-relief terrain at high depression angle. See Table 7.

Figure 33. Repeat sector at Blue Knob. This rolling farmland terrain was illuminated by Phase One from long range (19 km) across an intervening ridge. Note the considerable secondary incidence of trees. The viewing direction here is NE.

X-band results at Scranton and Blue Knob are relatively high for the category of forest/high-relief/high depression angle. The median of all eight Phase One X-band measurements of mean clutter strength shown in Figure 32 at these two sites is -19.9 dB. This value is even higher than the corresponding Phase One value in mountains, which is -21.6 dB. Only when we go to very high depression angles in the Phase Zero data (viz., 6- to 8-deg depression angle, moderately steep or steep forested terrain, eight patches, median value of mean clutter strength = -19.7 dB) do we see general results close to the measured Phase One X-band results at Scranton and Blue Knob. We may speculate that the high X-band values of mean clutter strength at Scranton and Blue Knob may be due to the urban component in these measurements, especially at Scranton. The median value of Phase One X-band measurements of mean clutter strength at Blue Knob only is -22.1 dB, which is slightly lower than the Phase One X-band mountain value and fits in better with Phase One X-band values in the other four forested terrain categories. We measured a similar multifrequency mean clutter strength characteristic as the Scranton and Blue Knob characteristics shown in Figure 33 at Brazeau, at least insofar as the Brazeau characteristic also shows strongly decreasing mean strength, UHF to S-band, and then an increase, S- to X-band. Brazeau is a northern wilderness forested site, also measured at high depression angle, but of low-relief in the repeat sector. Being a wilderness site, the corresponding (but smaller, viz., 2 dB) rise in mean strength, S- to X-band, at Brazeau cannot be attributed to cultural features.

4.1.3.2 Forest/High-Relief/Low Depression Angle. Table 7 shows that we have four sites which fall into the category of forest/high-relief/low depression angle. A photograph of the terrain at one of these sites, Woking, is shown in Figure 34. Terrain profiles for the repeat sectors at these sites are shown in Figure 35. All four sites are located in Alberta. Multifrequency mean clutter strengths measured over the repeat sectors at these four sites are shown in Figure 36. Again, a general trend is observed of decreasing mean strength with increasing frequency in the data of Figure 36 due to increasing vegetative absorption of RF energy with increasing frequency. In these low depression angle data, this trend extends monotonically from UHF to X-band and accounts for a decrease of 8.2 dB (see Table 11) in mean strength over this range. However, there is a countertrend at very low frequencies such that mean clutter strengths at VHF are 2.7 dB lower than at UHF. This drop in clutter strength at VHF is believed to be caused by multipath loss due to forward reflections from the intervening terrain between the radar and the repeat sector clutter patch at these very low depression angles.

Woking. This is illustrated clearly in the Woking data. Woking is a solidly forested site (i.e., land cover = 43). The repeat sector patch at 4- to 9.9-km range is illuminated at grazing incidence (i.e., depression angle = 0.2 deg). Terrain elevations rise with increasing range in the repeat sector patch, gradually at first over the near ranges in the patch (i.e., landform = 2, inclined) and then more rapidly at farther ranges in the patch (i.e., landform = 7, moderately steep). As a result, moderately steep terrain is viewed at the far end of the patch at grazing incidence over intervening low-relief terrain (noticeable in Figure 34). This is not brought out too clearly in the Woking DTED terrain profile of Figure 35. The multifrequency mean clutter strength characteristic of Woking (see Figure E-53) shows a clear-cut 10-dB decrease of mean strength from UHF to X-band largely attributable, we expect, to increasing absorption, which causes σ° to decrease with increasing frequency from the rising forested terrain in this repeat sector.* This character-

* See also Figure E-51, which shows clutter strength versus range at Woking. Note the unusual feature of decreasing L-band clutter strength with increasing range from 7.5 to 10 km in these data.

istic (Figure E-53) also shows a sharp drop of 7.5 dB at VHF from UHF, possibly attributable to multipath propagation loss caused by terrain reflections at grazing incidence over the intervening low-relief terrain, even though this terrain is solidly forested. Some of the helicopter propagation measurements at Brazeau indicated that forward multipath reflections can occur at VHF from forested terrain or from openings in the forested terrain at very low illumination angles. Altogether, this Woking characteristic is quite similar to the forest/high-relief/high depression angle characteristic of Figure 32, except for the pronounced dip of the Woking characteristic at VHF (and the unusually high X-band values in the Scranton and Blue Knob data previously discussed in Section 4.1.3.1).

At Woking the landform classification is 2-7. Thus, the high-relief nature of this terrain enters as a secondary component in this classification (i.e., 7 = moderately steep), and the low-relief primary component (i.e., 2 = inclined) reflects the low-relief nature of the intervening terrain, which may be causing a 7.5-dB propagation loss in clutter strength at VHF. Observe in Table 7 that three of the other four sites in this forest/high-relief/low depression angle category have similar 2-7 or 3-7 landform classifications (in contrast to the forest/high-relief/high depression angle sites that have high-relief terrain entering as the primary landform classification). However, these other three sites do not all reflect the simple canonical Woking situation of steep forested terrain viewed in the distance at grazing incidence over low-relief terrain.

Cold Lake. At Cold Lake a similar situation does exist where a moderately steep forested ridge is viewed in the distance over undulating, largely wooded terrain which has been opened in places for agriculture (i.e., note the secondary component of agriculture in the land cover classification = 43-21 at Cold Lake). A very similar multifrequency mean strength characteristic is obtained at Cold Lake (see Figure E-48) as at Woking (see Figure E-53), except that at Cold Lake the drop in mean strength from UHF to VHF seen at Woking does not occur, although neither does the VHF mean strength rise significantly from UHF as it does at Blue Knob and Scranton. This characteristic indicates that the existence and degree of VHF multipath is very dependent on terrain specifics. In the lower two bands at Cold Lake, mean clutter strength at vertical polarization is several decibels stronger than at horizontal polarization.

Peace River South II. However, at Peace River South II, for which the repeat sector patch has the same landform classification of 2-7 as Woking, the situation is quite different from that at Woking. At Peace River, Phase One was set up on one side of the river valley and looked across the relatively broad deep river valley to the repeat sector patch beginning on the far bank and extending beyond (see Figures 11 and 12 for aerial photos of the Peace River repeat sector). On the far bank the terrain was moderately steep (landform = 7) and wooded but transitioned to gradually rising inclined (landform = 2) farmland beyond the bank. The low-relief terrain in the patch occurs at longer ranges beyond the high-relief terrain at the beginning of the patch, unlike Woking and Cold Lake. The Peace River multifrequency mean clutter strength characteristic (see Figure E-63) is remarkably similar to the Woking characteristic (Figure E-53), except that it shows no drop at VHF due to multipath loss. The intervening river valley terrain at Peace River would not be expected to support multipath. Thus, at VHF, mean strengths at Peace River from the far bank of the river valley are almost identical to those from the ridge at Cold Lake (see Figure E-48). As at Cold Lake, Peace River mean strengths at vertical polarization at VHF and UHF are several decibels stronger than those at horizontal polarization. At L-band, mean strengths at Peace River show remarkably little variation with polarization and resolution and are remarkably similar to those at Woking.

Figure 34. Forested terrain at Woking. Phase One tower-top view looking SE into repeat sector.

Penhold II. Penhold II is the remaining site in the group of four forest/high-relief/low depression angle sites. The situation at Penhold is quite different from the other three; there is rolling farmland terrain with a substantial incidence of trees (10 to 30 percent) occurring in shelter belts and woodlots (not forest). Such terrain may be referred to as "parkland" in geographical terminology. The terrain within the repeat sector patch at Penhold is remarkably similar in land cover and landform classification to that at Blue Knob (see Table 7), although at Blue Knob the intervening terrain is forest and the depression angles are quite different for these two sites. The parkland terrain at these two sites gives multifrequency mean clutter strength characteristics much more like forest than open farmland (see Figures E-57 and E-39, respectively). The secondary component of scattered trees on these farmland landscapes dominates their clutter characteristics. Our ground clutter terrain classification system may eventually specify parkland as a

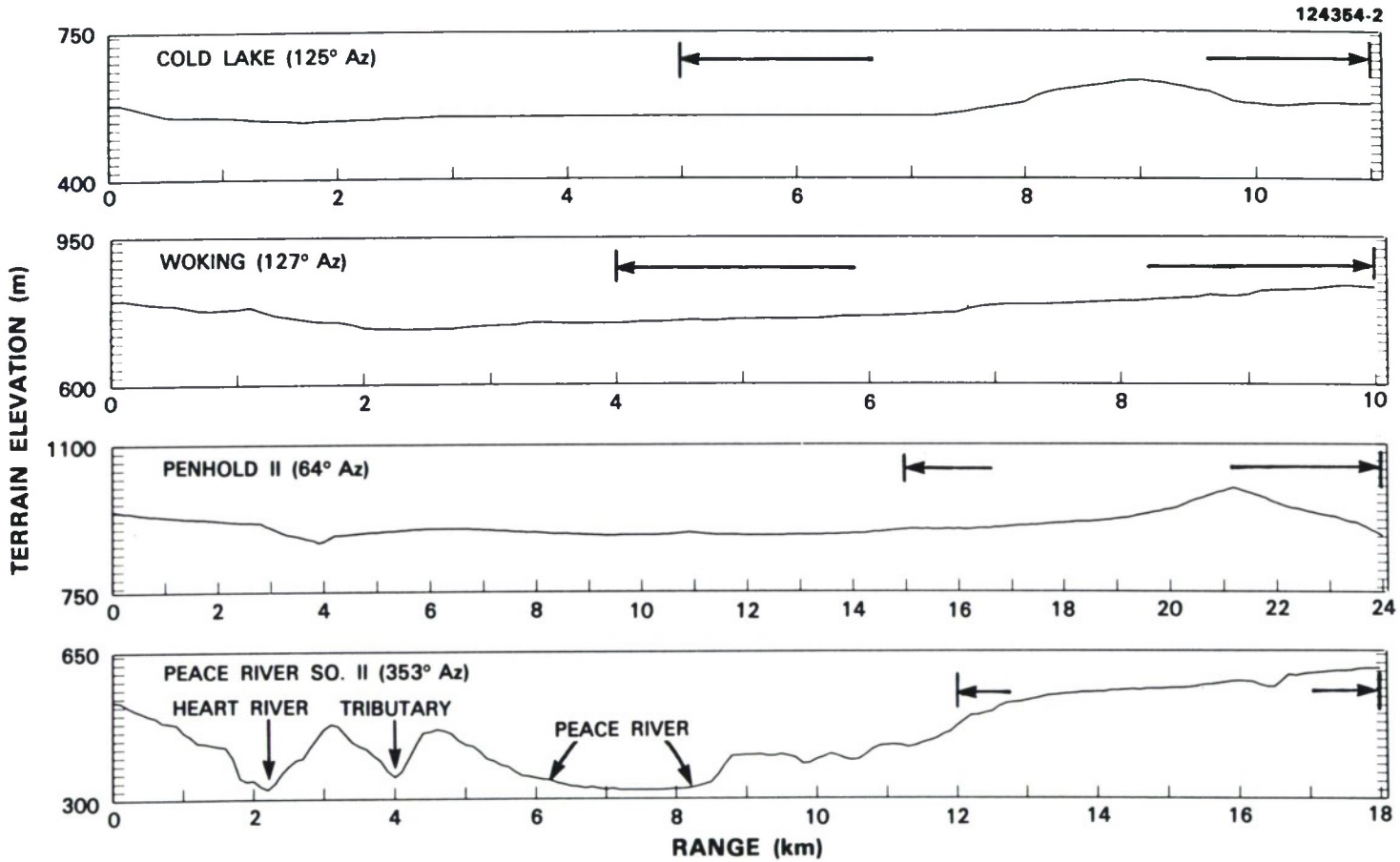

Figure 35. DTED terrain profiles at Cold Lake, Woking, Penhold II, and Peace River South II. Elevation in meters above mean sea level, 20 m between tick marks. Range extent of repeat sectors is indicated by horizontal arrows.

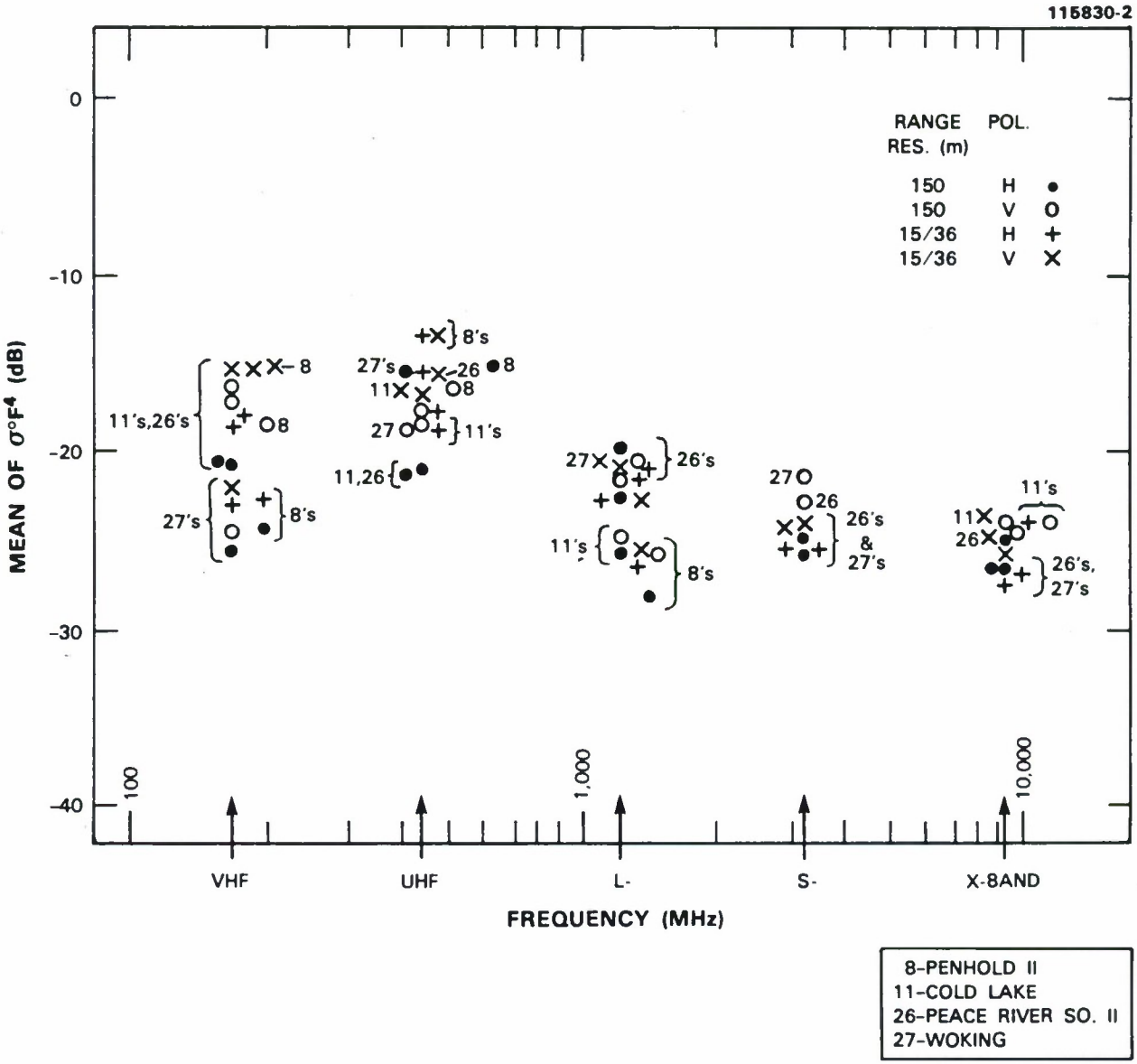

Figure 36. Mean clutter strength versus frequency for forest/high-relief terrain at low depression angle. See Table 7.

separate specific category in addition to forest and farmland. At Blue Knob, the intervening forested terrain is not supportive of multipath at the high depression angle involved, so the VHF mean clutter strength is high (see Figure E-39). At Penhold, we view gradually rising (i.e., secondary component of landform = 2, inclined) agricultural land with increasing range in the repeat sector across rolling parkland terrain potentially supportive of some VHF multipath and thus accounting for the drop in mean strengths at Penhold from UHF to VHF (see Figure E-57).*

Phase Zero. The Phase Zero X-band results are now discussed as they relate to the forest/high-relief/ low depression angle category. At Cold Lake and Peace River South II, the Phase One measurements were performed with six tower sections extended, which resulted in a substantially higher antenna mast height (99 ft) than Phase Zero (50 ft). A higher mast height results in slightly higher depression angles, which can result in higher clutter strength. At Cold Lake, the Phase One depression angle increased from the Phase Zero depression angle by 0.11 deg. This increase may contribute to the fact that the Phase Zero repeat sector mean strength at Cold Lake was -29.3 dB, which is 4.3 dB weaker than the Phase One X-band value (at 150-m range resolution, horizontal polarization) of -25.0 dB. At Peace River, the Phase One depression angle increased from Phase Zero by only 0.06 deg. Here, the Phase Zero repeat sector mean strength was -26.8 dB, or only 0.3 dB weaker than the Phase One X-band value (at 150-m range resolution, horizontal polarization) of -26.5 dB. At Woking, Phase One had three tower sections extended (59.1 ft), more nearly matching the Phase Zero mast height. The Phase Zero repeat sector mean strength at Woking was -24.5 dB, compared with the Phase One X-band value (at 150-m range resolution, horizontal polarization) of -26.3 dB. Across all 11 Phase Zero patches from seven sites containing high-relief forested terrain illuminated at low depression angles between 0 and 0.2 deg, the median value of mean clutter strength was -26.2 dB. This value is in close agreement with the Phase One X-band value assigned to this category (i.e., the median of data from three sites times four waveforms, see Table 11) of -25.0 dB.

Summary. In summary, these four sites involve four quite different terrain situations, yet as a group they exhibit the generally decreasing mean strength with increasing frequency characteristic, indicating domination by trees at substantial illumination angle (where here the substantial illumination angles arise from high-relief terrain slopes rather than high depression angles). Also, all four sites exhibit a reduction or at least leveling off of VHF mean strengths compared to UHF, usually explainable by greater or lesser amounts of multipath loss at the low depression angles involved over intervening low-relief terrain.

4.1.3.3 Forest/Low-Relief/High Depression Angle. Table 7 shows that we have two sites, Brazeau and Puskwaskau, that fall into the category of forest/low-relief/high depression angle. A photograph of the terrain at Puskwaskau is shown in Figure 3(a). A photograph of the terrain at Brazeau is shown in Figure 37. Terrain profiles of the repeat sectors at these two sites are shown in Figure 38. Both locations are fire tower sites situated in the boreal forest wilderness of northern Alberta. As such, both are located on prominent heights of land with good 360-deg visibility of low-relief forested wilderness terrain to far horizons (at both sites, we extended the Phase One antenna tower to six sections or ~100 ft). Therefore, we regard the repeat sectors at these two sites as unequivocably or canonically representative of general low-relief virgin forest illuminated from above and relatively uncontaminated by specific dominating

* The polarization differences in VHF mean clutter strengths in Figure E-57 (vertical polarization greater than horizontal polarization) corroborate the existence of VHF multipath at Penhold II (i.e., horizontal polarization reflection coefficients greater than vertical polarization).

terrain features and/or cultural features and/or propagation effects. Multifrequency mean clutter strengths measured over the repeat sectors at Brazeau and Puskwaskau are shown in Figure 39. Results from both seasonal visits to Brazeau are included in Figure 39, Brazeau (1), a winter visit, and Brazeau (2), a summer visit (numbers within parentheses following site name indicate visit number). Again, a general trend is observed of decreasing mean strength with increasing frequency in the data of Figure 39 due to increasing vegetative absorption of RF energy with increasing frequency. This trend extends monotonically from VHF to S-band and accounts for a decrease of 15.1 dB (see Table 11) over this range. As in Figure 32, a small reversal is observed in this trend such that mean strengths increase by 2.8 dB as frequency increases from S- to X-band. We shall compare these X-band data later in this section with some Phase Zero data.

Puskwaskau. First we discuss Puskwaskau. Within the repeat sector at Puskwaskau, the terrain gradually falls away (landform = 2, inclined) from the height of land upon which the radar is situated with increasing range over the repeat sector range from 1 to 6.9 km. The forest cover within the Puskwaskau repeat sector is largely deciduous aspen with some young spruce in the understory and occasional small clear patches of spruce [land cover = 43, mixed forest, see Figure 3(a)]. At the time the measurements were made (early autumn, see Table 1) there had been a recent snowfall, and the deciduous leaves were mostly off the trees. The X-band transmitter had failed five sites earlier at Plateau Mountain and was not repaired until Peace River South II, the site following Puskwaskau (see Table A-25), so there are no X-band results shown for Puskwaskau in Figure 39.

Brazeau. We now turn to Brazeau. We emphasized Brazeau in the measurements with two Phase One data collection visits to establish summer/winter seasonal variations in forest (setup numbers 17 and 24, see Table 1) and also with helicopter propagation measurements (indicated in Table A-1). The repeat sector at Brazeau is at longer range (i.e., from 4 to 9.9 km) than at Puskwaskau and is beyond the falloff from the local hilltop on which the radar is situated. Hence, the terrain within the repeat sector is undulating (landform = 3) rather than inclined. Within the repeat sector at Brazeau, the forest is of more composite nature or less homogeneous than at Puskwaskau, with more distinct separate patches of evergreen spruce and deciduous aspen, some openings of nonforested wetland and a small lake, and some 20-ft-wide cut lines cleared through the forest by the oil and gas industry (land cover = 42-62-41). A color infrared aerial photo of terrain in the center of the Brazeau repeat sector at relatively large scale (1:10,000) is shown in Figure 40. The second visit to Brazeau immediately preceded the Puskwaskau measurements, and hence, also falls within the above-mentioned set of five sites for which we have no X-band data.

Seasonal Variations at Brazeau. Repeat sector mean clutter strengths from both Brazeau visits are plotted separately from Puskwaskau in Figure 41 so that we may more easily focus on seasonal variations in these data. Seasonal variations in mean clutter strength at Brazeau as indicated in Figure 41 are small. During the first visit there, from 26 March to 13 April 1983, there was moderate to deep snow (6 in to 3 ft) on the ground, and some new snow fell during the visit. The site setup area required plowing of snow (1 to 1-1/2 ft) for access. There was some snow in the branches of the spruce. The deciduous aspen was not yet leaved out. During the second visit, from 25 August to 13 September, there was, of course, no snow; and the deciduous leaves were still mostly on the aspen, although beginning to fall. At first observation, the Brazeau seasonal variations in Figure 41 appear quite small, especially on the scale of variation that occurs with changing RF frequency. The tight clustering of data within groups by frequency band for measurements taken five months apart with independent setups seems remarkable and provides a positive indication of long-term calibration consistency (see also Tables A-11 through A-13). Closer examination reveals, however, that the second visit

Figure 37. Brazeau repeat sector. Looking south from site center.

mean strengths are generally 1 or 2 dB stronger than the first visit mean strengths (always true in the UHF and L-band data; true in the S-band data with one exception; not true at VHF, where first visit measurements are usually slightly stronger). Most of these small differences are less than our nominal calibration accuracy (2 dB rms), so we cannot unreservedly attribute them just to seasonal changes, as opposed to calibration variations in our equipment. General discussion of seasonal variation in the Phase One data is provided later in Section 7.2.

Polarization. There is little significant dependence of clutter mean strength on polarization evident in the forested results of Figures 39 and 41. For example, at 150-m range resolution and VHF, although mean strength at vertical polarization is 4.4 dB stronger than at horizontal polarization for the first Brazeau visit, the exact opposite is true at Puskwaskau where mean strength at horizontal polarization is 4.3 dB stronger than at vertical. And if, remaining at 150-m range resolution, we look to higher frequencies at Puskwaskau (see Figure E-67), we see, alternately, vertical stronger than horizontal by 3.1 dB at

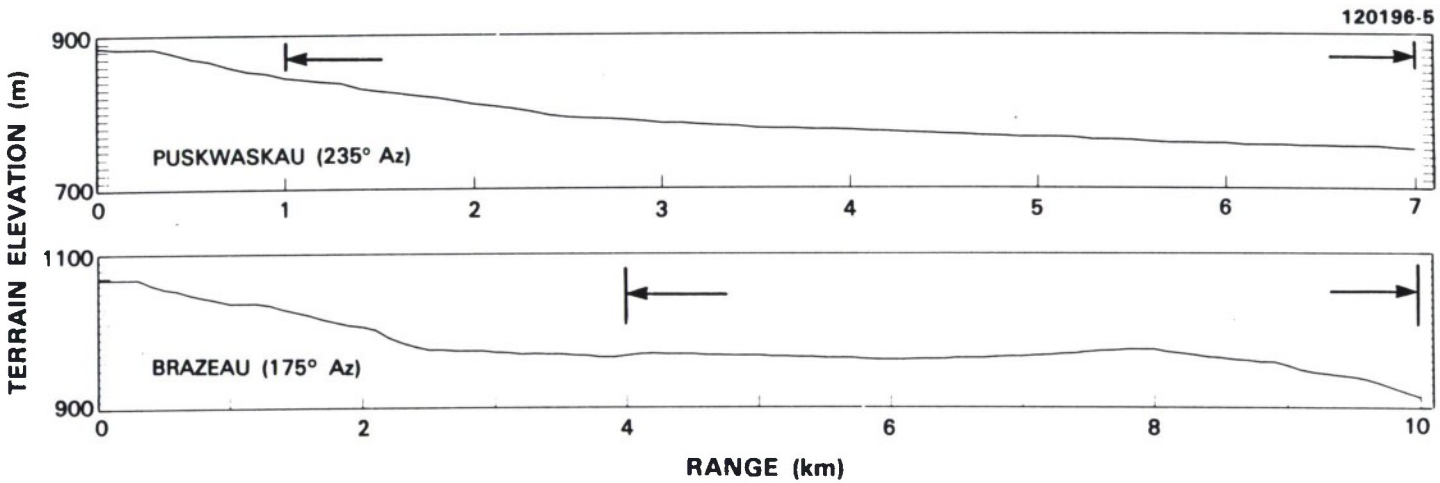

Figure 38. DTED terrain profiles at Puskwaskau and Brazeau. Elevation in meters above mean sea level, 10 m between tick marks. Range extent of repeat sectors is indicated by horizontal arrows.

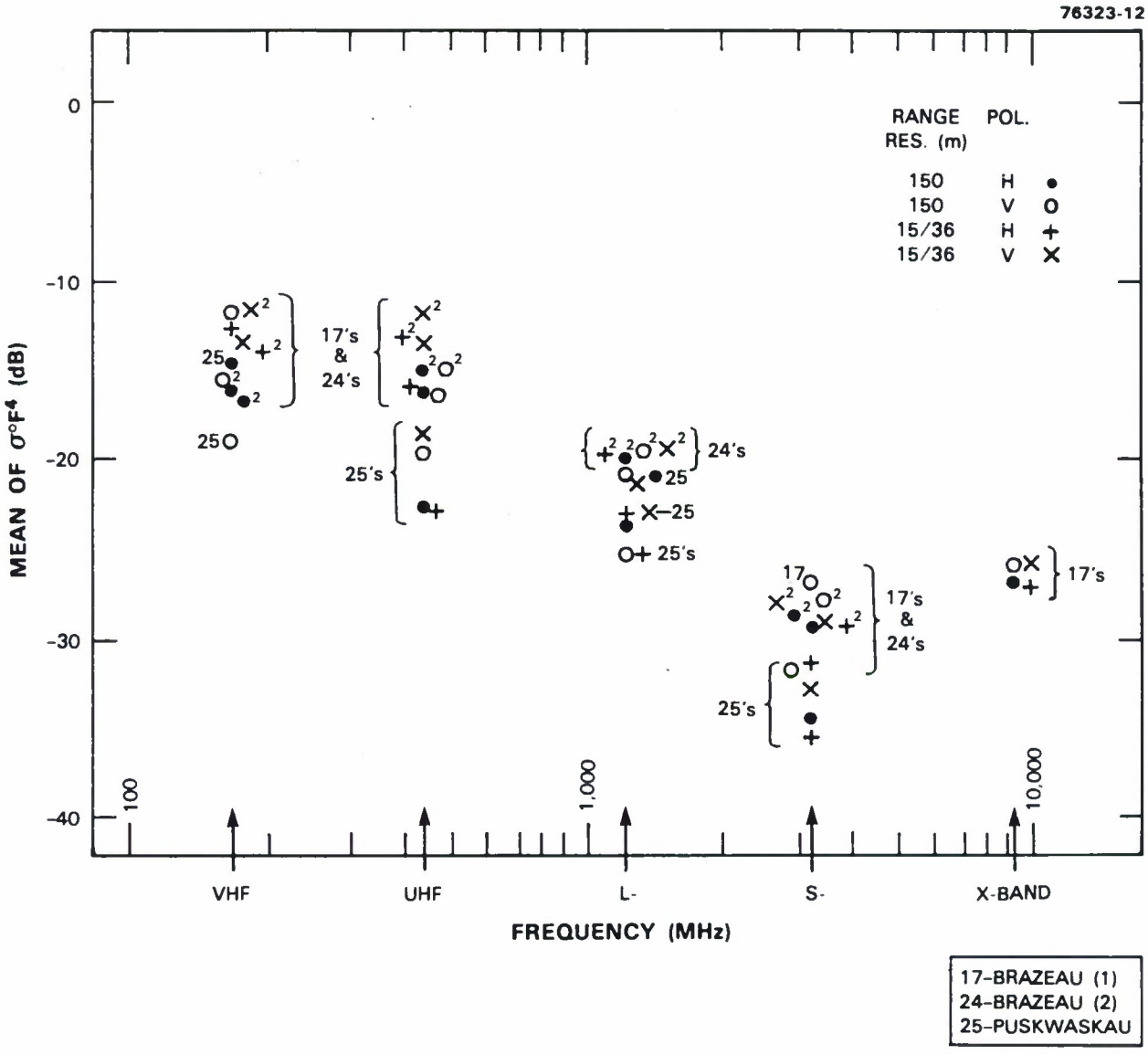

Figure 39. Mean clutter strength versus frequency for forest/low-relief terrain at high depression angle. See Table 7. There were two seasonal visits to Brazeau; the second visit results are indicated by superscript 2's to the upper right of the plot symbol.

Figure 40. CIR aerial photo of terrain in Brazeau repeat sector. Scale = 1:10,000. North is to the left.

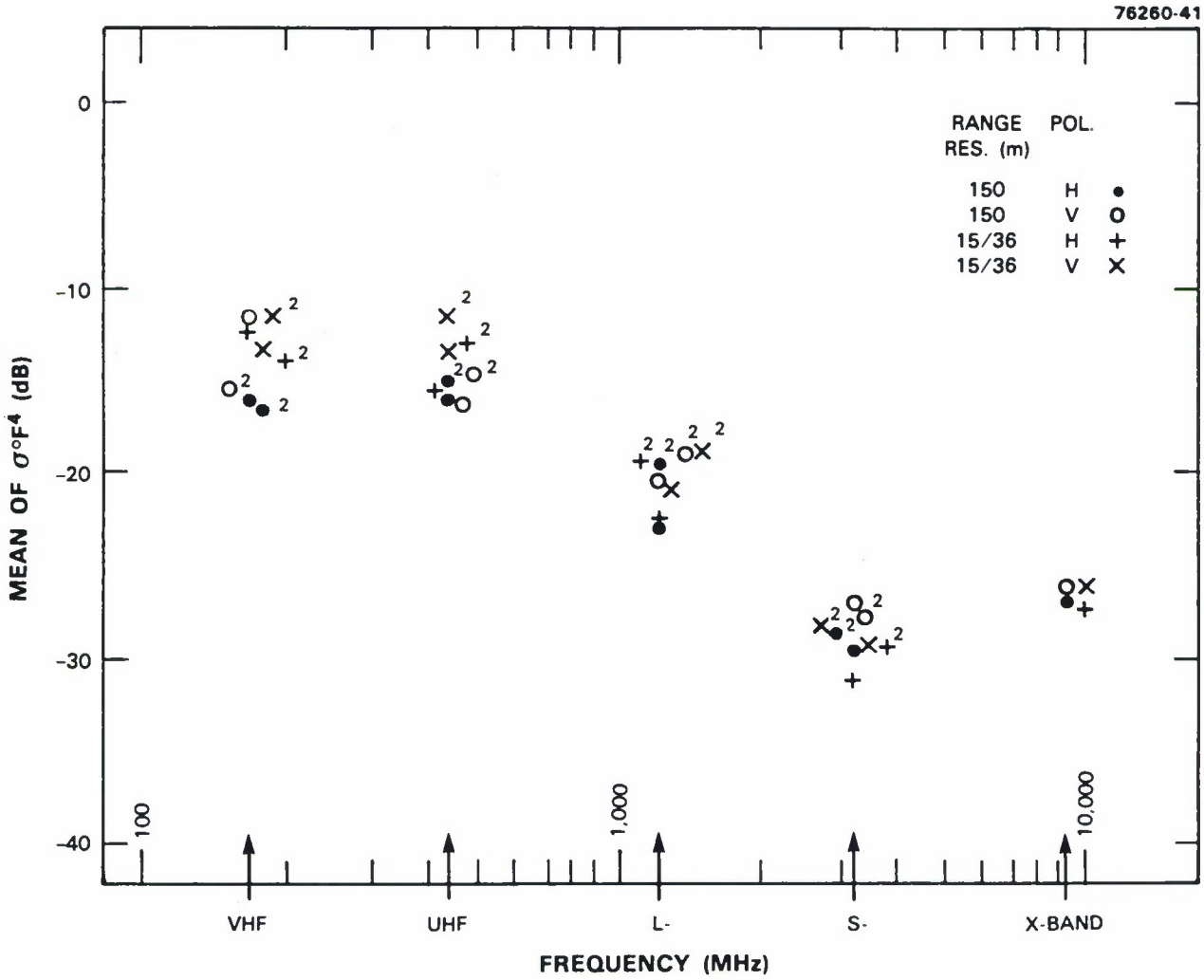

Figure 41. Seasonal variations in mean clutter strength at Brazeau. Repeat sector data. First visit, winter, 26 March to 13 April 1983. Second visit, summer, 25 August to 13 September 1983. Second visit results indicated with superscript 2's. X-band inoperable on second visit.

UHF, horizontal again stronger than vertical by 4.2 dB at L-band (like VHF), and vertical again stronger than horizontal by 2.6 dB at S-band (like UHF).

Phase Zero. Mean clutter strengths rise at Brazeau (1) from S- to X-band, as previously mentioned. These data are the only Phase One repeat sector data we have available for this terrain class of forest/ low-relief/high depression angle.* However, Phase Zero made measurements of 36 purely or homogeneously forested, low-relief terrain patches in the high depression angle regime between 1 and 2 deg like Brazeau and Puskwaskau, and the median value of mean clutter strength across all 36 measurements was -31.8 dB. This is significantly lower than the value of -26.5 dB given by the Phase One Brazeau repeat sector results. This lower Phase Zero value for this terrain class would continue the monotonic decrease of mean clutter strength with increasing frequency from S- to X-band. The Phase Zero measurement (with 50-ft antenna mast) of the Brazeau repeat sector provided a mean strength of -32.2 dB, close to its overall median in this terrain type of -31.8 dB (compare with the Phase One measurement of -26.9 dB, 150-m pulse, horizontal polarization, 100-ft mast).

4.1.3.4 Forest/Low-Relief/Intermediate Depression Angle. Table 7 indicates five sites that fall into the general category of forest/low-relief/intermediate depression angle. As a group, the repeat sectors of these sites are more representative of composite landscape in which forest predominates but in which the forest is broken by open areas of agricultural land or wetland or rangeland or areas of open water, as is indicated by the composite nature of the land cover classification in Table 7, rather than solid homogeneous forest such as Woking or Puskwaskau. This factor is illustrated by the photograph of Figure 42 that shows the partially open forested terrain in the Wainwright repeat sector. Terrain profiles for these forest/low-relief/intermediate depression angle sites are shown in Figure 43. Multifrequency mean clutter strengths measured over the repeat sectors at these five sites are shown in Figure 44.

The most striking thing about the data of Figure 44 is that, by and large, these measurements at intermediate depression angle in composite forest terrain no longer show a trend of decreasing mean strength with increasing frequency due to increasing vegetative absorption of RF energy that has been observed up until now at higher illumination angles (due to higher depression angles and/or higher terrain slopes) in forest terrain. Instead, the trend of mean strength with frequency in Figure 44 is beginning to be one of frequency independence. As defined by the medians of measurements by frequency band as displayed in Table 11, the characteristic of mean strength with frequency is within 0.6 dB of a constant value of -29.2 dB at three bands (UHF, L-, and X-band). About this constant value, the mean strength does rise by 3 dB at VHF to -26.2 dB (perhaps due to less vegetative absorption) and does drop by 2.9 dB at S-band to -32.1 dB. But within ±3 dB, the mean strength in this terrain category is constant at all five frequency bands.

This is the first time in this report that we have made this observation of frequency invariance of mean clutter strength in the Phase One measurements. In fact, this is a central observation that comes out of our measurement program. We shall see that not only in composite forest terrain at intermediate angles but also in composite or pure farmland terrain at intermediate angles, mean clutter strength is relatively

* In Appendix B, we reduce some Brazeau survey data. These data also show mean strength increasing from S- to X-band in forest terrain (see Table B-2). However, at -29.8 dB, the mean value at X-band of the survey data is weaker than the repeat sector data of Figure 39 and more in line with the Phase Zero results.

Figure 42. Partially open forested terrain at Wainwright. Looking SSE from weather station, visible just right of center, in repeat sector. Hummocky sand dunes partly covered by aspen forest. Some wetland and open water of a prairie slough beyond.

invariant with frequency at about the same gross level of about -30 dB (see Figures 60 and 98). This simple generality covers most terrain types as they occur most frequently for ground-based radar (as will be discussed in Section 4.3), and together with our two observed major exceptions to this rule, namely, that forest observed at high angles results in decreasing mean clutter strength with increasing frequency due to increasing vegetative absorption and that farmland observed at low angles results in increasing mean clutter strength with increasing frequency due to decreasing multipath propagation loss, constitute Phase One findings of major importance.

Why is there no longer a significant trend of decreasing mean clutter strength with increasing frequency in the results for the five composite forest sites at intermediate depression angle, as shown in

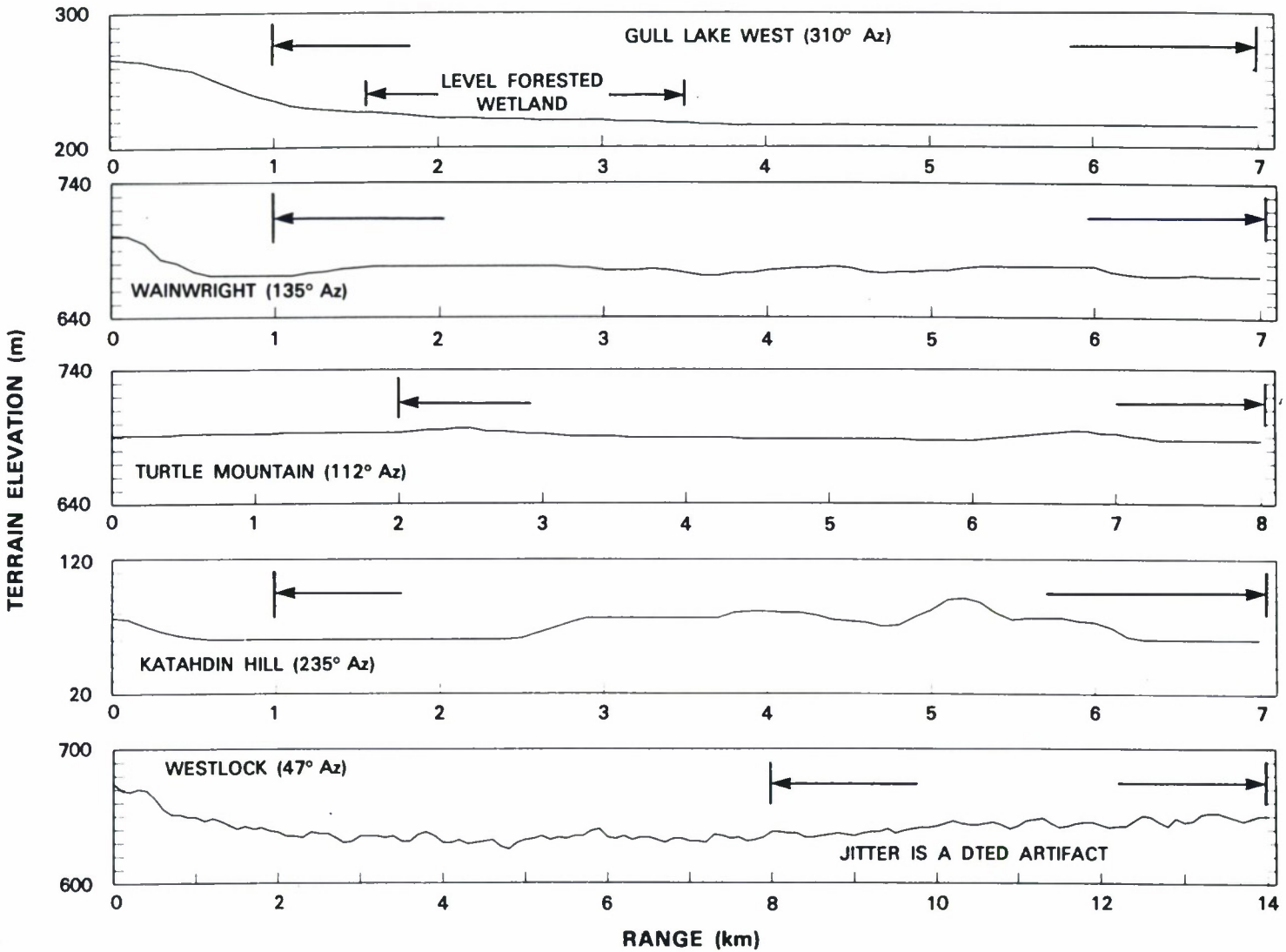

Figure 43. DTED terrain profiles at Gull Lake West, Wainwright, Turtle Mountain, Katahdin Hill, and Westlock. Elevation in meters above mean sea level, 10 m between tick marks. Range extent of repeat sectors is indicated by horizontal arrows.

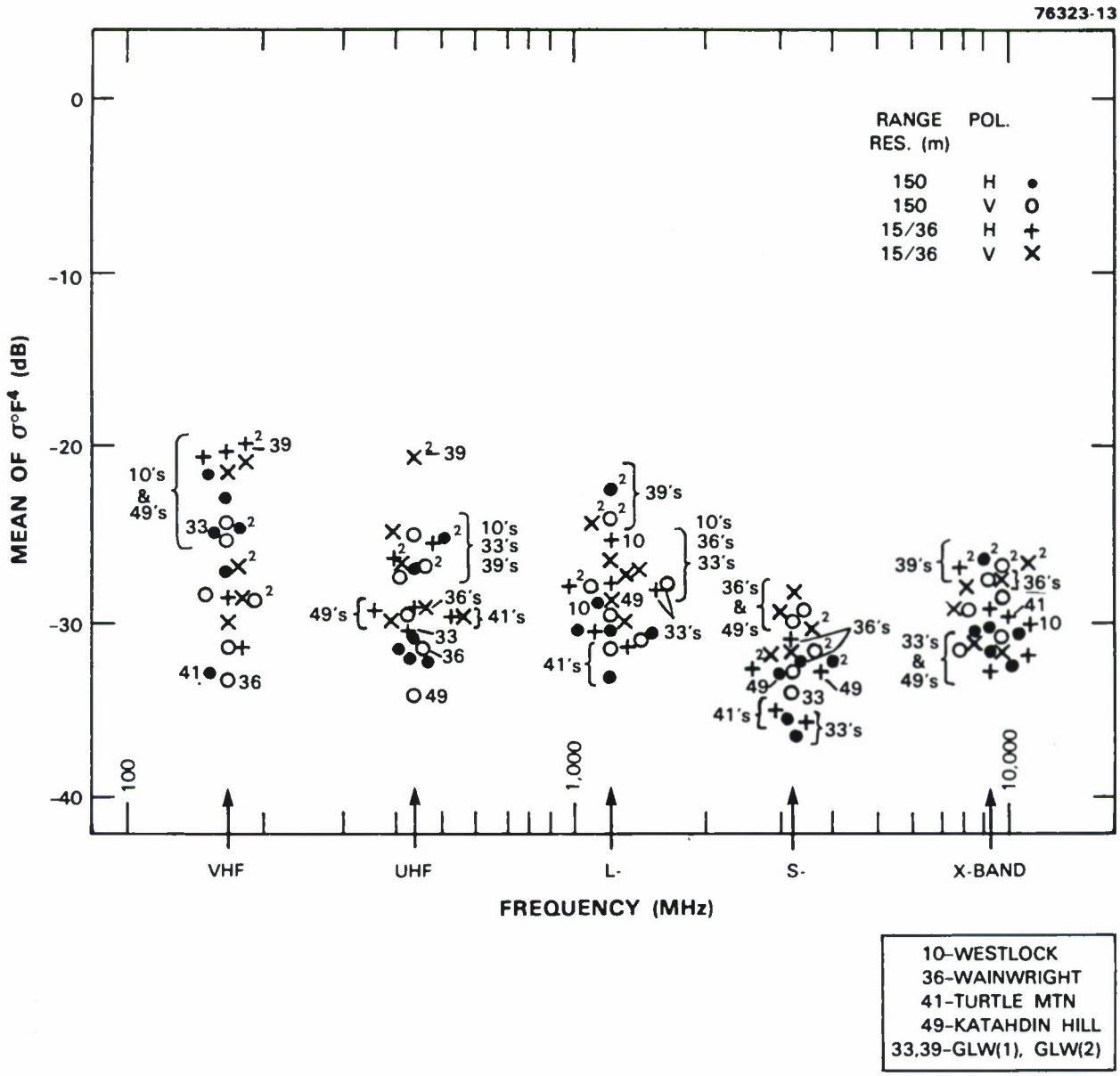

Figure 44. Mean clutter strength versus frequency for forest/low-relief terrain at intermediate depression angle. See Table 7.

Figure 44? We speculate that it is partly because, at the lower depression angles, the incident energy is less likely to penetrate the forest as a continuous absorbing medium but instead is more likely to be reflected back by individual high trees sticking up as scattering objects. This transition in type of phenomenon from a continuously illuminated surface at high angles to a sea of discrete scatterers at lower angles is aided by the discontinuous nature of the land cover at these five sites.

Although in gross terrain terms these five sites all provide composite forest terrain observed at intermediate depression angle in their repeat sectors, in fact all five sites are quite different from each other in physical detail, and their commonality was not immediately apparent until the descriptive studies converged to grossly similar summary data. The results at each of these sites will be discussed in turn. This discussion provides some appreciation for the diversity and complexity of landscape (i.e., every site is different), and as a result, the variability and scatter of clutter measurements, even within a common terrain category.

Gull Lake West. At Gull Lake West, Manitoba, we are looking out from a 100-ft-high ridge, initially onto very homogeneous level forested wetland (from 1.6 to 3.5 km), and then, beyond this forested wetland, onto a nonforested shallow, swampy, but basically open pond area (from 4.3 to 5 km), then to a distinct higher sand dune and beach area constituting the shoreline of Lake Winnipeg (between 5 and 6 km), and then to the open water of Lake Winnipeg itself. We opened the discussion of the Gull Lake West results in Section 2.2.2.1, and we refer back to Figures 4 through 9 in what follows. Phase One visited Gull Lake West twice to establish seasonal dependencies, from 15 to 25 February 1984 (winter) and from 2 to 12 May 1984 (spring). Second visit results are flagged with small superscript 2's in Figure 44 and in Figure 9. Data showing mean clutter strength versus range in five bands for both winter and spring visits are shown in Figure 7.

Several observations are made about these Gull Lake West data. The first observation concerns the lack of very much overall frequency dependence in the results, even when we restrict the area of observation to just the level forested wetland from 1 to 3.5 km in Figure 7, although we do observe some depression angle dependence in these data. Thus, in Figure 7, in the range interval from 3 to 3.5 km, winter season mean strengths from the level forested wetland are within a few decibels of -30 dB in all bands, except at L-band where they are closer to -26 dB. However, in the range interval from 2 to 2.5 km where the depression angle is higher, winter season mean strengths from the level forested wetland in all bands are higher, within a few decibels of -22.5 dB, except at S-band where they are closer to -28 dB. That is, although containing an expected variation with depression angle, these level forested wetland range gates at Gull Lake West do not show a trend of decreasing strength with increasing frequency due to increasing vegetative absorption that we saw in low-relief forest at Puskwaskau and Brazeau. Note that these sector display data of Figure 7 are corrected range gate by range gate for gain variation on the elevation antenna beam (see Appendix E, Section E.3). Evidently, the lack of very much overall frequency dependence in the repeat sector mean strengths of Figure 9 is not just due to the existence of transition zones between forest, open water, and sand dune regions in the nonhomogeneous Gull Lake West repeat sector but largely exists within these homogeneous subregions as well.

Seasonal Variations at Gull Lake West. The second Gull Lake West observation concerns seasonal variations. There are more large point-by-point seasonal variations in the Gull Lake West data of Figure 9 than in the Brazeau data of Figure 41, with the results from the spring visit usually stronger. We further

observe in Figure 9 that, in the available two season data at VHF, there are essentially no seasonal variations; at UHF, two second visit results are 5 and 6 dB stronger than first visit results; at L-band, a second visit result is 8.07 dB stronger than first visit* with other second visit results 2 or 3 dB stronger than first; at S-band, all second visit results are stronger than first, with the biggest difference equal to 4 dB; and at X-band, an unusually good clustering of the four different waveform results within groups by site visit, and good separation between these two groups yields a relatively clear-cut general result at X-band that the second visit mean clutter strengths are stronger than the first by 5 dB or so.

Why are the second visit (spring) mean strengths often significantly stronger than the first visit (winter) mean strengths at Gull Lake from UHF to X-band? We do not know. Certainly, during the first visit conditions were very wintry, with deep snow cover, deciduous leaves and needles off,† frozen snow-covered marshlands, and lake ice piled high along the Lake Winnipeg shoreline. And during the second visit, conditions were very springlike, with the snow and ice gone, and the deciduous foliage beginning to emerge. However, we do make the general comment: What appear to be large seasonal variations just on the basis of differences in mean strength over the whole repeat sector in Figure 9 appear to have much less significance when measured against the scale of variation in Figure 7. In fact, the overall impression of the data in Figure 7 is of quite good seasonal repeatability, in that the general profiles of mean clutter strength versus range repeat quite well, with only what appear to be largely second-order seasonal effects. This impression raises the general point that one should not too simplistically interpret variations of mean clutter strength with season over large spatial regions. Because mean clutter strength shifts with season does not usually mean that a constant return from a whole region of homogeneous land cover shifts uniformly by that amount simply due to the presence or absence of snow. For example, the 6.2-dB seasonal difference in the 36-m range resolution, vertical polarization UHF results in Figure 9 is observed in Figure 7 (second profile from top) to be largely caused by greater than 10-dB differences in the 4 or 5 range gates around 1.4 km because over the rest of the profile the seasonal differences are more on the order of 2 or 3 dB. We do not know what change in clutter and/or propagation conditions caused such large seasonal differences in these gates. As another example, the 4.7-dB seasonal difference in the 15-m range resolution, vertical polarization X-band results in Figure 9 is observed in Figure 7 (bottom profile) to be strongly contributed to by 20-dB differences in the region around 6.25 km. There is no terrain beyond 6 km in the repeat sector at Gull Lake West; that is, beyond 6 km, we are past the beach and onto Lake Winnipeg proper. We may only speculate as to why the spring visit returns‡ are so much stronger

---

* At 150-m pulse length, horizontal polarization. This 8.07-dB difference is the largest seasonal difference in mean strength in our repeat sector data base.

† The primary component in the forested wetland was tamarack, a deciduous evergreen.

‡ The spring visit shows lake clutter from waves in these range gates (see Figure 5). The returns in these gates do drop quickly, X- to S- to L-band in the spring visit results in Figure 7, as would be expected of lake clutter. The fact that VHF and UHF returns are stronger in this region may be due to ground clutter in the sidelobes of the wider azimuth antenna patterns in these bands.

than the winter visit returns* at X-band in these range gates on Lake Winnipeg. These examples point out that processes of natural seasonal change on landscape are complex and variable, cell to cell over large spatial regions. The main purpose here is not to resolve differences in every cell, but to answer the first-order question of what may be expected in terms of general change in mean strength with season over large spatial regions. We answer this question statistically in Section 7.2 by combining all of the measured seasonal differences in repeat sector mean strengths in a histogram. From this current discussion we would expect that seasonal differences in individual resolution cells (rather than in complete repeat sectors) would be much greater.

S-Band Dip at Gull Lake West. Our final Gull Lake West observation concerns the pronounced S-band dip in Figure 9 between L- and X-band. If it were not for this dip, the data as a whole in Figure 9 are relatively frequency independent, with just a slight trend of decreasing mean strength with increasing frequency of about 3 dB from VHF to X-band (based on the medians of the groups of measurements in each frequency band). However, the S-band measurements (still based on the median) dip about 4.5 dB below the trend. This is not the first time that we have seen an S-band dip in mean clutter strength frequency characteristics (e.g., Scranton, Blue Knob, and Brazeau). Does S-band slightly minimize ground clutter for some terrain types? We think the answer is yes. Or could the S-band measurements, in showing such a dip, have a small calibration error? We think the answer is no. However, one caveat concerning S-band calibration is that our second visit to Gull Lake falls within a set of eight sites beginning with Corinne (see Table A-25) in which all S-band clutter measurements were augmented by 4 dB, based on the external calibration tests. This problem was caused by a broken cable shield, which remained undetected for a while.† Even with this adjustment, second visit S-band results show a dip, but one may wonder if the adjustment was enough. Without this adjustment, second visit S-band results would match first visit S-band results more closely at Gull Lake, but the S-band dip would be more pronounced. Note that external calibration tests were not performed for the first visit to Gull Lake West (see Table A-1), nor did we find a useful daily reference target there during the first visit. One may wonder if S-band was mistakenly calibrated a bit low and undetected at the first visit to Gull Lake West. However, we have no concrete reason to think so. We present these considerations here to indicate what was involved in trying to maintain precision calibration of five truck-borne radars over three years. We shall discuss such matters more as this report proceeds.

---

* In the winter visit, are returns low between 6 and 6.5 km due to relatively smooth ice in this region? Then, is an ice ridge at the edge of open water at 6.75 km causing the spikes of increased clutter strength in this region?

† The broken cable shield caused higher than normal VSWRs, which were properly included in our calibration even before we found their cause. Even with increased VSWR thus accounted for, external calibration tests showed 4-dB additional loss due to the broken cable shield, which we incorporated in the S-band calibration constant at these sites.

Katahdin Hill. The next site to be discussed in the category of forest/low-relief/intermediate depression angle is Katahdin Hill, Massachusetts. Katahdin Hill is our own site at Lincoln Laboratory, just above the parking lot in front of the main entrance to Lincoln Laboratory. A photograph of the Phase One equipment at Katahdin Hill and the nearby hilly forested terrain typical of eastern Massachusetts is shown in Figure 45. We have a large data base of measurements of the Katahdin Hill repeat sector, acquired on a once-a-week basis from November 1984 to August 1985, during which time Phase One was set up on Katahdin Hill following its return from its major site tour through the west (see Section A.1). A report is available summarizing temporal and spectral characteristics at L-band (and X-band to a lesser degree) of some particular wooded cells in this sector based on this long sequence of weekly measurements [1]. However, we have not yet examined this set of weekly measurements in terms of mean strengths over the complete sector. Thus, the Katahdin Hill repeat sector results of this report are based only on the data acquired there as the last site in the Phase One measurement tour from 25 September to 19 October 1984. During this time, measurement procedures at Katahdin Hill were the same as at any of the other Phase One measurement sites.*

The hilly wooded terrain in the repeat sector at Katahdin Hill contains a dozen or so significant hills, typically separated by 1 km or so, with the hilltops typically 100 to 150 ft higher than the low areas between them. This terrain is classified as primarily hummocky (landform = 5), which is the highest relief category that we include as low-relief (see Table 4). The first kilometer or so of this repeat sector is level, some of which is used as farmland. Most of the repeat sector is relatively intensely settled and is criss-crossed with roads and highways and a rail line. The suburban town of Lincoln occurs within the repeat sector. However, many of these cultural features are hidden from view to Phase One beneath the trees that substantially cover much of the sector. These trees are typical of the eastern forest, being largely a mixed deciduous forest with occasional evergreen stands (e.g., hemlock). A large pond, Sandy Pond, about 1 km in extent, lies within the sector. Many of the hilltops in the sector have cultural features, such as water towers or radio masts that are visible to Phase One.

Measured multifrequency clutter mean strengths for the Katahdin Hill repeat sector are shown in Figure E-85. From UHF to X-band, this characteristic is largely frequency invariant at about the -30.5-dB level. However, clutter strengths at VHF abruptly rise 8 dB or so above this constant level to about the -22.5-dB level. This significantly stronger VHF clutter compared with the higher bands at Katahdin Hill may be due to decreased vegetative absorption of RF energy and hence increased diffuse reradiation at VHF on some of the steeper hillsides in the sector when compared to the higher bands. Note that we do have a high-relief secondary component for landform in this repeat sector (i.e., landform = 4, rolling, see Table 4). In any event, the idea of frequency independence in mean clutter strength at about -30 dB for

---

* We mention that at Katahdin Hill (1), the first site in the Phase One measurement tour, our data collection procedures were not yet finalized. As a result we did not establish a repeat sector, although several small patches were repeatedly measured. Thus, although nominally we have seven repeated site visits, only six are utilized in this report (see Table D-1).

Figure 45. Hilly forested terrain at Katahdin Hill. Camera viewing direction is NW across Hanscom Field. Phase One antenna tower erected to 100 ft visible at right.

this terrain class seems markedly reasonable in light of the Katahdin Hill UHF to X-band results but markedly unreasonable in light of the Katahdin Hill VHF results. This contradiction may reflect the mixture of low-relief/high-relief landform in the sector (i.e., LF = 5-4, see Table 7).

Turtle Mountain. The third site in the category of forest/low-relief/intermediate depression angle is Turtle Mountain, Manitoba. Turtle Mountain is an unusual site, near the Manitoba/North Dakota border, where we were up on a large forested glacial deposit, 20 or 30 km across, and which is several hundred feet above the surrounding prairie. On top of this large glacial deposit, the terrain is hummocky knob-and-kettle topography, of approximately 50-ft relief about a relatively unvarying mean level. The area is covered with many small lakes in the depressional areas. Aside from the lakes, the land cover is a mixed deciduous forest of aspen, poplar, birch, and some burr oak, with very occasional stands of

Figure 46. Hummocky forest at Turtle Mountain. View along access road beside Phase One setup area showing hummocky topography. Phase One antenna tower visible above trees in center of photo.

spruce. A photograph of the hummocky forested Turtle Mountain terrain is shown in Figure 46. The Turtle Mountain DTED data of Figure 43 do not capture the hummocky nature of this terrain very accurately. Phase One used six antenna tower sections at Turtle Mountain, but the site area proper had little inherent terrain elevation advantage and was just a clearing in the 50- to 60-ft trees, resulting in about 40 ft of antenna height above the trees. The repeat sector, from 2 to 7.9 km to the southeast, lay entirely within this knob-and-kettle forested terrain containing many small lakes, with its farthest range gates barely within the area atop the plateau given over to the International Peace Garden that straddles the international boundary there.

Multifrequency mean clutter strengths for the Turtle Mountain repeat sector are shown in Figure E-82. As with the Katahdin Hill data, once again we see a strong confirmation of the idea of frequency

independence for this terrain category, at about the -30-dB level (actually, at about -31 dB in these Turtle Mountain data), with no exception at VHF. Turtle Mountain is among the eight sites following Corinne in which S-band results were augmented by 4 dB to compensate for a power loss due to a faulty cable shield, as determined from results of external calibration tests at these sites (see Gull Lake discussion earlier in this section). One may wonder if slightly more than 4 dB might have been required as a result of this problem at Turtle Mountain in order to raise the S-band data in Figure E-82 more into line with the data at other frequencies. In all of these Turtle Mountain results in Figure E-82, the vertical polarization result is always a decibel or so stronger than the corresponding horizontal polarization result.

Wainwright. The fourth site in the five forested/low-relief/intermediate depression angle group of sites is Wainwright, Alberta. The Wainwright site is located within Camp Wainwright, a Canadian Forces Base in Alberta, near the Saskatchewan border. At Wainwright, we were located on a small hill (Hart Hill) about 100 ft higher than general elevations of the hummocky terrain in the repeat sector farther out to the southeast at ranges from 1 to 6.9 km. At Wainwright, we only extended one antenna tower section because our ground anchors had become loose, but the repeat sector visibility was not affected (i.e., no close-in mask). The terrain in the wasteland prairie Wainwright repeat sector is largely tree and/or shrub covered. At Wainwright, however, we are still at latitudes of prairie rangeland, not in the dense boreal forest wilderness farther north. Nevertheless, within the repeat sector at Wainwright, 54 percent of the area is covered with deciduous aspen trees (typically, to 45- or 50-ft heights) and 32 percent of the area is covered with shrubby or scrubby mixed rangeland (e.g., willow, typically to 15-ft heights). These trees and scrub growth generally occur in patches or groves with openings between them of herbaceous or grassy rangeland (7 percent of the area). Other openings include nonforested wetland (6 percent of the area) and a few small lakes, including Hart Lake (0.6 percent of the area). Thus, rather than continuous forest at Wainwright, we have patches of trees on a hummocky prairie landscape. A photograph of the Wainwright repeat sector terrain is shown in Figure 42.

Multifrequency mean clutter strengths for Wainwright are shown in Figure E-78. As with Turtle Mountain, in these Wainwright data we see strong confirmation of the idea of frequency independence at a level of about -30 dB for this terrain category (the median level through these Wainwright results is at -29.9 dB). If, in clutter modeling, we average results across nominally similar sites to reach generality (as we do here), we must be careful to avoid situations where no single site is like the average. These Wainwright results in Figure E-78 and the previous Turtle Mountain results in Figure E-82 clearly show that single sites can provide mean clutter strengths that are in large measure invariant with RF frequency, VHF to X-band, at or about the -30-dB level. At Wainwright, horizontally polarized mean strengths are stronger than vertical at VHF but weaker than vertical at S- and X-bands (with little difference with polarization existing at UHF and L-band).

Westlock. The final site in the terrain category of forest/low-relief/intermediate depression angle is Westlock, Alberta. At Westlock, about 45 mi north of Edmonton, we are farther north in Alberta than at Wainwright and are on the northern edge of the prairie farmland and in a transitional zone between the prairie and the northern boreal forest wilderness. The Westlock site was located on a local height of ground on undulating prairie farmland. The Phase One antenna tower was fully extended (i.e., six tower sections, nominally 100 ft, see Table A-5). Looking out into the repeat sector to the northeast, over the

first 8 km the undulating prairie farmland (with scattered groves of aspen) gradually declines in elevation by 175 ft (i.e., approximately 0.25-deg average terrain slope), then on the average levels out (although the terrain is still locally undulating) in a lowland area. The terrain then gradually transitions to forest with scattered open areas of nonforested wetland at 8- to 12-km range and gradually begins to rise (still locally undulating) by about 50 ft from 12- to 14-km range with some of this rising land again being under agriculture. At a much larger scale, this forested area, which begins at 8 km in the repeat sector, is not just local woods on the prairie but the beginning of the northern forest. The local variations (i.e., jitter) in the Westlock DTED data of Figure 43 are a DTED artifact and do not represent the nature of the actual terrain.

We selected the prairie-to-forest transitional region of the Westlock repeat sector at ranges from 8 to 13.9 km as the repeat sector clutter patch. Within this area, the land cover is 59 percent mixed forest, 25 percent agricultural land (partly cropland, partly pasture), and 14 percent nonforested wetland. In addition, 1 percent of the land cover in the repeat sector is shrubby rangeland, and 1 percent is built-up due to roads, power and telephone lines, and farm buildings. At the time we were at Westlock (15 to 25 November 1982), temperatures varied from +10°F to -13°F, most of the local ground area was covered by a 6-in layer of old powdered snow on fields that were either bare (i.e., plowed) or stubble-filled, and deciduous leaves were off the trees.

Westlock is one of a group of 11 sites (setup numbers 6 to 16, see Table A-25) where a major S-band hardware problem involving both a faulty RF limiter and a faulty circulator in the S-band receiver occurred. Although the S-band calibration data showed significant errors, it took some time to identify and fix the faults, and it was decided not to compromise the Phase One schedule for the sake of S-band. As a result, no S-band data are available for Westlock. Also at Westlock, the X-band transmitter required repairs, but a full set of X-band data was collected. As at most sites, VHF data were acquired during the small hours of the night to minimize VHF interference.

Four-frequency results of measured mean clutter strength for the repeat sector patch at Westlock are shown in Figure E-89. Unlike any of the other sites in this group (except possibly Gull Lake West), a clear-cut trend of gradually decreasing mean strength with increasing frequency is seen, in which clutter strengths drop by about 3 dB from VHF to UHF, by about 2 dB from UHF to L-band, and again by about 2 dB from L- to X-band, summing up to about 7 dB from -23 dB at VHF to -30 dB at X-band (averaged over the different waveforms). A constant level of -30 dB, which we have raised as a possibility for this general terrain class, does not work very well in modeling these Westlock data.

Why does Westlock alone, among the sites in this forest/low-relief/intermediate depression angle category, show this typical characteristic of decreasing mean strength with increasing frequency that is usually associated with vegetative absorption at higher angles of illumination in forest? Why, for example, are the Westlock repeat sector results so different from Wainwright? Both sites have low depression angles,* low terrain slopes, and patchy tree cover with openings. We do not know the answer. Still, this trend at Westlock only covers 7 dB, VHF to X-band, compared to 15 dB and more in the higher depression angle regime (viz., 1 to 2 deg) at Puskwaskau and Brazeau.

* In fact, of these two similar sites, Wainwright has the higher depression angle; on this basis, it should be Wainwright, not Westlock, with decreasing mean strength with increasing frequency.

4.1.3.5 Forest/Low-Relief/Low Depression Angle. Table 7 indicates that there are two sites, Sandridge and Dundurn, both on the central Canadian prairies, that fall into the terrain category of forest/ low-relief/low depression angle. In general terms, these two sites have a very constant mean elevation (i.e., no long rolls or undulations in the terrain at either site), with a sparse, stunted tree, or scrub brush vegetation cover. At Sandridge, the terrain is very level over many square miles around the site and covered with a sparse stunted deciduous forest. A photograph of the Sandridge terrain is shown in Figure 47. At Dundurn, the terrain is of a pebbly texture, where many small hillocks rise 25 or 35 ft above a very level substrate. This hummocky terrain has a vegetation cover consisting of patches of deciduous aspen trees, other patches of shrub and brush, with some open areas of native grassland between the patches of trees and brush. A photograph of the Dundurn terrain is shown in Figure 48. Therefore, at both of these sites, Phase One looks out from a setup area with no local terrain elevation advantage into repeat sectors of constant mean elevation containing scrubby vegetation. At both sites, the repeat sectors extend from 1 to 6.9 km in range. Also, at both sites, Phase One used three antenna tower sections to provide a mast height of about 60 ft (see Table A-5). Repeat sector terrain profiles for these sites are shown in Figure 49. These DTED data do not capture the 10-m Dundurn hummocks accurately (see description in this section).

Multifrequency mean clutter strengths measured over the repeat sectors at Sandridge and Dundurn are shown in Figure 50. Sector displays showing mean clutter strength versus range for the Sandridge and Dundurn repeat sectors are shown in Figures 51 and 52, respectively. In contrast to other forested sites, which at high illumination angles (due to high terrain slopes and/or high depression angles) showed a strong trend of decreasing mean clutter strength with increasing frequency and which at intermediate illumination angles showed either very slightly decreasing or no variation of mean clutter strength with increasing frequency, we now see in the results of Figure 50 — and for the first time in forest terrain — a moderate but significant trend of increasing mean clutter strength with increasing frequency. In terms of the median positions of the set of measurements of different waveforms in each band (see Table 11), mean clutter strength rises monotonically in this terrain category from -43.6 dB at VHF to -35.4 dB at X-band, an increase of 8.2 dB. This variation may be largely due to multipath propagation loss, possibly caused by ground reflections from the level open terrain around the Phase One setup areas at these two sites.

Sandridge. We now consider these two sites in more detail. At Sandridge, Manitoba, the terrain is very level. For example, on a 1:50,000 scale topographic map with 25-ft contour intervals, only three or four contour lines meander through the Sandridge repeat sector, all at 900-ft elevation [above mean sea level (MSL)]. The site is north of the black earth agricultural belt (where our Altona II and Headingley sites are located) but still south of the northern forests in a region of relatively poor soils (the interlake region between Lake Winnipeg and Lake Manitoba). These soils support sparse stunted trees in a deciduous forest of scrub aspen and burr oak, usually rising only 30 or 35 ft, which occur in large clones or patches, with occasional openings among them of nonforested wetland and pastureland.

Multifrequency mean clutter strengths for Sandridge are shown in Figure E-93. From UHF to X-band we see only a very slight indication of increasing clutter strength with increasing frequency (e.g., for 150-m range resolution, horizontal polarization, mean clutter strengths are: -38.66 dB at UHF, -37.74 dB at L-band, -37.28 dB at S-band, and -37.64 dB at X-band). Modeling these results as constant and independent of frequency over this range would perhaps be more appropriate than gradually increas-

ing clutter strength with frequency. Note that the constant value of around -37 dB is substantially less than the constant level of -30 dB discussed in conjunction with the forest/low-relief/intermediate depression angle terrain category in the previous section. This weaker clutter may be due to lower angles of illumination (i.e., slightly lower depression angle, zero terrain slopes). At VHF, however, the mean strengths of the Sandridge repeat sector in Figure E-93 are observed to drop abruptly to a level of about -45 dB, or 8 dB weaker than the otherwise approximately constant level of -37 dB. This decrease in VHF clutter strength at Sandridge may have been caused by multipath propagation loss resulting from terrain reflections, possibly from the somewhat more open terrain extending for several hundred feet around the setup area, or, less likely, from openings within, or even through, the sparse stunted forest farther out. However, the sector displays of Figure 51 do not show a trend of decreasing clutter strength with increasing range at VHF that would be expected from multipath; although, contradictorily, such a trend is evident at UHF, L-band (particularly so), and S-band. At Sandridge, the Phase One equipment was set up just to the west off a north-south paved secondary road through the stunted forest. Although generally the vegetation came within 50 ft or so of the road, near the setup area the terrain remained fairly open back several hundred feet or so from the road, perhaps due to sandy soil conditions. Such openings were not uncommon in the area, although on a percent-area basis most of the terrain was tree covered. The Sandridge measurements were performed from 12 to 21 May 1984, at which time the deciduous foliage was beginning to emerge.

Dundurn. Although belonging to the same general terrain class, Dundurn is different in detailed terrain characteristics from Sandridge. Camp Dundurn is a Canadian Forces Base on the central Saskatchewan prairie just south of Saskatoon. The repeat sector at Dundurn is within a wasteland hummocky sand dune area used for training, with hummocks approximately 25 to 35 ft high distributed randomly over a very level underlying mean surface. For example, on a 1:50,000 scale topographic map with 25-ft contour intervals, the Dundurn repeat sector is covered with many tiny closed contours, all at either 1700 or 1725 ft elevation (above MSL), and typically of 100- or 200-m extent, and several hundred meter separation. The hummocks are vegetated with aspen groves and patches of shrub and brush cover (e.g., chokecherry). Thus, what is visible to Phase One in the repeat sector at Dundurn are the usually vegetated tops of many hummocks, typically separated by several hundred meters, with the low areas between the hummocks shadowed. Dundurn was measured from 3 to 13 April 1984, three sites before Sandridge, before the deciduous foliage was out. Multifrequency mean clutter strengths for the Dundurn repeat sector are shown in Figure E-97. In each band, the group of measurements at the different waveforms clusters remarkably tightly in these Dundurn data. Overall, Figure E-97 portrays quite a different characteristic of clutter strength versus frequency than that of Sandridge (Figure E-93), except for the unusually good coincidence of results at VHF and X-band for the two sites. Rather than first rising, VHF to UHF, and then staying relatively constant, UHF to X-band, as did mean clutter strengths at Sandridge, at Dundurn mean clutter strengths first drop sharply, from about -42 dB at VHF to about -48 dB at UHF, and then rise in a strong monotonic manner from about -48 dB at UHF to about -36 dB at X-band. The UHF to X-band part of this characteristic is typical of what occurs in a multipath situation where large multipath propagation loss occurs at low frequency, with the loss decreasing with increasing frequency. This assumption of multipath propagation conditions is borne out in the sector displays of Figure 52, which show strong trends of decreasing clutter strength with increasing range, particularly in the lower bands.

The Phase One setup area at Dundurn was in the southeast corner of the camp airfield. Although no longer used, the airfield area was still maintained as a level grassy cleared area bounded by service

Figure 47. Level scrub forest at Sandridge. Phase One tower-top view looking SSE.

roads just outside the built-up area of the camp. Looking northwest into the repeat sector from the Phase One setup position, the terrain in the first 0.5 km, although off the airfield proper but adjacent to it, was relatively level and open and quite imaginable as supportive of multipath, before the onset of hummocky sand dunes and patches of aspen that are definitely in existence at 1-km range and beyond and probably not very supportive of multipath. Because the suggestion of multipath is strong in both Figures 50 and 52, why is mean clutter strength at VHF stronger than at UHF? In fact, the relatively strong VHF mean clutter strength in the Dundurn repeat sector was caused by a few particularly strong clutter cells of strength between -30 and -35 dB in the first six range gates in the sector between 1.0 and 1.2 km (see Figure 52). This is the region where the hummocks first began. Other than the hummocks and aspen patches, there were no other obvious physical sources for these strong cells. These cells are 4 to 7 dB stronger at VHF than UHF. Estimates of F^4 at these cells due to multipath are -2 dB at VHF and +11 dB at UHF

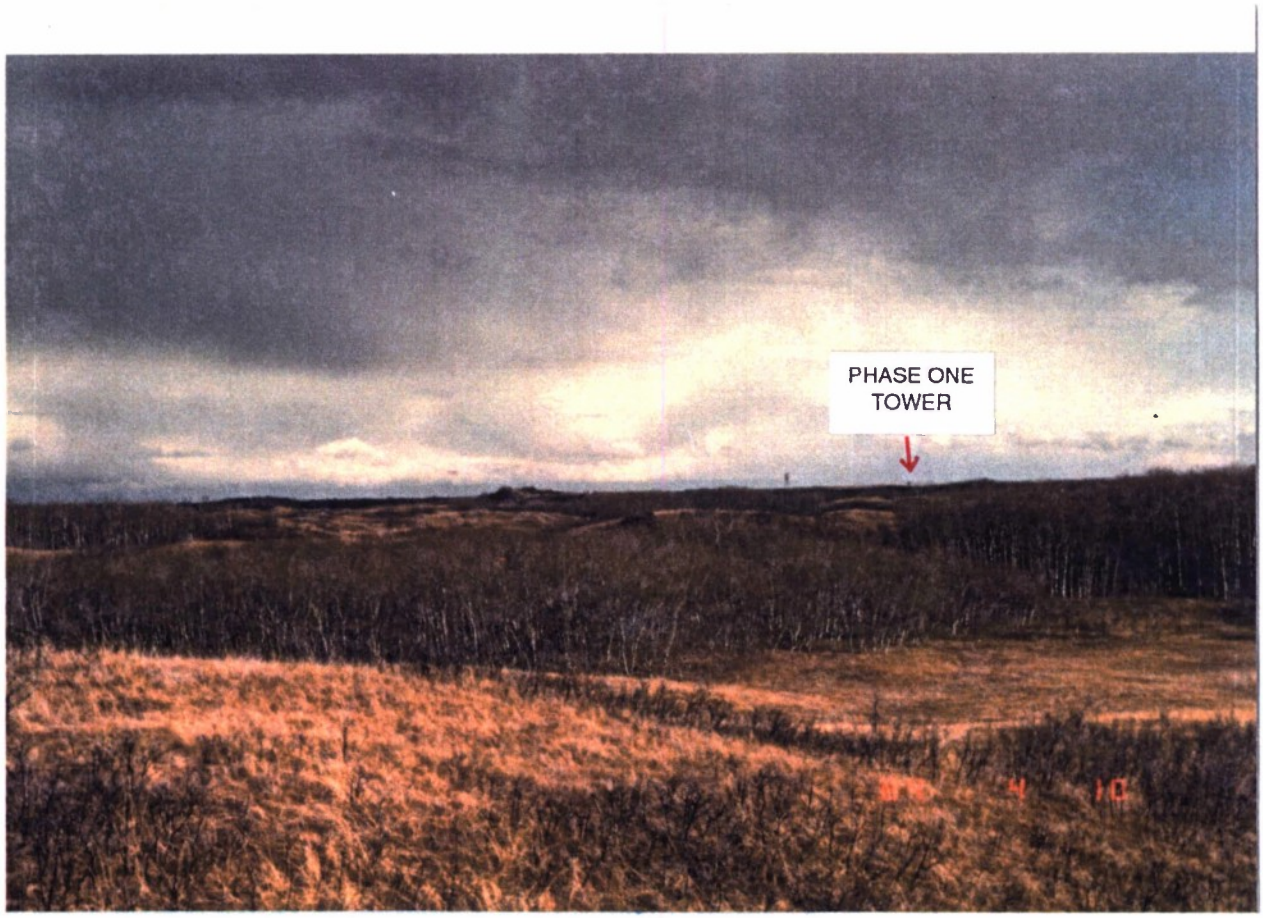

Figure 48. Hummocky scrub forest at Dundurn. View from remote weather station ESE back toward site center. Camp Dundurn water tower visible on horizon just right of center. Phase One tower visible as black dot on horizon 0.7 in to the right of water tower.

(i.e., elevation angle to top of hummocks ≈ 0.44 deg, see Figure B-4). Thus, the suggestion is that the intrinsic σ° from these vegetated hummocks is significantly greater at VHF than UHF. We shall see this same result (i.e., intrinsic σ° greater at VHF than at UHF) in Section 4.1.5 for desert (two sites) and frozen marshlands. Except for these first few cells at Dundurn, the VHF clutter falls off very quickly with increasing range, with UHF, L-, and S-band falling off similarly but at higher levels, and X-band falling off hardly at all, as would be expected in a multipath situation.

Summary. In light of these observations, the fact that VHF mean clutter strengths over the Dundurn repeat sector so closely match those at Sandridge in Figure 50 is obviously something of a coincidence. Nevertheless, in summarizing the commonality of these sites, we observe at both sites that X-band mean

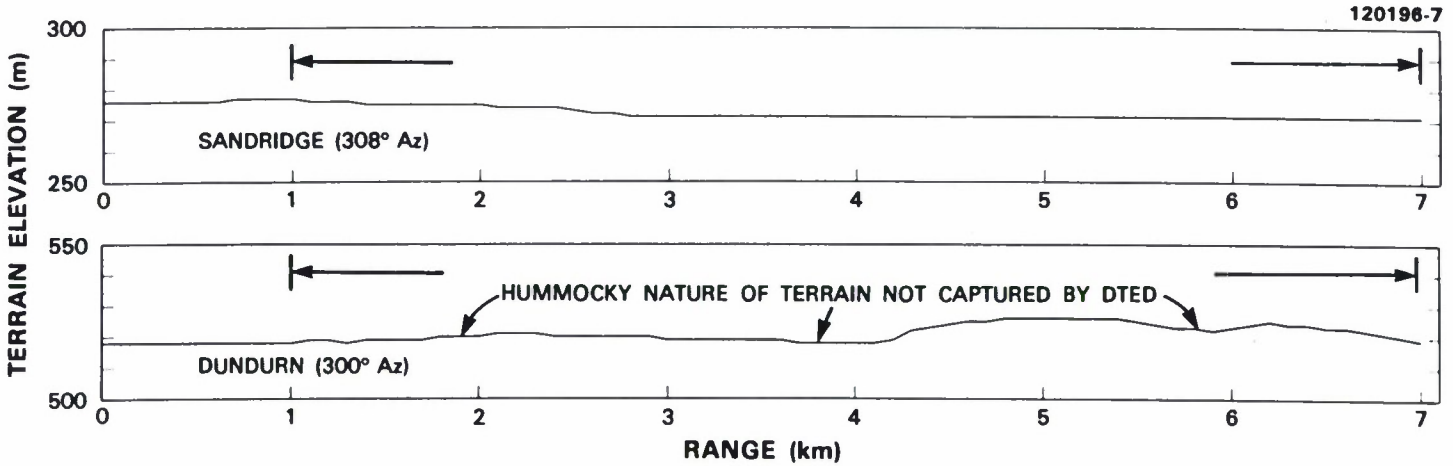

Figure 49. DTED terrain profiles at Sandridge and Dundurn. Elevation in meters above mean sea level, 10 m between tick marks. Range extent of repeat sectors is indicated by horizontal arrows.

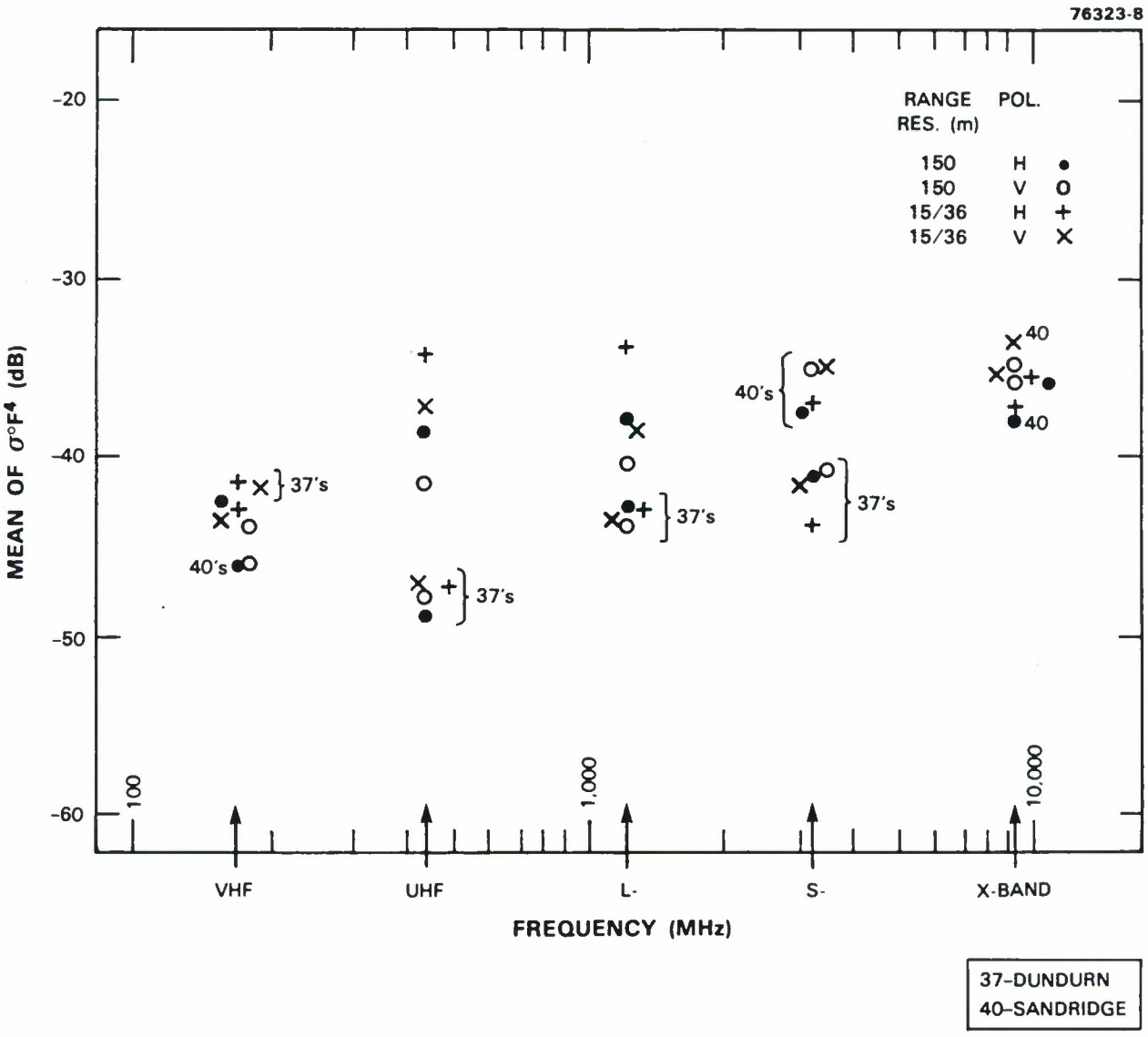

Figure 50. Mean clutter strength versus frequency for forest/low-relief terrain at low depression angle. See Table 7.

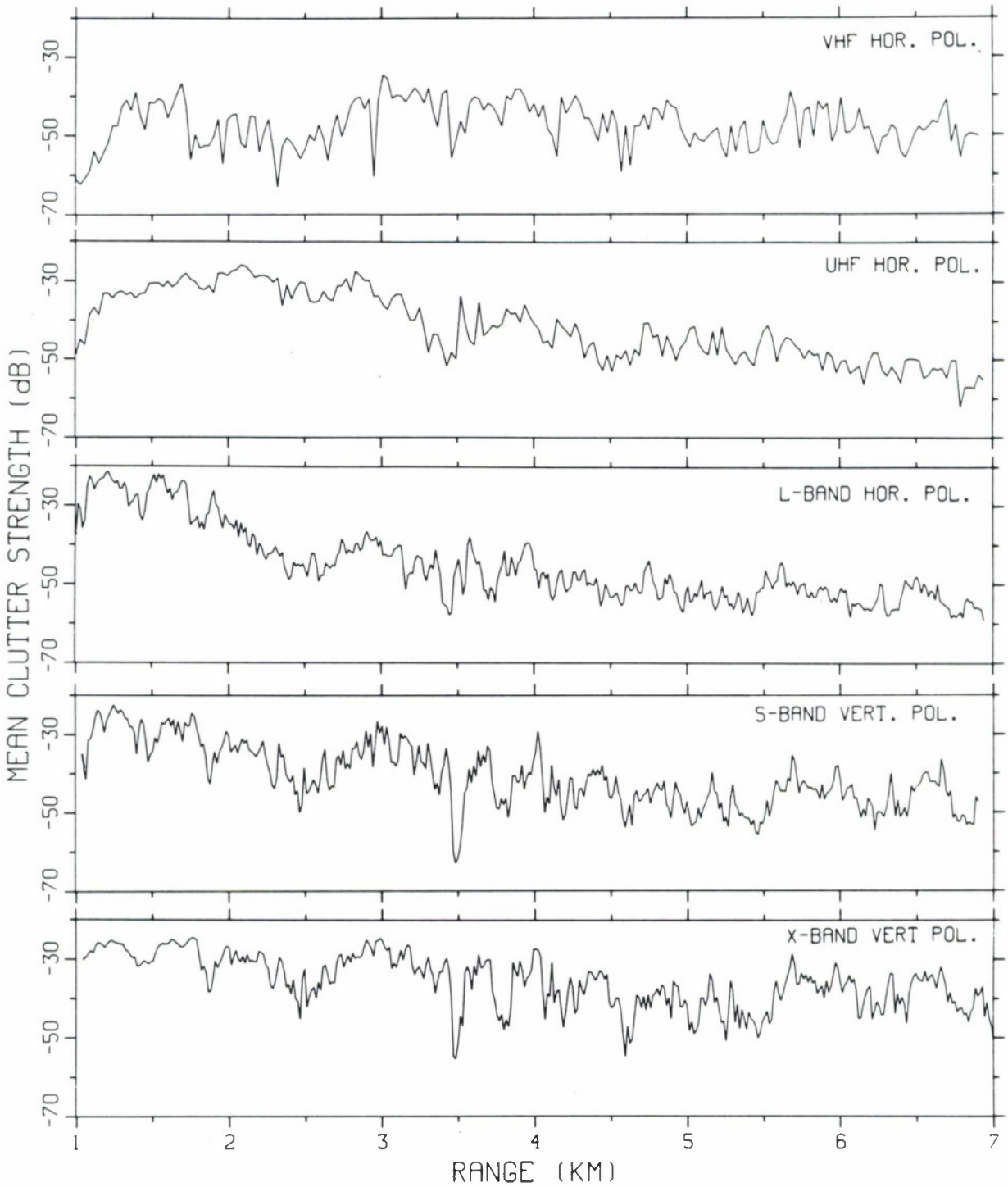

Figure 51. Mean clutter strength versus range at Sandridge. Repeat sector data. Vertical polarization for S- and X-bands and horizontal polarization for VHF, UHF, and L-band, 15/36-m pulse length. Data shown range gate by range gate, averaged in azimuth over 20 deg.

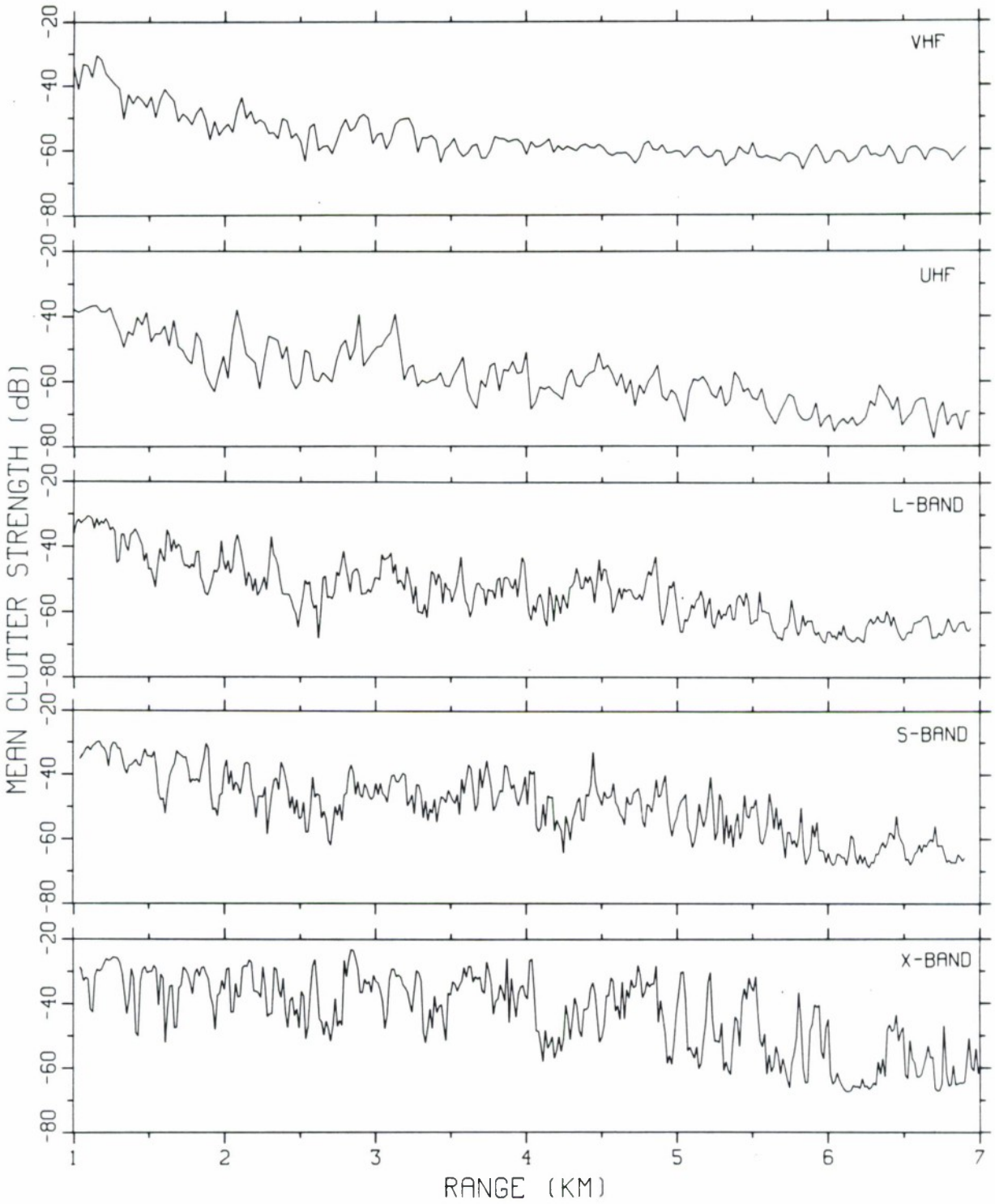

Figure 52. Mean clutter strength versus range at Dundurn. Repeat sector data. Vertical polarization, 15/36-m pulse length. Data shown range gate by range gate, averaged in azimuth over 30 deg.

clutter strengths are very similar (less coincidental, on the basis of relatively constant mean strengths through both complete sectors) at a level of -35.4 dB (see Table 11) and significantly weaker than forest/low-relief terrain at higher depression angles. This low X-band value of mean clutter strength for the forest/low-relief/low depression angle terrain category is very closely corroborated by the Phase Zero results, where, over all 43 Phase Zero patches of forest/low-relief terrain measured at depression angles below 0.3 deg, the median value of mean clutter strength is -35.48 dB.* So not only do we have what appears to be a valid general result at X-band for this forest/low-relief/low depression angle terrain category, significantly weaker than other forest terrain categories, but also we may expect clutter strengths at VHF to be generally lower than this X-band level perhaps partially due to multipath loss if the terrain and site area are somewhat open. Based on Sandridge and Dundurn results, how much clutter strengths fall off from X-band as frequency decreases depends on the details of how the multipath sets up. Based on Sandridge alone, which is our best example of a very level forested site, one might expect that, in a similarly level but denser forest with less opportunity for terrain multipath, multifrequency mean clutter strengths might be relatively invariant with frequency in the -35- to -37-dB range.

4.1.4 Agricultural Terrain

In following subsections we present multifrequency mean clutter strengths from agricultural terrain in three regimes of relief, as shown in Table 7. Multipath exists in many of these results to cause specific variations in mean clutter strength through the propagation factor, depending on the specific variations of terrain elevation involved. Furthermore, unlike forest, the dominant clutter sources in agricultural terrain are often specific discrete vertical objects associated with man's use of the land, and clutter strengths can depend quite specifically on what particular discretes exist and how they are distributed ov er any given repeat sector. In fact, one may argue that farmland clutter is quite a different, more heterogeneous and less stationary, statistical random process than forest clutter. Or one may argue it is not properly a statistical process at all, but deterministic, in that farmland clutter is so dominated by occasional strong isolated discrete cells in a weakly scattering background and that many of the strong cells occur in definite, culturally determined, spatial patterns.

As a result of this multifold specificity affecting mean clutter strengths in agricultural terrain, there are fewer general trends of mean clutter strength to discuss in agricultural terrain than in forest terrain. The trends that are found depend on our approach of reaching beyond specificity toward generality by combining measurements from a number of nominally similar repeat sectors in our multisite measurement program, thereby averaging out specific effects of propagation and/or discrete sources in individual measurements. By this means, two basic trends of variation of mean clutter strength in agricultural terrain are observed. First, in agricultural terrain that is of high-relief or moderately low-relief (i.e., terrain slopes > 1 deg), mean clutter strengths tend to be largely frequency independent, VHF through X-band, at about the -30-dB level. Second, in agricultural terrain that is either level or of very low-relief (i.e., terrain slopes < 1 deg), as frequency decreases below L-band through UHF to VHF, effective mean clutter strengths drop off dramatically. This latter effect is due to the generally decreasing intensity of illumination of such open level surfaces due to increasing multipath propagation loss with decreasing frequency. That is, clutter sources are being illuminated, and clutter returns are being received, well down

* For mean clutter strength of the Sandridge repeat sector, Phase Zero and Phase One (150 m, horizontal polarization) measured –36.3 and –37.6 dB, respectively; correspondingly, for Dundurn, –37.3 and –35.7 dB, respectively.

into the horizon plane null on the multipath lobing elevation pattern, and the width of this null and hence the amount of multipath propagation loss increases as the effective height of the antenna in wavelengths decreases with decreasing frequency.

In addition to the above two observations, we shall also observe that, in major contrast with forested terrain, mean clutter strengths in agricultural terrain, whatever its relief, are independent of depression angle at all five Phase One frequencies. Independence of mean clutter strength with depression angle in agricultural terrain agrees with the earlier Phase Zero findings at X-band. These earlier findings made a major point of the fact, however, that spreads in clutter amplitude distributions from large spatial regions (particularly in low-relief agricultural terrain, but in other terrain types as well) decrease rapidly with increasing depression angle. The reasons for this are as follows. In low-relief farmland, dominant clutter sources are large discrete vertical objects. At low angles, strong returns are received from these discrete sources, but much of the intervening terrain is either shadowed or provides very weak returns due to the illumination being at grazing incidence. As a result, in low-relief farmland at low depression angle, clutter amplitude distributions have a very large spread. As depression angle increases, the intervening terrain between strong discrete sources comes under stronger illumination, the weak returns from these regions rapidly increase, and as a result spreads in amplitude distributions rapidly decrease. However, the strong returns from the discrete objects at the high ends of the distributions tend to be relatively independent of depression angle and continue to dominate their mean strength. In contrast, low-relief forest is much more a homogeneous scattering medium, not dominated by large discrete objects. Nevertheless, at low angles in level forest, a large amount of microshadowing still occurs. As angle increases, the shadowing gradually decreases, as a result the amplitude distributions gradually tighten up, and their mean strengths — not dominated here by large singular discrete sources — gradually rise.

For now, our first emphasis in this report is on determining multifrequency trends of the means, not the spreads, of clutter amplitude distributions from 42 repeat sectors. However, our ground clutter model specifies both means and spreads of clutter amplitude distributions, tying each to their major dependencies as observed in our measurements. Thus, our model divides open farmland into a closely graduated set of depression angle regimes to provide the important dependency of spread on depression angle. We repeat, though, that here we are mainly bolstering this model by showing that, in high-relief or moderately low-relief agricultural terrain, mean clutter strengths are approximately invariant with frequency at about the -30-dB level; whereas, in very low-relief agricultural terrain, mean clutter strengths rise from low levels at VHF and UHF (viz., approximately -56 and -41 dB, respectively) up to the same approximately -30-dB level in the microwave bands.

4.1.4.1 Agricultural/High-Relief Terrain. Table 7 indicates that we have three sites within the category of agricultural/high-relief terrain. Repeat sector terrain profiles for these sites are shown in Figure 53. Recall that high-relief terrain is determined by slopes that are > 2 deg (see Table 4). Note in Table 7 that the high-relief landform classes that cause these three sites to group together as high-relief are rolling (LF = 4) and moderately steep (LF = 7).

Multifrequency mean clutter strengths measured over the repeat sectors at these three sites are shown in Figure 54. No clear trend emerges in these data. Mean strengths are observed to rise from VHF to UHF and L-band and then to drop again at S- and X-band. However, such particular variations are

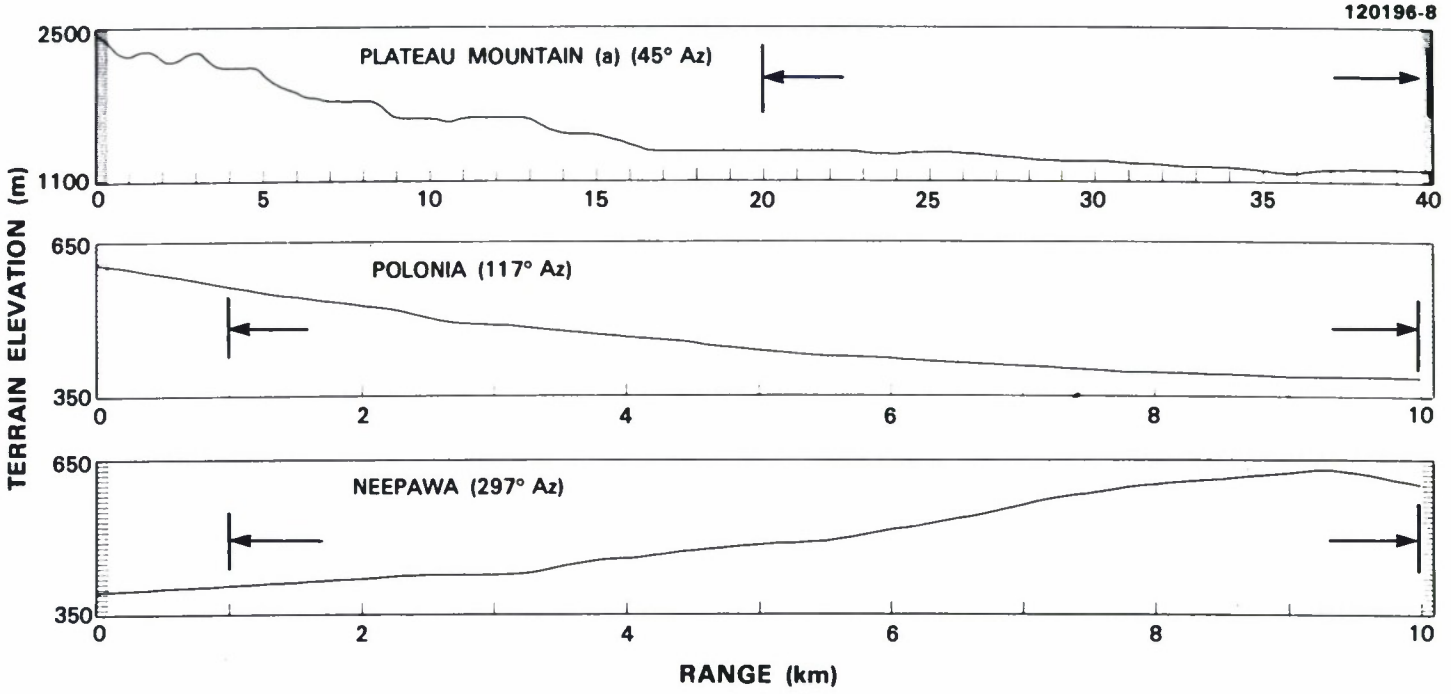

Figure 53. DTED terrain profiles at Plateau Mountain (a), Polonia, and Neepawa. Elevation in meters above mean sea level, 10 or 20 m between tick marks. Range extent of repeat sectors is indicated by horizontal arrows.

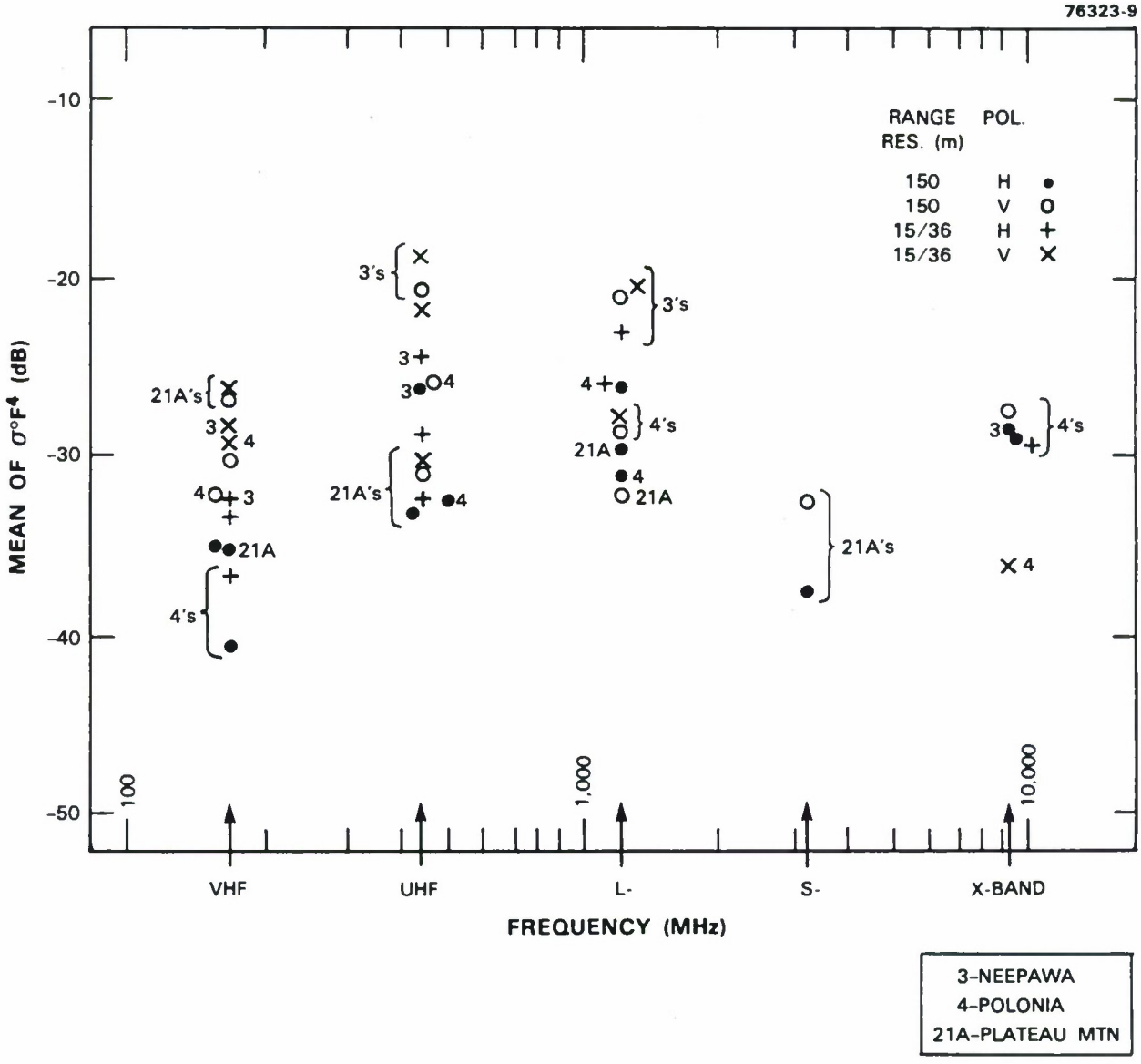

Figure 54. Mean clutter strength versus frequency for agricultural/high-relief terrain. See Table 7.

considered to be caused by specific terrain and propagation characteristics and not to be generally representative of agricultural/high-relief terrain. About all that can be said of the mean clutter strength data in Figure 54 that is generally representative of agricultural/high-relief terrain is that they largely lie in the range from -20 to -40 dB, and that in a very gross sense they can be represented by an approximate level of about -30 dB (actually, -29 dB is the median of all the points plotted in Figure 54).

Plateau Mountain. We now discuss each of the three agricultural high-relief sites in turn. We begin with Plateau Mountain (see Figure 27). Plateau Mountain was the only site at which two repeat sectors were selected. One of these sectors, namely, repeat sector (b) looking to the west at steep rocky mountain peaks, has been discussed in Section 4.1.2. Here, the other Plateau Mountain repeat sector, namely, repeat sector (a), is discussed. In repeat sector (a), Phase One looks at long ranges to the northeast, down off the top of Plateau Mountain, to rolling prairie rangeland beyond at ranges from 20 to 40 km. The elevation on Plateau Mountain is 8121 ft above MSL. Over the first 20 km, the terrain in repeat sector (a) to the northeast is almost entirely masked, except for the odd peak (e.g., Sentinel Peak) as the terrain elevation rapidly falls off down the side of the mountain and over the forested foothills below. We do not expect any significant multipath to have occurred over this 20 km of rough, masked terrain between the radar and the repeat sector clutter patch. Beyond these forested foothills, at about 20 km, the rolling rangeland of the high prairie comes into view, at typical elevations of about 4100 ft above MSL. Thus, repeat sector (a) at Plateau Mountain is the most airbornelike measurement situation that exists in the 42 Phase One repeat sectors (i.e., large elevation difference ≈ 4000 ft; long range = 20 to 40 km; relatively large depression angle = 2.3 deg; no multipath in the neighborhood of the radar).

Mean clutter strengths are provided from repeat sector (a) at Plateau Mountain over the range interval from 20 to 40 km. The rangeland terrain in this interval has substantial relief, on the order of 500 ft. Several roads and a creek bottom traverse the sector. A small village and various scattered ranch buildings exist within the sector. Thus, although predominantly rangeland (i.e., 73 percent), the sector is by no means discrete free. Twenty-four percent of the sector is farmland. The sector is tree free, except for a few small patches of trees at the beginning of the sector at ranges of 20 to 22 km. The Plateau Mountain measurements were in June, with crops up and grass high in repeat sector (a).

Mean clutter strengths for repeat sector (a) at Plateau Mountain are shown in Figure E-100. The X-band transmitter failed at Plateau Mountain and remained out of operation for five sites (see Table A-25). High range resolution data were not taken at L- and S-band in repeat sector (a) at Plateau Mountain due to the diminished sensitivity at such long ranges and the many samples involved over such a long range interval. In the remaining data in Figure E-100, frequency invariant results are observed at about the -32-dB level overall. At VHF, vertically polarized mean strengths are about 7.5 dB stronger than horizontal, which coincidentally is about the same amount that vertical was stronger than horizontal for repeat sector (b), looking west from Plateau Mountain at mountainous terrain (see Figure E-30). At UHF, however, vertically polarized mean strength in repeat sector (a) is only about 2 dB stronger than horizontal, resulting in a tightly clustered group of measurements by polarization and resolution.

Neepawa and Polonia. Neepawa and Polonia constitute a pair of sites in Manitoba that are separated by 8 km and where the repeat sectors face each other. That is, the Neepawa repeat sector is centered in azimuth on the Polonia setup position and vice versa. Both repeat sectors cover 1 to 10 km in range.

The consequence is that the same terrain is observed from two different directions. Dominating the low-relief prairie in the general area where Neepawa and Polonia are situated is Riding Mountain escarpment, a major terrain feature rising 1000 ft off the prairie floor. Polonia is situated near the top of the escarpment. The repeat sector at Polonia looks southeast down the side of the escarpment (landform = 7, moderately steep) to the more level prairie farther out and contains the Neepawa site at 8-km range. The repeat sector at Neepawa looks northwest, first across slightly inclined terrain (landform = 2) rising gradually towards the escarpment, and then, beginning at about 5-km range, up the side of the escarpment (landform = 7) to the Polonia site at 8-km range, and past it. Although the escarpment is visually a very striking terrain feature, visible from a long distance and appearing to rise very steeply, in fact the terrain slopes on the side of the escarpment are only about 2 deg. The land cover throughout this area is primarily cropland, but there is a significant secondary component of woodland, mainly aspen, that occurs in patches and groves. The incidence of trees on the moderately steep terrain on the side of the escarpment is greater, but there are still large open areas of cropland on the side of the escarpment. A photograph of this terrain from near the Polonia site looking down the side of the escarpment towards the Neepawa site is shown in Figure 55.

Neepawa and Polonia, together with Shilo, constituted the first shakedown tour of three Canadian sites conducted in February and March of 1982 (see Appendix A, Section A.1). The Phase One equipment was not yet fully configured for this first tour, and in particular, we lacked the S-band transmitter. Weather conditions were wintry with temperatures below freezing most of the time, and most of the prairie landscape was covered with an inch or two of crusty snow and ice. Occasional snow flurries left dustings of light snow. Towards the end of the stay at Neepawa, a thaw period was encountered, which turned the pasture setup area into a quagmire and hampered data collection. This was followed by an ice storm and blizzard with 40-kn winds that caused the antenna rotator to fail, all of which prevented us from obtaining most of the X-band repeat sector data at Neepawa.

Mean clutter strengths versus frequency for the Neepawa and Polonia repeat sectors are shown in Figures E-109 and E-104. At first consideration, there appears to be a remarkable degree of similarity in the overall characteristics of mean strength versus frequency at these two sites. This is somewhat surprising, as the measurement geometries at these two sites are quite different, even though it is the same terrain that is being viewed.

Neepawa. First, the Neepawa site will be discussed in more detail. At Neepawa, the rising escarpment is viewed in the distance over a relatively open low-relief terrain surface that we would expect to be supportive of multipath. The peak of the first multipath lobe would occur about 1.5 deg above this surface at VHF, about 0.6 deg above this surface at UHF, and about 0.2 deg above this surface at L-band (see Figure B-4). The surface is inclined about 0.5 deg towards the escarpment, so these beams actually first peak at about 2.0, 1.1, and 0.7 deg, respectively, above the local horizontal at the Phase One antenna. The Polonia site at 8-km range is at 1.4-deg elevation above the local horizontal at Neepawa. This suggests the following. At VHF, although even the terrain at long ranges high up on the escarpment does not reach maximum illumination at the peak gain of the first multipath lobe, nevertheless the terrain rises away from the Phase One site at a gradually increasing rate, resulting in much of this terrain being illuminated, not down in the horizon plane null as on level terrain, but well up on the side of the first

Figure 55. Polonia repeat sector. View is SE down the side of Riding Mountain escarpment and out onto cropland barely discernible in far distance beyond trees.

multipath lobe, although not as high as the peak. At UHF, the peak of the first multipath lobe does fully illuminate the steeply rising terrain up the side of the escarpment, theoretically providing 12-dB peak gain over free space assuming unity reflection coefficient, or 7.8-dB gain augmentation averaged over the full lobe. At L-band, the first two multipath lobes illuminate the rising terrain up the side of the escarpment, theoretically providing similar gain augmentation. Indeed, in the Neepawa results of Figure E-109, mean strengths at UHF and L-band are about 10 dB stronger than at VHF, which is probably indicative of fuller illumination of the escarpment at the higher frequencies. These observations are also borne out in the sector display results of Figure E-107. Of course, the actual multipath situation at Neepawa may have been considerably more complex than indicated by this simple heuristic discussion (e.g., multiple specular reflections might occur along this upward sloping terrain), but this discussion does encourage thinking about the sorts of dominant influences multipath can cause in the clutter measurements at Neepawa.

Two final comments are made on the Neepawa data of Figure E-109. First, in these Neepawa data, vertically polarized mean strengths are typically 4 or 5 dB stronger than horizontal in all three available bands. These variations with polarization run counter to our multipath argument if the assumption is made that terrain reflection coefficients are higher at horizontal polarization than at vertical. Higher reflection coefficients at horizontal polarization would provide stronger lobes, and hence, dominant clutter strengths from the distant escarpment (under multipath enhanced illumination) would be stronger at horizontal polarization than at vertical, not weaker, as is observed. Second, can it be argued that the high Neepawa clutter strengths at UHF and L-band are caused by high terrain slopes on the side of the escarpment, with VHF weaker because of multipath loss? Although the terrain slopes are relatively high on the side of the escarpment (viz., 2 deg), so are they in the rolling terrain of Plateau Mountain repeat sector (a). However, in this latter situation, which is unaugmented by multipath, mean strengths at UHF and L-band are, on the average, close to 10 dB weaker than at Neepawa; VHF mean strengths at Plateau Mountain are similar to those at Neepawa, suggesting no large VHF multipath loss at Neepawa.

Polonia. We now turn to Polonia. Looking down the side of the escarpment from Polonia, we still expect multipath, although to a lesser degree than from the more open prairie at Neepawa. The side of the escarpment at the near ranges in the Polonia repeat sector, although definitely containing substantial open cropland smooth enough and extensive enough to provide reflecting Fresnel zones, also contains meandering wooded gullies eroded down the side of the escarpment, which would tend to reduce multipath. If we assume that dominant multipath contributions arise from the local terrain nearby the Phase One setup position (which is often true), then we are led to understand how the essential geometry at Polonia is roughly similar to that at Neepawa. This factor explains the similar mean strength versus frequency characteristics of Figures E-109 and E-104, even though at first consideration the scenes seem so different (i.e., Neepawa looks over level terrain at a specific terrain feature rising in the distance; whereas, Polonia observes level prairie from a high position).

This essential geometry at Polonia is as follows. Consider the side of the escarpment to be the reflecting surface causing multipath lobing (see Section B.2). For the three-section antenna mast, the peak of the first lobe occurs at 1.5, 0.6, and 0.2 deg above this surface, at VHF, UHF, and L-band, respectively. However, this reflecting terrain surface is tilted at 2 deg. Therefore, the peak of the first lobe occurs at 0.5, 1.4, and 1.8 deg of depression angle below the local horizontal at the Phase One antenna at VHF, UHF, and L-band, respectively. The terrain at the Neepawa setup position, 8 km out in the repeat sector, is viewed at 1.6-deg depression angle from the Polonia antenna. In terms of range out into the repeat sector, the peak of the first lobe illuminates the prairie at 25.8, 9.2, and 7.2 km at VHF, UHF, and L-band, respectively. However, mean clutter strengths are being computed only over the 1- to 10-km range interval in the Polonia repeat sector. Thus, at least according to this simple analysis, we see how the 1- to 10-km interval is illuminated on the underside of the first multipath lobe at VHF, but that at UHF and L-band parts of this range interval are illuminated at the peak gain of the multipath pattern. This begins to explain why the effective mean clutter strengths in Figure 54 are so much stronger at UHF and L-band than at VHF at Polonia and provides a similar multifrequency characteristic as do the Neepawa results. The similarity arises from the fact that, in both measurement situations, multipath lobing patterns occur as a result of reflections from the local terrain surface around the setup position, and in both situations terrain at far ranges in the repeat sector rises above the plane of the local surface up into the lobing pattern.

Note that in every case by polarization and resolution at VHF, UHF, and L-band, the Neepawa measurement of mean clutter strength is stronger than the Polonia measurement (by 4.5 dB on the average). One might at first consider that this is because the escarpment terrain viewed from Neepawa is high-relief; whereas, the prairie terrain viewed from Polonia is low-relief. This may be part of the answer because the escarpment terrain is rougher (i.e., gullied and broken) than the prairie terrain as well as being inclined at 2 deg. In terms of grazing angle, however, the Neepawa setup area is illuminated from Polonia at about 1.1 deg above the plane of the local surface (assuming 0.5-deg local terrain slope); whereas, the Polonia setup area is illuminated from Neepawa at about 0.6 deg above the plane of the local surface (assuming 2-deg local terrain slope). Because of the simplicity of this geometrical computation, little significance should be attributed to this 0.5-deg difference in grazing angles. But what this computation does do is diminish somewhat the argument that it is the higher escarpment terrain slopes making mean strengths measured from Neepawa so significantly higher than mean strengths measured from Polonia. In fact, the grazing angles seen from Polonia compute slightly higher. Thus, we are inclined to believe that the differences in mean strength are more due to fuller illumination from Neepawa than from Polonia, which is indeed indicated in the multipath computations discussed above. This latter belief is somewhat buttressed because the single available X-band measurement of mean strength from Neepawa is almost identical (within 0.5 dB) to the corresponding measurement from Polonia, and of course, illumination is no longer an issue at X-band.

Although the Polonia clutter data discussed to this point are for the 1- to 10-km range interval in the repeat sector, in fact the radar was quite high and had good visibility out over low-relief prairie farmland to very long range. In Appendix B, Section B.2, we discuss how it is often multipath from the local hillside slope that dominates propagation in these situations such that the illumination of clutter sources in the far field is the result of the direct ray in the horizontal direction (i.e., at 0-deg depression angle) interfering with a horizontally directed multipath ray from the local hillside slope (refer to Figure B-3). At Polonia, the 2-deg local hillside slope involved happens to be such that it is the peak of the second multipath lobe at UHF that horizontally illuminates the far-field clutter sources, with a resultant theoretical 12-dB multipath gain augmentation in clutter strength. This situation is depicted in Figure 56. Measured cumulative clutter amplitude distributions for the Polonia repeat sector over a longer range interval from 1 to 47 km are shown in Figure 57. Indeed, mean clutter strengths in these distributions are 5 to 8 dB stronger at UHF than in the other four bands, which we believe is the result of this multipath augmentation at UHF. Similar cumulative results for the 1- to 11.4-km range interval in the Neepawa repeat sector are shown in Figure 58, where the reduced clutter strength at VHF has already been explained as due to the fact that the top of the escarpment does not reach the peak of the first VHF lobe. In these two figures, two specific propagation effects are seen causing both significantly stronger (i.e., UHF data in Figure 57) and weaker (i.e., VHF data in Figure 58) clutter in what are otherwise tightly clustered multifrequency clutter measurements in this prairie farmland terrain. Later, in Section 4.1.4.3, similar cumulative distributions from Shilo will be shown, situated in similar terrain 80 km away from the escarpment (and so, unlike Neepawa and Polonia, not dominated by it), in which multipath dominates the measurements in yet a different manner.

Summary. After the foregoing specific discussions of Plateau Mountain (a), Neepawa, and Polonia, it may seem that we are mixing apples and oranges by combining their data into one terrain class. However, in terms of specifics, every ground clutter measurement situation is different; and we are

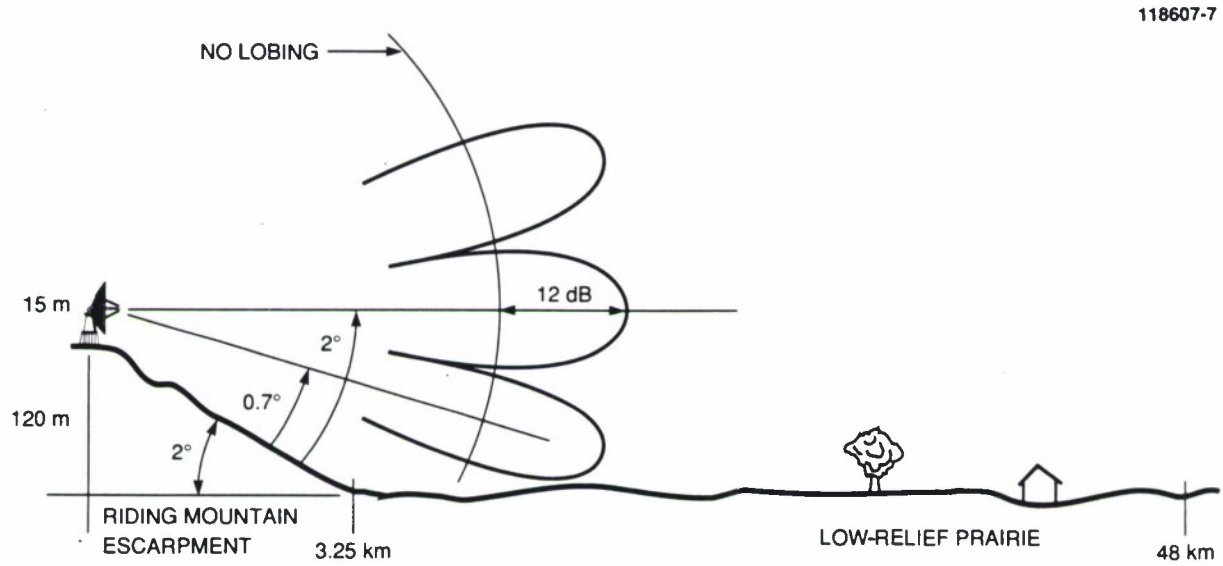

Figure 56. UHF multipath lobing at Polonia, Manitoba.

attempting to discover useful generalities as they come through at the overall level of terrain description as provided in Table 7. This table illustrates the gross similarity in landform, land cover, and high (non-zero) illumination angles for these three sites; and some evidence of gross similarity in the mean strengths of the clutter from these three sites is seen. We have argued, somewhat heuristically, that high UHF and L-band mean clutter strengths at Neepawa in Figure 54 and, to a lesser degree, at Polonia are due to multipath propagation enhancement. In addition, we showed another propagation enhancement at UHF in long-range Polonia data. These discussions of propagation effects at Polonia and Neepawa, and their lack at Plateau Mountain (a), serve as good examples of the significant role propagation plays in low-angle ground clutter from open terrain. We have argued that the way to generalize beyond specific propagation effects is to combine measurements from many sites. As an example, whereas at Neepawa and Polonia UHF mean clutter strengths were augmented by specific effects of propagation, we shall see in the next section that at Beiseker UHF mean clutter strengths are reduced by specific propagation effects.

4.1.4.2 Moderately Low-Relief Agricultural Terrain. Table 7 shows three sites within the category of moderately low-relief agricultural terrain. A photograph of the terrain at one of these sites, Magrath, along with an X-band PPI clutter map is shown in Figure 59. Recall that moderately low-relief terrain is defined as having terrain slopes between 1 and 2 deg (see Section 3.3). Note in Table 7 that it is the presence of inclined terrain (of landform class = 2, see Table 4) as the highest sloped terrain category in all three repeat sectors that results in grouping them together as moderately low-relief sites. When scanning vertically down the landform column over all three groups of agricultural sites in Table 7, the

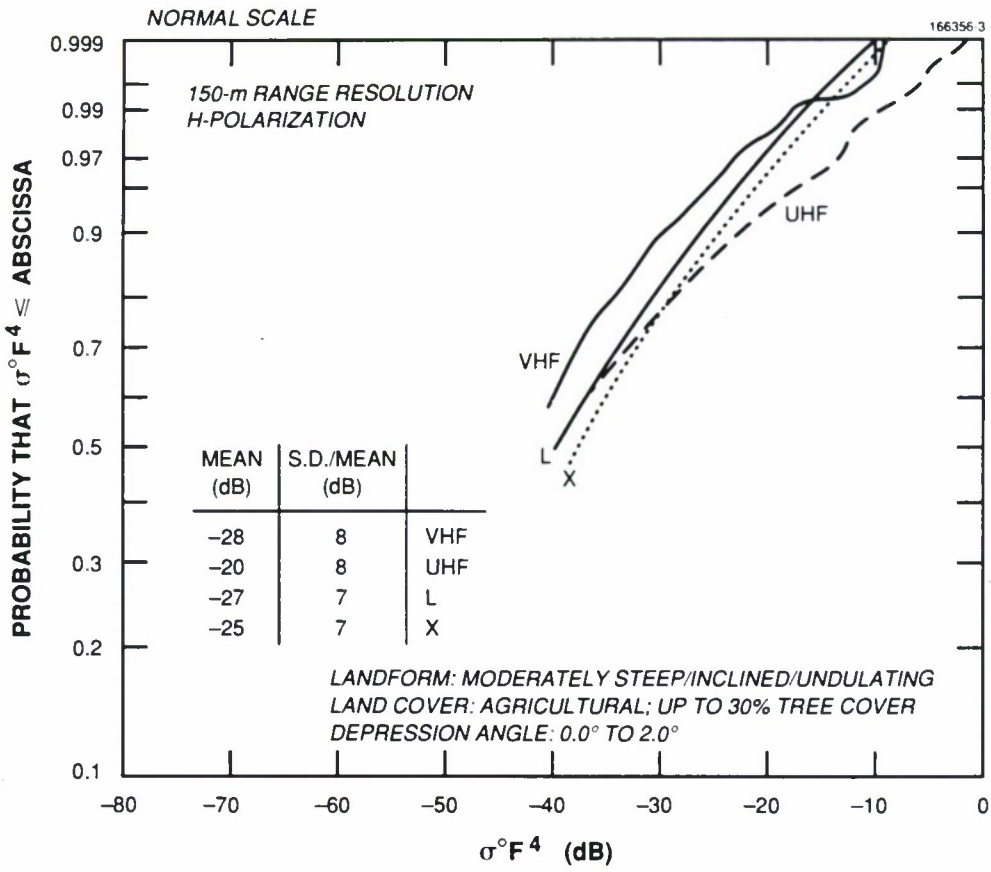

Figure 57. Measured multifrequency ground clutter amplitude statistics at Polonia, Manitoba. Range, 1.0 to 47.0 km. Azimuth, 107 to 127 deg.

following observations are made: high-relief components in the first group (landform = 4 or 7, terrain slopes > 2 deg), the universal presence of inclined terrain (landform = 2, terrain slopes between 1 and 2 deg) as the highest sloped terrain in the second group, and the universal absence of anything but level or undulating terrain (landform = 1 or 3, terrain slopes < 1 deg) in the third group. In terms of depression angle, Table 7 indicates that the three moderately low-relief agricultural sites span a relatively wide range from 1.2 to 0.4 deg. In terms of land cover, Table 7 indicates that these three sites are substantially solid cropland with occasional components of rangeland but with very few trees (in contrast with the high-relief agricultural sites, two of which had substantial incidence of trees, i.e., secondary component of land cover = 41). In terms of range extent, Table 7 indicates that, as with depression angle and correlated with it, the repeat sectors at these three sites provide considerable variation, extending over a near interval of 1 to 6.9 km at Beulah, an intermediate interval of 5 to 10.9 km at Magrath, and a relatively far interval of 8 to 17 km at Beiseker.

Multifrequency mean clutter strengths measured over the repeat sectors at the three moderately low-relief agricultural sites are shown in Figure 60. In general terms, the basic message of Figure 60 is one of frequency independence at an overall level of about -30 dB. (The median level of all the points plotted

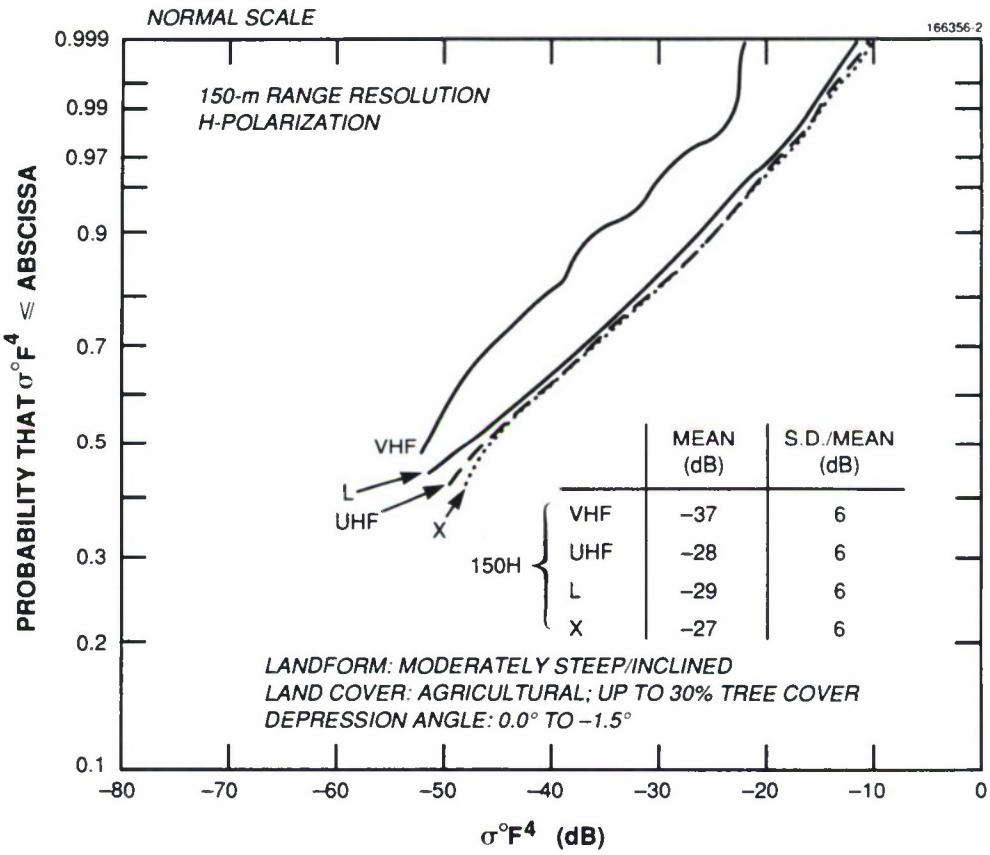

Figure 58. Measured multifrequency ground clutter amplitude statistics at Neepawa, Manitoba. Range, 1.0 to 11.4 km. Azimuth, 287 to 307 deg.

in Figure 60 is at -29.6 dB.) In more specific terms, the UHF and S-band clusters of mean clutter strength in Figure 60 cover similar ranges of variation, VHF mean strengths are greater than UHF, L-band mean strengths cluster more tightly and towards the high end of the UHF and S-band data, and again (see Scranton, Blue Knob, Brazeau, and Gull Lake West discussions) a slight S-band dip occurs between L- and X-band. Such minor specific variations may be quite dependent on these particular three sites. That is, if we had selected a different group of moderately low-relief agricultural sites, we may have obtained different minor variations around the -30-dB overall level but probably would not have obtained a very different overall level. When statistical processing of all Phase One 360-deg survey data into clutter patch histograms is complete (i.e., thousands of clutter patches, not just 42 repeat sectors), we will be able to present results in which small variations have more statistical significance.

All three moderately low-relief agricultural sites were on agricultural terrain that had significant relief (hundreds of feet) over long macrocorrelation intervals (many kilometers). Thus, at each of these sites, Phase One set up on a local topographic high and looked out into a repeat sector in which the terrain elevation fell off down the side of the hill that we were set up on and up the side of the next hill. That

is, the view was over one macrowavelength of terrain elevation variation. DTED terrain profiles for the Magrath and Beiseker repeat sectors are shown in Figure 61. This explains how the significant "inclined" component in landform classification arose in these repeat sectors. The land was first inclined away from Phase One and then, farther out in the repeat sector, inclined towards Phase One. Even though strong multipath generally occurred on these open farmland landscapes, the terrain inclinations between 1 and 2 deg were enough to first steer the multipath lobes down (recall that the angle to the peak of the first multipath lobe above the local ground slope is nominally at 1.5, 0.6, and 0.2 deg at VHF, UHF, and L-band, respectively, for the 60-ft antenna mast, see Figure B-4) and then to cause the farther out terrain to rise up through them. That is, the distant rising terrain in these repeat sectors was well illuminated at all frequencies on the multipath lobing pattern, giving rise to roughly frequency independent mean clutter strengths at about the -30-dB level. The effects of multipath in such terrain are discussed more fully in Appendix B, Section B.2. Frequency independence of mean clutter strength is definitely not the case on very low-relief agricultural terrain (see Section 4.1.4.3). Thus, perhaps surprisingly, VHF and UHF clutter strengths on open low-relief agricultural terrain depend strongly on whether the terrain has long gentle inclinations.

Phase Zero. Table 11 shows that the median value of mean clutter strength at X-band over all Phase One repeat sector measurements at the three moderately low-relief agricultural sites is -28.4 dB. Compare this value with what Phase Zero measured in similar terrain. Over 724 patches classified primarily as agricultural low-relief (but with all kinds of secondary classifiers, and not restricted just to moderately low-relief), the median value of mean clutter strength measured by Phase Zero was -31.6 dB, which is significantly lower by 3.2 dB from the above Phase One value of -28.4 dB. If from this set of patches, we consider only the subsets that are purely classified as inclined agricultural patches with no secondary classification, thereby restricting terrain slopes to the same 1- to 2-deg range of the Phase One repeat sectors in this terrain category, we are left with 35 patches for which the median value of mean strength is -33.3 dB. Thus, it appears that the Phase One estimate of mean clutter strength for this terrain category based on three sites only may be several decibels high. The Phase Zero estimates are within 1 dB of the lower Phase One value at S-band for this terrain category, namely, -32.5 dB. Site-by-site comparisons of repeat sector X-band mean clutter strengths in decibels measured by Phase Zero and Phase One (for the 150-m pulse, horizontal polarization) for Beiseker and Magrath are, respectively: Beiseker, -25.7 versus -31.6, -30.3, -31.0 (three seasonal visits); Magrath, -32.4 versus -32.4 (i.e., exact correspondence).

Beulah. Each moderately low-relief agricultural site will now be discussed in more detail. At Beulah, North Dakota, Phase One was on the top of a hill at 2064 ft above MSL, and first looked down the side of this hill to low-lying terrain around Antelope Creek at about 1800 ft above MSL and between 3- and 4-km range, and then up the side of the terrain rising out of Antelope Creek to elevations of about 1950 ft above MSL at 7-km range. The presence of strip mine spoil piles 30 to 50 ft high at about 1-km range in this repeat sector would act to diminish the effects of multipath at Beulah, although the terrain in Antelope Creek valley and the rising terrain beyond was directly visible from the 60-ft antenna mast. Beulah was measured in June 1984 with leaves out and crops growing. A photograph of the inclined farmland terrain at far range in the Beulah repeat sector is shown in Figure 62.

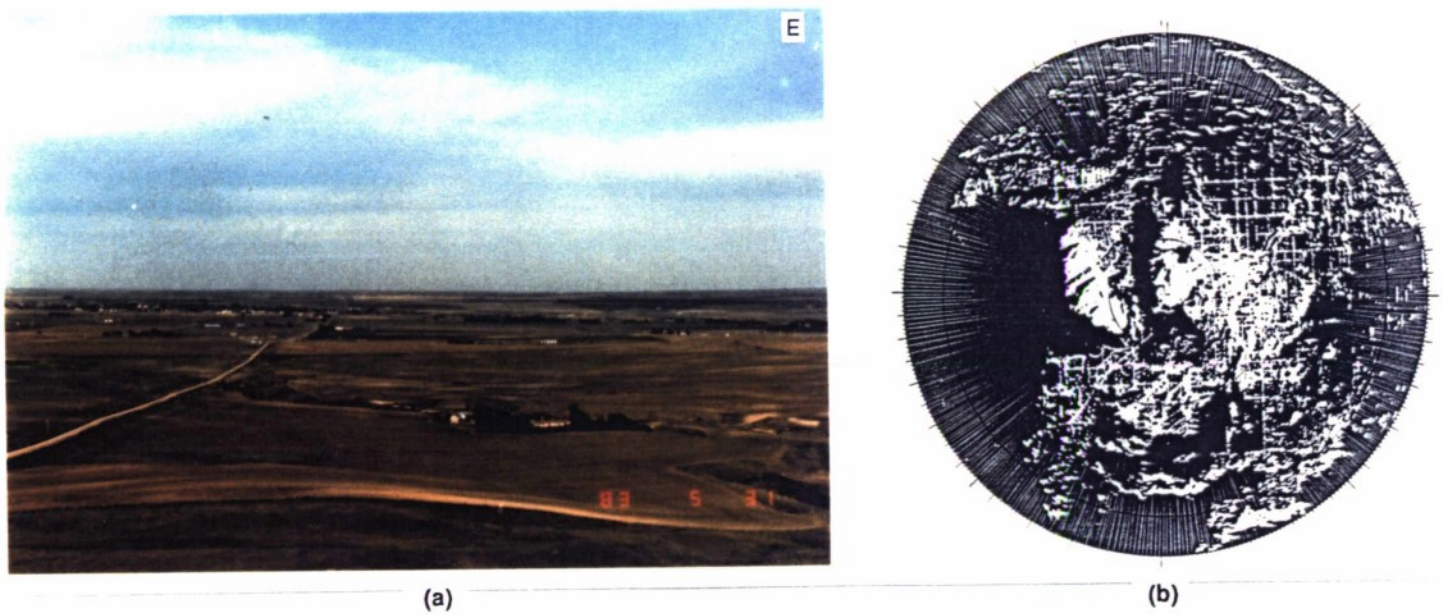

Figure 59. Agricultural terrain at Magrath. (a) Phase One tower-top view looking east and (b) X-band PPI clutter map. North is zenith. Maximum range = 24 km.

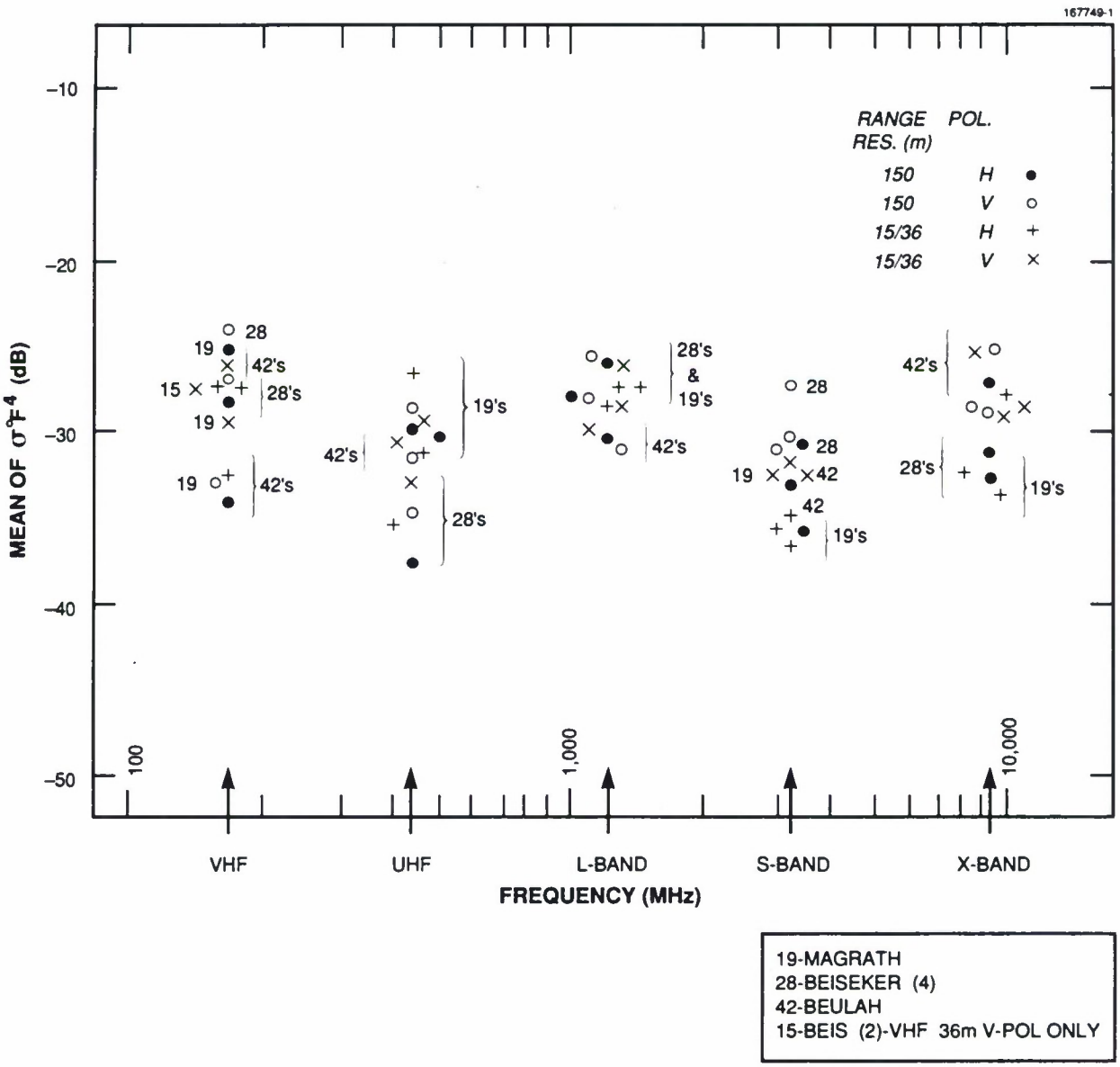

Figure 60. Mean clutter strength versus frequency for agricultural/moderately low-relief terrain. See Table 7.

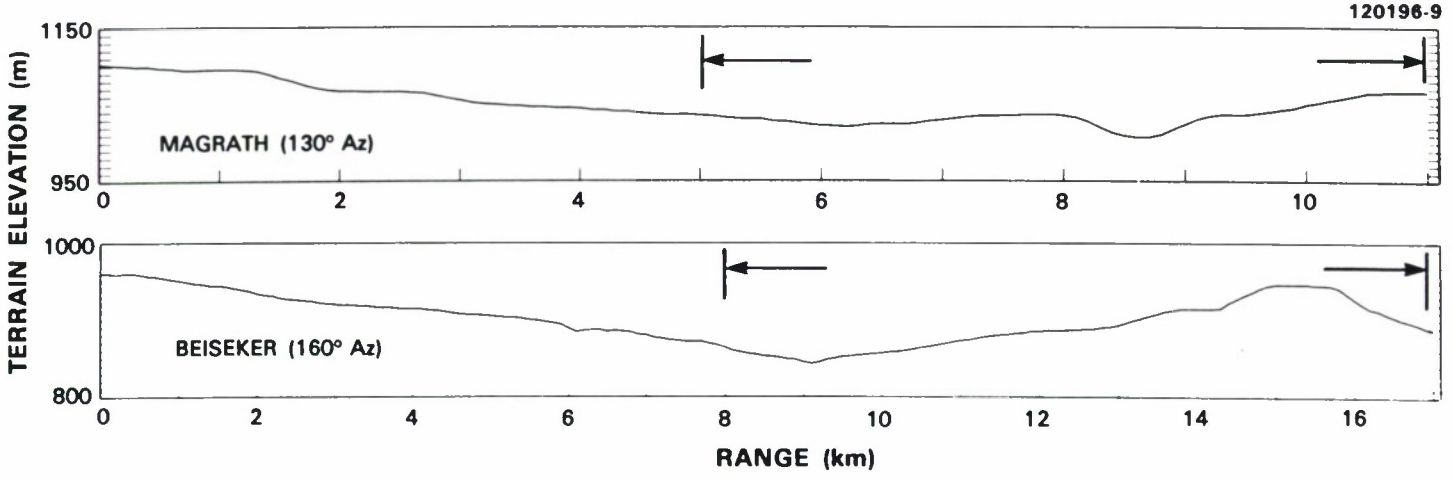

Figure 61. DTED terrain profiles at Magrath and Beiseker. Elevation in meters above mean sea level, 10 m between tick marks. Range extent of repeat sectors is indicated by horizontal arrows.

Mean clutter strengths versus frequency for the Beulah repeat sector are shown in Figure E-113. In this figure, we observe vertically polarized mean strengths stronger than horizontal at VHF by 7 or 8 dB [like Plateau Mountain (b)], almost no variation with polarization or resolution (i.e., a tight cluster) at UHF very nearly at the -30-dB level, a slight S-band dip between L- and X-band, but altogether, in general terms, relatively frequency invariant results near the -30-dB level.

Magrath. At Magrath, Alberta, Phase One was on the top of a hill at 3675 ft above MSL, and in the repeat sector first looked down the side of this hill to low-lying terrain along Pothole Creek at elevations of about 3200 ft above MSL at 8- to 9-km range and then up the terrain rising beyond Pothole Creek to elevations of about 3500 ft above MSL at 11-km range. At longer ranges, this terrain continues to rise up the Milk River Ridge, a significant terrain feature in southern Alberta. Within the Magrath repeat sector, the land is 75 percent farmland, 22 percent rangeland, 1 percent built-up, and 2 percent water, as in streams, irrigation canals, and reservoirs. Much of the farmland around Magrath is irrigated. The natural terrain around Magrath is almost treeless (the percent tree cover in our Magrath repeat sector, as derived from 1:10,000 scale aerial photos, is zero). We occasionally refer to Magrath as the canonical tree-free site. Lack of trees does not affect mean clutter strength significantly, but it does affect spread in clutter amplitude distributions. Magrath was measured in late May/early June of 1983, at a very similar time of year as Beulah. Severe wind conditions (averaging 25 to 35 mph with gusts of 45 to 65 mph) occurred on several occasions at Magrath and slowed down Phase One operations. Both ground-based and helicopter-based propagation measurements were conducted at Magrath to establish the multipath environment there. In these measurements, Phase One was the transmitter, and the receiver was either on a helicopter flying vertical ascents/descents or at our manually transportable 70-ft calibration tower (see Figure A-10) where the receive antenna was cranked up and down.

Mean clutter strengths versus frequency for the Magrath repeat sector are shown in Figure E-118. In contrast to the Beulah results of Figure E-113, at Magrath horizontally polarized mean strength was observed to be 8 dB stronger than vertical for the 150-m pulse at VHF — just the opposite to what we observed at Beulah. Otherwise, there is a great deal of similarity between the Magrath and Beulah results, including tight clusters at UHF and L-band, a slight S-band dip between L- and X-band, and overall levels remarkably similar near -30 dB.

Beiseker. We now turn to Beiseker. A photograph of the Beiseker terrain is shown in Figure 63. Beiseker was one of our most intensively investigated sites. For example, Phase One made four visits to Beiseker to establish seasonal variations in clutter. The most visits Phase One made to any other site was two. Also, we made ground-based and helicopter-borne propagation tests there for three of the four visits to establish the multipath properties at the site. In addition, we performed special Phase One external calibration tests at Beiseker involving balloon-borne spheres and moving spheres sliding down a 45-deg line to corroborate our standard tower-mounted corner reflector and standard gain antenna calibration tests (for a discussion of these standard tests, see Appendix A). Finally, we arranged to bring Phase Zero to Beiseker while Phase One was there, measured the same clutter at nearly the same time (i.e., sequentially, not simultaneously) from nearly the same place (i.e., the two radars were set up side by side), and performed a relatively in-depth analysis of the resulting coincident data, partly to corroborate the calibrations of the two radars and partly to understand the differences in measurements that can arise largely due to differing multipath effects as a result of the different elevation beamwidths (viz., 23 deg for

Phase Zero, 3 deg for Phase One at X-band). We performed Phase Zero/Phase One coincident clutter measurements at one other site, Knolls, Utah, where the terrain measured was canonically flat desert in the neighborhood of the Bonneville salt flats (see Section 4.1.5).

At Beiseker, the measurement position was on a local topographic high point at 3180 ft above MSL. A three-dimensional oblique view of the Beiseker terrain generated from DTED is shown in Figure 64. The repeat sector was directed SSE. In this direction, the terrain elevation gradually fell away to elevations of about 2775 ft above MSL in the neighborhood of the Rosebud River at about 9-km range, and then the terrain elevations gradually rose beyond the river to about 3125 ft above MSL at about 17-km range. The land cover in the repeat sector was 88 percent farmland, 11 percent rangeland, and 1 percent nonforested wetland. An aerial photo of all of the terrain in the Beiseker repeat sector at 1:50,000 scale is shown in Figure 65. A CIR aerial photo of some of the terrain (centered at 12 km, 157 deg) in the Beiseker repeat sector at 1:10,000 scale is shown in Figure 66. With a little scrutiny the terrain in Figure 66 can be located within the aerial photo of Figure 65.

Figure 67 shows mean clutter strength versus frequency for the Beiseker repeat sector for all four Phase One visits. Figure 67 is repeated in Appendix E with additional explanatory notes. We begin by making several general observations about the data in Figure 67. First, there is very little general variation with season from visit to visit across the four visits. Second, the data generally support the idea of frequency independence of mean clutter strength in moderately low-relief farmland at about the -30-dB level. (The median value of all the mean clutter strengths plotted in Figure 67 is -29.5 dB.) Third, UHF mean strengths are generally about 6 dB weaker than the other four bands. This is due to a site-specific UHF multipath propagation loss in the Beiseker repeat sector, which will be explained shortly.

Seasonal Variations at Beiseker. The visit-to-visit variations in mean clutter strength shown in Figure 67 are now discussed in more detail. First, some capsule comments describing the seasonal state of the Beiseker terrain for each of the four visits are given. Photographs of the terrain for each of the four visits are provided in Appendix E. The first visit to Beiseker was a fall visit from 18 October to 13 November 1982. At this time there were mostly stubbly and plowed fields without much snow. Crops had been harvested. Two inches of wet snow fell on arrival day but mostly melted off in the next few days. Light snow occasionally fell during early morning hours but usually disappeared later in the day. Daytime temperatures through the data collection period varied from 41°F to 60°F.

The second visit to Beiseker was a winter visit from 12 February to 24 February 1983. The fields were covered with 2 to 10 cm of crusted snow during the entire visit; however, stubble was sticking up through the snow in some fields. Daytime temperatures through the data collection period varied from 13°F to 42°F.

The third visit to Beiseker was a summer visit from 6 August to 24 August 1983. At this time, there were mostly fields containing mature crops, primarily grains (e.g., wheat, barley, oats) but also rapeseed and alfalfa. Harvesting of some crops had begun, so some fields were bare. However, we obtained most of the data with the crops still up. Daytime temperatures through the data collection period varied from 63°F to 80°F.

Figure 62. Inclined cropland at Beulah. Typical strip farming cropland at far range in repeat sector looking ESE up rising terrain.

The fourth visit to Beiseker was planned to be an annual repeat of the first visit to provide year-to-year variations, in contrast to the seasonal variations provided by the first three visits. However, scheduling did not work out, so the fourth visit was a later fall visit from 16 November to 26 November 1983. At this time, there were quite wintry fields, as in the February visit, but without the old crusted snow. During this visit, there was usually some new light snow in the morning, which would not completely disappear in the afternoon. The ground was frozen at all times, and, also at all times, the view was basically of white fields, although with thin snow cover and with stubble sticking through. Daytime temperatures during the data collection period varied from 14°F to 30°F.

Figure 63. Beiseker terrain looking west. Phase One equipment visible in middle distance. August 1983.

Thus, across the four Beiseker visits, we experienced quite different seasonal status of the agricultural field surfaces. A major reason we chose Beiseker for four seasonal visits was because the clutter returns at Beiseker were strongly affected by multipath at all frequencies. We believed that the varying seasonal states of the field surfaces might more significantly affect clutter returns through varying reflection coefficients and hence varying multipath effects than through seasonal effects on the clutter sources themselves, many of which tend to be discrete vertical objects.

The seasonal variations in mean clutter strength at Beiseker, as shown in Figure 67, do little to support the view that very significant changes in multipath occurred with changing season at Beiseker. One can find occasional 5- and 6-dB differences* in mean strength with season in these data (e.g., between each of the first three visits and the fourth visit, at VHF, vertical polarization, 150-m pulse; and between second and fourth visits and second and first visits at L-band, horizontal polarization, with the 150-m

* And even one of 7.07 dB, the maximum Beiseker seasonal difference in mean strength for fourth visit minus second visit, L-band, 150-m pulse, vertical polarization.

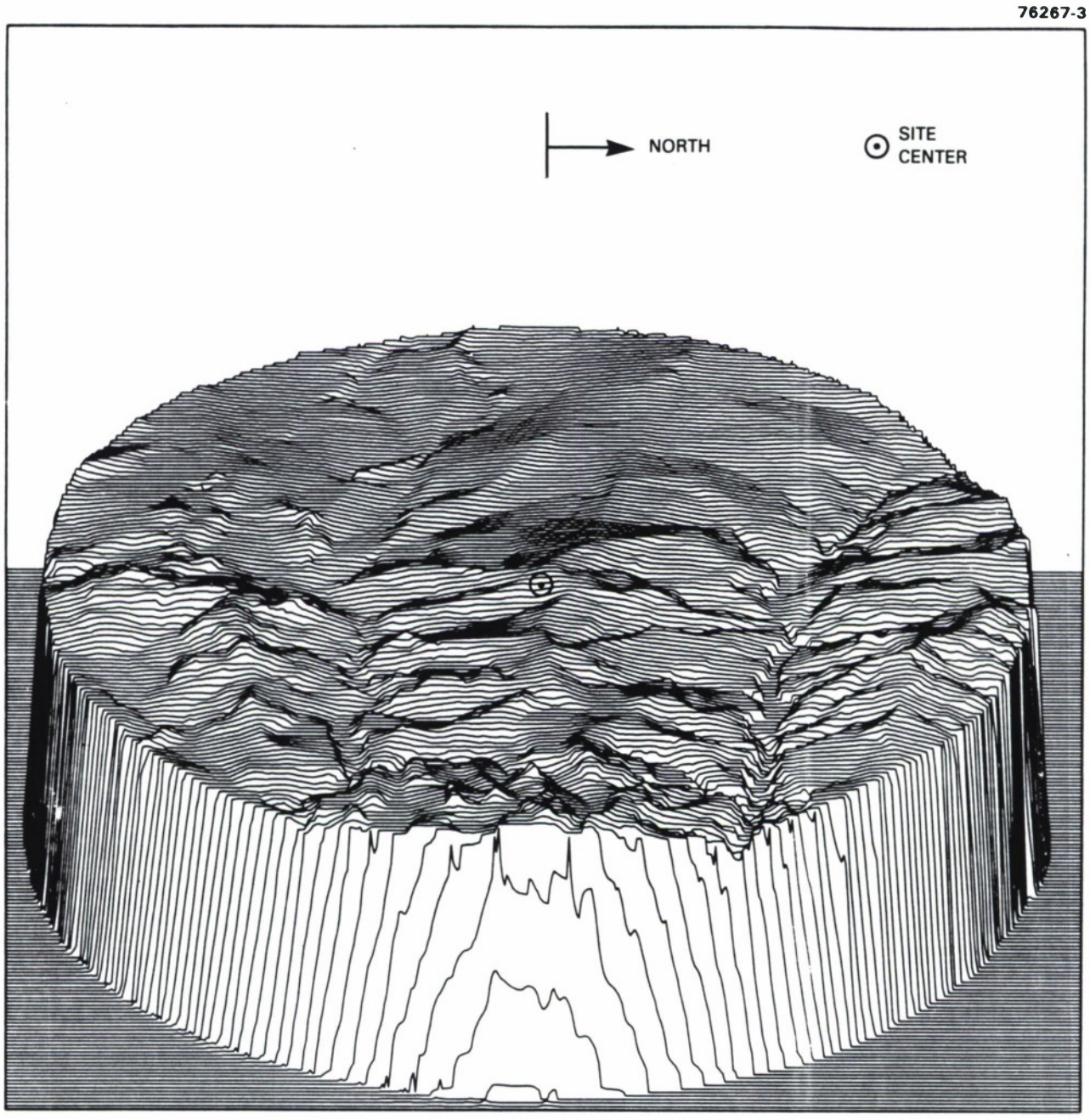

Figure 64. Three-dimensional oblique view of terrain at Beiseker, Alberta. Clutter measurement site is at the center of the diagram. Maximum range = 20 km. West is at zenith to better show the major east-west oriented waves on this terrain. Peak-to-valley relief is about 100 m. Based on data provided to DMA Format Level One by Defence Cartographic Mapping and Charting Establishment, Ottawa.

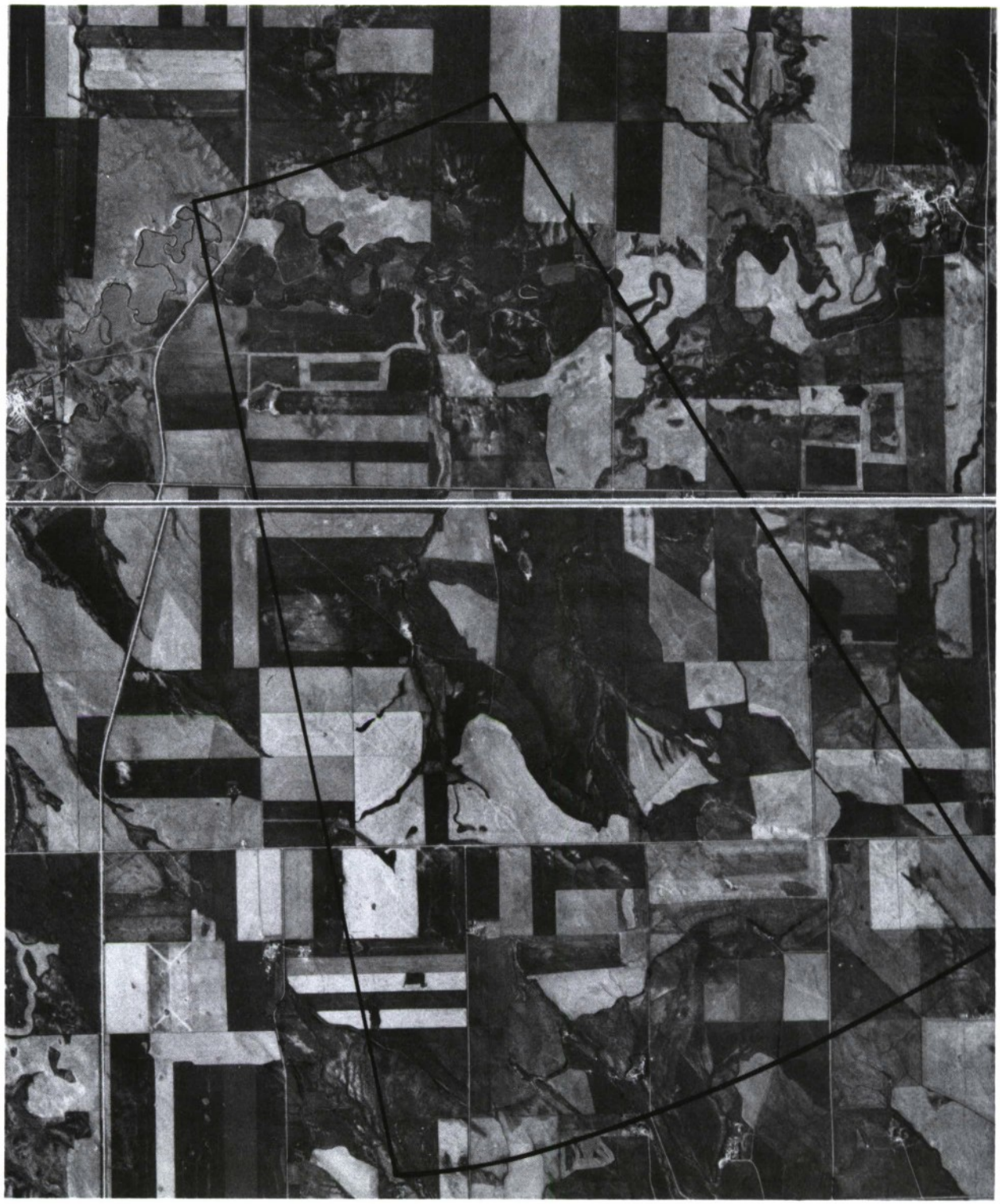

Figure 65. Aerial photo of repeat sector at Beiseker. Scale = 1:50,000. North is up.

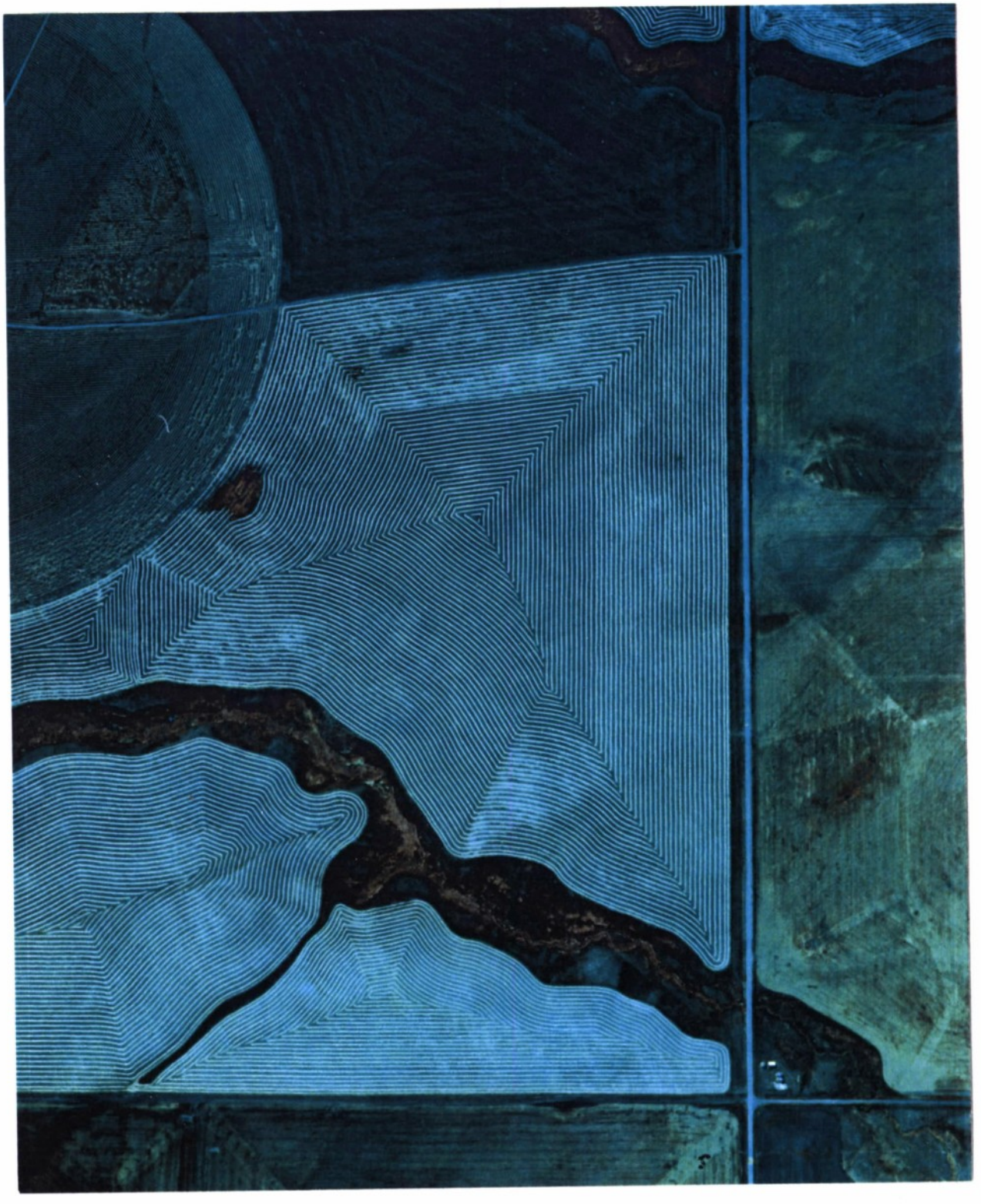

Figure 66. CIR aerial photo of repeat sector at Beiseker. Scale = 1:10,000. North is to the right.

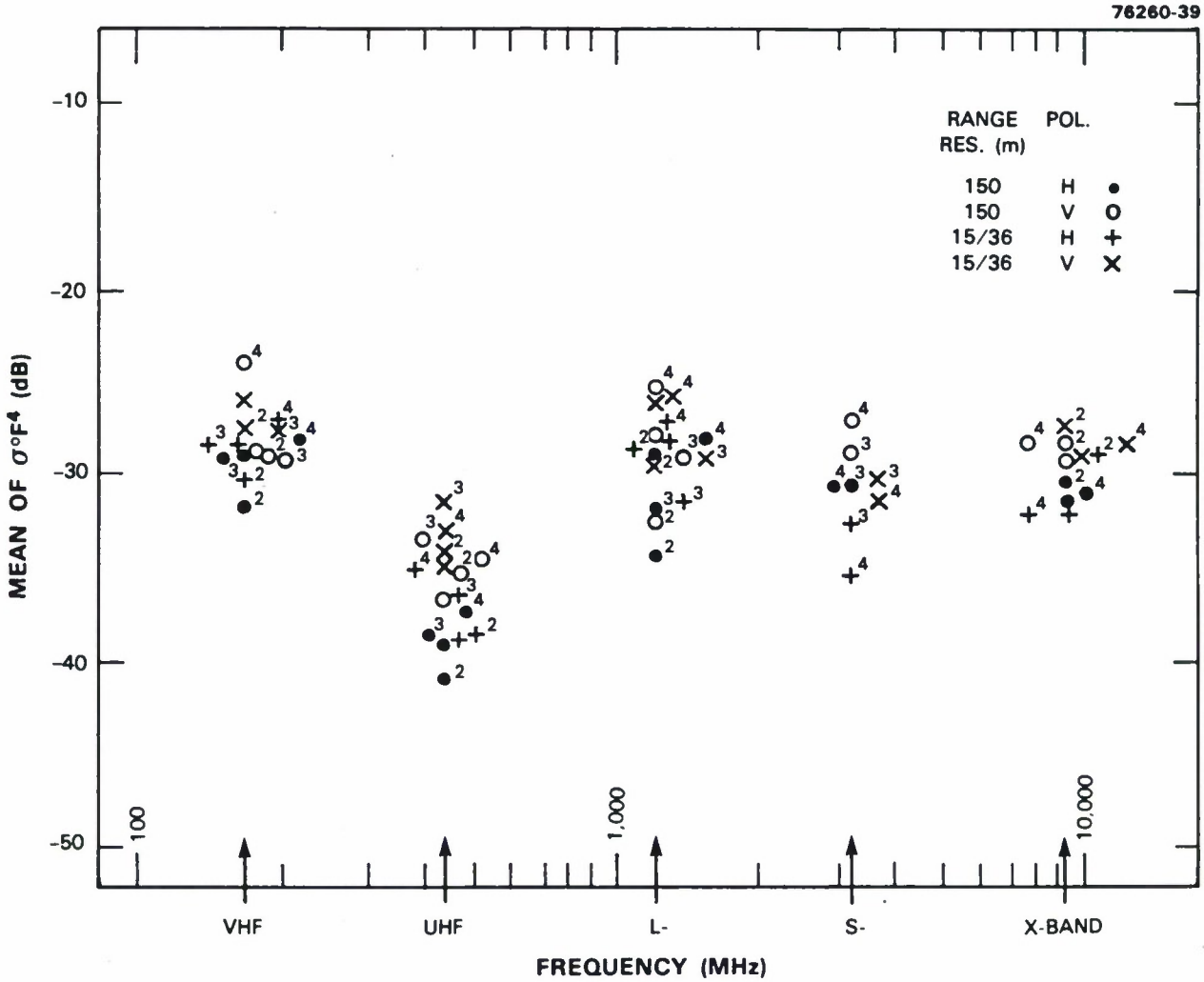

Figure 67. Seasonal variations in mean clutter strength at Beiseker. Repeat sector data. First visit, fall (18 October to 13 November 1982). Second visit, winter (12 February to 24 February 1983). Third visit, summer (6 August to 24 August 1983). Fourth visit, late fall (16 November to 26 November 1983). Second, third, and fourth visit results indicated by superscripts to the upper right.

pulse), but most of the Beiseker seasonal variations in mean strength are < 3 or 4 dB. Assuming all 88 differences in Figure 67 to be positive numbers (i.e., absolute values), 74 percent are ≤ 3.0 dB; 91 percent are ≤ 4.0 dB; the modal (i.e., most likely) difference is 1.0 dB; the median difference is 1.7 dB; the mean difference is 2.0 dB; and the standard deviation is 1.5 dB. Furthermore, these variations do not exhibit any obvious particular pattern.

Certainly, the summer visit results (i.e., third visit) with crops in the fields do not stand out from the other three visits without crops. There is an indication that the fourth visit results are strongest and the second visit results weakest at VHF, UHF, and L-band (where multipath effects might be stronger) in the 150-m pulse data, especially at horizontal polarization. However, this indication is less pronounced in the 15/36-m pulse data. Visually, fourth and second visits provided relatively similar-looking field surfaces compared to the other visits. In examining the data of Figure 67 beyond this, we need to be aware of the notes in Figure E-126 (i.e., no S-band data for first and second visits; no X-band data for third visit; questionable VHF data at 36-m resolution for second visit; no VHF 36-m data at vertical polarization for fourth visit; a shorter range interval, viz., 8.0 to 13.9 km, for the S-band 15-m results, both polarizations, for third and fourth visits). A selected set of the seasonal differences in Figure 67 are included in our overall histogram of seasonal differences in mean clutter strength (for a given frequency, polarization, and pulse length) measured in six Phase One repeated visits presented and discussed in Section 7.2.

It is fair to conclude from the data of Figure 67 that seasonal variations in clutter returns at a given site are quite small (e.g., several decibels) compared to the sorts of spatial variations that can occur in similar terrain from site to site. However, these several decibels may be highly significant in the operations of a particular radar at a particular site.

Multipath at Beiseker. We now consider multipath in the Beiseker repeat sector and how it explains the UHF dip in the data of Figure 67. The situation is illustrated by the sketch in Figure 68. From Beiseker site center, looking into the repeat sector, for the first kilometer out from the radar, the terrain was inclined away from the radar at a relatively constant angle of 1.4 deg, like a tilted flat surface. For the next 700 m the terrain leveled out, and then beyond 1.7 km, proceeded to continue to fall off in elevation towards the Rosebud River. The DTED profile of Figure 61, for which the source map was at 1:250,000 scale, does not capture these details. Thus, the first kilometer of 1.4-deg tilted flat surface would be expected to dominate multipath characteristics. Indeed, for the 57-ft antenna mast height, the second null (i.e., the first null above the horizon plane null) on the UHF multipath lobing pattern in elevation occurs at 1.12 deg above the plane of this tilted surface, assuming unity reflection coefficient from the tilted surface (see Figure B-4). Thus, with respect to local horizontal at the Phase One antenna, this null occurs at 0.28-deg depression angle below the horizontal, which is close to the depression angle at which we illuminate the centroid of the repeat sector range interval from 8 to 17 km (viz., 0.39 deg). Thus, at UHF, the rising terrain from beyond the Rosebud River that constitutes the repeat sector interval is weakly illuminated in a null of the multipath lobing pattern. In fact, this null, centered at 0.28-deg depression angle, has an angular width from 0.47-deg depression angle to 0.09-deg depression angle in which there is a propagation loss (i.e., $F < 1$). This angular width covers most of the repeat sector range interval from 8 to 17 km and explains the approximately 6-dB weaker mean clutter strengths at UHF over this interval compared with the other bands in Figure 67.

Looking more closely at Figure 67, we observe that the VHF mean strengths are slightly stronger than the L-, S-, and X-band mean strengths. (The median of all the VHF mean strengths in Figure 67 is -28.6 dB; the median of all the L-, S-, and X-band mean strengths is -29.4 dB.) The peak of the first VHF lobe on the multipath lobing pattern occurs at 1.48 deg above the tilted surface or at 0-deg depression angle. As a result, at VHF illumination is enhanced (i.e., $F > 1$) over the complete range interval from 8 to 17 km. Thus, effective clutter strengths are slightly augmented at VHF compared with the higher bands that cast multiple lobes over this interval and hence obtain effective gain averaged over both peaks and nulls.

In considering multipath effects on clutter strengths in the manner discussed above for Beiseker, and similarly at other sites in this report, it is often important to know the terrain slope near the Phase One radar. Obtaining terrain slope from topographic contour maps is often relatively crude (e.g., typical contour interval = 25 ft)* and results in approximating the real terrain with sloped facets running from contour line to contour line. One is left with the question of determining which facets provide active reflecting Fresnel zones causing the multipath. Then the effective Phase One antenna mast height that controls the periodicity of the multipath lobing is the height above the plane of this facet, which can be less than or greater than the actual mast height. These matters are discussed in Section B.2 of Appendix B.

At Beiseker, the crude faceted topographic map model left ambiguity in explaining the UHF dip in mean clutter strengths in Figure 67. As a result, and as part of our special emphasis of Beiseker, we carefully ran our own survey of terrain elevations into the repeat sector, nominally every 50 m for the first 6 km. (We also surveyed into the repeat sector at Cochrane, every 25 m for the first 315 m.) This Beiseker survey unambiguously provided the 1.4-deg terrain slope causing multipath and thus explained the relatively weak effective clutter strengths at UHF.

4.1.4.3 Very Low-Relief Agricultural Terrain. Table 7 indicates that we have six sites within the category of very low-relief agricultural terrain with terrain slopes of less than 1 deg. A photograph of the terrain in the repeat sector at one of these sites, Pakowki Lake, is shown in Figure 69. In Table 7, the only landform classes occurring for the repeat sectors at these sites are 1, level and 3, undulating. Note in particular the absence of landform class 2, inclined, or any other landform classes of greater relief. The only land cover classes occurring are 21, cropland, with occasional secondary occurrence of 31, herbaceous rangeland, but no occurrence of dramatically different types of land cover. (The town of Wolseley originally occurred in the far ranges of the Wolseley repeat sector from 10 to 12 km, but we removed the last 2 km from this sector.) Thus, this group of repeat sectors is unequivocally just general low-relief farmland relatively uncontaminated by the sorts of specific terrain features in relief or land cover that so often dominate our measurements.

There is a large range of depression angles for these six sites in Table 7, from 1.2 to 0.15 deg. Three of the sites, Orion, Wolseley, and Rosetown Hill, although looking at level and/or undulating cropland

* That is, the contour interval is usually 25 ft in the large scale 1:50,000 maps available for most of our Canadian sites. The contour interval is usually much greater, i.e., 100 ft, in the 1:250,000 scale DTED source maps.

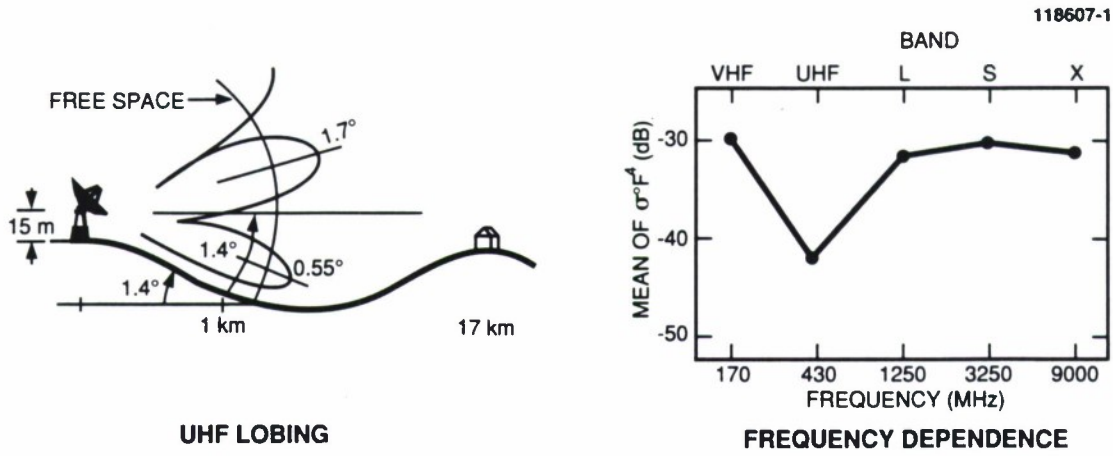

Figure 68. Effects of UHF multipath on clutter strength at Beiseker, Alberta.

in their repeat sectors, were set up on hills 335, 180, and 98 ft, respectively, above their repeat sectors (leading to depression angles of 1.2, 0.5, and 0.4 deg, respectively). The other three sites all had little or no terrain elevation advantage over their repeat sectors; they illuminated their repeat sectors at 0.3-, 0.2-, and 0.15-deg depression angle. DTED terrain profiles through the repeat sectors of these six sites are shown in Figure 70.

As with any six different locations on the surface of the earth, there are some differences among these six sites. Pakowki Lake and Orion, like Neepawa and Polonia previously discussed, provide another pair of repeat sectors looking at one another. However, unlike Neepawa and Polonia, Pakowki Lake and Orion are separated by 19.5 km, so their respective repeat sector range intervals, each extending from 1 to 10 km, essentially do not overlap (or, more precisely, only provide a common overlapping interval in their last 0.5 km). These two sites occur in relatively dry prairie grassland terrain in southeastern Alberta under irrigation for agriculture (note that each has a secondary land cover component of rangeland). The lake bed of Pakowki Lake is usually dry (and was when we measured there). The Orion site looks down from its hilltop location out across undulating terrain towards the dry lake bed at about 22 km range. The terrain falls off fairly quickly in the first 2 km of the Orion repeat sector, but then falls off much more slowly,

at an average slope of about 0.2 deg. The Pakowki Lake site is located near the dry lake bed and looks back toward Orion. The terrain very gradually rises through the Pakowki Lake repeat sector at 0.17 deg. An aerial photo of the terrain in the Pakowki Lake repeat sector is shown in Figure 71.

Of these six sites, some have significant incidence of trees (e.g., Wolseley and Shilo) and some do not. Some are on hills, some are not, and one, Corinne, is situated on the extremely level Regina Plain in southern Saskatchewan. Some are dry and approaching rangeland conditions, others are black-earth cropland with plenty of average rainfall. At these six sites, by coincidence, almost all of the Phase One measurements were obtained in winter season, December through March (see Table 1), except for Corinne, which was measured in April but still before any crops were up. However, recall that clutter measurements from our four seasonal visits to Beiseker showed little variation with season in agricultural terrain. At the five winter season sites, there were generally several inches of snow on the fields, and the fields were either plowed or stubble, with the stubble sticking through the snow [see Figure 3(b)].

Multifrequency mean clutter strengths measured over the repeat sectors at the six very low-relief agricultural sites are shown in Figure 72. This characteristic is remarkably different from that of Figure 60 for moderately low-relief agricultural sites. As in the moderately low-relief data, the very low-relief data show essential invariance of mean clutter strength with frequency at L-, S-, and X-bands, but unlike the moderately low-relief data that also hold this level at UHF and VHF, the very low-relief data drop to lower levels at UHF and much lower levels at VHF. If we go to the median value of all the mean strengths plotted in each band in Figure 72 (see Table 11), this value holds constant within a few tenths of a decibel of -31 dB at L-, S-, and X-bands, but drops 10 dB to -41 dB at UHF, and drops 25 dB to -56 dB at VHF. These large decreases in effective clutter strength at UHF and VHF on very low-relief agricultural terrain are due to multipath loss entering through the propagation factor. That is, at these open agricultural sites, forward terrain reflections cause multipath lobing on the vertical elevation beam of the antenna, and the terrain is so level that, at the lower frequencies, the returns from the clutter sources are received well down in the first (i.e., horizon plane) null, increasingly so as frequency decreases from L-band to UHF to VHF.

Thus, as a group, these very low-relief sites provide a very different multifrequency mean strength characteristic than the previous moderately low-relief group. At the very low-relief sites, first the terrain does not slope away from the site enough to tilt the lobing pattern down very much, and second, terrain elevation variations farther out are not large enough to cause the far-out illuminated terrain to rise back up through the lobing pattern with increasing range through the repeat sector. Rather, the levelness of the terrain at very low-relief sites constrains the effective gain of the illumination to be locked deep into the horizon plane null at VHF and UHF. Our terrain classification system effectively finds such level sites by separating inclined terrain of landform = 2 (1 deg < terrain slopes < 2 deg) from level or undulating terrain of landform = 1 or 3 (terrain slopes < 1 deg). Given the complexities in clutter from real terrain, we feel fortunate that our classification system provides us this important correlative, and hence, predictive capability on the basis of what, at root, is a fairly coarse classifier.

Hilltop Versus Level Sites. That this classification procedure is actually setting a threshold within a spectrum of terrain and propagation influences, and not just separating black and white situations, may be appreciated more by comparing, within the very low-relief sites, the multifrequency mean strength characteristics from the hilltop sites with those from the level sites. For the three hilltop sites, Orion,

Rosetown Hill, and Wolseley, the mean strengths at UHF cluster very tightly at a median level of mean strength of -39 dB. (This cluster provides as good site-to-site repeatability as we ever see, such that all 12 measurements fall within a range of +4 dB and -6 dB about the median.) For two of these hilltop sites, Orion and Rosetown Hill, the mean strengths at VHF also cluster closely, at a median level of -48 dB (over a range of +3 dB and -8 dB about this level). For the three level sites, Corinne, Shilo, and Pakowki Lake, the UHF and VHF groups of mean strengths also cluster quite well, at median levels of -46 dB and -57.5 dB, respectively. Thus, in terms of median values of clustered groups of measurements of mean strength, level sites provide 7 dB and 9.5 dB lower mean strengths, or increased multipath propagation losses, compared with hilltop sites, at UHF and VHF, respectively, all in very low-relief agricultural terrain with terrain slopes < 1 deg. The reason for this, as discussed elsewhere (see Appendix B, Section B.2), is that, for the hilltop sites, the terrain sloping away from the site tilts the multipath lobing pattern down, causing the effective antenna gain against the farther out level terrain to start to rise, but not enough to clearly get out of the null and up on the peak of the pattern, as happens in moderately low-relief terrain with terrain slopes between 1 and 2 deg.

Rosetown Hill is a classic example of this situation with a definite local hill rising 100 ft or so above surrounding level terrain. Thus, in the repeat sector direction, the terrain drops 98 ft in the first 2.5 km away from the site (i.e., 0.7-deg terrain slope), and then levels out, with the repeat sector mean strength range interval starting at 4 km.* On the other hand, the situation remaining to be discussed from the above examples, namely, Wolseley at VHF, is different. A photograph of the Wolseley terrain is shown in Figure 73. Wolseley is less of a clear-cut local hilltop situation, and more just a general topographic high, with the terrain gradually falling away in the repeat sector direction towards the Qu'Appelle River valley at 25-km range. The terrain falls faster (150 ft) over the first 6 km (0.4 deg terrain slope) and slower (25 ft) over the next 4 km that constitute the repeat sector range interval. At VHF, with its broader horizon plane null, these terrain variations are not enough to substantially increase the illumination, and at VHF the Wolseley mean strength data fit the level terrain group much better than the hilltop group (in fact, at a median level of -62 dB, and with a range about this of ± 5 dB, the Wolseley VHF mean strengths are actually lower than most of the level terrain data). At UHF, however, the Wolseley terrain elevation variations are enough to increase the gain on the elevation lobing pattern as with the other hilltop sites in very low-relief agricultural terrain.

At the Phase One microwave frequencies, L-, S-, and X-band, mean strengths for these very low-relief agricultural sites are invariant with frequency, as discussed above, and invariant between the hilltop and level sites. The fact that mean strengths separate between these two groups at VHF and UHF is an indication that depression angle can be used as the separation parameter (i.e., 0.4 deg ≤ depression angle ≤ 1.2 deg for the hilltop sites, 0.15 deg ≤ depression angle ≤ 0.3 deg for the level sites, see Table 7). The fact that depression angle does not separate mean strengths in low-relief agricultural terrain in the microwave bands has been observed previously in the Phase Zero X-band data. Although mean strengths of clutter amplitude distributions do not vary with depression angle in agricultural terrain in the microwave bands, the spreads or dispersions in these distributions vary extremely rapidly with depression angle, decreasing as

* The Rosetown Hill DTED terrain profile in Figure 70 does not capture these details accurately.

Figure 69. Very low-relief cropland in Pakowki Lake repeat sector. Range = 4 km, viewing direction is NNW. Irrigation ditch on level cropland.

depression angle rises. This was also observed in the Phase Zero data. Thus, our model for the behavior of these distributions in agricultural terrain is based on small gradations in depression angle, even though microwave mean strengths are invariant with both frequency and depression angle in such terrain.

Phase Zero. Table 11 shows that the median value of mean clutter strength at X-band over all Phase One repeat sector measurements at the six very low-relief agricultural sites is -31.5 dB. This value will be compared with what Phase Zero measured in similar terrain. As previously mentioned, for 724 patches classified primarily as agricultural low-relief (not just very low-relief), the median value of mean clutter strength measured by Phase Zero was -31.6 dB, essentially identical to the Phase One value for very low-relief. If from this set of patches, the subsets that are purely classified as level and undulating

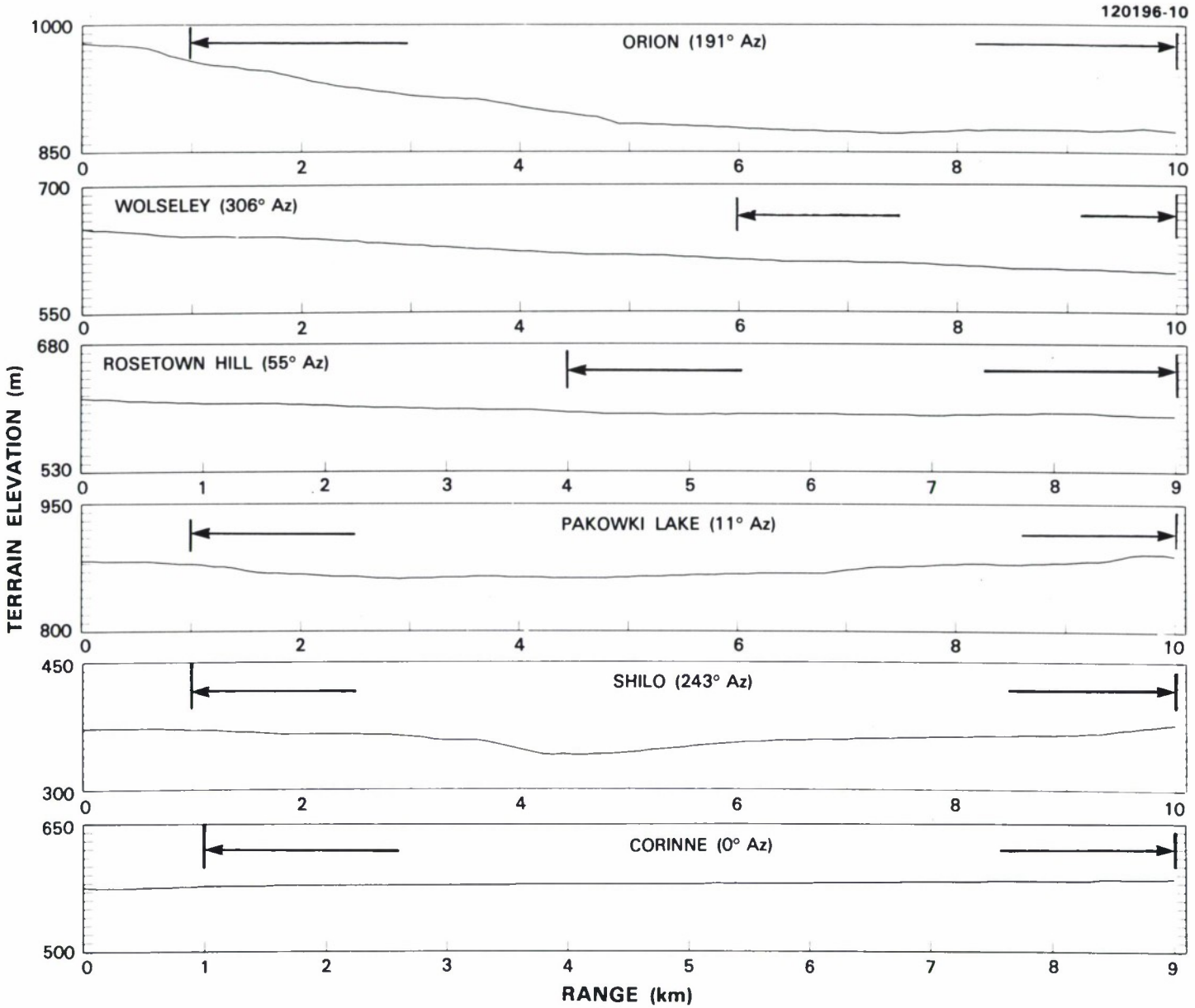

Figure 70. DTED terrain profiles in six very low-relief agricultural repeat sectors. Elevation in meters above mean sea level, 10 m between tick marks. Range extent of repeat sectors is indicated by horizontal arrows.

Figure 71. Aerial photo of repeat sector at Pakowki Lake. Scale = 1:50,000. North is up.

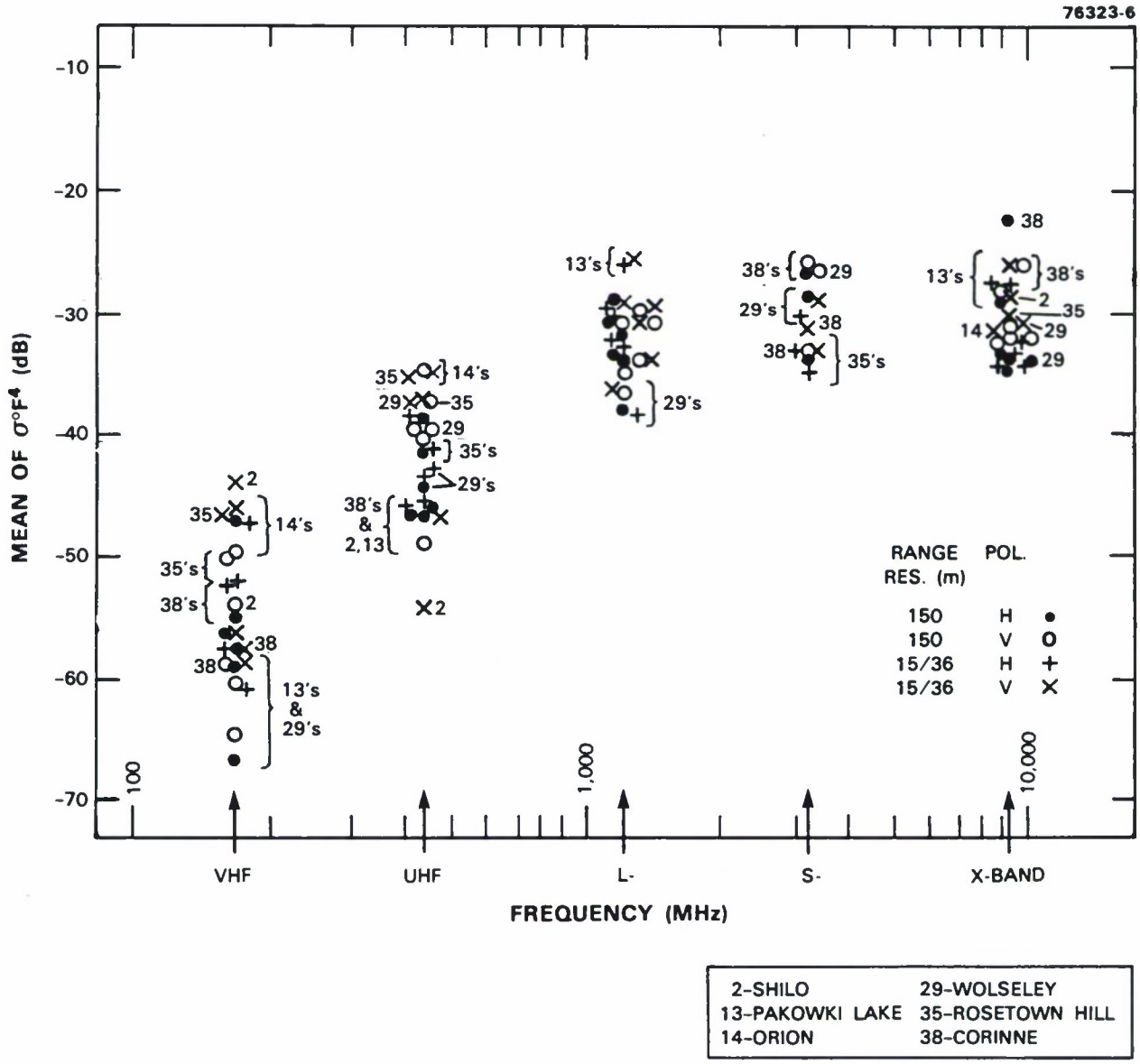

Figure 72. Mean clutter strength versus frequency for agricultural/very low-relief terrain. See Table 7.

cropland with no complicating secondary classification are considered, thereby restricting terrain slopes to be < 1 deg as in the very low-relief repeat sectors, there remain 85 and 77 patches, respectively. The median values of mean clutter strength are equal to -33.6 dB and -32.0 dB, undulating higher than level as expected, or -33.1 dB over both level and undulating patches. The Phase One median value of -31.5 dB in this terrain category matches these Phase Zero values quite closely. For five of the six* Phase One sites with repeat sectors in this terrain group, comparisons of repeat sector mean strength between Phase Zero and Phase One (150-m pulse, horizontal polarization), respectively, are as follows: Rosetown Hill, -34.2 versus -34.4 dB; Pakowki Lake, -30.2 versus -29.3 dB; Shilo, -36.1 versus -34.9 dB; Orion, -30.9 versus -34.0 dB; Corinne, -29.6 versus -22.6 dB. On the whole, the correspondence between Phase Zero and Phase One results in the above list is regarded as excellent, especially because multipath propagation is strongly at work in these measurements, and the resultant values of propagation factor F would be expected to be significantly different between Phase Zero and Phase One, given their different vertical antenna beamwidths of 23 and 3 deg, respectively (and slightly different tower heights of 50 and 59.1 ft, respectively).

The one significant deviation in the above list is Corinne, with a difference of 7 dB, Phase One higher. Looking ahead to Figure 78, we see that, in 11 X-band Phase One mean strength measurements of the Corinne repeat sector at three antenna heights and both pulse lengths and polarizations, the particular value of -22.6 dB (for three tower sections = 59.1 ft, 150-m pulse, horizontal polarization) compared with Phase Zero in the above list stands apart as being significantly stronger than the remaining ten which form a close group. The median level in this close group of 10 mean strengths is -28.3 dB, much closer to the Phase Zero measurement of -29.6 dB. Presumably, the strong -22.6-dB value is just a particular outcome of variable multipath illumination as tower heights, beamwidths, polarizations, and resolutions vary.

Shilo. We now discuss results from Shilo, Manitoba. Shilo was the first Canadian site, measured in February 1982. The weather was very cold while we were at Shilo, with daytime highs not rising above -20°F for most of the month-long stay there (see Appendix A). The terrain at Shilo was open prairie farmland strongly supportive of multipath. Terrain relief was low, less than 50 m over 10- to 20-km range extents, but the terrain was not dead level. The site position itself provided little elevation advantage over surrounding terrain, just 20 ft over the midpoint of the repeat sector. A photograph of the agricultural terrain in the repeat sector to the southwest at Shilo is shown in Figure 74. The terrain shown in this photograph is within geometric line-of-sight of the Phase One antenna. In such terrain, dominant clutter sources are vertical discretes. Phase Zero results are available for this Shilo terrain, including terrain elevation profiles, aerial photos, and X-band clutter results showing the discrete nature of the clutter and the typical discrete clutter sources.

Cumulative clutter amplitude distributions for the Shilo repeat sector at VHF, UHF, L-, and X-bands are shown in Figure 75. (The S-band transmitter was not operational at the first three Canadian sites; see Appendix A.) These distributions are formed by accumulating left to right across the underlying histogram. They include all samples within the range and azimuth limits specified, including those at radar

* The Phase Zero value for the Wolseley repeat sector with the town of Wolseley removed is not presently available.

Figure 73. Very low-relief cropland at Wolseley. Phase One tower-top view looking NNW toward repeat sector.

noise level, but are only shown as they emerge above the noise to the right of the maximum noise-contaminated bin. As such, they are absolute measures of probability of occurrence (i.e., percentile level) within the distribution; increasing radar sensitivity would affect these distributions only by extending them farther to the left.

We observe that the spreads in the clutter amplitude distributions of Figure 75, as given by the ratio of standard deviation to mean, increase significantly with increasing frequency. This is caused by the resolution cell size of the radar decreasing with increasing frequency due to the decreasing azimuth beamwidth with increasing frequency (see Table 2). That is, as resolution cell size decreases, less averaging occurs within a cell, and more variation occurs from cell to cell. This is an important general effect and is incorporated in our clutter model.

Figure 74. Shilo repeat sector looking west. Very low-relief cropland.

A strong trend of increasing strength with increasing frequency is seen in the Shilo clutter amplitude statistics shown in Figure 75. This is the result of multipath decreasing the effective illumination of the clutter sources at the lower frequencies. This is illustrated in Figure 76. To the right in Figure 76, mean clutter strength is plotted versus frequency for the Shilo repeat sector (over a reduced range interval compared to Figure 75; in Figure 76, the range interval is that given in Table 7). To the left in Figure 76 are graphics illustrating how multipath causes the strong trend in mean clutter strength. Thus, on low-relief open terrain such as that at Shilo, strong forward terrain reflections cause multipath lobing on the free-space antenna pattern. At VHF these lobes are broad. As a result, backscatter from typical clutter sources such as trees and buildings is received well on the underside of the first multipath lobe, and effective clutter strengths are much reduced. This is entirely the result of propagation effects (i.e., multipath) entering clutter strength $\sigma^{o}F^{4}$ through the propagation factor F. Now, as indicated in the upper graphic in Figure 76, as frequency increases, the multipath lobes become narrower, and the first lobe is pressed

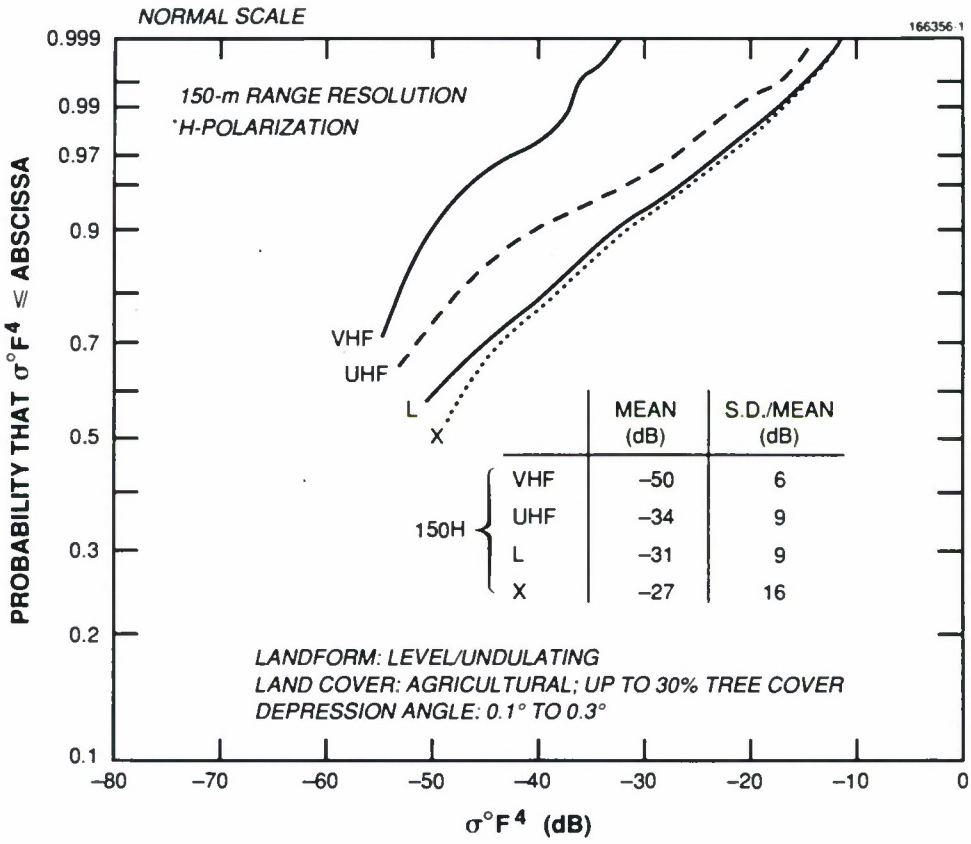

Figure 75. Measured multifrequency ground clutter amplitude statistics at Shilo, Manitoba. Range, 1.0 to 21.85 km. Azimuth, 228 to 258 deg.

closer and closer to the ground. As a result, effective clutter strengths rise until, in the microwave regime, typical clutter sources such as trees and buildings start to subtend a number of lobes and the effect starts to average out. The Shilo results of Figures 75 and 76 may be compared with the Polonia and Neepawa results of Figures 57 and 58, discussed previously in Section 4.1.4.1. The Shilo results show quite a different multifrequency mean clutter strength characteristic than at Polonia or Neepawa, from generally similar terrain to Polonia and Neepawa but under different multipath illumination conditions.

Antenna Height Variations at Shilo. At Shilo, we made some repeat sector measurements with only one antenna tower section extended, resulting in a reduced tower height of nominally 30 ft, as well as more complete measurements at a nominal height of 60 ft. Photographs of Phase One at Shilo with only one tower section extended are shown in Figures A-2 and A-3. Table A-5 gives exact antenna heights for different tower extensions. Table 8 indicates that, at X-band, out of five comparisons where similar measurements (i.e., same waveforms, same ranges) were available at both short and tall tower heights at Shilo, the short tower resulted in slightly stronger mean clutter strength three times, the tall tower gave slightly stronger clutter one time, and both towers gave the same mean strength one time. Thus, at X-band,

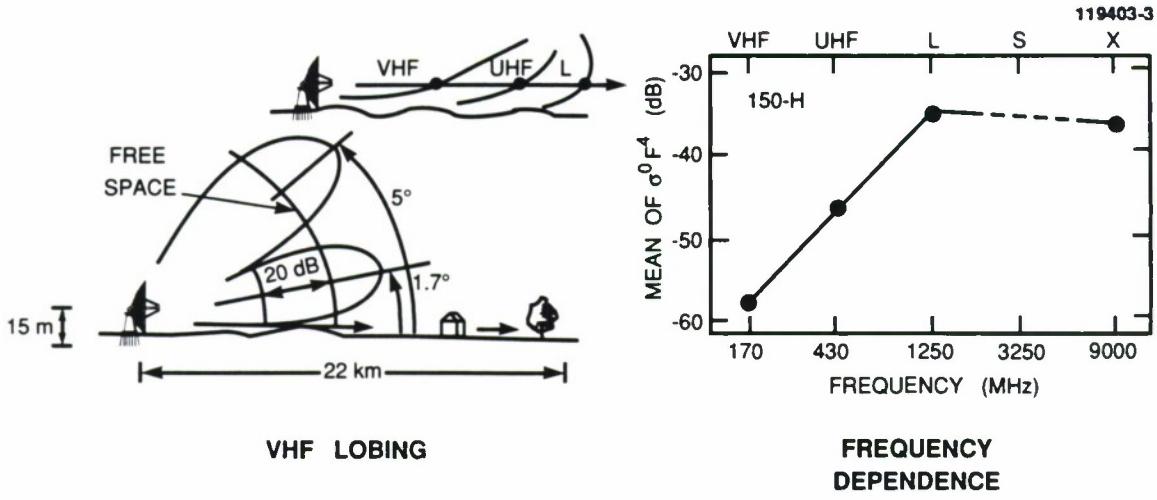

Figure 76. Effects of multipath on clutter strength at Shilo, Manitoba.

these antenna tower heights appear to have little effect on measured clutter strength over the ranges indicated in Table 8. Whether the tower is tall or short, the propagation lobes are narrow enough so that numerous lobes are subtended over typical sources such as trees and buildings, and changes in antenna height cause only minor variations in clutter strength as the lobes shift around over the sources.

However, at UHF, it is a different story. In Table 8, out of two available comparisons, the shorter tower in both cases resulted in much decreased (i.e., by 9 and 13 dB) mean clutter strength, even though the tall tower mean clutter strength was 10 to 15 dB weaker than that at X-band. That is, at UHF, even with the tall tower, there is a 10- to 15-dB multipath loss caused by illumination on the underside of the first propagation lobe, and this loss increases to 23 dB as tower height decreases from 60 to 30 ft and the first null-width broadens. This 9- to 13-dB decrease in mean clutter strength shown in the UHF data of Table 8 is approximately predictable by evaluating the propagation factor in the simple situation of multipath on a plane conducting surface, assuming a clutter source height of 15 m (i.e., like a tree or a house) at 5-km range. In these Shilo measurements, where multipath propagation loss substantially reduces clutter strength at VHF and UHF on open low-relief agricultural terrain, the amount of the loss depends significantly on antenna height.

TABLE 8

Short Tower and Tall Tower Clutter Strengths at Shilo[1]

Band	Waveform[2]	Range (km)	Tower Height[3] with Stronger Clutter	How Much Stronger (dB)	Approximate Mean Strength of Stronger Clutter (dB)
X	150 H	1–21.7	Short	2	–30 ±3
	150 H	1–10.3	Short	3	
	150 V	1–10.4	—	0	
	15 H	1–5.7	Short	3	
	15 V	1–10.4	Tall	3	
UHF	36 H	1–12.3	Tall	9	–45 ±5
	36 V	1–12.3	Tall	13	

Notes:
1. Low-relief farmland
   Some tree cover (up to 30 percent)
   Snow cover
2. Range resolution = 15, 36, 150 m; polarization = horizontal (H) or vertical (V)
3. Short = 30 ft; Tall = 60 ft

Antenna Height Variations at Suffield and Lethbridge West. At Suffield and Lethbridge West, as at Shilo, some repeat sector measurements were obtained with both one and three antenna tower sections extended. We briefly digress to discuss differences in repeat sector mean clutter strength with antenna height at Suffield and Lethbridge West, even though these two sites do not provide very low-relief agricultural terrain in their repeat sectors. Then we return to discuss antenna height variations at Corinne, the last very low-relief agricultural site yet to be discussed in this section. In the Suffield repeat sector (i.e., grassland plus discrete, 7 to 11.9 km, see Table 10 and Section 4.2), differences of the tall tower minus the short tower repeat sector mean strengths were 5.1, 2.5, -0.7, and 1.8 dB at VHF, UHF, L-, and X-band, respectively. In the Lethbridge West repeat sector (i.e., urban, 6 to 11.9 km, see Table 7 and Section 4.1.1), differences of the tall tower minus the short tower repeat sector mean strengths were 9.3, 10.2, 5.2, and -3.5 dB at VHF, UHF, L-, and X-band, respectively. These differences are averages of differences between individual experiments of like waveform (i.e., like polarization and pulse length) in each band. As expected, the differences are more significant at the lower frequencies and are greater at Lethbridge West where the terrain is quite level (even though the clutter is from relatively high urban sources) than at Suffield where the relief, although low, is significant (i.e., 50 m). We may further compare Suffield differences with Shilo, where the terrain profiles are quite similar (see Figures 70 and 85), and wonder why the tall tower UHF mean strength is 9 to 13 dB stronger than the short tower mean strength at Shilo but only 2 to 3 dB stronger at Suffield. We presume the answer has to do with multipath illumination specifics (i.e., different local terrain inclinations, different clutter source heights, etc.).

Antenna Height Variations at Corinne. We now turn to Corinne, the last very low-relief agricultural site, and the clutter measurements at different tower heights conducted there. In the preceding discussion and elsewhere in this report (e.g., Appendix B, also see Sections 4.1.1 and 3.2.1), we have discussed the fact that, in a multipath-dominated situation, the geometrical factors of antenna height, range, and clutter source height affect the amplitudes of received clutter returns. It is impracticable, however, to compute accurately the actual varying multipath illumination across the vertical extent of every clutter source. To provide empirical statistical insight into these matters, we now show multifrequency measurements of mean clutter strength for the Corinne repeat sector using three different Phase One antenna tower heights. An aerial photo of the repeat sector at Corinne is shown in Figure 77. A photograph of the Corinne terrain is shown in Figure 16(a). We selected Corinne for this sequence of tower height measurements because it is a canonically level farmland site with only farmland discretes rising as clutter sources above level fields.* The repeat sector azimuth extent at Corinne, 60 deg, is broader than at the other sites, allowing more statistical averaging to take place (i.e., more clutter sources). In such a "laboratory demonstration" type of environment, we should more easily than at other sites be able to understand real effects of multipath propagation on ground clutter. Indeed, similar tower height measurements were performed at Corinne earlier with Phase Zero at X-band only, and results are available in which these Phase Zero measurements are interpreted by means of propagation analysis and which show that, on the average, the X-band mean clutter strengths rose 6 dB when the Phase Zero mast was raised from 20 to 50 ft.

Figure 78 shows mean clutter strengths versus frequency for the Corinne repeat sector with three antenna tower heights. In this figure, the superscripts "L" and "M" appended, usually to the upper right of a data point, but occasionally to the upper left, stand for low tower (one antenna tower section) and medium tower (two sections), respectively (note: do not confuse the "L" superscript for low tower with L-band). The three-section (our standard height) high tower data are not superscripted. See Table A-5 for actual Phase One antenna center heights in feet for each band. What is seen in Figure 78 is relatively strong dependence of mean strength on frequency, but relatively weak dependence of mean strength on antenna height. Additional results are provided in Table 9. Median levels of mean strength over all repeat sector experiments in each band at both polarizations and pulse lengths are shown in Table 9; whereas, Figure 78 shows mean strengths from only one representative (i.e., "digest") experiment for each polarization and pulse length in each band.† Based on the many experiments underlying Table 9, differences of the tall tower (three sections) minus the low tower (one section) mean strengths were 5.1, 6.7, 5.6, 1.6, and 3.9 dB at VHF, UHF, L-, S-, and X-bands, respectively. Differences of the tall tower (three sections) minus the medium tower (two sections) mean strengths were 2.8, 2.2, 1.7, -1.2, and 2.6 dB at VHF, UHF, L-, S-, and X-bands, respectively. Differences of the medium tower (2 sections) minus the low tower (one section) mean strengths were 2.3, 4.5, 3.9, 2.8, and

---

* Corinne is the only site where we obtained Phase One measurements with one, two, and three antenna tower sections extended. At three other sites, Shilo, Suffield, and Lethbridge West, we obtained measurements with one and three antenna tower sections extended (see Table A-1).

† Furthermore, Figure 78 shows results over the complete 60-deg azimuth extent from 330 to 30 deg of the Corinne repeat sector (which required combining multiple experiments). Table 9 shows results over the complete 60-deg sector only for the 150-m pulse length experiments. For the 15/36-m pulse length experiments, Table 9 shows results from 330 to 30 deg at VHF and UHF, from 330 to 0 deg at L- and S-bands, and from 330 to 350 deg at X-band (i.e., individual experiments).

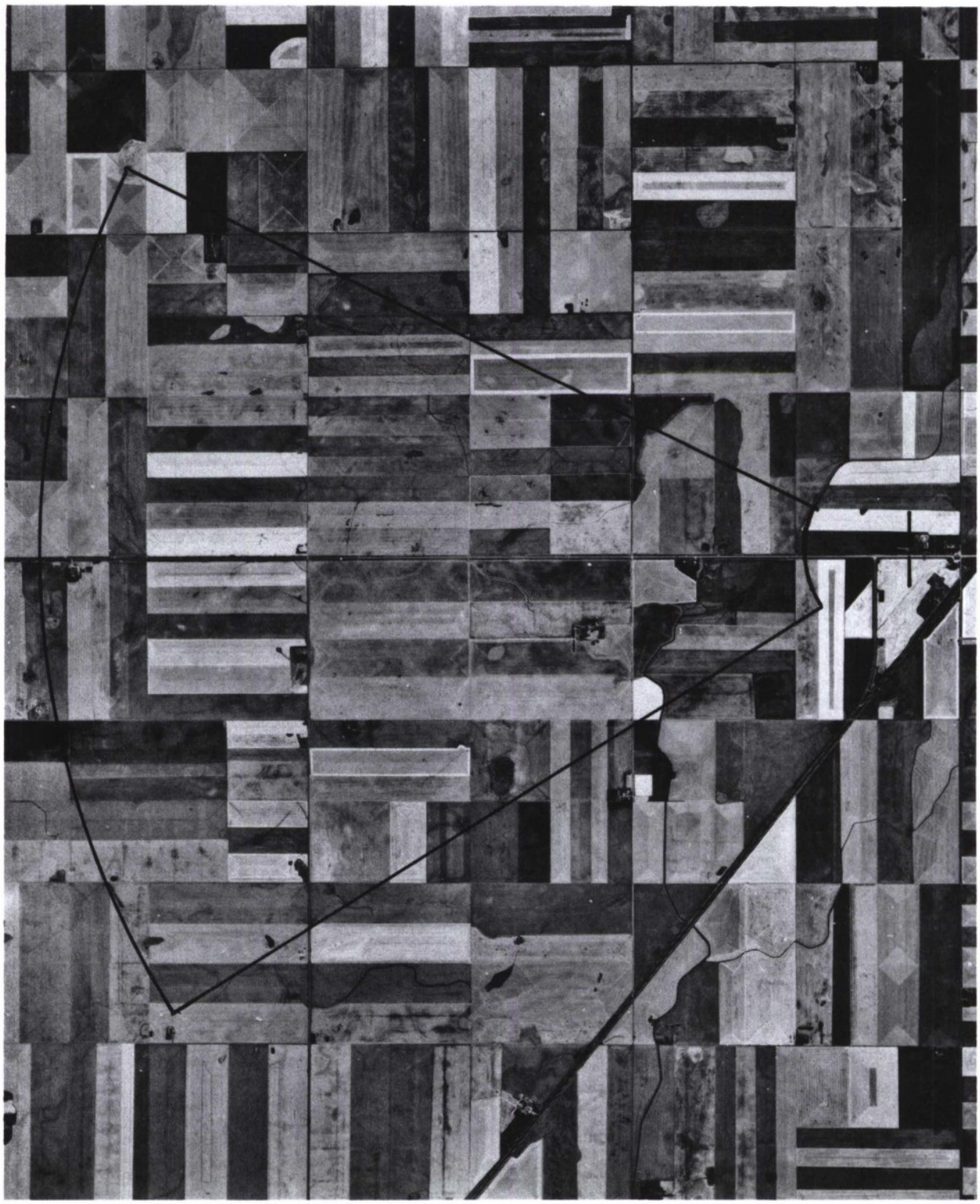

Figure 77. Aerial photo of repeat sector at Corinne. Scale = 1:50,000. North is to the left.

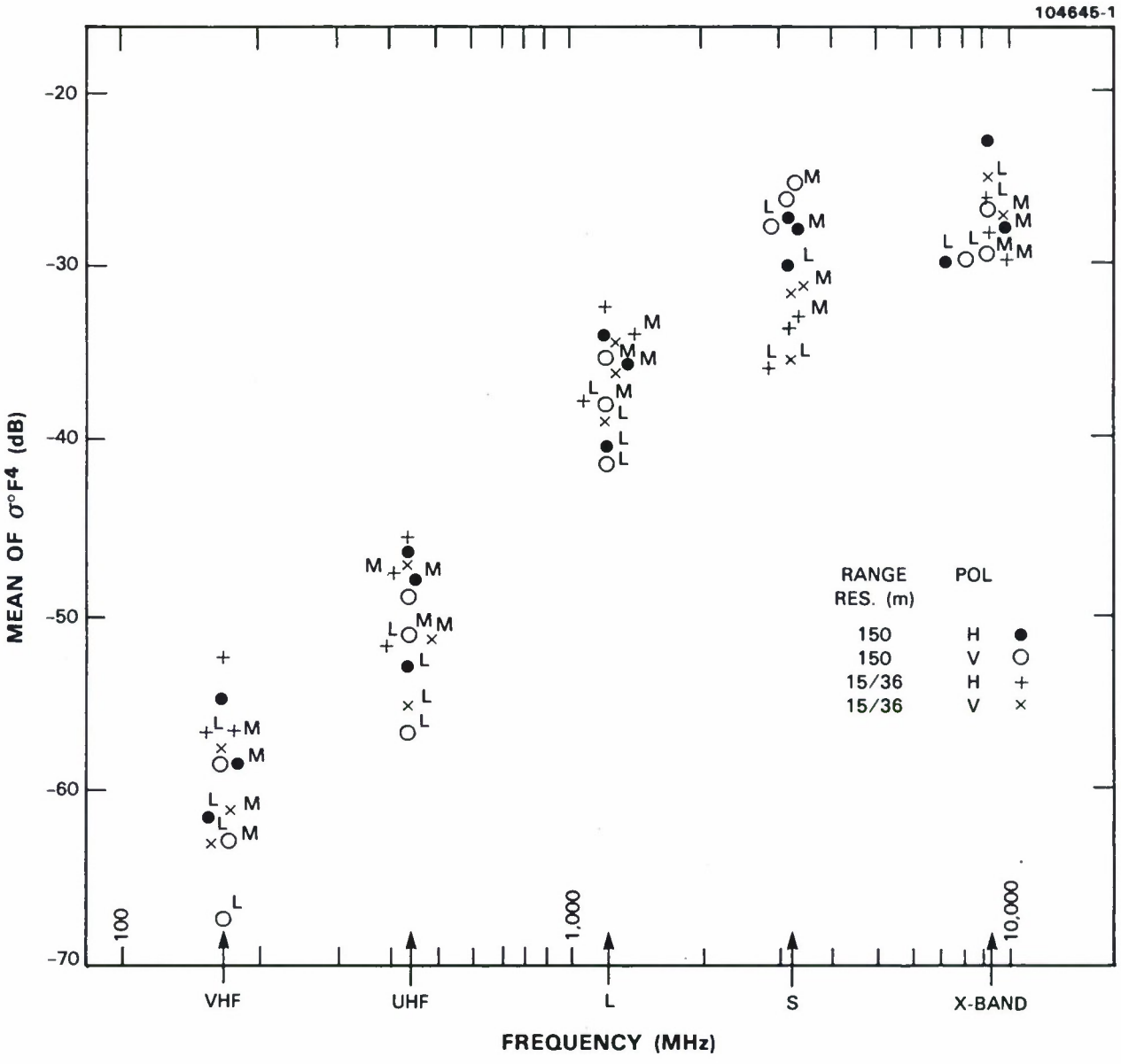

Figure 78. Mean clutter strength versus frequency at Corinne for three antenna heights. Repeat sector data; level farmland; antenna heights = 54 – 59 ft (3 tower sections, no superscript), = 41 – 46 ft (2 tower sections, superscript "M"), and = 27 – 32 ft (1 tower section, superscript "L"), see Table A-5; at S-band, the high resolution range interval (4.0 – 8.9 km) is shorter than that for the other 18 frequency band/waveform combinations (1.0 – 8.9 km).

1.3 dB at VHF, UHF, L-, S-, and X-bands, respectively. These differences are averages of differences between individual experiments of like waveform (i.e., like polarization and pulse length) in each band (i.e., they are not just the differences of the median numbers entered in Table 9)*. These differences in repeat sector mean clutter strength with antenna height at Corinne are less at VHF and UHF than those observed at Shilo and Lethbridge West. Figure 20 shows how mean clutter strength varies with range in a complex way for one, two, and three tower sections extended at Corinne, at UHF, L-, and X-band. Overall, mean clutter strengths over the Corinne repeat sector increase with antenna height by 5 to 7 dB in the low bands and by 2 to 4 dB in the high bands. On the other hand, for any antenna height, mean strengths increase strongly and monotonically with frequency by 28 dB overall for both the high and medium antennas and by 32 dB overall for the low antenna.

These results can be understood on the basis of multipath lobing on the Phase One antenna pattern. Consider the height to the peak of the first multipath lobe. Assuming perfect reflection off a flat surface at all frequencies, a not unreasonable assumption at Corinne, the height to the peak of the first lobe varies directly with range and inversely with frequency and antenna height. That is, all of these variations are linear (or inverse linear), so variations with range, frequency, and antenna height all count the same and play off against each other equally. The range interval of the Corinne repeat sector is from 1 to 8.9 km. Range to the spherical earth horizon (another good approximation at Corinne) from the lowest antenna height, namely, 27.5 ft, is 11.9 km, so we have line-of-sight geometric visibility of the complete repeat sector from all antenna positions and no over-the-horizon diffraction effects. The frequencies vary over a 55:1 range from 167 to 9200 MHz (see Table A-6). On the other hand, the tower heights, with from one to three tower sections extended, vary only over a 2:1 range (see Table A-5). This is the main reason why frequency has such a strong effect in Figure 78, and tower height a much weaker effect.

TABLE 9

Median Values of Mean Clutter Strength Versus Antenna Height for the Corinne Repeat Sector

	Median Level of Mean Clutter Strength (dB)				
	VHF	**UHF**	**L-Band**	**S-Band**	**X-Band**
High Tower	-55	-46	-34	-30	-27
Medium Tower	-57	-48	-34	-31	-29
Low Tower	-62	-53	-38	-33	-30

Note: Medianized over all measurements in sort file (see Section 6.1) at both polarizations and both pulse lengths for each antenna height in each band.

* The 3.9-dB average difference between tall tower and low tower at X-band separates into average differences by waveform, for 150-m pulse, horizontal polarization and vertical polarization, then 15-m pulse, horizontal polarization and vertical polarization, respectively, as: 3.5, 4.7, –0.5, and 8.1 dB.

For three tower sections raised, the height above ground of the peak of the first multipath lobe at 1 km (the beginning of the repeat sector), at 4.95 km (the midpoint of the repeat sector), and at 8.9 km (the end point of the repeat sector) is: at VHF, 26, 128, and 230 m, respectively; at L-band, 4, 18, and 33 m respectively; and at X-band, 0.5, 2 and 4 m, respectively. For one tower section raised, the height above ground of the peak of the first multipath lobe at 1, 4.95, and 8.9 km is: at VHF, 49, 241, and 433 m; at L-band, 7, 36, and 65 m; and at X-band, 0.8, 4, and 7 m. Thus, at VHF, for all ranges within the repeat sector and the three antenna heights, most clutter sources, such as buildings, telephone poles, fence lines, etc. are well below the peak of the first lobe. The gain at which such objects are illuminated is well down on the underside of the first multipath lobe, accounting for the weak clutter strengths there. The increases in antenna height over a 2:1 range only cause relatively minor 5- or 7-dB increases in the overall VHF illumination, which overall is very weak due to 30-dB multipath loss. At X-band, on the other hand, for all ranges within the repeat sector and the three antenna heights, many clutter sources are higher than the peak of the first multipath lobe and are fully illuminated by multiple lobes. Thus, we expect and see less variation with antenna height at X-band. At L-band, we are in between, with clutter sources fully illuminated at close ranges at all three antenna heights. However, with increasing range and decreasing antenna height, we gradually decrease the illumination until at longer ranges we have weak illumination at all three antenna heights. Thus, at L-band, we see 5- to 8-dB average multipath loss over the complete sector for the three antenna heights, and a 4-dB increase in mean strength with antenna heights.

Two final comments are made on the S-band data in Figure 78. First, the 15-m pulse length results are for a shorter range interval, namely, 4 to 8.9 km, than all the other results. Second, Corinne is where the shield broke on the S-band antenna cable connector, leading to a difference in calibration constant of 4 dB. The shield broke between acquisition of the high and medium tower data. Thus, the low and medium tower S-band results in Figure 78 are all augmented by 4 dB compared with the high tower results.

Antenna Height Effects; Phase Zero Versus Phase One. We now conclude the subject of antenna height effects on clutter by comparing Phase Zero and Phase One mean clutter strength results at similar and differing antenna heights for repeat sectors at various sites covering many terrain types. From all the sites, we have available a set of 30 sites where Phase Zero and Phase One made measurements from nearly identical locations, and where we have good X-band data from both instruments (see Table A-25 for seven Phase One sites with no X-band data). At all 30 sites, Phase Zero used its 50-ft antenna mast height. For 22 sites, Phase One used its 59.1-ft X-band mast height, which we regard as reasonably close to the Phase Zero height. For eight sites, Phase One used its 99-ft X-band mast height, which is twice as high as the Phase Zero mast height. For each site, we take the difference of the Phase One mean clutter strength in the repeat sector (150-m pulse length, horizontal polarization) minus the Phase Zero mean clutter strength in the repeat sector (usually at 150-m pulse length, occasionally at 75-m pulse length, always at horizontal polarization). Across the 22 sites for which Phase One and Phase Zero had similar antenna heights, of the 22 differences in mean strength, the mean difference was -0.01 dB, and the standard deviation was 3.9 dB. (Of the 22 differences in depression angle to sector midpoint, Phase One minus Phase Zero, the mean difference was 0.02 deg with a standard deviation of 0.01 deg; note that small differences in location and hence site height as well as mast height contribute to this.) However, across the eight sites for which Phase One had twice as high an antenna as Phase Zero, of the eight differences in mean strength, the mean difference was 4.9 dB, with a standard deviation of 3.2 dB. (Of these eight differences in depression angle, the mean difference was 0.12 deg with a standard deviation of 0.06 deg.)

This study provides two important results. First, it provides an answer to the question, "Do Phase One and Phase Zero get the same answers when they measure the same clutter?" This study answers yes, even to a precision (obviously somewhat fortuitous) of 0.01 dB. It provides reassurance regarding calibration of both instruments.

Second, this study shows that a 100-ft mast measures X-band clutter, on the average, 4.9 dB stronger than a 50- or 60-ft mast. This extends the previous study of Phase Zero mast height on the level open farmland at Corinne where mean clutter strengths increase an average of 6 dB when the Phase Zero mast was raised from 20 to 50 ft. This difference was interpreted by means of propagation analysis. Recall from the preceding Corinne discussion that, in the Phase One repeat sector at Corinne, the average difference of tall 59-ft tower minus low 32-ft tower X-band mean clutter strength over many repeated measured differences in mean strength by like waveform was 3.9 dB. Here, in this Phase Zero/Phase One comparison study, we see a similar mast height effect covering eight sites with much more general terrain types, not just level open terrain.* The mean increase in depression angle with the higher mast at these eight sites is only 0.12 deg. Although small differences in depression angle are important, in our measurements of different clutter patches of varying depression angle with fixed mast height mean strengths do not rise as much as 4.9 dB with an increase of only 0.12 deg in depression angle.

4.1.5 Desert, Marsh, or Grassland

Table 7 shows four sites within the category of desert, marsh, or grassland. These sites are quite different from each other in terrain characteristics. They are discussed in two regimes of depression angle, high and low, with each depression angle regime containing two sites.

If these sites are quite different from one another, what is there about them that makes us group them together? First, they are all open or nonforested sites. This alone does not distinguish them from the agricultural sites, which, taken together, cover a very wide variety of different scenes in open terrain. What does distinguish them from the sites we classify as agricultural is their lack of a cultural overlay of discrete man-made influences and objects. These four open sites are largely in their original natural states, and their repeat sectors have the original natural vegetation as land cover on generally level or low-relief terrain. The multifrequency characteristics of mean clutter strength at these four sites are different from any of the other sites, but as a group they all have considerably lower mean clutter strengths than our other terrain categories at corresponding depression angles, with one interesting exception which we shall discuss presently.

Repeat sector terrain elevation profiles generated from DTED for these four sites are shown in Figure 79. The situations at these sites are as follows. At Booker Mountain, the site is on a high peak 3 mi northeast of the town of Tonopah in Nevada. The repeat sector begins 12 km to the southeast on the relatively level (but slightly undulating) desert floor 1570 ft below. This desert repeat sector is barren

* Of the eight sites only three were open and supportive of multipath. At these three sites, the increased clutter strength with higher antennas may have been contributed to by increased illumination of low sources on the underside of the first multipath propagation lobe. However, the remaining five sites, all forested and thus not supportive of X-band multipath, provided similar increases in mean clutter strength with higher antennas as did the open sites.

in places and covered with desert brush vegetation (e.g., sagebrush, greasewood) in other places. Figure 80 shows a photograph of this Booker Mountain measurement situation and an X-band PPI clutter map measured there.

At Vananda East, the site is on the edge of a 350-ft-high bluff in Montana. From the site, one looks to the northeast down off the steep edge of the bluff and out 3.6 km to the beginning of the repeat sector. The terrain below the bluff is low-relief undulating grassland without roads, buildings, or other cultural discretes, and only very infrequent small occurrences of pine. There is significant relief within the repeat sector from 100 to 150 ft with maximum slopes between 1 and 2 deg. A photograph of Phase One at Vananda East is shown in Figure 81 (see also Figure A-11).

At Knolls, the site is on the Great Salt Lake Desert in Utah, 25 mi east of the Bonneville Race Track, and 60 mi north of the Dugway military range. From a 25-ft-high local hill, one looks to the northwest across a railroad and the interstate highway to a very level repeat sector (i.e., only one contour line meanders through the repeat sector on a topographic map with 5-ft contour intervals) containing mostly barren salt and mud flats, but with some scrubby desert vegetation in places. The interstate highway and railroad are not included in the repeat sector range interval from 3 to 6.5 km. A Phase One tower-top view of the Knolls salt flats is shown in Figure 82.

At Big Grass Marsh, the site is in the middle of a large, level wetland area in Manitoba, approximately 20 mi long in the north-south direction by 10 mi across. The Big Grass Marsh measurements were made in February 1984, so it was a frozen snow-covered marsh from which we measured backscatter.* In contrast, the measurements at Knolls, Booker Mountain, and Vananda East were summer measurements, all between 18 June and 4 August 1984. The marsh is traversed by several straight gravel roads. Some of the marsh, where the water table is not right at the surface, is used for pasture or for growing hay in summer. The terrain under foot, where walkable, is rough and bumpy. For the Phase One setup area at Big Grass Marsh, we just eased off to the north side of an east-west gravel road. From there the repeat sector looked north, across nonforested wetland with some minor hayfields, to the edge of an extensive region of open water in the last 0.5 km of the repeat sector beyond 6-km range. This water was frozen and snow covered when we were there. At the shoreline of the open water region, at 6-km range, there were three very small patches of deciduous aspen trees. In addition, there were two very small patches of aspen at the left edge of the repeat sector at 3-km range and one very small patch of aspen at 2-deg azimuth, 5-km range. Otherwise, the natural vegetation was dormant marshland grasses and tall aquatic vegetation (e.g., cattails and bulrushes) over most of the sector with much of the higher vegetation sticking through the snow cover. The center area of the sector was actually slightly higher, by 3 ft or so, than our setup position. A Phase One tower-top view of the repeat sector at Big Grass Marsh is shown in Figure 83.

---

* The first data collection day at Big Grass Marsh was 4 February 1984. A full-scale prairie blizzard occurred that day. During this storm, snow accumulation was significant, temperature dropped to –5°F, and winds averaged 25 to 40 mph, gusting to 50 mph. On subsequent data collection days, skies were clear, but the landscape was snow-covered and frozen at all times. Partly because of this blizzard, the surrounding terrain was 100 percent covered with a moderately deep snow cover, 6 in to 3 ft.

Multifrequency mean clutter strengths measured over the repeat sectors at Booker Mountain, Vananda East, Knolls, and Big Grass Marsh are shown in Figure 84. Mean strengths range over 53 dB in Figure 84, from -23.1 dB at X-band, 150-m pulse, vertical polarization for the Nevada desert measured from Booker Mountain to -76.1 dB at UHF, 150-m pulse, horizontal polarization at Big Grass Marsh in Manitoba (see Table C-4 for examples showing validity of weak clutter measurements at Big Grass Marsh). There is a much greater range of strengths for this set of relatively level, open, discrete-free sites than for any of the other groups of sites. Keep in mind that we observe these similar surfaces at quite different geometries with effective site elevation advantages of -3, 25, 342, and 1570 ft and depression angles of 0.2, 0.3, 1.0, and 1.8 deg for Big Grass Marsh, Knolls, Vananda East, and Booker Mountain, respectively. What is driving these strengths over wide ranges are large amounts of multipath loss at the lower frequencies at the two sites, Knolls and Big Grass Marsh, with little or no elevation advantage. The two high sites, Vananda East and Booker Mountain, provide what we expect are largely intrinsic σ°s in Figure 84.

Depression angle largely accounts for the variability in Figure 84, both where large multipath loss exists (e.g., at VHF, mean strengths increase with increasing depression angle by over 40 dB from Big Grass Marsh and Knolls to Vananda East and Booker Mountain) and where it does not (e.g., at X-band, mean strengths also increase with increasing depression angle, by over 20 dB, in the same order across these sites and are similar to the Phase Zero range of variation with depression angle over similar terrain types). Reasonable similarity is seen in mean strength versus frequency characteristics at Booker Mountain and Vananda East, where Booker Mountain provides a higher depression angle, but Vananda East has higher terrain slopes. Remarkable similarity is seen in the L-band data at these two sites. At both sites X-band mean strengths as a tight group have jumped up to be 12 or 14 dB stronger than at the lower bands.* At the lower sites, skimming over the mud flats in Utah or skimming over the frozen marsh in Manitoba provides significantly lower mean strengths than looking down at the Nevada desert at 2 deg or at the Montana grassland at 1 deg.

Mean clutter strengths are shown individually for these four sites in Figures E-156, E-161, E-165, and E-171. We now comment briefly on each of these in turn. At Booker Mountain, Figure E-156, mean strengths are relatively constant from UHF to L- to S-band but are slightly higher at VHF and much (i.e., 15 dB) higher at X-band; mean strengths at vertical polarization are stronger than at horizontal by 5 to 7 dB at VHF and UHF and by 2 to 4 dB at S- and X-band; but mean strengths at L-band form a remarkably tight cluster within 0.5 dB of -39.5 dB at all four combinations of polarization and pulse length (with vertical still slightly stronger than horizontal). At Vananda East, Figure E-161, there are remarkable coincidences with Booker Mountain. Again, there is a very tight cluster of mean strengths at L-band at essentially the identical level (i.e., -39.7 versus -39.6 dB at Booker Mountain) and, as mentioned earlier, a similar large 15-dB increase in clutter strength to the -25- to -27-dB range at X-band. However, at Vananda East, mean strengths stay approximately constant near the -40-dB level, VHF to L-band, and begin to rise from L- through S-band by several decibels before the large increase to X-band. As at Booker Mountain, at Vananda East mean strengths at vertical polarization are 2 to 3 dB stronger than at horizontal at S- and X-bands, but at Vananda East there are no similar differences with polarization in the lower bands as there were at Booker Mountain.

* This is the exception mentioned in the second paragraph of Section 4.1.5.

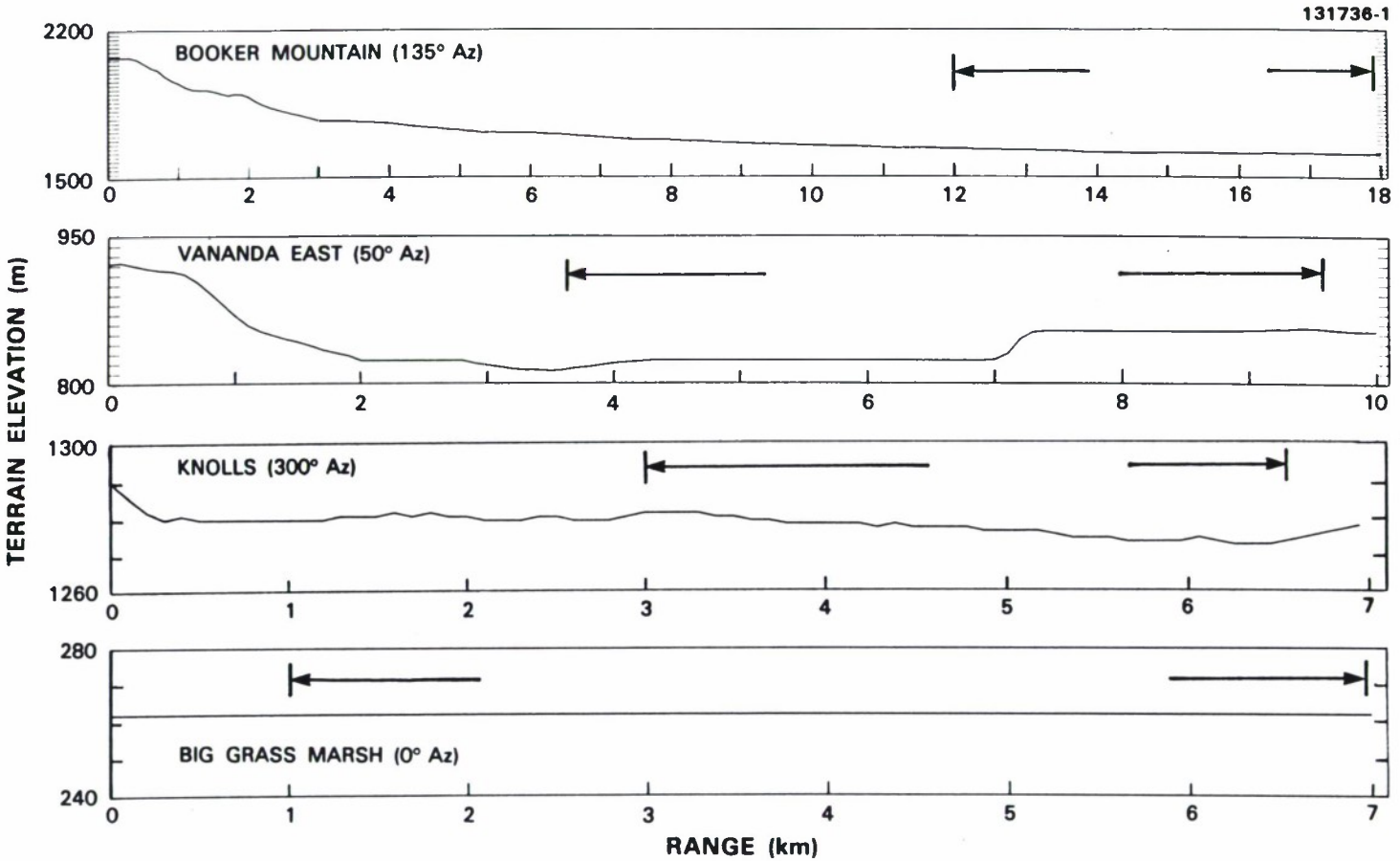

Figure 79. DTED terrain profiles at Booker Mountain, Vananda East, Knolls, and Big Grass Marsh. Elevation in meters above mean sea level, 10 and 20 m between tick marks. Range extent of repeat sectors is indicated by horizontal arrows.

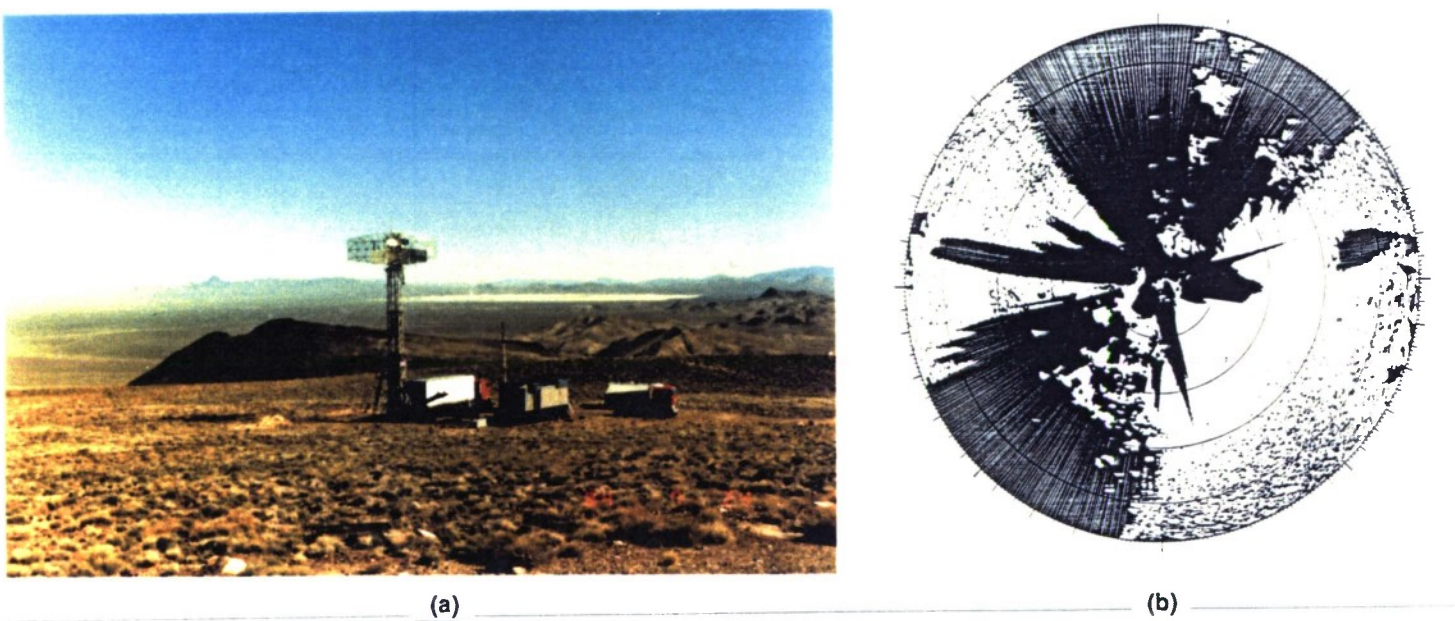

(a) (b)

Figure 80. Low-relief desert terrain viewed from Booker Mountain. (a) Looking SE past equipment on site down onto desert floor in repeat sector beyond and (b) X-band PPI clutter map. North is zenith. Max range = 24 km.

Figure 81. Phase One at Vananda East. Antenna tower barely visible on high bluff to right of center. Clutter measurements from grassland at high depression angle.

At Knolls, in Figure E-165, there is substantial multipath loss at VHF, UHF, and L-band, a remarkably tight cluster of X-band mean strengths at all four combinations of polarization and pulse length, and a monotonic rise in mean strengths, L- to X-band, largely the result of multipath propagation loss entering through the propagation factor. At Big Grass Marsh, in Figure E-171, we see as at Knolls substantial multipath loss at VHF, UHF, and L-band; we see low resolution stronger than high at S-band but high resolution stronger than low at L-band, indicative of several interfering scatterers in dominant resolution cells; and, as at Knolls, we see a strong monotonic increase in mean strengths, here from UHF to X-band, again due to effects of multipath illumination. Note that, just due to multipath effects alone, mean strengths at VHF should be weaker than at UHF. Surprisingly, at both Big Grass Marsh and Knolls, mean strengths at VHF are generally 5 to 10 dB stronger than at UHF. Looking back to the multipath-free situations of Booker Mountain and Vananda East, mean strengths are also substantially stronger at VHF

Figure 82. Salt flats at Knolls. Phase One tower-top view looking WSW.

than at UHF at Booker Mountain and at least equal at Vananda East. Thus, across three of these four sites, there appears to be the suggestion of intrinsic σ°s at VHF being substantially greater than at UHF (with substantial equivalence at the fourth site, Vananda East).

Phase Zero. We now compare Phase Zero and Phase One measurements of mean clutter strength in the repeat sectors at these four sites. Phase Zero measured Booker Mountain in June 1982 at -28.1 dB, or 2.5 dB weaker than the Phase One July measurement (at 150-m pulse length, horizontal polarization). Phase Zero measured Vananda East in July 1982 at -28.9 dB, or 1.2 dB weaker than the Phase One August measurement. Phase Zero measured Knolls in June 1982 at -36.0 dB in an enlarged repeat sector containing the interstate highway, which was 2.4 dB stronger than the Phase One June measurement in the same enlarged repeat sector. Finally, Phase Zero measured Big Grass Marsh in February 1980 at -39.6 dB, or 5.1 dB stronger than the Phase One February measurement. All in all, we have reasonable correspondence within the general range of 1 to 5 dB between Phase Zero and Phase One measurements at these four sites.

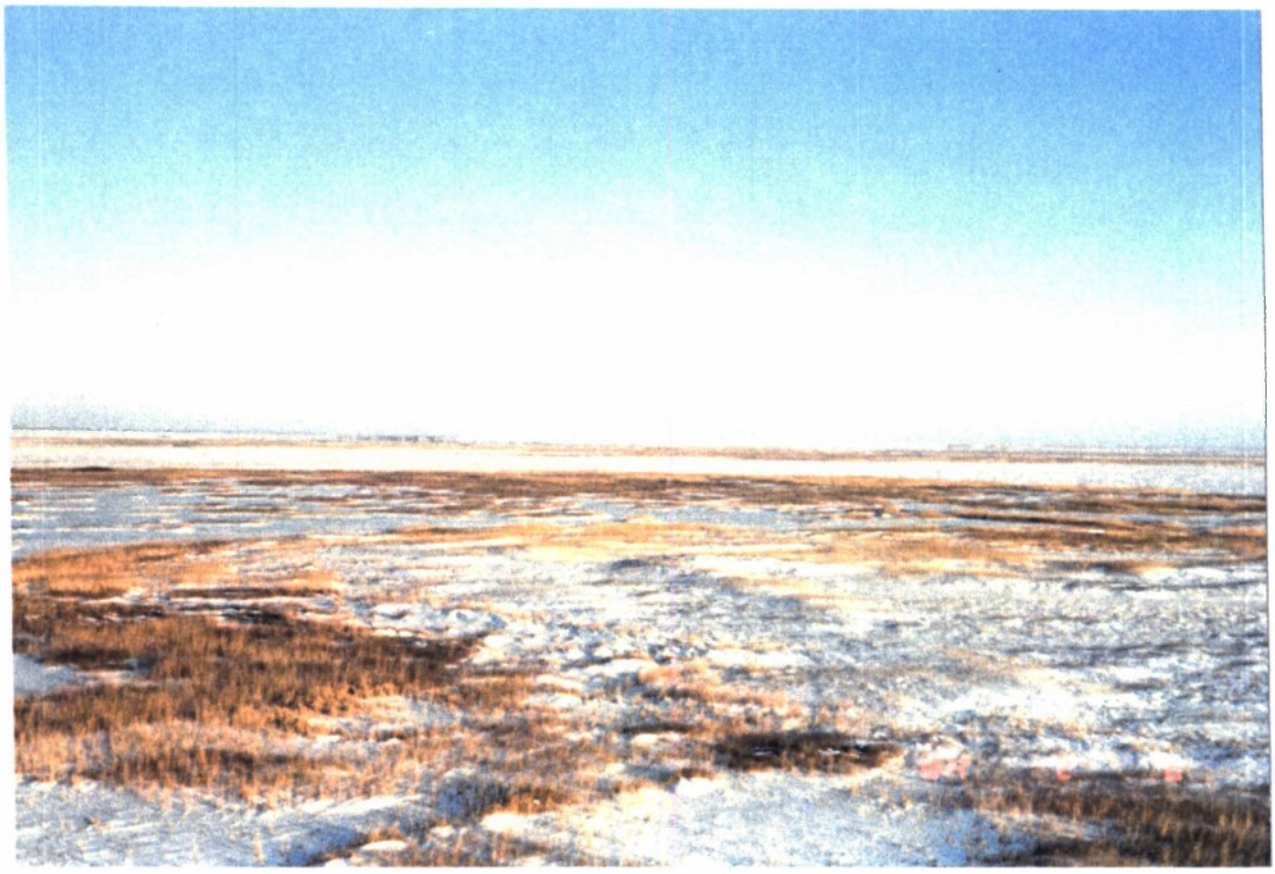

Figure 83. Big Grass Marsh. Phase One tower-top view looking north into repeat sector.

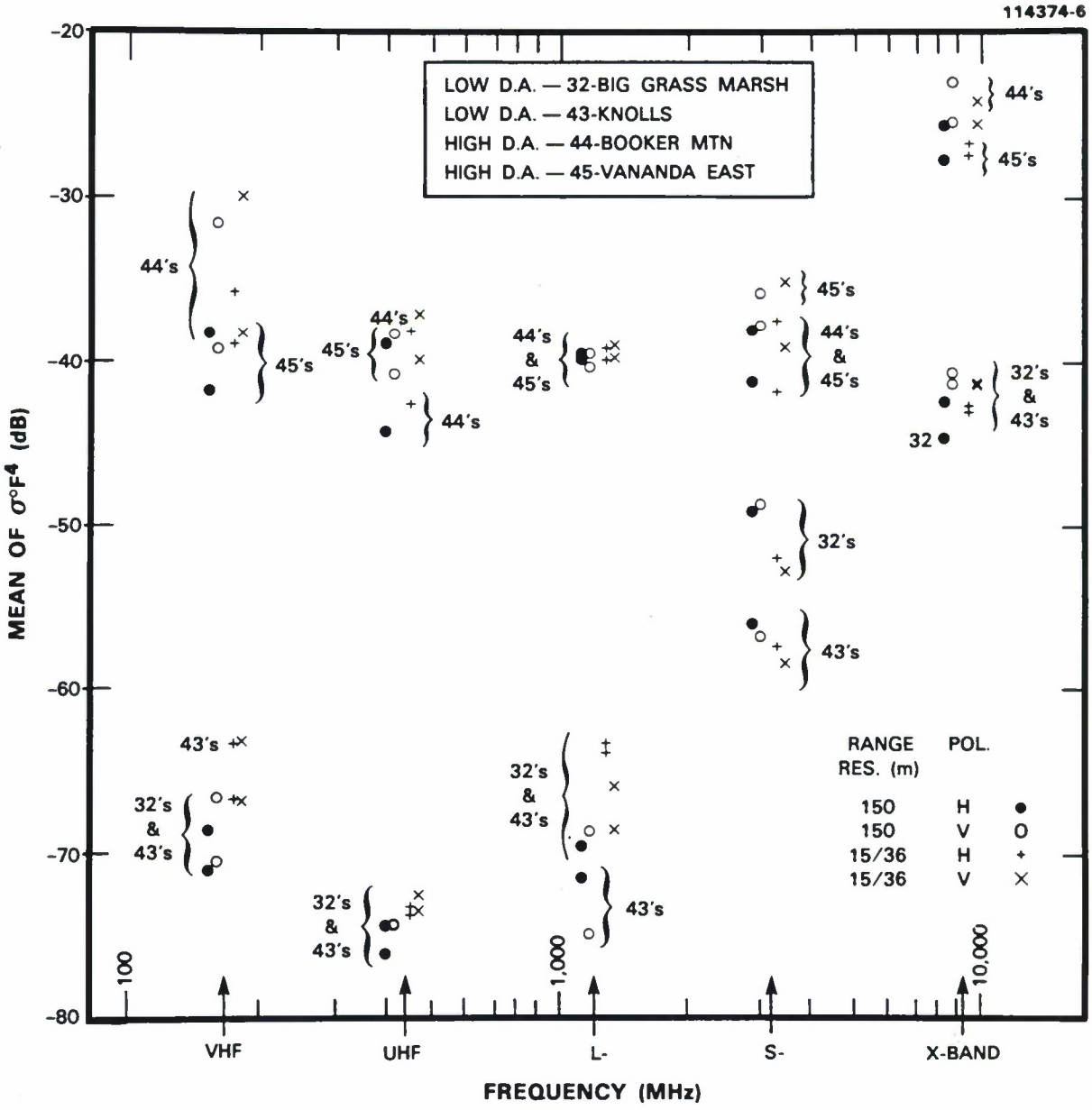

Figure 84. Mean clutter strength versus frequency for desert, marsh, or grassland (few discretes) at high and low depression angle. See Table 7.

4.2 FOUR COMPLEX REPEAT SECTORS

The Phase One equipment obtained ground clutter measurements at 42 different sites (e.g., see Table 1). The preceding section was based on discussing measurements at groups of sites of common terrain type. Within these groups of sites, as indicated in Table 7, we discussed results for 38 different repeat sectors, which leaves repeat sectors at four Phase One sites yet to be discussed. Terrain descriptions for these four repeat sectors are shown in Table 10.

TABLE 10
Terrain Descriptions of Four Repeat Sectors

Location	Depression Angle (deg)	Land-form	Land Cover	Range (km)	Azimuth (deg)	Setup Number
Wachusett Mountain, Mass.	2.1	5-4	43-21-11	8-13.9	156-176	46
Cochrane, Alta.	1.7	7-2	31/32-21/22-41/43-11	1-10	220-240	6,16
Suffield, Alta.	0.3	3-5-9	31-62-52-12	7-12.9	125-135	12
Spruce Home, Sask.	0.3	1	21-41	3-8.9	40-50	34

The results of mean clutter strength versus frequency for these four sites are discussed in this section. For various reasons, each site is transitional between various pairs of terrain groups as defined in Section 4.1. We could have made a case for all-inclusivity and forced these four sites into terrain groups as defined by just their primary terrain classifiers. To have done so would not have upset the general multifrequency trends of mean clutter strength within these terrain groups very much. That is, the abnormalities in the multifrequency mean strength characteristics at these four sites would have been swamped out by the other sites in the groups. Elsewhere, our goal has been to average out overly specific effects of terrain and propagation. Here, however, in these four sites, we believe we have differences that are more general in character, and to do proper justice to our measurements at these four sites (which have very interesting features), we separate them from our other sites and discuss them individually.

We have stated that every ground clutter measurement scenario is different. This is at the root of the intractability that ground clutter has posed to prediction. That is, at macroscale, where we accumulate resolution cell-by-resolution cell returns over a number of square kilometers, we get a different answer for mean strength across the ensemble of cell-by-cell returns for each different measurement scenario. Our approach in this report is to uncover trends in multifrequency mean clutter strength by site type, over and above

macroscale variability. The specific discussions of multifrequency mean clutter strength at four particular sites in this section, each transitioning general terrain groups, help illustrate such modeling philosophy.

Wachusett Mountain. These four sites are discussed in order of decreasing depression angle. DTED terrain elevation profiles for the repeat sectors at these sites are shown in Figure 85. We begin with Wachusett Mountain at 2.1-deg depression angle. This is among the highest depression angles within all of the 42 Phase One repeat sectors (compare with Plateau Mountain (a) at 2.3 deg; Puskwaskau, also at 2.1 deg; and Polonia at 2.0 deg). Wachusett Mountain is a single, isolated, monadnock peak in central Massachusetts rising 1000 ft above a hilly wooded peneplain. From this peak, we look SSE down to the repeat sector at 8- to 13.9-km range. Within this range interval, the land cover is primarily mixed eastern forest. However, there are agricultural clearings and scattered buildings along low-lying ground. One paved road runs north-south through the sector, and the Quinapoxet River meanders across the sector. The topography is hummocky and rolling hills, typically of about 100-ft relief, but as great as 270 ft in the extreme, and providing terrain slopes as great as 5 deg. Our Wachusett Mountain measurements were in summer season (i.e., August) with deciduous trees fully leaved out. A Phase One tower-top view of the Wachusett Mountain repeat sector is shown in Figure 86.

Multifrequency mean clutter strengths for the Wachusett Mountain repeat sector are shown in Figure 87. This is a very tight data set showing unusually little variation with polarization and resolution, indicative of a more uniform Rayleigh-like and less discrete-dominated scattering medium provided by the forest (see also low ratios of standard deviation to mean, generally in the 2- to 3-dB range, or approaching 4 dB at S- and X-band, Tables D-2 through D-6). Mean strengths at vertical polarization are, however, 1 or 2 dB stronger than at horizontal in every measurement in Figure 87. We see the typical decrease of mean strength with increasing frequency, VHF to L- and S-band, in Figure 87 that we associate with forest illuminated at high angle. Five-frequency sector displays showing mean clutter strength versus range in the Wachusett Mountain repeat sector are shown in Figure E-173.

The two terrain categories we have that the Wachusett Mountain repeat sector might fit are forest/high-relief/high depression angle and forest/low-relief/high depression angle (see Table 7). The Wachusett Mountain repeat sector landform classification is transitional between the high end of low-relief (i.e., primary LF = 5, hummocky) and the low end of high-relief (i.e., secondary LF = 4, rolling).* First, considering low-relief, and comparing Figure 87 with Figure 39, we first observe that the Wachusett Mountain data are towards the low end of the Puskwaskau and Brazeau data but still quite within their general range at VHF, UHF, and L-band. This puzzles us a bit; we would expect the steeper Wachusett terrain to result in the Wachusett data being towards the high end of the Puskwaskau and Brazeau data because these latter sites are of lower relief. At S-band, the Wachusett Mountain results are remarkably close to the Brazeau results (and, indeed, higher than Puskwaskau). At X-band, however, Wachusett Mountain mean strengths jump up to be 5 or 6 dB greater than Brazeau. Previously, we argued that Brazeau X-band mean strengths were already too high for this terrain category, based on extensive Phase Zero measurements.

---

* Our landform class numbers are not always in increasing order of relief. "Rolling," number 4, is of higher relief than "hummocky," number 5. See Table 4.

Suppose we consider including Wachusett Mountain in the forest/high-relief/high depression angle category, on the basis of its high-relief secondary landform classifier of "rolling." Comparing Figure 87 with Figure 32, we see that the high Wachusett Mountain X-band mean strengths very satisfactorily match those at Scranton and Blue Knob. However, Wachusett Mountain mean strengths are a bit low at S-band, and very much too low (8 dB or more) at VHF, UHF, and L-band, compared with the high-relief Scranton and Blue Knob data. *The conclusion is that dominant terrain classifiers can vary with RF frequency; the Wachusett Mountain repeat sector is high-relief at X-band and low-relief at VHF, UHF, and L-band.*

Finally, let us compare Wachusett Mountain results with Katahdin Hill results (Figure E-76) because Katahdin Hill is very similar hilly wooded Massachusetts terrain (almost identical landform and land cover classification, see Table 7), although illuminated at a much lower depression angle. Indeed, the multifrequency mean strength characteristics at these two sites are very similar in trend, VHF to S-band, except the Katahdin Hill mean strengths are generally about 8 dB weaker due to the lower depression angle (0.4 deg at Katahdin Hill, compared to 2.1 deg at Wachusett Mountain). However, at X-band, Katahdin Hill mean strengths stay down at their UHF, L-, and S-band level, unlike the significant X-band increase at Wachusett Mountain.

Cochrane. Cochrane results will now be discussed. Cochrane is 30 mi west of Calgary, on a high bluff 684 ft above the Bow River. A three-dimensional oblique view of the terrain at Cochrane to 20-km range, generated from DMA digital terrain elevation data (DTED), is shown in Figure 88. Terrain elevation profiles through the Cochrane repeat sector are shown in Figures 10 and 85.* The repeat sector looks southwest, first across the river and the town of Cochrane in the river valley, and then up rough, moderately steep, inclined rangeland terrain rising towards the Rocky Mountains, visible on the horizon at 40-mi range. An aerial photo showing the terrain in the Cochrane repeat sector is shown in Figure 89. Within the repeat sector, the land cover is predominantly rangeland with some urban and some agriculture and with 11 percent tree cover scattered in patches. Figure 91 shows a telephoto view looking from site center southwest into the repeat sector at Cochrane, together with some interpretation.

Multifrequency mean clutter strengths are shown for Cochrane in Figure 90. As apparent in Figure 90, Cochrane was a seasonally revisited site with first visit in summer (August) and second visit in winter (February/March). What is seen in Figure 90 is frequency invariance near the -20-dB level, except for the first visit, L-band, which is 6 dB weaker. We also see little variation with resolution and polarization, except at VHF especially with the 150-m pulse, where mean strength at vertical polarization is 8 dB stronger than at horizontal polarization for both visits.

---

* The Cochrane terrain profile of Figure 10 (225 deg) was manually generated from 1:50,000 scale maps; whereas, the profile of Figure 85 (230 deg) was generated from DCARTO data provided to DMA Format Level Two (see Figure 88) from the same maps. DMA also directly generated DTED for Cochrane, for which the source was 1:250,000 scale maps with 500-ft contour intervals. These latter data do not well approximate the Cochrane terrain (e.g., 100-m error in site elevation).

At first we would have expected mean strengths at Cochrane to be similar to repeat sector (a) at Plateau Mountain, where we looked down at high-relief rangeland at high depression angle. However, the Cochrane results are everywhere much stronger than the Plateau Mountain (a) results. We believe that the reason has to do with the 11 percent tree cover at Cochrane. These trees are generally on north-facing slopes as the terrain first rises quite steeply on the far visible banks of Jumping Pond Creek as it drains into the Bow, then farther out at midrange in the repeat sector as the terrain rises steeply up to the Crawford Plateau, and finally at far ranges as the terrain rises sharply once more up to Copithorne Ridge. That is, at a depression angle of 1.7 deg, we view the forested "stair risers," not the more areally extensive rangeland "stair treads." This is quite evident in the photograph of Figure 91.

In this respect, there is much commonality between Cochrane and Blue Knob repeat sectors, even though these two measurement situations seem so different at first glance (i.e., eastern forest in Pennsylvania versus western rangeland in Alberta). The similarities are found by our classification system. Both are high-relief terrain, more open than forested, viewed at similar high depression angles, but each with similar secondary incidence of tree cover, 11 percent at Cochrane, 8.6 percent at Blue Knob, which dominates the mean clutter characteristics. Although Cochrane does not provide the characteristic decreasing mean clutter strength with increasing frequency of forest, surprisingly, if the Cochrane data of Figure 90 are overlaid on the Blue Knob data of Figure E-39, the Blue Knob data provide an almost exact upper envelope to the Cochrane results (i.e., discount the low horizontally polarized VHF results and the low, first visit, L-band results in the Cochrane data). Penhold II is another similar site to Cochrane and Blue Knob in terms of landform and land cover classification (see Table 7, Penhold II also is high-relief open terrain with 9.8 percent tree cover), except that the Penhold II repeat sector is viewed at low depression angle and, unlike Cochrane and Blue Knob, is affected by multipath. Nevertheless, overlaying the Penhold II data of Figure E-48 onto the Cochrane data of Figure 90 shows fair equivalence in gross mean levels, especially if now we lean towards first visit L-band results for Cochrane. Thus, there are three repeat sectors, each of high-relief open terrain with nominally 10 percent tree cover, although in overall visual effect seemingly very different from each other, with interesting similarities in their mean strengths. In earlier discussions of Blue Knob and Penhold II, we have raised the possibility of eventually separating the classification of open terrain with scattered 10 percent tree cover as parkland. The Cochrane results reinforce these earlier discussions.

Suffield. We now turn to our Suffield site,* which is located on Canadian Forces Base Suffield in southeastern Alberta. The Suffield terrain is native herbaceous rangeland. When standing at site center and looking into the repeat sector to the southeast, one sees only grass all the way out to the horizon. We measured Suffield in winter season (December/January) with several inches of snow cover on the grass. The landform is generally low-relief, although with some variety. From site center at an elevation of 2525 ft above MSL, the terrain gradually falls off to 2350 ft at 7-km range, the start of the repeat sector range interval, and then gradually rises back to 2500 ft at 13 km, the end of the repeat sector. In the

* At Suffield, we obtained measurements with both one and three sections extended on the Phase One antenna tower. Variations in mean clutter strength with antenna tower height at Suffield were briefly discussed in Section 4.1.4.3. In what follows here, all the Suffield results are with three tower sections extended.

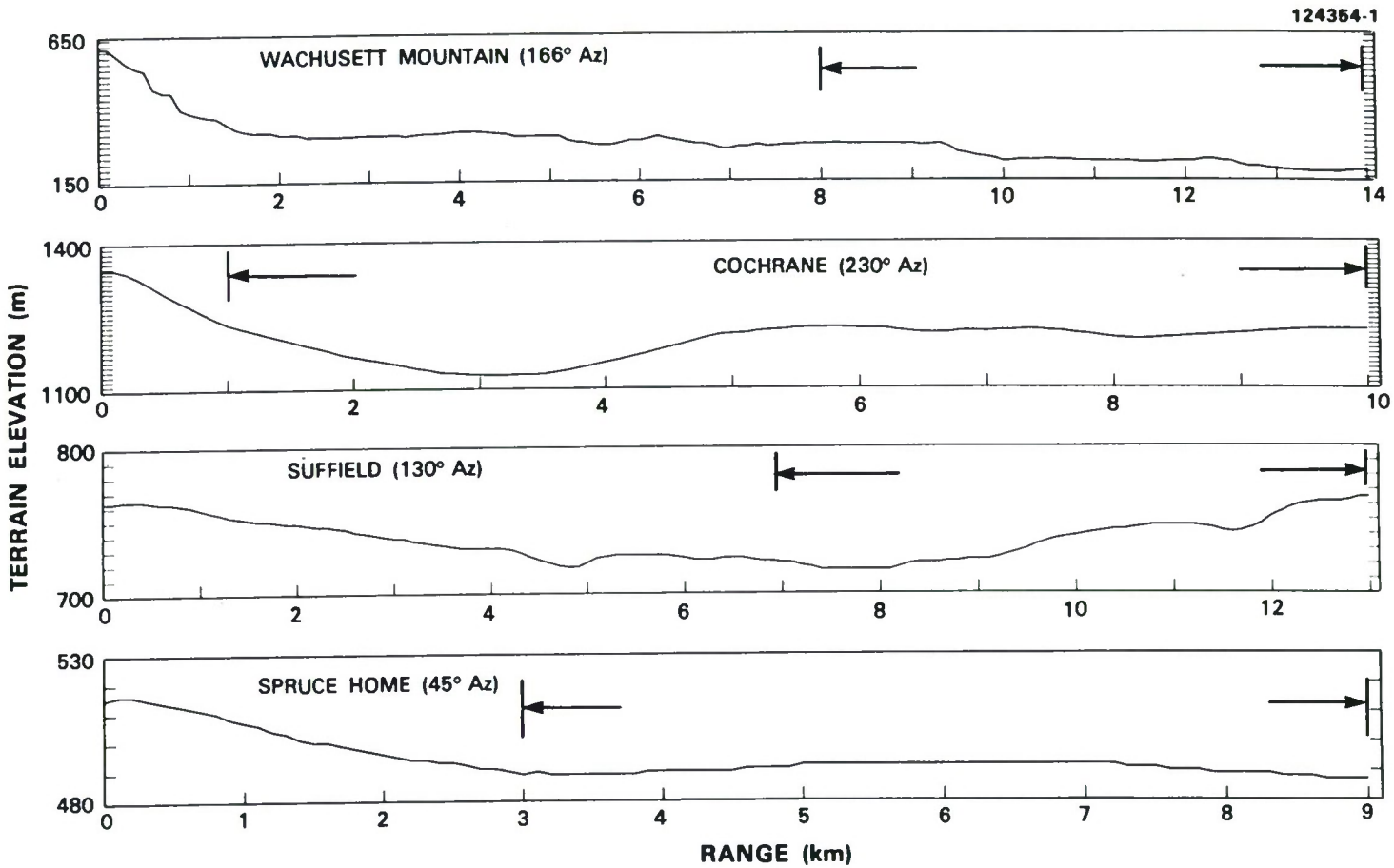

Figure 85. DTED terrain profiles at Wachusett Mountain, Cochrane, Suffield, and Spruce Home. Elevation in meters above mean sea level, 10 and 20 m between tick marks. Range extent of repeat sectors is indicated by horizontal arrows.

Figure 86. Repeat sector at Wachusett Mountain. Phase One tower-top view looking SSE into repeat sector.

low-lying terrain from 7 to 8 km, the terrain is broken; from 8 to 10 km, the terrain is undulating; from 10 to 11.5 km, the terrain is hummocky; from 11.5 to 12 km, the terrain is again broken; and finally, from 12 to 13 km, the terrain levels out, although with some undulations. There are some small prairie sloughs or ponds in the sector (2 pereent by area) and some low marshy areas (5 pereent by area) surrounded by sedge and eattails. Only one small isolated serub tree was found in the seetor, right in the front left corner of the seetor at 7-km range and 125-deg azimuth.

Thus, on this Suffield military range, we expeeted to measure diserete-free grassland elutter with a multifrequeney mean strength characteristie perhaps midway between Big Grass Marsh and Vananda East. The mean elutter strengths that were measured at Suffield are shown in Figure 92. These results look very mueh like those we measured on very low-relief farmland dominated by diserete sourees. After obtaining these results, we returned to Suffield for on-the-ground field surveillance to see what discretes we might have missed out in the seetor; a few were found. An Alberta Energy Corporation (AEC) natural gas compressor pumping station had been built sinee the date of our aerial photos. This building was a

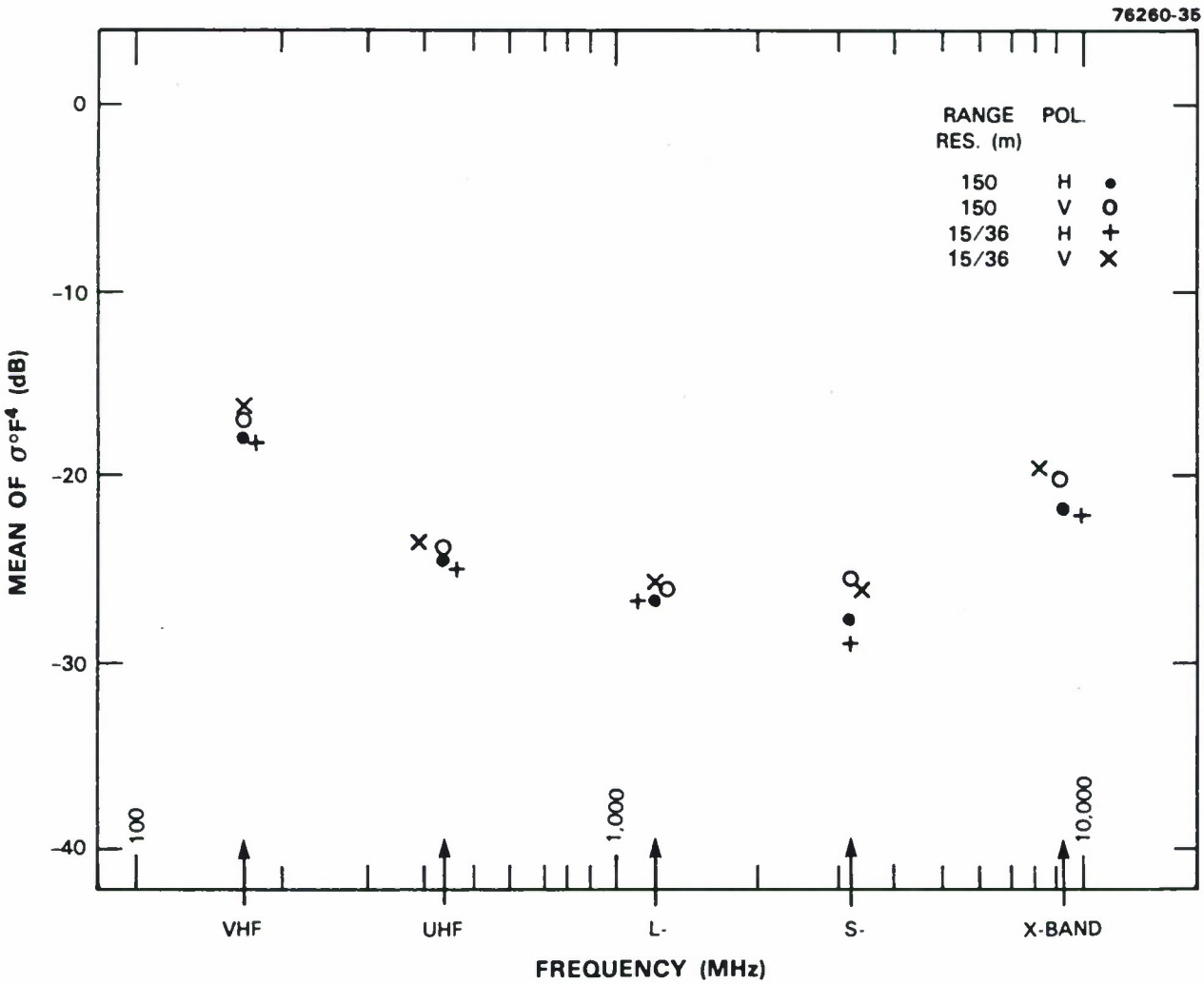

Figure 87. Mean clutter strength versus frequency at Wachusett Mountain.

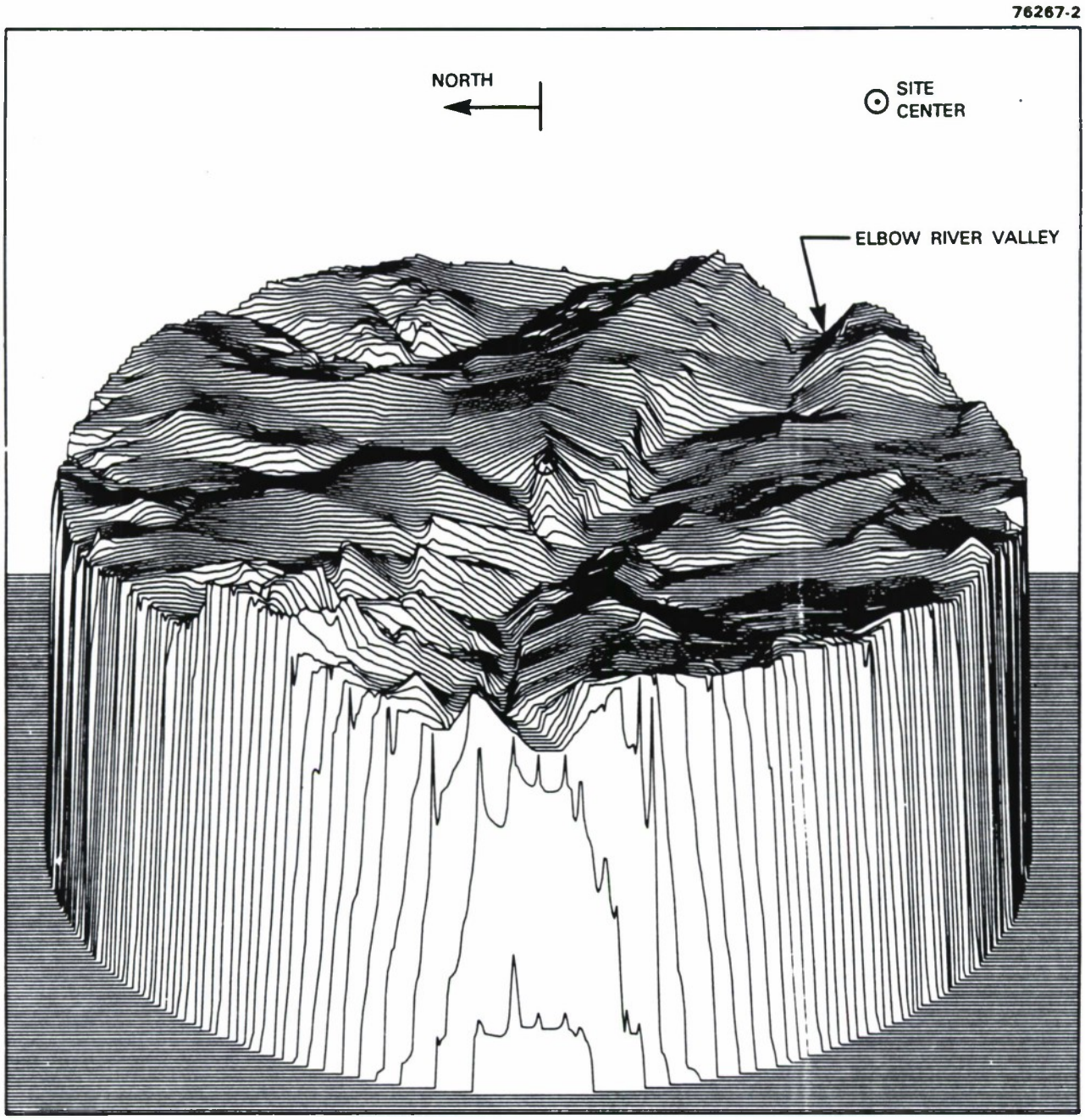

Figure 88. Three-dimensional oblique view of landform at Cochrane, Alberta. Clutter measurement site is at the center of the diagram. Maximum range = 20 km. East is at zenith to better show the Elbow River valley bisecting the region. Elevation difference between site center and river valley bottom is about 200 m. Based on data provided to DMA Format Level Two by Defence Cartographic Mapping and Charting Establishment, Ottawa.

Figure 89. Aerial photo of repeat sector at Cochrane. Scale = 1:50,000. North is to the left.

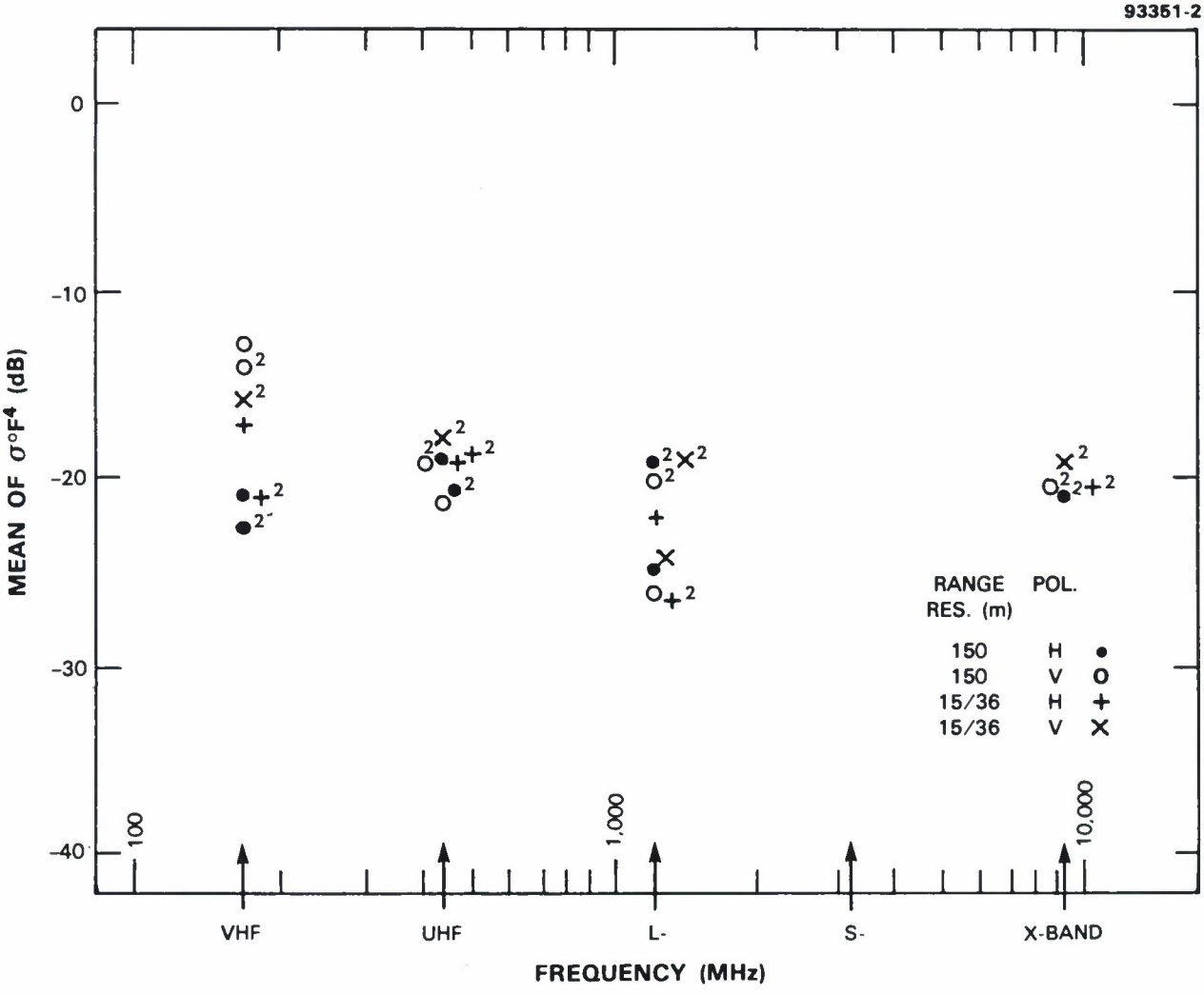

Figure 90. Mean clutter strength versus frequency at Cochrane. Repeat sector data. Two seasonal visits. First visit, summer, August 1982. Second visit, winter, February/March 1983. Second visit results indicated with superscript 2's. See Table A-25 to explain missing S- and X-band (first visit) data.

large, two to three story, rectangular metal barn with smaller outlying buildings and equipment located at 8.9-km range and 127-deg azimuth. A photograph of this building and the grassland around it is shown in Figure 93. Two smaller range buildings, also new, were nearby. All these buildings had power lines to them. We found another short stretch of power lines along a trail at 11.5 km. These power lines were just single wires on wooden poles.

These few discrete clutter sources, particularly those in the vicinity of the large AEC building, were enough to drive the Suffield repeat sector mean clutter strengths to high levels. This is evident by considering the results shown in Figures 94 and 95. These figures show the same measured data reduced and plotted different ways. Figure 94 shows the X-band clutter strength histogram for the Suffield repeat sector for the 15-m pulse length and at horizontal polarization. Figure 95 shows clutter strength versus range through the Suffield repeat sector, for the same X-band, 15-m pulse, horizontal polarization experiment, for five specific beam positions, namely, for 125.5, 126.5, 127.5, and 128.5 deg, which are the first four contiguous beam positions in the sector, and for 134.5 deg, which is the last beam position in the sector (recall that the X-band beamwidth is 1 deg, see Table A-6).

First, consider the histogram of Figure 94. This histogram was generated from the partially integrated data in which each sample was obtained by coherently integrating 32 of the 1024 pulses collected at a PRF of 2000 Hz in each range gate with step/scan antenna positioning. The first thing we draw attention to in this histogram is that in the clutter strength region from about -20 dB to about -45 or -50 dB, the histogram is very well behaved; the number of samples gradually diminishes with increasing strength in a very regular manner. In fact, over this region from -20 to -50 dB, the distribution of clutter strengths is very accurately represented by a Weibull distribution with a Weibull spread parameter of $a_w = 3.83$ (see Appendix C, Equation C-12.)* This well-behaved Weibull distribution of strengths measured from discrete-free Suffield grassland might well represent the areally extensive clutter background in general open farmland terrain, if one were inclined to develop a farmland clutter model in which a random clutter background is modeled separately from subsequently specified deterministic discrete clutter sources.

However, the next thing we draw attention to in the histogram of Figure 94 is that it contains a long high tail over the clutter strength region from -19 to +11 dB, caused by strong discretes of low percent occurrence. In fact, from -19 to +11 dB inclusive, there are 808 samples in the histogram of Figure 94, which constitutes 0.64 percent of the total number of samples in the histogram. This long high-side tail can barely be discerned in Figure 94. If we now turn to the sector display of Figure 95, it is evident that most of these strong values come from the vicinity of the large AEC building in the Suffield repeat sector. We first pause to describe the data in Figure 95 more specifically. These data involve no spatial averaging, but show clutter strength in individual resolution cells, range gate by range gate and beam position by beam position. In each resolution cell, the clutter strength shown is the temporal mean strength resulting from averaging 32 samples, each of which is a coherent average of 32 pulses recorded at a PRF of 2000 Hz. Generally, Figure 95 indicates that the clutter from this Suffield grassland is of a very spiky nature, with 30-dB fluctuations common, as individual cells drop into and out of direct

* In contrast, the distribution in Figure 94 is very poorly modeled as lognormal over the same region.

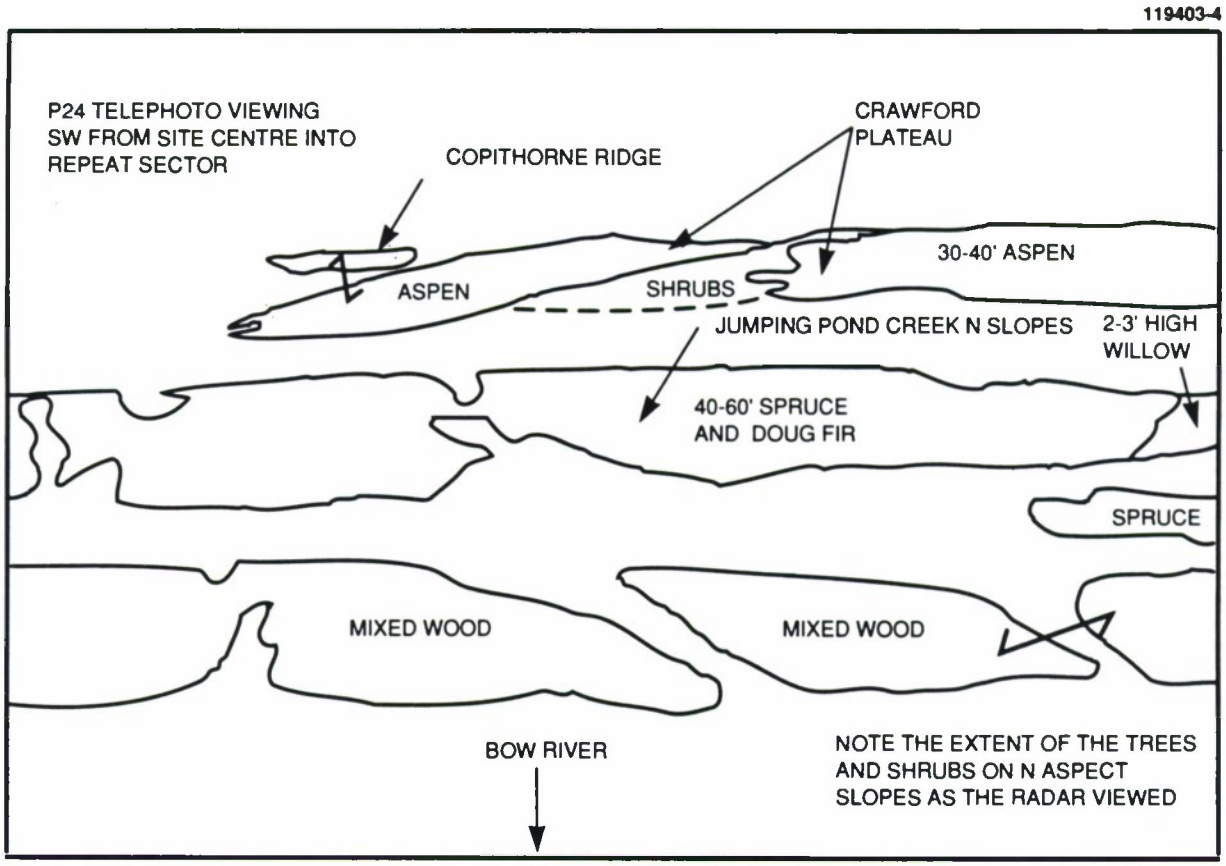

Figure 91 (a). Interpretation of some of the features in the Cochrane photo of Figure 91(b). This overlays Figure 91(b).

visibility at the low 0.3-deg depression angle involved. These data are a good example of the statistical nature of low-angle clutter, even on what is relatively homogeneous, discrete-free grassland (i.e., not constant σ°). Most of these clutter returns vary over the range from -20 to -50 or -60 dB or so. The major exception to this range of variation in the data of Figure 95 is the returns of strength >> -20 dB from cells in the near vicinity of the AEC building in the range interval from 8.8 to 9.0 km and at azimuths from 125.5 to 127.5 deg. For example, at the 127.5-deg azimuth position there is a strong specular flash directly from this building that raises the clutter return 30 dB or more above the envelope of the peaks in other cells not near the building. Although in the following beam position (i.e., 128.5 deg) no indication of the building remains, in the two preceding beam positions there is significant evidence of the building and associated discretes at levels > -20 dB spread over a number of range gates. Altogether, in these data there are 435 samples of strength ≥ -13 dB from the vicinity of the AEC building, which, if deleted, reduce the mean strength in the histogram of Figure 94 from -22.90 to -34.89 dB. Note that the general statistical nature of the grassland clutter at 134.5 deg, the final beam position in the sector, is

Figure 91 (b). Telephoto view from Cochrane site SW into repeat sector.

relatively similar in range of fluctuation to that 6 deg earlier (i.e., at 128.5 deg), except over the region from 7 to 8.5 km. This region is at the noise floor at 134.5 deg, where the noise level decreases with increasing range because R^4 STC attenuation was used in the experiment (see Figure A-17).

Thus, the data of Figures 94 and 95 indicate that a more appropriate value of X-band mean clutter strength (at 15-m pulse length, horizontal polarization) to represent discrete-free Suffield grassland is -34.9 dB, not the -22.9-dB value actually measured there and driven to be so large by the presence of the AEC building. In comparing this adjusted Suffield X-band mean clutter strength value of -34.9 dB for grassland at 0.3-deg depression angle with corresponding values from the two other grassland sites, we see in Figure 84 that it does indeed lie intermediate between the Big Grass Marsh value of -42.7 dB (level site, 0.2-deg depression angle) and the Vananda East value of -27.5 dB (high site, 1.0-deg depression angle).

We now proceed to similarly adjust Suffield repeat sector mean clutter strengths in other bands. We choose to do so at low resolution (i.e., 150-m pulse) because the low resolution data are much more clear-cut as to which samples come from the AEC building (we selected X-band, 15-m pulse in the preceding example to give as much resolution into the data as possible in this example). Thus, in the L-band (150-m pulse, horizontal polarization) histogram shown in Figure E-182, it is very obvious (and was confirmed in sector display plots like Figure 95) that there are four cells at $\sigma^{\circ}F^4$ levels of -4, -8, -16, and -17 dB providing samples (32 each) from the AEC building. When the samples from these four cells are removed from the histogram of Figure E-182, the mean strength of the histogram drops from -25.0 to -39.9 dB. Proceeding similarly in the other bands (at 150-m pulse length, horizontal polarization), we find that mean strengths adjust as follows: at X-band, from -21.7 to -33.9 dB; at S-band, from -25.3 to -43.2 dB; at L-band, from -25.0 to -39.9 dB; at UHF, from -36.8 to -40.3 dB; and at VHF, from -51.3 to -51.7 dB.

We now compare these adjusted Suffield mean clutter strengths (adjusted to be representative of grassland without the large AEC building discrete clutter source) with the other grassland sites (see Figure 84), particularly Vananda East, which has similar landform (i.e., 3-5) but at a higher depression angle. This comparison is made at 150-m pulse length and horizontal polarization. At UHF, L-, and S-band, the adjusted Suffield values are remarkably close to Vananda East values (the values are, for Suffield and Vananda East, respectively: at UHF, -40.3 versus -38.9 dB; at L-band, -39.9 versus -39.5 dB; at S-band, -43.2 versus -38.1 dB). Furthermore, in these three bands at both these grassland sites, mean clutter strengths are remarkably invariant with frequency at or near the -40-dB level. These -40-dB levels are the best estimates of mean clutter strength in these bands for canonical discrete-free grassland, and therefore, if we were to pursue the previous modeling discussion, are what we would assign as mean strengths to Weibull distributions for representing an areally extensive clutter background prior to deterministic specification of strong man-made discretes.

At VHF, although Vananda East mean clutter strength holds near the -40-dB level (viz., -41.7 dB), adjusted Suffield mean clutter strength drops to -51.7 dB (i.e., 10.0 dB weaker than Vananda East). This lower Suffield value is probably caused by VHF multipath loss from the hillside slope local to the antenna at Suffield (see Appendix C, Section C.2), which would not occur for the high bluff site at Vananda East. Note that, at VHF, the adjusted Suffield mean strength is only 0.4 dB weaker than the unadjusted value. This is because at VHF the cells containing the AEC building, although 25 to 30 dB stronger than surrounding cells, were 5 dB weaker than some cells at longer range (presumably strong due to multipath enhancement). This resulted in the mean clutter strength, dominated by these strong long-range cells, coincidentally being about equal to the strength of the cells containing the AEC building, so the inclusion of AEC cells has little effect on mean clutter strength.

At X-band, the Vananda East mean clutter strength jumps up from the -40-dB level in lower bands to -27.71 dB (remarked on earlier). The adjusted Suffield X-band mean clutter strength jumps up from -40 dB also, but to -33.9 dB,* a level 6 dB weaker than measured for grassland at Vananda East but still 11 dB stronger than measured for grassland at Big Grass Marsh.

In summary, the repeat sector values of mean clutter strength at Suffield, adjusted to be applicable to relatively discrete-free grassland by removal of cells containing the AEC building, are understandable

* Or to -34.9 dB for the 15-m pulse data of Figure 94.

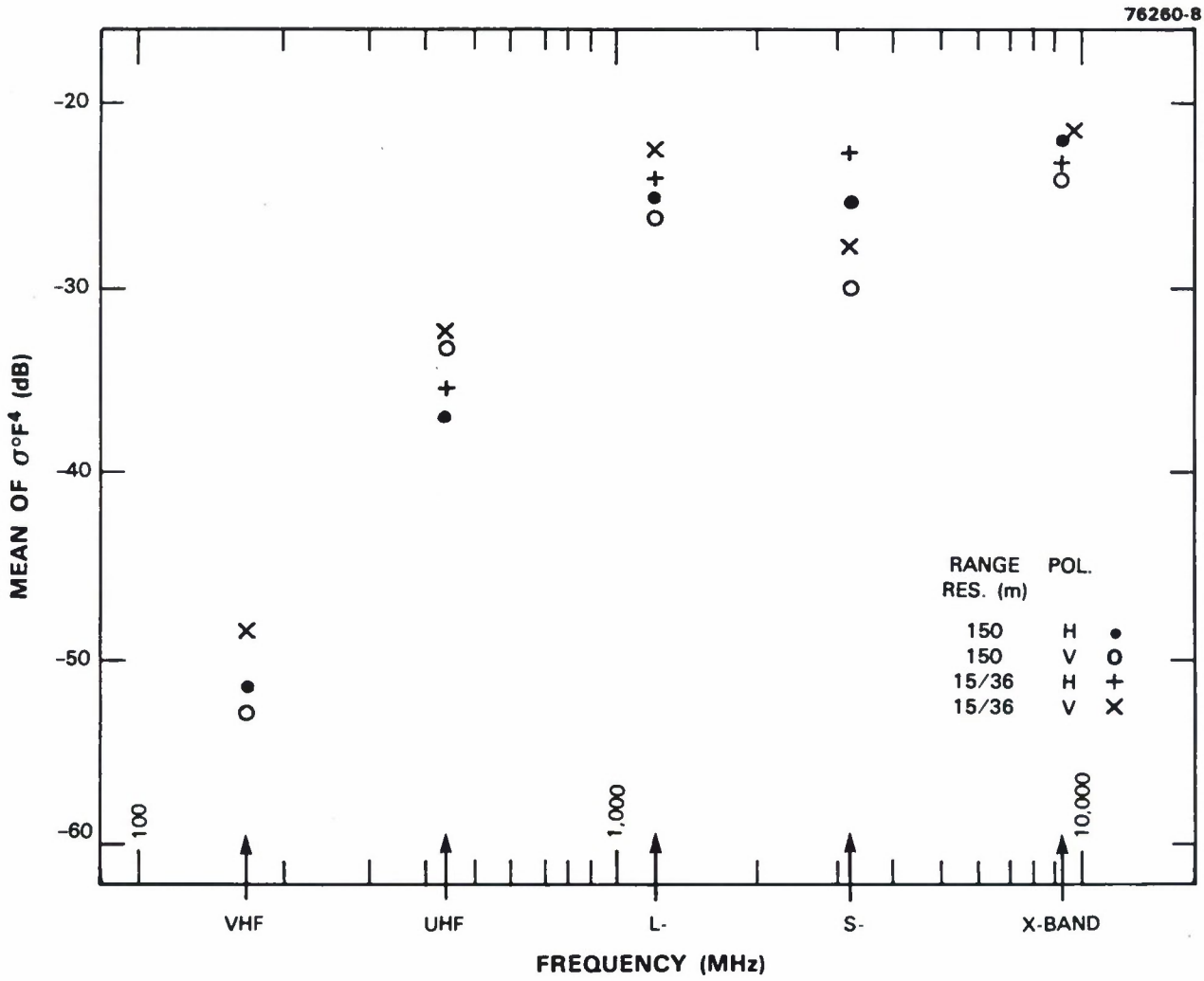

Figure 92. Mean clutter strength versus frequency at Suffield.

Figure 93. Alberta Energy Corporation natural gas compressor station on native herbaceous range in Suffield repeat sector. Range = 8.9 km, azimuth = 127 deg. Viewed from same direction as seen from Phase One.

and provide additional information within the context of the other discrete-free grassland sites, Vananda East (same 3-5 landform as Suffield) and Big Grass Marsh (landform = 1, level). The depression angle at Suffield, 0.3 deg, is intermediate between the depression angle at Big Grass Marsh, 0.2 deg, and that at Vananda East, 1.0 deg. As a result, at VHF and X-band, adjusted values of Suffield mean clutter strength for grassland lie intermediate between those at Big Grass Marsh and at Vananda East. At UHF, L-, and S-band, adjusted values of Suffield mean clutter strength are very nearly equivalent to those at Vananda East. Note that this technique of separately dealing with large man-made discretes in the clutter data is usually much more demanding than at Suffield because usually in farmland terrain many such sources exist. However, as mentioned earlier, such studies are being actively pursued in coordinated analyses of our Phase One data at DREO, Ottawa.

SITE = SUFFIELD RDF = RXTHIB.RDF;1

LC = 31 32 0 LF = 3 5 TC = 0 DA = 0.29 DAC = 2.05 PN = R99 DATE = 11-JAN-83

	SHDWUB	SHDWLB	SHDLSS		SHDW	SHDLSS			
MEAN	-22.90	-22.91	-19.07	WEIB0	0.104E+01	0.111E+01	SIG(MAX)		11
SD	-7.49	-7.49	-5.58	WEIB1	0.205E-01	0.300E-01	NDI(MAX)		-43
CDS	17.09	17.09	15.17	WEIR2	0.955E+00	0.924E+00	SAT(MAX)		999
CDK	34.53	34.53	30.69	WEISS	0.759E-01	0.290E+00	SIG(MIN)		-85
SPDL	-999.00	-999.00	-999.00	LDGB0	0.260E+01	0.257E+01	NDI(MIN)		-85
SPDR	15.53	15.54	13.68	LDGB1	0.503E-01	0.627E-01	SAT(MIN)		999
DBME	-49.60		-38.31	LDGR2	0.972E+00	0.961E+00	50	-51.0	-39.0
DBSD	12.32		9.18	LDGSS	0.285E+00	0.614E+00	70	-43.0	-34.0
DBCDS	0.40		0.06				90	-32.0	-27.0
DBCDK	3.02		5.25				99	-21.0	-16.0

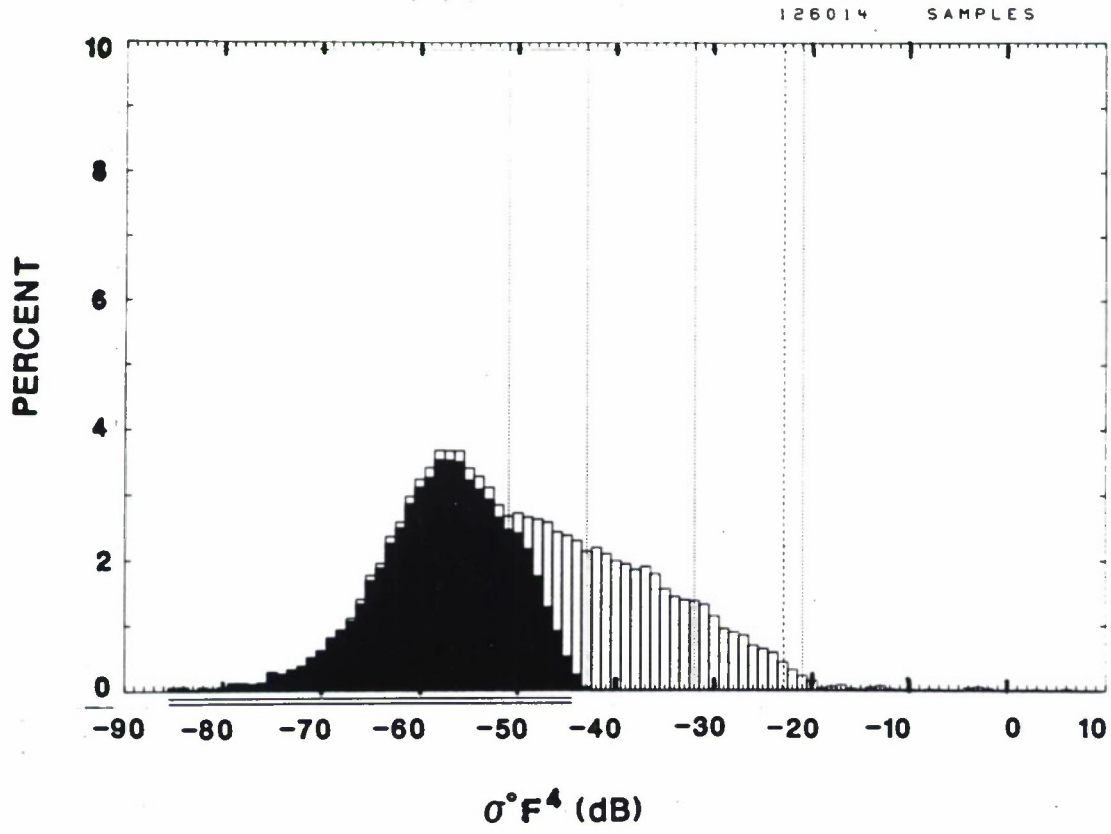

Figure 94. Clutter strength histogram for Suffield repeat sector. X-band, 15-m pulse, horizontal polarization. Digest experiment.

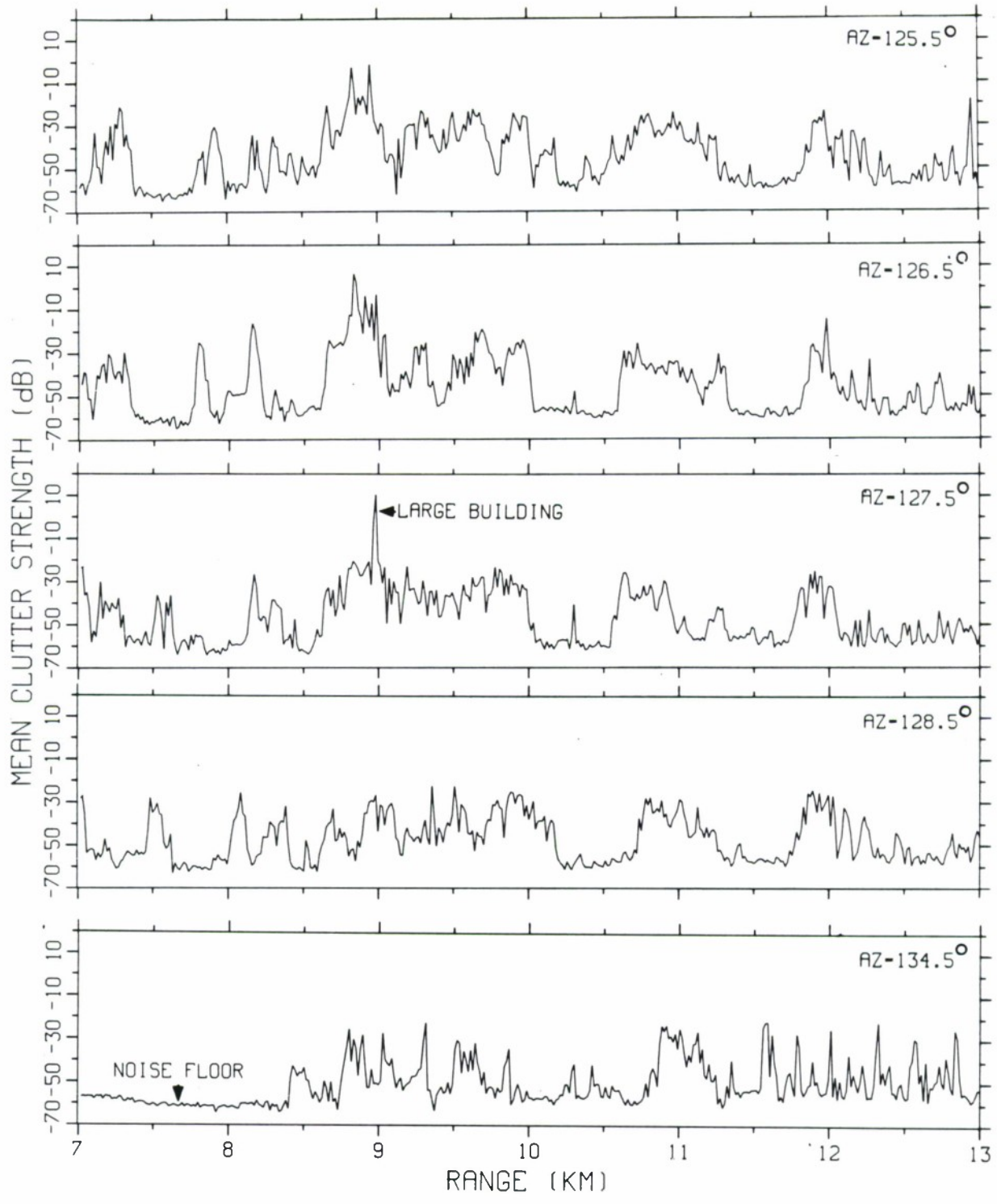

Figure 95. Mean clutter strength versus range at Suffield. Repeat sector data. X-band, 15-m pulse, horizontal polarization. Individual azimuth beam positions.

Spruce Home. We finish this section with a discussion of the Spruce Home results. Spruce Home is a northern site in Saskatchewan, 15 mi north of Prince Albert, in a transitional zone between the open prairie and the northern forest. As such, it is very similar to the Westlock site in northern Alberta. As at Westlock, the Spruce Home measurements were collected in winter season (early March 1984) with several inches of old snow on the ground and well before the spring thaw. Daytime temperatures during data collection ranged from -10°F to +28°F. A photograph of the Phase One equipment erected at Spruce Home is shown in Figure A-5. At Spruce Home, the site is on a small local hill, 63 ft above very level terrain farther out to the northeast in the repeat sector where we selected the range interval between 3- and 8.9-km range for data reduction. The DTED terrain profile through the Spruce Home repeat sector is shown in Figure 85. From site center, the terrain falls off in this direction by 53 ft in the first kilometer at 0.93-deg average terrain slope. The terrain is largely open farmland, but with many stands of trees and tree lines. Multifrequency mean clutter strengths for the Spruce Home repeat sector are shown in Figure 96.

The Spruce Home measurement scenario is strikingly similar to Rosetown Hill in many ways (nearly the same depression angle, 0.3 versus 0.4 deg; same purely level landform; similar range extent, 3 to 8.9 km versus 4 to 9 km for Rosetown Hill).* At both sites, we look down off a pronounced local hill (not just a topographic high) to very level agricultural terrain farther out. However, there are two significant differences between Spruce Home and Rosetown Hill. At Rosetown Hill, the terrain slopes away from the radar at 0.65 deg, compared to 0.93 deg at Spruce Home.† In both situations, this near-in, open, inclined terrain gives rise to strong forward terrain reflections and results in multipath lobing on the vertical antenna beam. In both cases, because of the terrain inclination, the lobing pattern is rotated down compared to the level terrain in the repeat sector farther out, but the lobing pattern is rotated down more at Spruce Home (i.e., 0.93 deg) than at Rosetown Hill (i.e., 0.65 deg). In neither case is this small rotation enough to bring the peak of the first VHF lobe, which occurs 1.48 deg above the inclined plane of the reflecting surface, to bear on the repeat sector range interval farther out. However, the small difference in terrain slope involved, namely, 0.28 deg, causes significant differences in VHF and UHF mean clutter strengths from the farther out range intervals. The Rosetown Hill data are shown in Figure E-140. Comparing these with the Spruce Home data of Figure 96, we see that, at both VHF and UHF, the Rosetown Hill mean strengths are about 9 dB weaker than the Spruce Home mean strengths.

However, we cannot attribute all of this 9-dB average difference to decreased multipath propagation loss at Spruce Home due to the 0.28 deg higher terrain slope there. The second significant difference between Spruce Home and Rosetown Hill is now addressed. This difference is the substantial secondary incidence of aspen trees (with a few spruce) in groves and tree lines at Spruce Home (i.e., land cover = 21-41) compared with no trees at Rosetown Hill (i.e., land cover = 21). These trees are evident in the photograph of Figure 97, which is a Phase One tower-top view northeast into the repeat sector at Spruce Home. The trees cause considerably stronger mean clutter strengths at Spruce Home compared

---

* Coincidentally, Rosetown Hill was the measurement site immediately following Spruce Home.

† It is the local terrain slope, not the hill height that is important. The hill height at Rosetown Hill is 98 ft, see Section 4.1.4.3, compared with 63 ft at Spruce Home.

with Rosetown Hill. For example, consider L-band, where repeat sectors at both sites should be well illuminated (i.e., peak of first multipath lobe at L-band occurs 0.2 deg above the plane of the reflecting surface). At both sites, the L-band mean strength data are remarkably tightly clustered (i.e., variations with polarization and resolution are very small; we have remarked on tight L-band clusters at a number of other sites as well, e.g., see Booker Mountain). However, the average L-band mean strength level at Spruce Home is at -24.8 dB, or 5.5 dB stronger than the average L-band mean strength level at Rosetown Hill of -30.3 dB. We believe this 5.5-dB difference is largely due to trees at Spruce Home. Note in Figure 96 that at Spruce Home the strong L-band mean strengths (i.e., -24.8 dB) are approximately maintained at S- and X-bands also (i.e., -25.5 and -25.8 dB, respectively). If we compare the Spruce Home mean strength data with the very low-relief agricultural data in Figure 72, in the microwave bands the Spruce Home data are at the very top or slightly above the very low-relief agricultural clusters due to trees. At UHF and VHF (vertical polarization only at VHF) the Spruce Home data are substantially above the very low-relief agricultural clusters, due both to trees and decreased multipath propagation loss. We refrain from including Spruce Home in with these very low-relief agricultural sites, partly because of the presence of trees as a secondary land cover classifier at Spruce Home (Table 7 shows that none of the very low-relief agricultural sites have such a secondary land cover classifier), but also partly because the 0.93-deg terrain slope of the hill of the Spruce Home site is just marginally within the 1-deg maximum slope we allow in very low-relief agricultural terrain.

Several final comments regarding Spruce Home will be made. First, note in Figure 96 that the multipath dominated measurements at VHF and UHF show mean strengths at vertical polarization much stronger than at horizontal. In fact, these Spruce Home polarization differences at VHF, namely, 12.3 dB for the 150-m pulse and 11.1 dB for the 36-m pulse, are the largest polarization differences seen across all of the sites in the repeat sector measurements. These differences support our argument of strong multipath at Spruce Home because we would expect higher reflection coefficients, stronger multipath, deeper nulls, and hence, more multipath propagation loss from the snow-covered Spruce Home reflecting surfaces at horizontal polarization than at vertical. We frequently observe similar but lesser effects of polarization in mean clutter strength caused by multipath (e.g., Rosetown Hill and Shilo). Next, Phase Zero measured the Spruce Home repeat sector at -27.9 dB mean strength on 29 October 1982 (i.e., with a light dusting of snow cover), which is very close to the Phase One value (at 150-m pulse length, horizontal polarization) of -26.8 dB measured 1-1/2 years later. Finally, these last two sites, Suffield and Spruce Home, although physically very different from each other, have, coincidentally, remarkably similar multifrequency mean clutter strength characteristics to each other.

4.3 SUMMARY OF MEAN GROUND CLUTTER STRENGTH VERSUS FREQUENCY BY TERRAIN TYPE

A major objective of this report is to show how mean ground clutter strength varies with frequency for various terrain types. Our approach for achieving this objective is to combine measurements from different sites within broad classes of similar terrain and depression angle, such that the results cluster within each category and separate between different categories. In the foregoing subsections of Section 4, we have presented and discussed in detail the clustering of the multifrequency mean strength data within

12 terrain categories. We have developed such clusters based on the repeat sector data base. Within each terrain category, we now specify the median level of the cluster of measured mean strengths in each of the five frequency bands, VHF, UHF, L-, S-, and X-band, as a general measure of mean strength at that frequency for that terrain category. In so doing, overly specific terrain and propagation effects in individual measurements are averaged out. The results are plotted in Figure 98 and tabulated in Table 11.

The results of Figure 98 and Table 11 generalize how mean ground clutter strength varies with frequency as a function of terrain type. These results are based on one unified program of measurements with accurate calibration and consistent data reduction throughout. In Figure 98 and Table 11, we have five broadly different terrain groups, namely, urban, mountains, forest, farmland, and a combined discrete-free category of desert, marsh, or grassland. We further partition many of these groups within several regimes of depression angle and/or terrain relief, such that there are 12 subcategories in all. A great deal of variability of mean clutter strength is observed in Figure 98 — in total 66 dB between mountains at VHF and desert or marshland at UHF. This extreme variability is what has plagued investigators attempting to understand and predict the performance of ground-based radars operating against clutter interference over the years. It is apparent that an orderly rationale of sorting through this variability on the basis of terrain type, depression angle, relief, and RF frequency reduces variability within class to that observed in the preceding Section 4 cluster plots* (or, in general, to within a one-sigma range of ± 3.2 dB, see Figure 110) and provides the separation between classes as observed in Figure 98.

We now discuss the results in Figure 98 and Table 11. For the most part, we leave all of the measurement-specific qualifications of these data to the preceding site-by-site discussions in Section 4 and focus more on pointing out the messages in these data. The clusters of mean strengths from which we obtained the medians of Figure 98 and Table 11 include mean strengths at both vertical and horizontal polarization and short and long pulse length. Variations with polarization and resolution, usually small, are more generally discussed subsequently in Section 5. In what follows we dwell for the first time on comparing and contrasting mean clutter strengths between classes, not on the degree of clustering of measurements from different sites within classes.

First, in Figure 98, focus on the two short-dashed curves at the top of the figure for mountain and urban clutter, providing very strong mean strengths in the -10- to -20-dB range. Mountain clutter at VHF provides the strongest mean clutter strengths measured at -7.6 dB. This falls rapidly by 14 dB with increasing frequency to levels of -21 and -22 dB at S- and X-bands. We believe that much of this trend of decreasing strength with increasing frequency in mountain terrain is caused by forest vegetation on steep mountain slopes. Urban complexes observed, as in the repeat sector measurements of this report, on low-relief open terrain provide large mean clutter strengths at high frequencies in the -10- to -12-dB range, partly because of their broadside aspect, but at low frequencies these large returns are decreased significantly by up to 10 dB through multipath loss. However, on the basis of the Phase Zero measurements, in more general composite terrain mean clutter strength from urban complexes at X-band is 12 dB weaker than on low-relief open terrain.

---

* For example, the "cluster plot" for forest/high-relief/high depression angle is Figure 32, and so on.

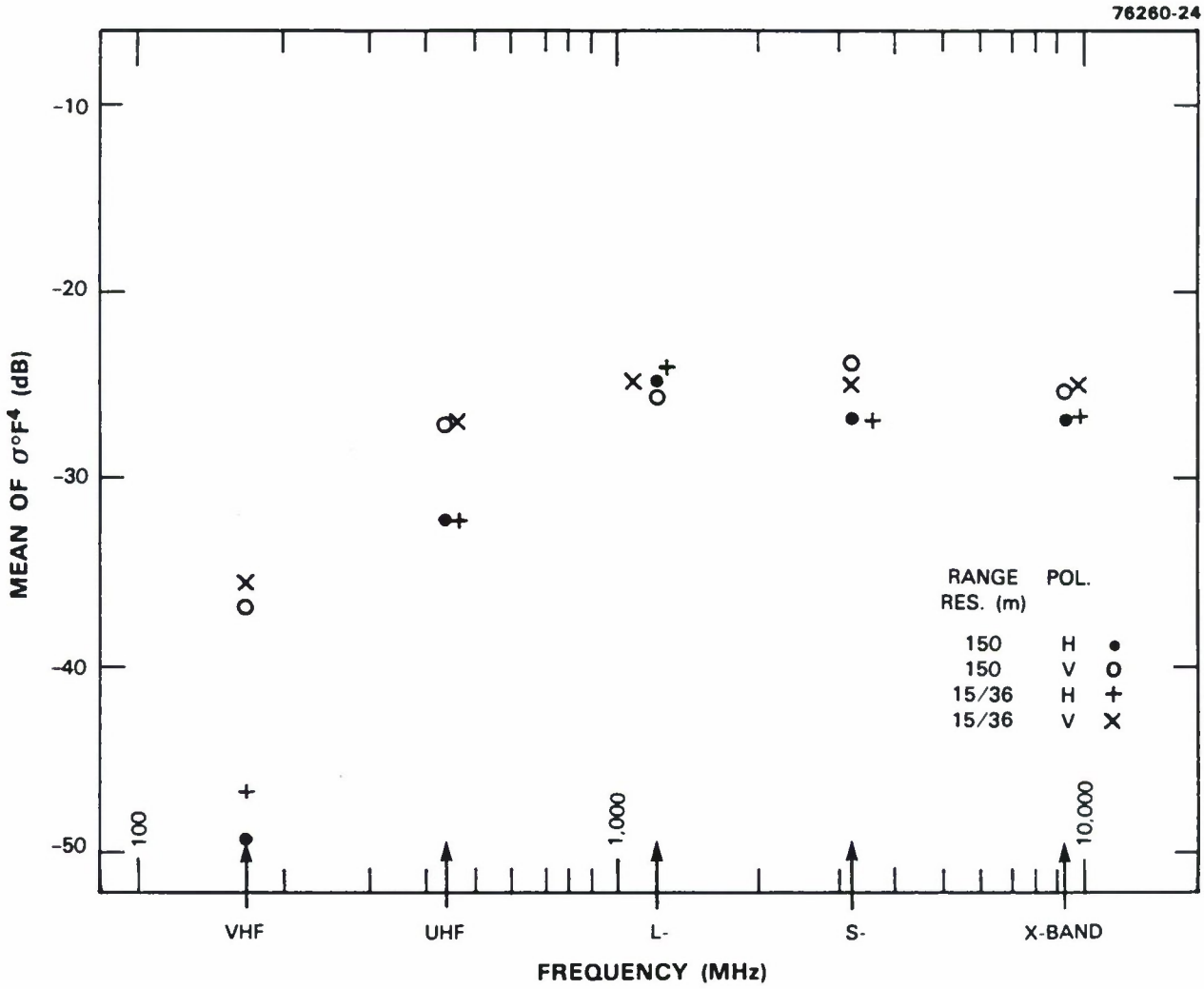

Figure 96. Mean clutter strength versus frequency at Spruce Home.

Figure 97. Secondary incidence of trees at Spruce Home. Phase One tower-top view looking NE into repeat sector. Arrow indicates position of remote weather station.

Next, in Figure 98, focus on the two long-dashed forest/high-relief curves near the top of the figure. These curves also show mean strengths decreasing with increasing frequency, as in mountains, but generally a few decibels weaker, partly due to less steep terrain slopes. Relatively little difference is seen between high and low depression angle in high-relief forest terrain at UHF, L-, and S-bands, indicating that terrain slopes are steep enough to largely overwhelm depression angle leverage on total illumination angle in such terrain. However, at VHF and X-band, depression angle is shown to be of more effect in high-relief forest terrain. At VHF, many of the measurement scenarios with low depression angle in high-relief forest terrain supported forward terrain reflections from the terrain between the radar and the farther out steep forest, and this led to multipath propagation loss in mean clutter strength from the steep forest. Thus, in Figure 98, mean clutter strengths in forest/high-relief/low depression angle terrain show a local countertrend decreasing from UHF to VHF by 3 dB. At X-band, the mean clutter strength in forest/high-relief terrain at high depression angle also shows a countertrend of increasing by 3 dB from S-band, and, in fact, is slightly higher than for mountains at X-band. From time to time, we have pointed out that 42 repeat sector terrain macropatches are not enough to iron out all site specificities in our results, and that this is the major reason why we are processing all of our 360-deg full coverage Phase One survey data to provide results from many more patches. In Figure 98, the fact that, at X-band, forest/high-relief/high depression angle mean strength rises above that of mountains is such a specificity. Phase Zero X-band measurements across many more patches show forest/high-relief/high depression angle mean strength to continue to decrease from its S-band value of -23.6 dB to an X-band value of -24.5 dB.

Next, in Figure 98, focus on the three low-relief forest curves indicated by "plus sign" plot symbols. In such terrain, mean clutter strengths vary strongly both with depression angle and RF frequency. At high depression angles in low-relief forest, mean clutter strengths decrease with increasing frequency. At low depression angles in low-relief forest, mean clutter strengths increase with increasing frequency. At any of the five frequencies, mean strength increases significantly with depression angle, more so at VHF (by 29 dB, from low to high depression angle) than at X-band (by 9 dB, from low to high depression angle). If we compare low-relief forest (plus signs) and high-relief forest (long dashes) both at high depression angle > 1 deg, we see little difference with relief at VHF, UHF, and L-band, but large 6-dB differences with relief at S- and X-band. This difference indicates that the degree of separation of clutter mean strength by terrain class can be a function of RF frequency; therefore, selection or specification of optimum terrain categories to separate clutter statistics can be frequency dependent. The rise in mean strengths from S- to X-band in low-relief forest at both high and intermediate depression angles is not borne out by Phase Zero data medianized over many more patches, which provides X-band values at or slightly below S-band in both cases (i.e., at -31.8 and -32.5 dB, respectively).

Next, in Figure 98, focus on the two farmland curves indicated by heavy solid lines midway in the figure. Then, in Table 11, notice that there is not significant separation in mean strengths between high-relief agricultural terrain (with terrain slopes > 2 deg) and moderately low-relief agricultural terrain (with terrain slopes between 1 and 2 deg). In these two terrain groups, there are random variations of the median level of mean strength by frequency band, with the former stronger at UHF and L-band, the latter stronger at VHF and S-band, and virtually identical levels at X-band, all within several decibels of -30 dB. Hence, we combine results from these two groups into one terrain category with terrain slopes > 1 deg. Although the combined cluster plot is not shown here, in Figure 98 the farmland curve annotated

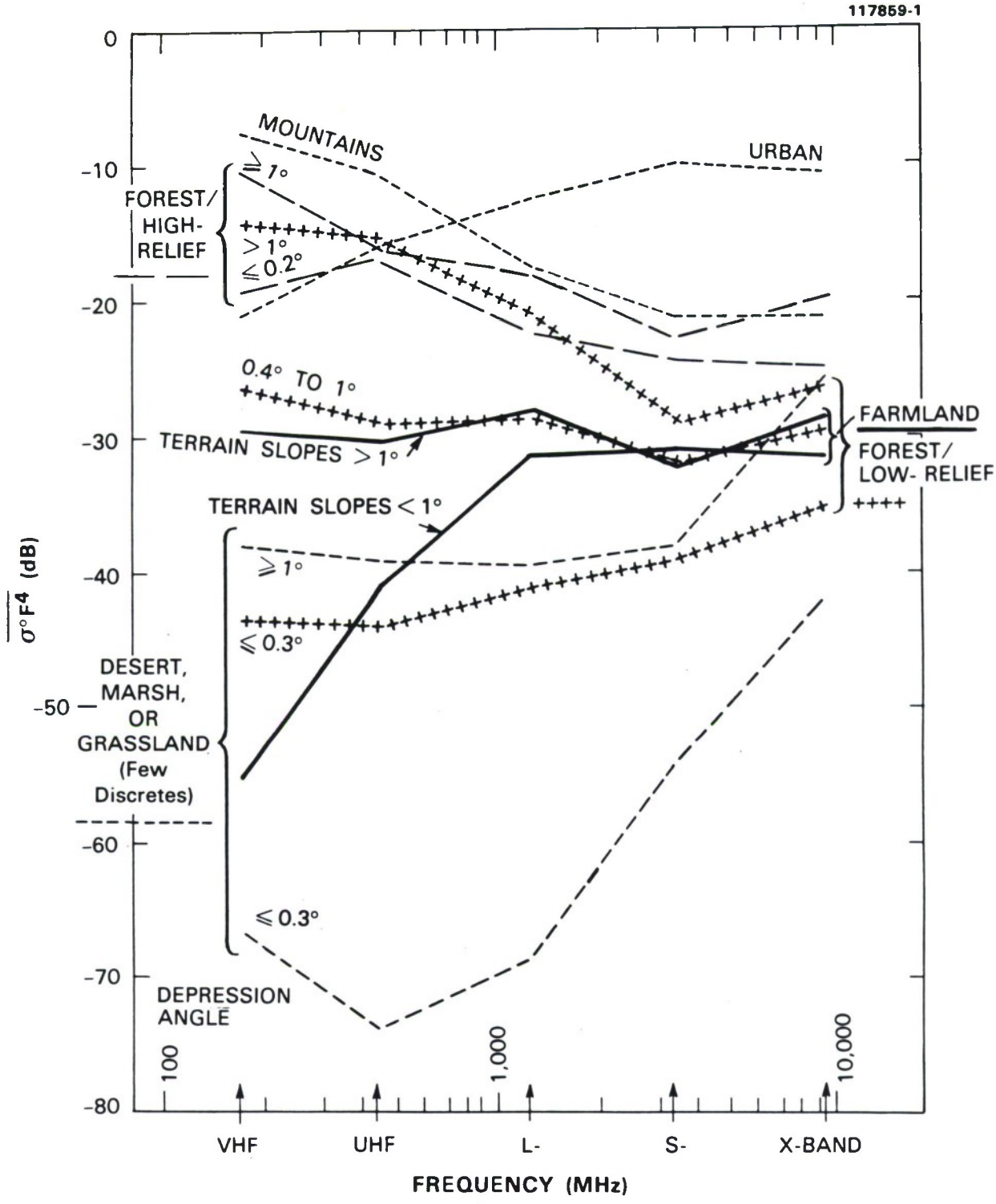

Figure 98. Mean clutter strength versus frequency for all measured terrain types. See Table 11 for numeric values.

TABLE 11

Median Value of Mean Clutter Strength Over M Repeat Sector Measurements* by Terrain Type and RF Frequency

Terrain Type	Median Value of $\overline{\sigma^{\circ}F^4}$ (dB)				
	Frequency Band				
	VHF	UHF	L-Band	S-Band	X-Band
URBAN	−20.9	−16.0	−12.6	−10.1	−10.8
MOUNTAINS	−7.6	−10.6	−17.5	−21.4	−21.6
FOREST/HIGH-RELIEF (Terrain Slopes >2°)					
High Depression Angle (>1°)	−10.5	−16.1	−18.2	−23.6	−19.9
Low Depression Angle (≤0.2°)	−19.5	−16.8	−22.6	−24.6	−25.0
FOREST/LOW-RELIEF (Terrain Slopes <2°)					
High Depression Angle (>1°)	−14.2	−15.7	−20.8	−29.3	−26.5
Intermediate Depression Angle (0.4° to 1°)	−26.2	−29.2	−28.6	−32.1	−29.7
Low Depression Angle (≤0.3°)	−43.6	−44.1	−41.4	−38.9	−35.4
AGRICULTURAL/HIGH-RELIEF (Terrain Slopes >2°)	−32.4	−27.3	−26.9	−34.8	−28.8
AGRICULTURAL/LOW-RELIEF					
Moderately Low-Relief (1°< Terrain Slopes <2°)	−27.5	−30.9	−28.1	−32.5	−28.4
Very Low-Relief (Terrain Slopes <1°)	−56.0	−41.1	−31.6	−30.9	−31.5
DESERT, MARSH, OR GRASSLAND (Few Discretes)					
High Depression Angle (≥1°)	−38.2	−39.4	−39.6	−37.9	−25.6
Low Depression Angle (≤0.3°)	−66.8	−74.0	−68.6	−54.4	−42.0

* Based on data in Tables D-2 through D-6; M varies with band and terrain type. See cluster plot figures for each terrain type.

as "terrain slopes > 1 deg" plots the median levels of the combined clusters of mean strength in each band. This curve is essentially invariant with frequency at the -30-dB level, with band-to-band fluctuations of at most 1 or 2 dB about this level. As discussed elsewhere, mean clutter strengths do not vary with depression angle in high-relief or moderately low-relief agricultural terrain, although the spreads in clutter amplitude distributions in such terrain are a very strong function of depression angle. Thus, in contrast to low-relief forest, in which mean clutter strengths vary strongly with both frequency and depression angle, in farmland mean strengths are invariant both with frequency and depression angle, except for very low-relief farmland.

As indicated in Figure 98, in very low-relief farmland, terrain slopes are less than 1 deg (and so are most depression angles, i.e., in such terrain there are usually few hills high enough to give much higher depression angles), and as a result there is a large multipath propagation loss at UHF (i.e., ≈ 10 dB) and VHF (i.e., ≈ 25 dB) in mean clutter strength below the nominal -30-dB level. The exact multipath propagation loss involved is very significantly dependent on the precise terrain slope of the hill upon which the radar is located, even in very low-relief terrain in which terrain slopes are less than 1 deg. In addition, the multipath propagation loss is theoretically dependent on geometric factors of antenna height, clutter source height, and distance between antenna and clutter source. In broad measure, our results do not show extreme sensitivity to clutter source height and range extent variations as they occur over the repeat sector matrix of patches. However, higher antennas generally provide somewhat stronger clutter; this matter is discussed and quantified in Section 4.1.4.3.

Note that there are remarkably small differences in mean clutter strength between farmland of moderate relief or greater (terrain slopes > 1 deg) and low-relief forest at intermediate depression angles. In fact, mean strengths in these two terrain categories even follow one another in band-to-band fluctuations near the -30-dB level in Figure 98, presumably just by coincidence. We have many sites in each of these two terrain classes (see Table 7). Thus, in much commonly occurring low-relief rural terrain, neither very level nor very steep, at intermediate depression angles, mean clutter strengths hover around the -30-dB level, irrespective of whether the terrain is forest or farmland.

Finally, in Figure 98, focus on the two short-dashed curves at the bottom of the figure for desert, marsh, or grassland, that is, for open terrain with very few discrete sources compared with farmland. On discrete-free desert, marsh, or grassland, mean clutter strength is weaker than for other terrain types. Again, at low depression angles, there is a large multipath loss due to decreased illumination at the lower frequencies, and this loss is greater and extends to higher frequencies than in farmland because the clutter sources are much lower in such terrain (e.g., a sagebrush bush) than in farmland (e.g., a silo). Note that propagation loss alone would continue to decrease mean clutter strength from UHF to VHF at low depression angles on open desert, marsh, or grassland. However, the data from desert and frozen marshland indicate that intrinsic σ°s actually rise substantially from UHF to VHF in such terrain, enough to more than compensate for increased propagation loss at low angles from UHF to VHF and to result in greater mean clutter strengths at VHF compared to UHF at both high and low depression angles. Our data from grassland indicate intrinsic σ°s at VHF equal to those at UHF.

We observe that mean clutter strength increases very strongly with depression angle in discrete-free desert, marsh, or grassland in all frequency bands, including VHF where much of the effect is caused by

multipath propagation, and X-band where multipath has less effect. More specifically, mean clutter strengths in Figure 98 for desert, marsh, or grassland increase from low to high depression angle by 30 dB or more at low frequencies and 16 dB at X-band as depression angle increases over the range from ≤ 0.3 deg to 1 or 2 deg.

If we compare mean clutter strength between desert, marsh, or grassland and forest at X-band in Figure 98, we observe that at low depression angles, mean strength in desert or marshland terrain is 5 or 6 dB weaker than in forest terrain. However, at high depression angles > 1 deg (and on the basis of two different Phase One measurement sites), mean strength in desert or grassland is equal to that in low-relief forest terrain (i.e., at X-band, looking down at sagebrush vegetation is equivalent to looking down at a forest canopy). This strong X-band desert or grassland clutter at high depression angle is 12 to 14 dB greater than at S-band and lower frequencies.

In this summary section, we have focused on median levels of clusters of measured mean clutter strengths for each combination of terrain type and frequency. We could provide more information based on these clusters of mean strengths than just their median levels. For example, we could provide similar tables to Table 11 showing median differences in mean strength with polarization and resolution within clusters by terrain type and frequency. Indeed, we do pursue such polarization and resolution studies somewhat in Section 5, to show such differences by frequency (viz., Tables 13 and 15) or by terrain type (viz., Tables 14 and 16), but not by both. If an investigator is interested in further pursuing such follow-on information regarding any of our clusters of mean strengths, he or she can straightforwardly reduce it himself or herself from the specification of clusters and values of mean strengths provided in this report. If, however, an investigator is interested in other statistical attributes of clustered clutter amplitude distributions besides the mean, for example, the median or other percentiles, or higher moments, he or she needs additional information. Subsequently, in Section 6, we provide medianized levels of higher moments and percentiles of clutter amplitude distributions within our same measurement clusters as specified here, by terrain type and frequency band.

5. GENERAL DEPENDENCIES OF MEAN GROUND CLUTTER STRENGTH WITH RADAR PARAMETERS

Tables D-2 through D-6 in Appendix D contain approximately 960 accurately calibrated and consistently reduced pairs of numbers for mean and standard deviation in ground clutter spatial amplitude distributions. Each pair has been centrally selected from a set of repeated measurements. In totality, these tables provide a wealth of information descriptive of ground clutter amplitude distributions over large spatial regions at near grazing incidence. These numbers were measured at 42 different places on the surface of the earth, but aside from site name, Tables D-2 through D-6 carry no terrain descriptive information such as is provided in Table D-1. In perusing Tables D-2 through D-6, one senses that there is considerable general information provided in them concerning dependencies of ground clutter on the main radar parameters of frequency, polarization, and resolution, over and above specific variations from site to site and terrain type to terrain type. What can we say about such general radar parameter dependencies of ground clutter, for example, for the benefit of radar engineers who need to design radars to perform in a variety of terrain types?

In following subsections in Section 5, the data of Tables D-2 through D-6 are reduced to provide general information on how mean ground clutter strength varies with frequency, polarization, and resolution. Variations with frequency are shown independent of terrain type (see Section 4 for frequency dependence by terrain type). Variations with polarization and resolution are shown three ways: (a) by frequency band independent of terrain type, (b) in an overall distribution independent of frequency and terrain type, and (c) by terrain type independent of frequency.

Tables D-2 through D-6 also contain general information on seasonal variation of ground clutter (seven of the site visits are repeats at different seasons). In addition, by including the set of day-to-day repeated measurements behind each entry in these tables for any given visit, information is available to provide general dependencies of ground clutter on day-to-day changes, primarily with weather. In Section 6, the data of Tables D-2 through D-6 are reduced to provide general information on how mean ground clutter strength varies with weather and season.

5.1 FREQUENCY DEPENDENCE

Before showing the general or non-terrain-specific frequency dependence of ground clutter, let us do what is sensible in averaging together results from all of our terrain types. For example, there are urban and rural terrain types. Within rural, we have extreme terrain types such as mountains and deserts as well as more commonly occurring general types of farmland and forest. Should we include urban terrain types? We think not. Urban stands apart as a special man-made terrain type. Should we include mountains and desert? It turns out that it really does not much matter, in terms of overall mean clutter strength. Mountains influence the overall level to be somewhat higher, desert to be somewhat lower, and these two influences tend to cancel. (In fact, including urban also does not much matter because the number of rural sites is so much greater.) So, somewhat arbitrarily, we decide to include all rural sites including mountains and desert for the sake of generality but to delete urban as really quite different in kind, not just degree, from rural.

All the rural mean strengths in Tables D-2 through D-6 are plotted as a scatter plot versus frequency, VHF through X-band, in Figure 99. Five urban sites, see Table 7, and six seasonal repeats, see Table D-1,

are deleted. Data are not available for Katahdin Hill (1) or North Truro. This leaves 37 rural sites. Multifrequency mean clutter strength data from these 37 sites for both pulse lengths and polarizations are plotted together in Figure 99. The resultant scatter plot is basically funnel-shaped* with wide scatter at VHF and decreasing scatter as frequency increases to X-band.

The central or median position of this scatter plot (which includes values for both pulse lengths and polarizations) is specified in each frequency band as a general non-site-specific measure of mean ground clutter strength. The results are tabulated in Table 12. These results indicate that general mean ground clutter strength is remarkably invariant with RF frequency, VHF through X-band, at or about the -30-dB level with no strong trend. More specifically, the mean of all five clutter strength numbers in Table 12 is -29.2 dB, and all five numbers lie within 1.7 dB of this. Mean strengths at VHF, UHF, and S-band are all within a fraction of 1 dB of -30 dB; mean strengths at L- and X-band are closer to -27.5 dB.

TABLE 12
General Dependence of Mean Ground Clutter Strength on Frequency

	Frequency Band				
	VHF	**UHF**	**L-Band**	**S-Band**	**X-Band**
Median value of mean clutter strength (dB)	–29.6	–30.3	–27.8	–30.7	–27.5
Standard deviation in mean clutter strength (dB) (i.e., one-sigma variation)	16.6	13.6	9.7	7.1	5.8
Number of repeat sector measurements	144	146	146	110	129

Notes: Median values of mean clutter strength over 37 rural sites. Also, one-sigma variations of mean strength in each band. Phase One repeat sector data, seasonal repeats not included.

In grossly averaging across many terrain types in this manner, we need to be careful that the result may be unlike any particular terrain type. In that case, we would never be designing for a real situation. In earlier discussions, we have remarked from time to time on approximate observed frequency invariance of mean clutter strength near the -30-dB level, both site-specific and terrain-type-specific. For example, Figure E-85 shows mean clutter strengths at one site, Wainwright, remarkably invariant near the -30-dB level. (Also see Figures E-80 and E-113.)

* Especially if we discount the desert (Knolls) and marsh (Big Grass Marsh) results that tend to separate out at the bottom of the plot at UHF, L-, and S-bands.

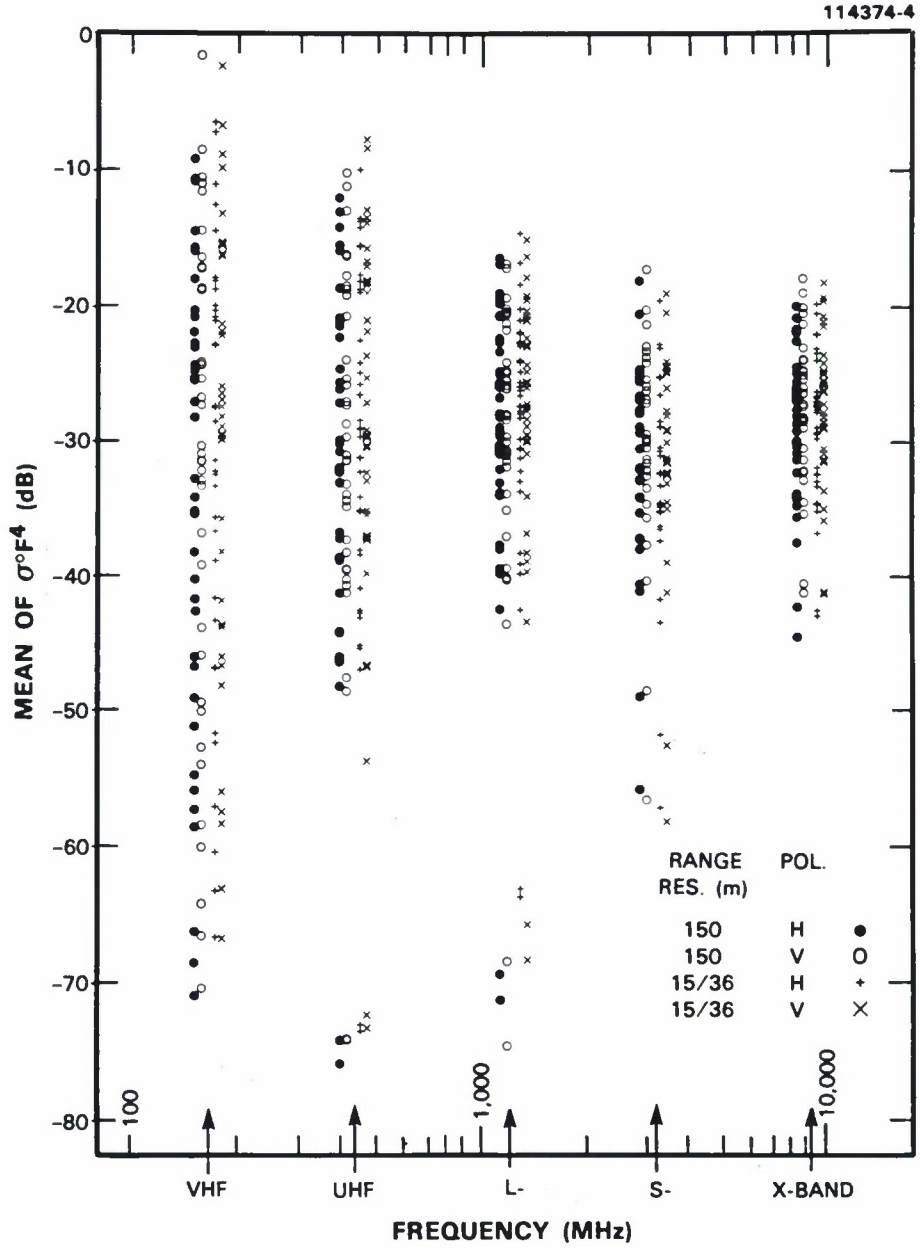

Figure 99. Mean clutter strength at 37 rural sites. Repeat sector data.

Besides characterizing the central level in our funnel plot, we also wish to quantify the spread whereby the funnel is wide at VHF and narrow at X-band. This is done by computing, for each band, the standard deviation or one-sigma range of variation of all the contributing mean strengths. The results are also shown in Table 12. To the extent that the mean strengths are distributed normally in each band (a fair approximation), this one-sigma variation is the range within which 68 percent of the values fall. There is a strong clear monotonic trend in Table 12 where this one-sigma range of variation decreases with increasing frequency from 16.6 dB at VHF to 5.8 dB at X-band. That is, mean clutter strengths in rural terrain vary much more at VHF than at X-band. The reasons are associated with VHF clutter strengths increasing in forest due to decreased vegetative absorption at VHF compared to the microwave bands and with VHF clutter strengths decreasing in open level farmland because of multipath loss. Our terrain-specific characteristics of mean strength with frequency do not have this problem of greatly increased variability at VHF. That is, bringing in terrain descriptive information improves our prediction accuracy.

5.2 POLARIZATION DEPENDENCE

Central (medianized) differences in mean clutter strength with polarization across all repeat sectors including seasonally repeated measurements are shown in Table 13. Each difference is computed as mean strength at vertical polarization in decibels minus mean strength at horizontal polarization in decibels. That is, each decibel difference represents the ratio of power received at vertical polarization to power received at horizontal polarization for otherwise comparable measurements. The medianized differences across all sites are shown in Table 13 for each RF frequency band, each range resolution, and for both range resolutions combined.

TABLE 13
Median Differences in Mean Clutter Strength with Polarization, VV-HH

Range Resolution	Differences (dB) in Mean Clutter Strength with Polarization, VV-HH (One-Sigma Variation, dB)				
	Frequency Band				
	VHF	UHF	L-Band	S-Band	X-Band
Low (150-m pulse length)	1.0 (4.5)	1.8 (2.8)	0.3 (2.3)	2.3 (1.8)	1.7 (1.6)
High (15 m at L-, S-, X-bands; 36 m at VHF and UHF)	1.6 (3.8)	2.0 (3.2)	0.4 (2.9)	2.3 (1.8)	1.7 (2.3)
Both	1.2 (4.1)	2.0 (3.0)	0.4 (2.6)	2.3 (1.8)	1.7 (2.0)

Notes: Phase One repeat sector data. All site visits. One-sigma variations are shown in parentheses.

The median differences of mean clutter strength with polarization in Table 13 are small, on the order of 2 dB or less. Recall that the nominal calibration accuracy is 2 dB rms across all the sites. Note that, specifically, the median differences with polarization in Table 13 are quite close to 2 dB, V-H, at UHF, S-, and X-bands, but a bit less at VHF, and near zero at L-band. Also note that there is very little difference in these median differences with range resolution, so we can concentrate on the bottom row that shows median differences across the set of experiments including both resolutions.

Is there really a ≈ 2-dB average difference in mean clutter strength with polarization, or could these data in Table 13 perhaps be finding small calibration errors as antenna polarization is changed? Even though calibration accuracy is specified at 2 dB rms over all the sites, in Table 13 we are considering differences in two measurements always conducted at the same site, often one immediately following the other, so calibration differences between them should be much less than 1 dB (see Tables A-12 and A-13) for everything up to the antennas. It is very unlikely that four out of five bands would have the same net errors in antenna gain, namely, V > H by 2 dB. That is, our external calibrations would have detected an error of 2 dB in antenna gain, e.g., see Table A-10. Thus, we accept the conclusion that, on the average, mean ground clutter strength is often 2 dB or so stronger at vertical polarization than at horizontal. The reason may be associated with the preferred vertical orientation of many discrete clutter sources.

Although average differences in mean clutter strength with polarization are small, individual differences in specific pairs of measurements can be greater. For example, if we consider all of the repeat sector measurements, still separated by frequency band but including measurements at both pulse lengths, and look for the largest-but-one* difference in mean clutter strength with polarization in each direction, V > H and H > V, respectively, we find the following: at VHF, 11.1 and 7.0 dB; at UHF, 6.8 and 3.2 dB; at L-band, 5.1 and 6.5 dB; at S-band, 5.1 and 4.6 dB; and at X-band, 5.5 and 4.0 dB.† Because of these occasional larger differences in mean strength with polarization, we now consider the one-sigma range of variation shown in Table 13, which specifies the larger, more significant, differences with polarization in terms of decreasing probability of occurrence. In Table 13, the one-sigma range of variation in mean strength with polarization about the mean difference, which is usually nonzero, decreases from 4.1 dB at VHF to 2.0 dB at X-band.

Even though there are larger polarization differences in mean strength at the lower bands than at the higher bands, we now combine the differences at all five bands and both pulse lengths into one overall histogram. This histogram is shown in Figure 100. The corresponding cumulative distribution is shown in Figure 101. The overall median polarization difference in mean clutter strength across all bands is 1.5 dB, V > H. The overall one-sigma range of variation across all bands is 2.8 dB. This histogram also demonstrates that larger polarization differences in mean clutter strength occur significantly frequently in ground clutter.

---

* Discount the largest difference in each direction, V > H and H > V, as the extreme statistical outlier.

† These largest-but-one differences with polarization, V > H and H > V, respectively, occur at the following sites by setup number and may be found in the individual site plots of mean strength in Appendix E: at VHF, 34 and 39; at UHF, 13 and 40; at L-band, 7 and 43; at S-band, 22 and 12; and at X-band, 48 and 38. Of these, six are at 150-m pulse length, and four are at 15/36-m pulse length. In the foregoing, no two setup numbers repeat, and the setup numbers occur randomly by site and terrain type.

The corresponding cumulative distribution of polarization differences in mean clutter strength in Figure 101 allows us to read probability of occurrence directly. For example, in 3 percent of the measurements, mean strength at horizontal polarization was stronger than at vertical by 5 dB or more (left tail); in another 3 percent of the measurements, mean strength at vertical was stronger than at horizontal by 7 dB or more (right tail). The remaining 94 percent of measurements had lesser differences in mean strength with polarization. Seventy-five percent of measurements had differences within the 2.8-dB one-sigma range of variation about the mean difference.

In the above, we have presented and discussed differences in mean clutter strength with polarization broken down by frequency band and resolution (i.e., Table 13), individually for worst-case (but one) measurements, and overall for all bands and both resolutions in terms of probability of occurrence (i.e., Figures 100 and 101). We now proceed to present differences in mean strength with polarization broken down by terrain type. Table 14 shows differences in mean clutter strength with polarization for our 12 terrain categories averaged across all five frequencies and both pulse lengths. On the whole, differences with polarization remain small when broken down into our 12 individual terrain categories. An exception is high-relief agricultural terrain, for which, in the measurements (see Figures E-100, E-104, and E-109), mean clutter strength at vertical polarization was, on the median average, 4.8 dB stronger than at horizontal polarization. Some small trends are observable in the data of Table 14. Thus, differences in mean strength with polarization increase with increasing depression angle in low-relief forest and in desert, marsh, or grassland, increase with increasing relief in low-relief agricultural terrain, but decrease with increasing depression angle in high-relief forest. The individual site data in Appendix E should be studied before too much statistical significance is attributed to any of these small trends.

5.3 RESOLUTION DEPENDENCE

The clutter coefficient σ° is equal to the RCS of the resolution cell divided by the area of the cell. This normalization by cell area means that, in homogeneous clutter where RCS increases directly with cell size, there is no dependence of σ° on spatial resolution. The real world of ground clutter is the antithesis of homogeneity. With real clutter, we need to think of distributions of varying σ° over a spatial region, not of a constant σ°. The spreads of these distributions are fundamentally dependent on spatial resolution, where increasing resolution results in less averaging within a cell and thus more cell-to-cell variability (e.g., see Figure 104). However, even for real heterogeneous clutter, the mean clutter strength of the spatial amplitude distribution over a fixed region, unlike any other statistical attribute of the distribution, is often relatively independent of spatial resolution.

To see why this is so, consider the following arguments. First, imagine a resolution cell of 150-m range resolution containing one telephone pole of 1 m^2 RCS in a clutter-free background. Let the σ° of the cell be x. Now imagine increasing range resolution to 15 m, so that 10 cells cover the region previously covered by the 150-m cell. Of these 10 cells, one will have a σ° of $10x$ (i.e., pole RCS stays the same at 1 m^2, cell size smaller by a factor of 10), and the other nine cells will have σ°s of zero. The mean clutter strength over all 10 cells at 15-m resolution is still x (i.e., one value of $10x$ averaged together with nine values of zero), the value for the 150-m cell.

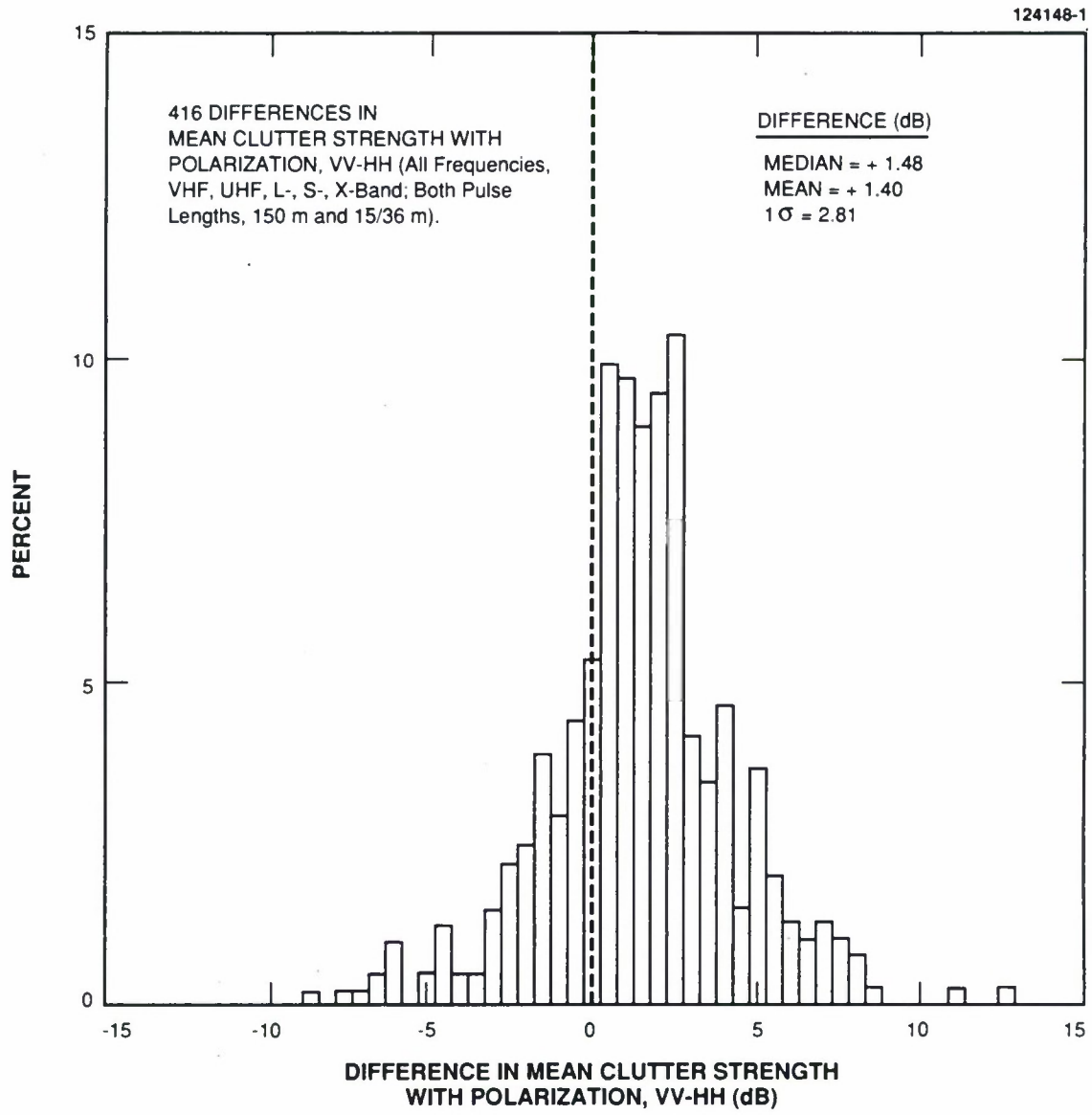

Figure 100. Histogram of differences in mean ground clutter strength with polarization, VV-HH. Phase One repeat sector data. All site visits, all five RF frequencies, both range resolutions.

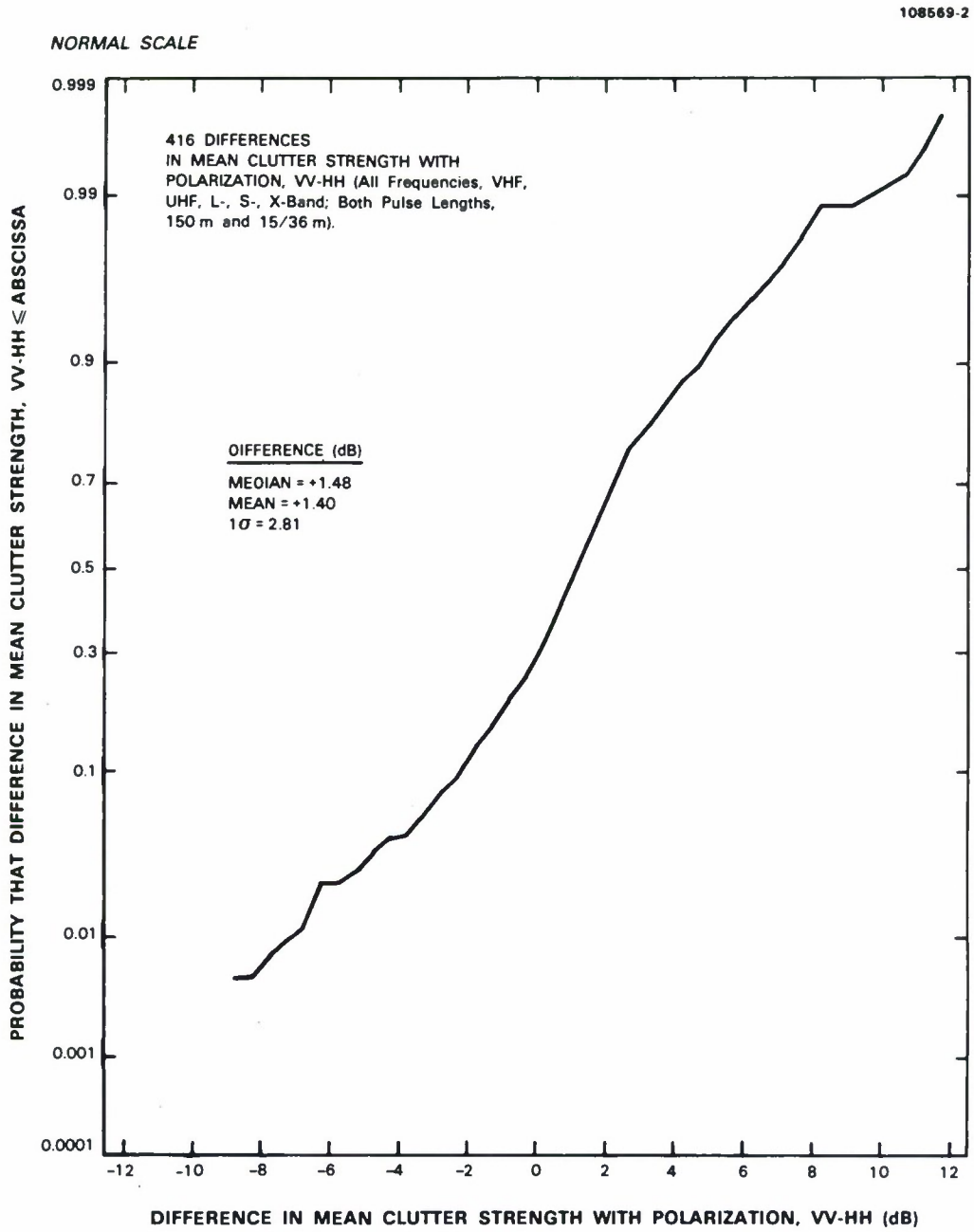

Figure 101. Cumulative distribution of differences in mean ground clutter strength with polarization, VV-HH. Phase One repeat sector data. All site visits, all five RF frequencies, both range resolutions.

TABLE 14
Average Differences in Mean Clutter Strength with Polarization, VV-HH, by Terrain Type

Terrain Type	Differences (dB) in Mean Clutter Strength with Polarization, VV-HH		
	Median	Mean	Standard Deviation
URBAN	1.07	0.66	2.76
MOUNTAINS	1.16	2.37	2.81
FOREST/HIGH-RELIEF			
High Depression Angle	0.56	1.25	1.75
Low Depression Angle	1.66	1.79	1.88
FOREST/LOW-RELIEF			
High Depression Angle	1.23	1.20	2.05
Intermediate Depression Angle	0.95	0.64	2.47
Low Depression Angle	0.16	–0.11	1.98
AGRICULTURAL/HIGH-RELIEF	4.80	3.64	3.79
AGRICULTURAL/LOW-RELIEF			
Moderately Low-Relief	2.51	1.74	3.17
Very Low-Relief	1.57	1.41	3.09
DESERT, MARSH, OR GRASSLAND (Few Discretes)			
High Depression Angle	2.37	2.19	2.50
Low Depression Angle	0.19	0.08	2.19

Notes: Repeat sector data. All sites, all five frequencies, both pulse lengths. Based on data in Tables D-2 through D-6.

Second, imagine a 150-m resolution cell containing 10 approximately equispaced telephone poles, each of 1 m^2 RCS. Assume that the 10 returns from these poles are of random phase (i.e., we can imagine the exact position of each pole within its 15-m domain to be random with respect to RF wavelength). Imagine illuminating all 10 poles in one big 150-m resolution cell. Because the phases of the 10 returns are random, powers and hence RCSs add, and the measured RCS is 10 m^2. Let the resultant $\sigma°$, obtained by dividing by the area of the 150-m cell, be x. Now imagine increasing range resolution to 15 m, so that

there is only one pole per cell. The RCS of each 15-m cell is now 1 m^2, or one-tenth that of the large cell, but the area of each small 15-m cell is also one-tenth that of the large 150-m cell, so that σ° of each small cell remains x as does the mean over all 10 small cells.

Thus, in power-additive situations where clutter sources within cells are randomly phased, mean clutter strengths over fixed spatial regions are independent of resolution. In voltage-additive situations where only several sources exist within a cell of fixed phases that can interfere constructively or destructively, separating the returns with higher resolution and averaging the resultant σ°s will not yield a mean σ° equal to the original single-cell value. To the extent that we see differences with resolution in mean clutter strengths in the Phase One results, it may indicate once more the domination of low-angle clutter by discrete sources with several (not one, not many) interfering discretes per cell. It would still be hard to imagine from such arguments, however, why there should be any overall bias in mean strength with resolution across many measurements (i.e., sometimes constructive interference, sometimes destructive).

We now turn to the measurement results showing differences in mean strength with range resolution. Table 15 shows such differences medianized across all of the repeat sector measurements for vertical polarization, horizontal polarization, and both polarizations combined. These medianized differences with resolution are very small, less than 2 dB everywhere. These slight differences might very well be indicative of calibration offsets. Calibration variations with pulse length can be caused by differences in matched filters, receiver bandwidths, pulse shapes, and resultant estimates of 3-dB pulse widths.

TABLE 15
Median Differences in Mean Ground Clutter Strength with Range Resolution, High-Low

Polarization	Differences (dB) in Mean Clutter Strength with Pulse Length, 15/36 m — 150 m (One-Sigma Variation, dB)				
	Frequency Band				
	VHF	UHF	L-Band	S-Band	X-Band
Vertical	1.9 (2.1)	1.5 (3.0)	0.9 (1.5)	–1.2 (1.8)	0.2 (2.5)
Horizontal	2.0 (1.6)	1.4 (1.4)	0.7 (3.0)	–0.9 (1.7)	0.0 (1.4)
Both	2.0 (1.9)	1.4 (2.3)	0.9 (2.3)	–1.0 (1.8)	0.2 (2.0)

Notes: Phase One repeat sector data. All site visits. One-sigma variations are shown in parentheses.

Now consider how changing polarization affects the results in Table 15. In a clutter measurement, if the polarization is switched, from vertical to horizontal, for example, the ensemble of effective scatterers is changed in the resolution cell, so one might expect to change individual resolution differences

in mean clutter strength by changing polarization. Therefore, one might also expect to change the one-sigma variation of resolution differences over many experiments with polarization. Indeed, we observe significant differences in the one-sigma ranges of variation in Table 15 between vertical and horizontal polarization in each band. However, in changing polarization, we do not change pulse shape, matched filter, or receiver bandwidth, so if there was a constant calibration offset with range resolution, it should be the same at vertical or horizontal polarization. Indeed, in Table 15, we observe medianized differences with resolution to be very nearly the same at vertical and horizontal polarization in each band. If we, therefore, take these differences as relative calibration offsets, we observe essentially no offset at X-band, plus and minus 1-dB offsets at L- and S-bands, respectively, and 1.4- and 2-dB offsets at UHF and VHF, respectively. In all of this speculative assumption of median difference with resolution as calibration offset, it is relative calibration we are considering. All we know is that, on the average over many measurements, we expect no difference with pulse length. If we observe a difference, we do not know which pulse is calibrated correctly, or if either pulse is. Further, we do not know how to convolve these median differences with resolution in Table 15 with the previously tabulated median differences with polarization in Table 13.

Now consider again the one-sigma range of variations of differences in mean strength with resolution, shown in parentheses in Table 15. Although randomly differing between vertical and horizontal polarization in each frequency band, there is no trend with frequency, unlike the previous corresponding variations with polarization in Table 13 where larger differences occurred at lower frequencies. Overall, in Table 15, the one-sigma range of variation in mean strength between Phase One range resolutions, i.e., 150 m versus 15/36 m, indicative of the phasing in and out of several dominant discrete scatterers per cell, is about 2 dB in each band. This result illustrates from another perspective that low-angle clutter contains discretes of stable phase and the extent to which a few such interfering discretes per resolution cell often occur. Cells containing many randomly phased contributors would not show such one-sigma differences with resolution.

We now combine all of the differences in mean strength with resolution across all repeat sectors, including all bands and both polarizations, in one histogram, as shown in Figure 102. The corresponding cumulative distribution is shown in Figure 103. The overall mean and median differences in this distribution are 0.81 and 0.85 dB, respectively; but these small numbers may be less significant than the corresponding specific numbers by frequency band, just discussed. We now discuss general differences by terrain type in the tails of these distributions. There is a predominance of farmland sites in these tails and a lack of woodland sites, which tends to support our arguments that resolution differences are caused by dominant cells containing several interfering discretes. There is only one clear exception to this, where a purely forested site with no qualifying second- and third-order classifiers appears only once, namely, Puskwaskau, with a -4.15-dB resolution difference, 15-m result minus 150-m result, at L-band and horizontal polarization, within the first 15 measurements in either tail. In contrast, in the center of the distribution where differences with resolution are small, the sites are predominantly forested. For example, over the 12 measurements where absolute differences in mean strength with resolution were ≤ 0.1 dB, eight came from forested sites, one from grassland, and one from desert (all presumably with

relatively fewer discretes) and only two from agricultural sites (both Beiseker, presumably with more discretes). Probabilities of occurrence of differences in mean strength with Phase One resolution, 150 m versus 15/36 m, across the complete repeat sector data base may be quantified from Figure 103. For example, 79 percent of measurements had differences within the 2.16-dB one-sigma range of variation about the mean difference.

Pursuing the general observation that discrete-dominated farmland terrain shows greater variation in mean clutter strength with resolution than does more homogeneous forest terrain, we now specifically sort the repeat sector mean strength data to show differences with resolution by terrain class. The results are shown in Table 16. Recall that we cannot ascribe much meaning to average differences in mean clutter strength with pulse length, but that we expect larger standard deviations of these differences in discrete-dominated terrain where a few major scatterers per resolution cell might provide returns that are voltage additive and which, therefore, could sum differently for different cell sizes. Indeed, Table 16 illustrates relatively large standard deviations of differences with resolution for urban terrain and agricultural terrain (especially very low-relief agricultural terrain, namely, 3.41 dB). Both terrain types, urban and agricultural, are obviously dominated by cultural (i.e., man-made) discrete clutter sources. In addition, a large value of standard deviation of differences in mean strength with resolution for desert, marsh, or grassland at low depression angle (i.e., Knolls and Big Grass Marsh), namely, 3.32 dB is seen in Table 16. We have argued that this terrain class is discrete free, but by this we mean free of the large cultural discretes that dominate farmland. The result of Table 16 would seem to indicate that when skimming at grazing incidence over the desert at Knolls or the frozen wetland at Big Grass Marsh, the backscatter is also, perhaps not unsurprisingly, dominated by discretes (i.e., voltage-additive situations), where here the discretes would be just minor variations in microtopography (i.e., small hillocks and hummocks) on the desert and marsh floors. That is, at grazing incidence, ground clutter is grainy; discretes can be large (i.e., water tower) or small (e.g., hillock), but whatever sticks up above the mean plane of the surface will be the localized source of the backscatter. Note that, as depression angle changes from low to high for desert, marsh, or grassland in Table 16, the standard deviation of differences in mean strength with resolution abruptly drops from 3.32 to 1.12 dB, indicating that the desert, marsh, or grassland floor stops being grainy and becomes much more homogeneous as the depression angle rises from grazing incidence to 1 or 2 deg (but see Figures E-156, E-161, E-165, and E-171 for specifics). Also, we would expect forested terrain to be less discrete-dominated than urban or farmland terrain, and indeed, we observe smaller standard deviations of differences in mean strength with resolution in forest (and in mountains, which are primarily forest covered) than in urban or agricultural terrain in Table 16. In addition, these standard deviations of differences are significantly lower in high-relief forest than in low-relief forest (i.e., higher slopes, more homogeneous) in Table 16.

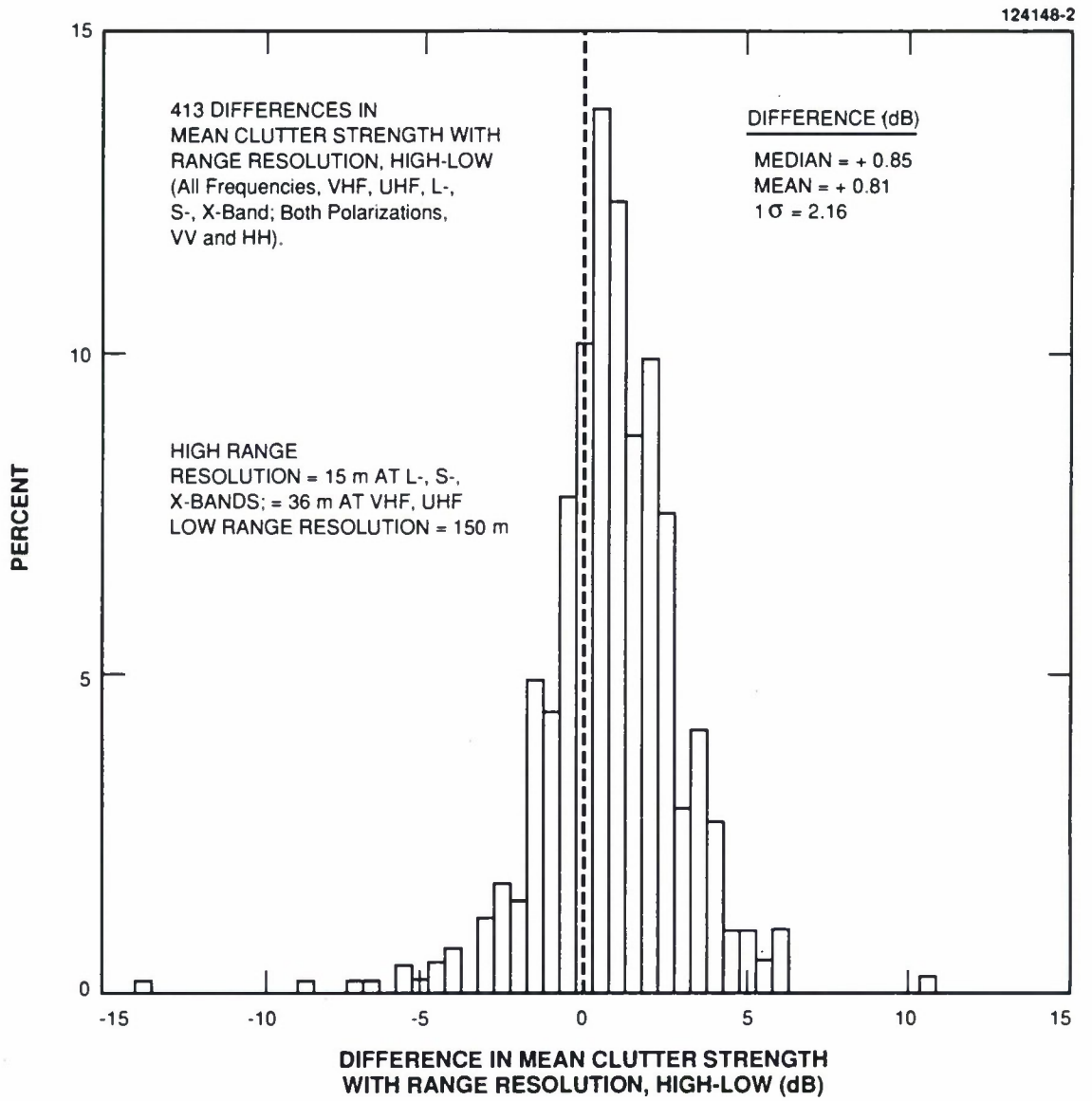

Figure 102. Histogram of differences in mean ground clutter strength with range resolution, high-low. Phase One repeat sector data. All site visits, all five RF frequencies, both polarizations.

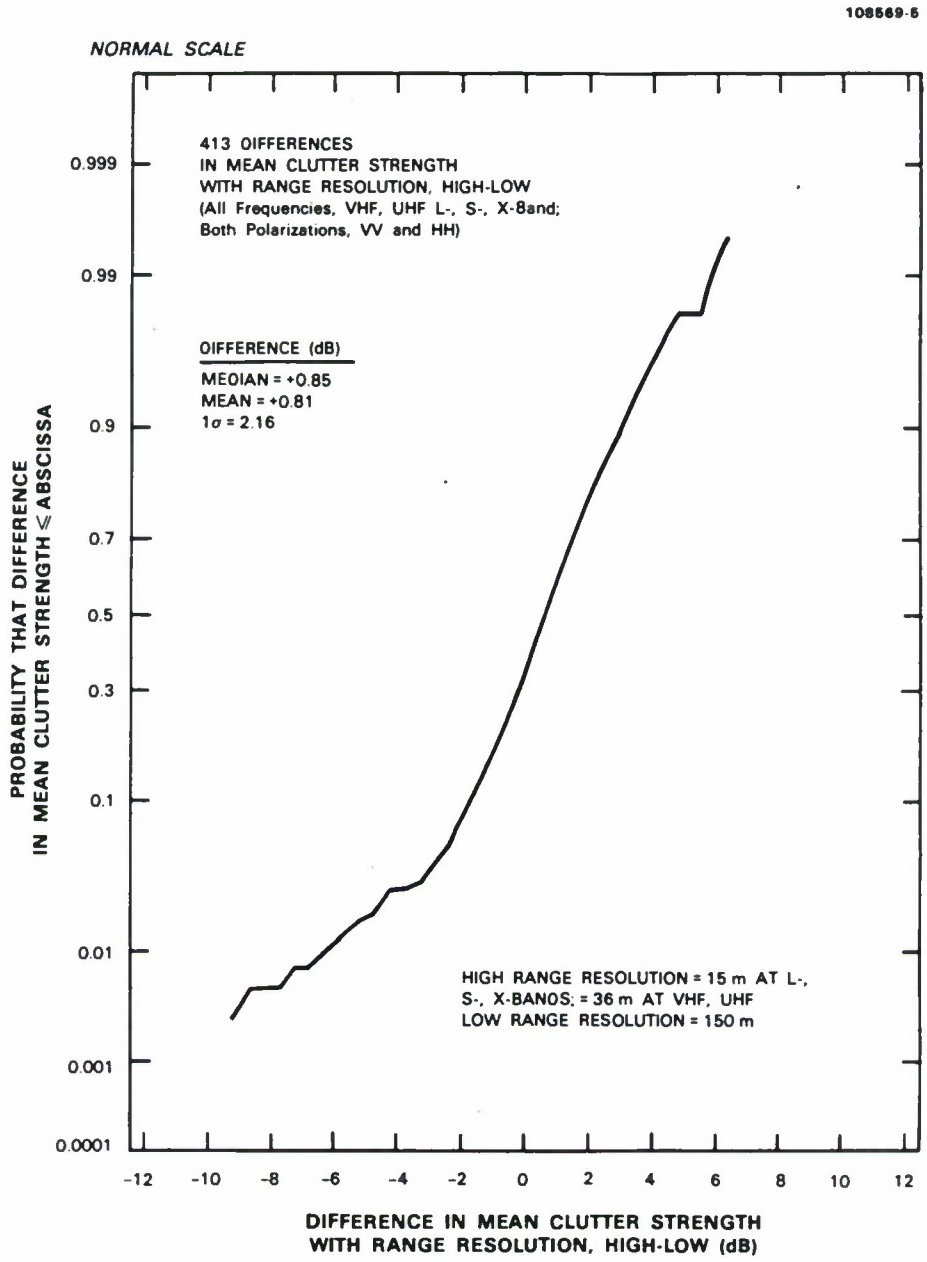

Figure 103. Cumulative distribution of differences in mean ground clutter strength with range resolution, high-low. Phase One repeat sector data. All site visits, all five RF frequencies, both polarizations.

TABLE 16
Average Differences in Mean Clutter Strength with Phase One Range Resolution, High-Low, by Terrain Type

Terrain Type	Differences (dB) in Mean Clutter Strength with Pulse Length 15/36 m – 150 m		
	Median	Mean	Standard Deviation
URBAN	0.81	0.87	2.12
MOUNTAINS	0.94	0.75	1.51
FOREST/HIGH-RELIEF			
High Depression Angle	0.11	0.17	1.25
Low Depression Angle	1.29	0.96	1.59
FOREST/LOW-RELIEF			
High Depression Angle	0.05	0.35	1.97
Intermediate Depression Angle	1.13	1.23	1.81
Low Depression Angle	1.12	1.18	1.87
AGRICULTURAL/HIGH-RELIEF	2.04	1.51	2.92
AGRICULTURAL/LOW-RELIEF			
Moderately Low-Relief	–0.48	–0.24	2.04
Very Low-Relief	1.30	1.02	3.41
DESERT, MARSH, OR GRASSLAND (Few Discretes)			
High Depression Angle	0.58	0.56	1.12
Low Depression Angle	1.79	1.81	3.32

Notes: Repeat sector data. All sites, all five frequencies, both polarizations. Based on data in Tables D-2 through D-6.

6. HIGHER MOMENTS AND PERCENTILES IN MEASURED GROUND CLUTTER SPATIAL AMPLITUDE DISTRIBUTIONS

The subject matter of this report is multifrequency low-angle ground clutter amplitude distributions from large spatial macroregions of visible terrain. Previously, we discussed mean levels (i.e., first moments) in such distributions. Here, in Section 6, we bring these distributions under more complete description by numerically specifying their higher moments, namely, the ratio of standard deviation to mean (which is a normalized measure of the second moment), the coefficient of skewness (or normalized third moment), and the coefficient of kurtosis (or normalized fourth moment), and several particular percentile levels in them, namely, the 50- (or median), 70-, and 90-percentile levels. Each of these six statistical attributes is provided as a median value of the particular attribute over a number of repeat sectors and measurements by frequency band within the same terrain groups as in Table 11. Thus, these higher moments and percentiles are generalized (i.e., central values) by terrain class and RF frequency.

Whereas the mean of the clutter amplitude distributions is largely independent of resolution but varies significantly with frequency in many terrain types, the dispersion or spread in these distributions is fundamentally dependent on resolution (the smaller the cell, the less the averaging within a cell and the greater the variability from cell to cell). As a result, all of the higher attributes presented in this section depend on resolution. An example of this result is shown in Figure 104, which shows the Weibull spread parameter a_w (which is directly dependent on and completely specified by the ratio of standard deviation to mean, see Appendix C, Equation C.13) as a function of Phase One spatial resolution over the repeat sector at three different sites. In Figure 104 the 20-element Phase One parameter matrix (i.e., five frequencies, two polarizations, two range resolutions) is providing 10 different values of spatial resolution as the azimuth beamwidth varies from 13 deg at VHF to 1 deg at X-band (see Table A-6) and as the range resolution varies between 150 m and 15 m (at L-, S-, X-bands) or 36 m (at VHF and UHF). For any given plot symbol in this figure, the symbol occurs for the five frequencies left to right in order, X-band to VHF. We believe the strong trends shown in Figure 104 are basically trends with resolution, although any dependence of spread on frequency is also included. Many such figures are behind the dependency of spread in our clutter model on resolution and depression angle for a given terrain type.

Because of the dependence of dispersion or spread in clutter amplitude distributions on spatial resolution, the generalized results by terrain class for higher moments and percentiles are separated, in different tables, between those applicable for the wide pulse (i.e., 150 m) and those applicable for the narrow pulse (i.e., 15 m at L-, S-, and X-bands; 36 m at VHF and UHF). In these tables, the variations with range resolution can be observed by comparing and contrasting between pairs of tables, and the essential variations with azimuth resolution can be observed by comparing and contrasting between different frequency bands in any given table. Many of the trends in these tables with terrain type and depression angle are carried over into our clutter model.

6.1 EVOLUTION OF ANALYSIS

The generalized information provided in Section 6 on third and fourth moments and percentile levels within major terrain classes was produced somewhat differently, and from a slightly different statistical

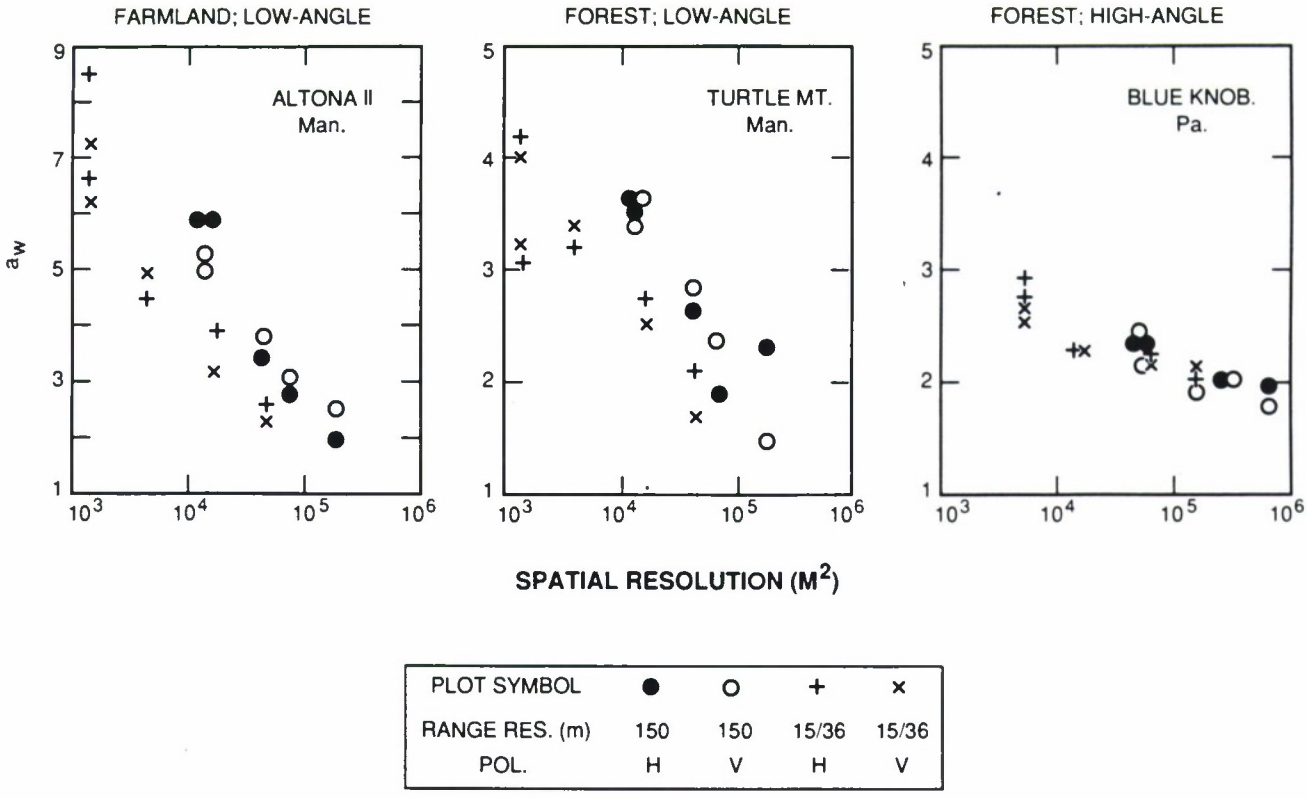

Figure 104. Weibull spread parameter a_w, versus radar spatial resolution at three clutter measurement sites. Repeat sector data. Spatial resolution depends on beamwidth (13 deg at VHF, 5 deg at UHF, 3 deg at L-band, 1 deg at S- and X-band) and pulse length (150 m or 15/36 m). In each figure, each plot symbol appears five times, once for each radar frequency, in order of decreasing frequency left-to-right as beamwidth increases.

population, than the similar information on mean and standard deviation. To see why this is so, a brief history is provided of the Phase One data reduction and analysis effort. This capsule history illustrates what our overall approach has been for coming to grips with and unraveling the information in our voluminous Phase One data base.

From 1982 to 1984, the Phase One equipment was collecting clutter measurement data in the field, and raw tapes were being sent back to Lincoln Laboratory for calibration. The calibration effort, in which raw A/D counts were converted pulse by pulse to absolute values of clutter cross section and stored on Calibrated Clutter Tapes (CCTs), largely kept up with the collection process (see Appendix A for more discussion of this calibration effort). However, in the beginning, the Lincoln Laboratory central computer facility could only store several sites' worth of CCTs (about 70 per site) at any time. Our approach was to look at the CCTs one site at a time as the calibrated data became available, moving tapes into and out of the computer room as we proceeded. We concentrated on our repeat sector measurements (although not exclusively). We ran all the repeat sector experiments through a clutter patch histogram program,

which, for a given range interval in the sector, produced the histogram of samples collected over all the cells in that interval in 1-dB bins, as well as many statistical attributes describing the histogram, including all the higher moments and percentiles, goodness-of-fit information, for example, to Weibull and lognormal distributions, effects of noise and saturation, and effects of coherency and integration gain. We also ran our sector display program for many repeat sector experiments showing σ° versus range and made PPI spatial displays of clutter at various σ° threshold settings.

Initially in this analysis effort, there were a number of interfacing and evolving processes under way that were centrally important to the analysis effort and that required us to iterate our results. These included software growth and debugging, calibration evolution, and increasingly refined terrain descriptions and ground truth.

During this process, we analyzed a large amount of data at each site. We summarized results across sites by generating a set of 20 best "digest" repeat sector clutter patch histograms of amplitude statistics (i.e., five frequencies, two polarizations, two resolutions) for one common range interval at each site. From these results, we maintained and kept current a gradually lengthening, consistent, and correct list of means and standard deviations at each site. It was from this set of data that we abstracted to get our best insights into frequency dependence of clutter and to generate the multifrequency "funnel" plots of mean strength that we used in oral briefings to summarize the results of our program as it proceeded. The final status of this carefully monitored list of numbers is given in Tables D-2 through D-6. The trend analysis of this report is largely based on these files. This sequence of activity, however, did not directly lead to a capability for computer-automated generation and storage of clutter patch histograms and subsequent automated ensembling and trend analysis of these histograms.

However, our plans for obtaining an automated Phase One patch processing capability were proceeding. Several key prerequisite tasks necessary to achieve this capability were eventually completed. First, we finished production of our partially integrated Phase One data base (see Appendix A). This reduced the volume of our data from 3601 to 228 tapes while maintaining its spatial resolution, allowed us to make the complete data base available for direct access in the Lincoln Laboratory computer room, and brought it all into uniform and correct final calibration. Second, we completed production of a comprehensive Phase One Master File data base management system that gives logical access to all 12,726 experiments and many high level data collection parameters of each. Third, we finished specification in range and azimuth extent of all 3440 clutter patches at all of our sites, finalized their terrain descriptions and classifications, and made them available on computer files. Fourth, we completed implementation of intersection software. This software automatically finds all of the experiments in the Master File providing measurement coverage of a given clutter patch. This software then generates a clutter amplitude histogram from the integrated tapes for each such intersecting experiment with that patch and stores it on magnetic tape with its terrain classifications from the patch specification file. Finally, this intersection software provides a high level summary file of modeling information, containing important clutter attributes (e.g., mean, standard deviation, etc.) and terrain descriptors (e.g., landform, land cover, depression angle) for each stored histogram. This capability has been subsequently used to process all of our 360-deg coverage Phase One survey data (as opposed to the repeat data, see Appendix A) within clutter patch histograms (upwards of 100,000 histograms in all), by means of which we plan to obtain improved statistical rigor (i.e., more samples) and increased accuracy in our predictions.

This automated Phase One patch histogram production capability only became available late (i.e., mid-1988) in our repeat sector analysis activity. However, we used this capability to process across our complete repeat sector data base. As a result, we now have an archival repeat sector clutter patch histogram data base stored on three magnetic tapes. This data base consists of a clutter amplitude histogram with statistical attributes of the histogram and terrain classifiers for a specified repeat sector range interval at each site common to all 20 waveforms for each of our 4465 repeat sector experiments. All histograms within this data base are of consistent and finalized calibration. In addition, we have the overview summary file containing important statistical attributes and terrain descriptions for each histogram in a single, easily manipulated file. We call this summary file the repeat sector sort file.

The repeat sector sort file was used to obtain the medianized results by terrain class for skewness and kurtosis and 50-, 70-, and 90-percentiles presented in Section 6. Thus, these results were obtained differently than were the similar generalized results for means and standard deviations. The fundamental difference is that the repeat sector sort file results for higher moments and percentiles are averaged over all the repeat sector experiments, including the day-to-day repeats of which there are nominally four per experiment; whereas, the earlier results for mean and standard deviation were obtained from a set (viz., Tables D-2 through D-6) in which only the best of these day-to-day repeats was included. To the extent that the repeated experiments repeat exactly, the statistics do not change. We did remove from the repeat sector sort file a number of specialized experiments (e.g., different antenna tower heights at any one site) and occasional anomalous or obviously bad experiments. Also, we did reproduce our earlier generalized results for mean and standard deviation using the repeat sector sort file and obtained essentially identical results as are presented here. But we do mention this difference in underlying technique between how we generated centrally (i.e., medianized) representative values within general terrain classes of means and standard deviations on the one hand, and the higher moments and percentiles on the other.

6.2 RATIO OF STANDARD DEVIATION TO MEAN

Values for ratios of standard deviation to mean in repeat sector ground clutter amplitude distributions at all Phase One measurement sites are plotted in Figures 105 and 106 for urban sites and rural sites, respectively. For each repeat sector, values are plotted for each of the 20 combinations in the radar parameter matrix (i.e., five frequencies, two polarizations, two resolutions). In Figures 105 and 106, very large values of standard deviation-to-mean ratios are generally observed in both urban and rural terrain, resulting from the long high-side tail in these amplitude distributions caused by isolated strong returns from discrete sources over a wide range of amplitudes. In particular, in the urban data of Figure 105 at X-band, there is a clear-cut separation between narrow pulse and wide pulse results such that the narrow pulse data have much higher spreads than the wide pulse data; in the lower frequency bands there remains relatively good separation (i.e., little overlap) between narrow pulse and wide pulse results. Spreads in the urban data, as given by ratio of standard deviation to mean, are never less than about 5 dB in Figure 105.

Maximum spreads in the rural data in Figure 106 can be about as large as in the urban data. The average spreads in the rural data are somewhat less than in the urban data, and minimum observed spreads in the rural data are much less than in urban data, and in a number of measurements, approach values close to unity (i.e., ratios of standard deviation to mean near 0 dB) indicative of Rayleigh statistics.

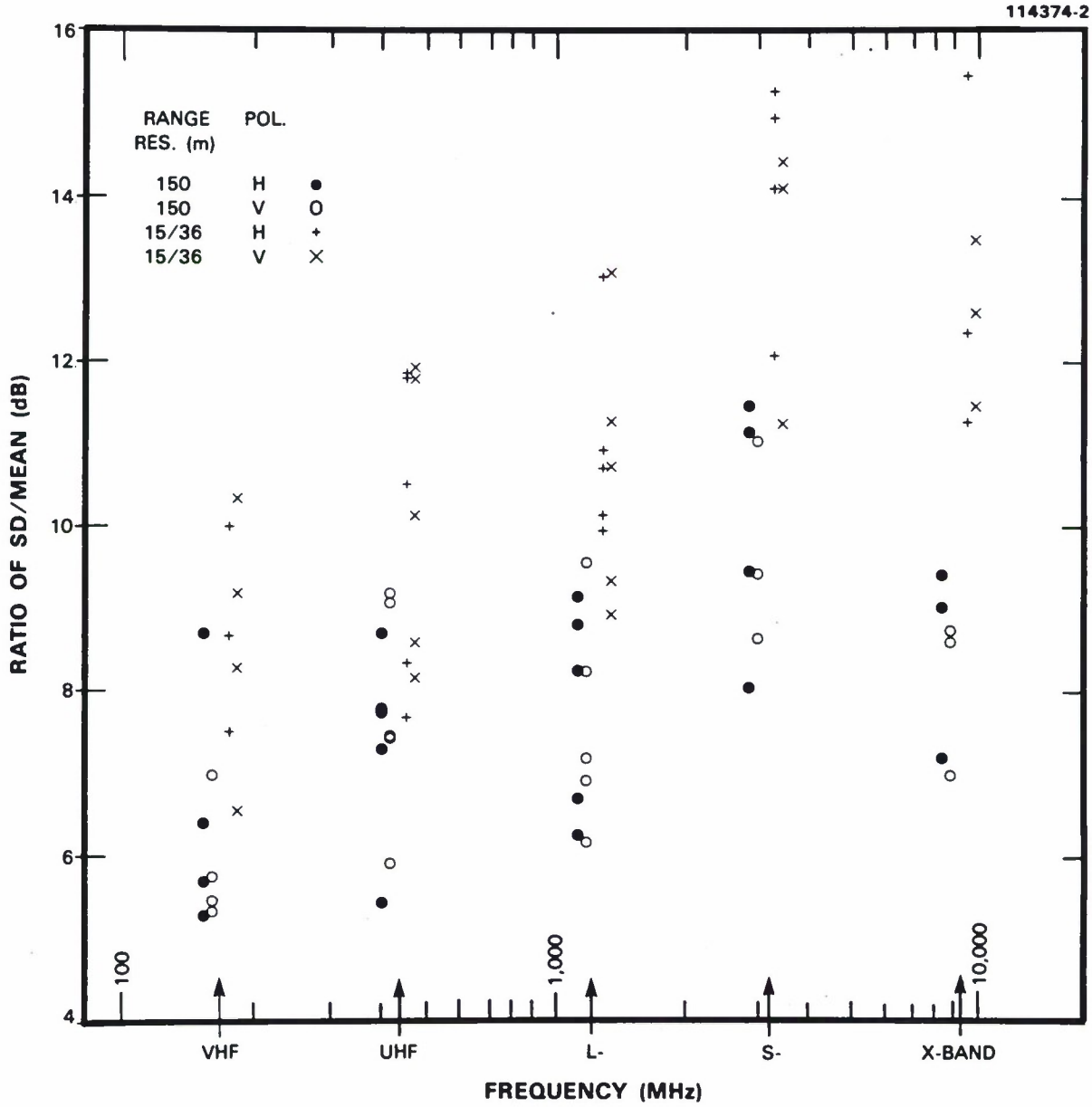

Figure 105. Ratio of standard deviation to mean in clutter amplitude distributions at five urban sites. Repeat sector data.

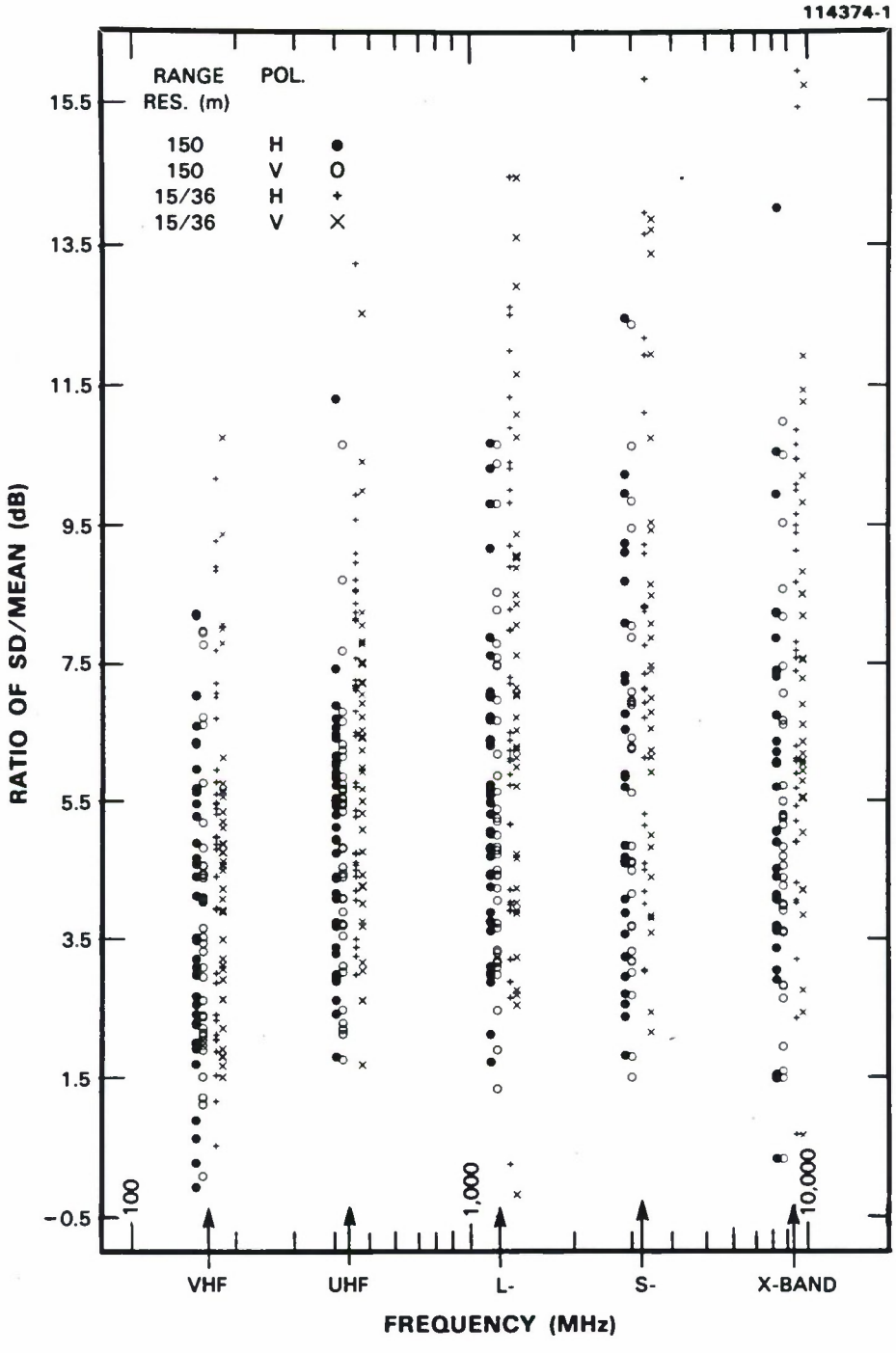

Figure 106. Ratio of standard deviation to mean in clutter amplitude distributions at 37 rural sites. Repeat sector data.

Figures 105 and 106 separate the measured values of ratio of standard deviation to mean into only two terrain types, urban and rural. We now proceed to separate these values within our total 12-category set of terrain types, as given by Table 7. Tables 17 and 18 show ratios of standard deviation to mean for ground clutter spatial amplitude distributions, by frequency band in all 12 terrain classes, for the Phase One wide pulse and narrow pulse, respectively. These numbers are medianized and hence generalized from groups of repeat sector measurements with a variable number of measurements in each group. Measurements at both polarizations are included in these groups.

The ratio of standard deviation to mean is the fundamental statistical measure of dispersion or spread in the distribution. When the ratio is equal to unity, it is indicative of Rayleigh statistics. Most of the results in Tables 17 and 18 are considerably greater than unity, indicating the extreme cell-to-cell variability existing in low-angle ground clutter statistics. This variability occurs because, at angles near grazing incidence, returns are measured over a wide range of strengths from all of the vertical features rising above the mean elevation of the clutter patch.

The underlying trends observed in Tables 17 and 18 are as follows. A comparison of Tables 17 and 18 shows that the ratio of standard deviation to mean usually increases with increasing range resolution. In either table, a weak trend is observed where the ratio of standard deviation to mean tends to increase as azimuth beamwidth decreases from VHF to X-band (e.g., agricultural/high-relief; marsh/low depression angle). For a given spatial resolution (i.e., for a given frequency band in either table), the ratio of standard deviation to mean usually decreases with increasing depression angle. We observe large ratios of standard deviation to mean in urban and agricultural terrain dominated by discrete objects; smaller ratios exist in forest, particularly at high angles, and in mountains, where steep forested slopes also prevail. As angle of illumination increases in forested terrain, we begin to move from the low angle, spiky, discrete- and shadow-dominated widely spread Weibull regime toward more airbornelike fuller illumination and more homogeneous backscatter of the narrowly spread Rayleigh regime.

It is evident that these observed trends in ratios of standard deviation to mean in Tables 17 and 18 are less well defined than the trends in mean strength previously discussed. Analysis of our more comprehensive Phase One survey data should improve the accuracy of such observed trends in ratios of standard deviation to mean.

6.3 SKEWNESS AND KURTOSIS

The coefficients of skewness and kurtosis are normalized measures of the third and fourth central moments, respectively, of any distribution. They are defined in Appendix C. Skewness is a measure of asymmetry in the distribution. Kurtosis is a measure of concentration about the mean. General values of skewness for the measured low-angle ground clutter amplitude distributions for the low and high range resolution waveforms are given in Tables 19 and 20, respectively. Corresponding values of kurtosis are given in Tables 21 and 22. All these values in Tables 19 through 22 are medianized over groups of individual repeat sector measurements within each of our 12 general terrain classes for each RF frequency band. The number of different repeat sectors in each group is shown in Table 7. Measurements at both vertical and horizontal polarizations are included. These results were obtained from our repeat sector sort file, which includes day-to-day repeated measurements.

TABLE 17

Median Value of Ratio of Standard Deviation to Mean in Ground Clutter Amplitude Distributions over Many Repeat Sector Measurements* by Terrain Type for the Phase One Low Range Resolution Waveform†

Terrain Type	Median Value of SD/Mean (dB)				
	Frequency Band				
	VHF	UHF	L-Band	S-Band	X-Band
URBAN	5.7	7.6	7.7	9.5	8.7
MOUNTAINS	2.7	4.1	3.4	4.5	3.6
FOREST/HIGH-RELIEF (Terrain Slopes > 2°)					
High Depression Angle (>1°)	2.9	3.1	4.2	4.6	4.3
Low Depression Angle (≤ 0.2°)	5.0	5.3	4.3	2.1	4.8
FOREST/LOW-RELIEF (Terrain Slopes < 2°)					
High Depression Angle (> 1°)	3.5	3.7	3.6	3.5	3.8
Intermediate Depression Angle (0.4° to 1°)	2.9	4.3	4.2	4.7	4.6
Low Depression Angle (≤ 0.3°)	5.3	3.7	4.6	5.2	4.6
AGRICULTURAL/HIGH-RELIEF (Terrain Slopes > 2°)	4.9	5.8	6.1	6.4	7.1
AGRICULTURAL/LOW-RELIEF					
Moderately Low-Relief (1° < Terrain Slopes < 2°)	5.8	5.5	7.4	6.7	5.8
Very Low-Relief (Terrain Slopes < 1°)	4.4	6.7	7.7	9.3	6.7
DESERT, MARSH, OR GRASSLAND (Few Discretes)					
High Depression Angle (≥ 1°)	3.8	5.7	5.6	2.2	0.9
Low Depression Angle (≤ 0.3°)	1.7	2.7	5.9	7.2	4.6

* Based on data in Tables D-2 through D-6.

† Low range resolution = 150 m.

TABLE 18

Median Value of Ratio of Standard Deviation to Mean in Ground Clutter Amplitude Distributions over Many Repeat Sector Measurements* by Terrain Type for the Phase One High Range Resolution Waveform†

Terrain Type	Median Value of SD/Mean (dB)				
	Frequency Band				
	VHF	UHF	L-Band	S-Band	X-Band
URBAN	8.7	10.3	10.7	14.1	12.5
MOUNTAINS	3.4	5.4	2.8	4.0	4.1
FOREST/HIGH-RELIEF (Terrain Slopes > 2°)					
High Depression Angle (>1°)	4.2	4.3	6.1	7.3	6.7
Low Depression Angle (≤ 0.2°)	5.5	5.5	4.2	2.7	5.4
FOREST/LOW-RELIEF (Terrain Slopes < 2°)					
High Depression Angle (> 1°)	2.8	5.2	3.9	4.7	5.4
Intermediate Depression Angle (0.4° to 1°)	3.6	5.6	6.0	6.5	6.1
Low Depression Angle (≤ 0.3°)	6.1	4.5	8.3	7.6	6.6
AGRICULTURAL/HIGH-RELIEF (Terrain Slopes > 2°)	5.8	7.4	8.6	—	9.3
AGRICULTURAL/LOW-RELIEF					
Moderately Low-Relief (1° < Terrain Slopes < 2°)	7.5	7.9	9.7	8.3	7.2
Very Low-Relief (Terrain Slopes < 1°)	5.1	8.6	11.1	13.6	10.4
DESERT, MARSH, OR GRASSLAND (Few Discretes)					
High Depression Angle (≥ 1°)	5.5	8.2	9.2	3.7	1.7
Low Depression Angle (≤ 0.3°)	1.6	3.5	1.7	11.6	7.3

* Based on data in Tables D-2 through D-6.

† High range resolution = 15 m at L-, S-, and X-bands and = 36 m at VHF and UHF.

These higher moments can be of particular interest to theoretical workers in ground clutter who treat clutter as a correlated noise process. Such workers may model the process, for example, such that the scatterers follow a correlated Gamma distribution. Then the clutter amplitude returns are K-distributed. The K-distribution has built into it the mechanisms to handle the correlation physics of the underlying phenomenon [5]. This is in contrast to our simpler approach here of just providing empirical descriptions of these distributions and their important observed parametric dependencies.

The way higher moments are often used in theoretical studies is as follows. Any measured amplitude distribution can be normalized to have zero mean (by subtracting the actual mean from each sample) and unity standard deviation (by dividing each sample by the actual standard deviation). It is then straightforward to match mean and standard deviation of the measured normalized distribution to the theoretical K-distribution or to appropriate descriptive-only distributions such as Weibull or lognormal. The goodness-of-fit then depends on how well the higher moments follow the match. Such theoretical studies into clutter correlation are thus based on the behavior of third and fourth moments. We also mention that clutter correlation is important in radar detection performance. For example, false alarm rates dramatically rise in spatially correlated clutter as opposed to uncorrelated clutter with the same amplitude distribution [6].

Rayleigh statistics may be taken as a point-of-departure in interpreting coefficients of skewness and kurtosis. For Rayleigh statistics, skewness = 2 (or 3.01 dB) and kurtosis = 9 (or 9.54 dB). The numbers of Tables 19 through 22 usually show skewness and kurtosis to be considerably greater than Rayleigh, a consequence of the widely dispersed high-side tail caused by the fundamental discrete and spiky nature of low-angle clutter. We do see, though, as with standard deviation, that where we would expect to be encountering more Rayleigh-like conditions, for example, with increasing illumination angle in forest, these numbers tend to get smaller; and where we expect a more discrete-dominated spiky process, for example, at low angles in agricultural terrain or in urban terrain, these numbers tend to be bigger. We see a strong dependence on range resolution where the numbers are larger for higher resolution. We interpret the indicated variation where the numbers tend to increase with increasing frequency to really be more due to the decreasing azimuth beamwidth with increasing frequency.

We observe skewness and kurtosis numbers relatively close to Rayleigh for mountains at VHF and low range resolution (viz., 2.93 dB and 7.88 dB, respectively). Standard deviations and ratios of percentile levels also indicate statistics approaching Rayleigh in this situation. The reason for this is that, in looking at mountains, we are looking predominantly at steeply forested slopes under full illumination. In addition, low range resolution and VHF reduces the spatial resolution to its minimum, thus providing more scatterers in each cell and giving Rayleigh statistics a better chance for realization. The slight undershoot of Rayleigh numbers may be due to clutter amplitude distributions in mountainous terrain often having an enhanced low-side tail.

TABLE 19
Median Values of Skewness over All Repeat Sector Measurements by Terrain Type for the Low Resolution Waveform*

Terrain Type	Median Values of Skewness (dB)				
	Frequency Band				
	VHF	UHF	L-Band	S-Band	X-Band
URBAN	6.88	8.87	9.84	12.67	11.14
MOUNTAINS	2.93	4.42	5.46	5.60	6.07
FOREST/HIGH-RELIEF					
High Depression Angle	6.56	6.53	9.34	9.55	9.88
Low Depression Angle	6.14	6.12	7.82	8.54	7.31
FOREST/LOW-RELIEF					
High Depression Angle	6.48	5.12	6.07	6.84	7.90
Intermediate Depression Angle	5.26	7.88	7.68	9.04	8.17
Low Depression Angle	6.34	5.73	7.04	7.79	8.07
AGRICULTURAL/HIGH-RELIEF	7.17	8.02	10.02	11.82	11.38
AGRICULTURAL/LOW-RELIEF					
Moderately Low-Relief	8.13	7.19	9.53	11.00	9.68
Very Low-Relief	6.93	8.82	10.06	10.57	11.07
DESERT, MARSH, OR GRASSLAND (Few Discretes)					
High Depression Angle	5.43	8.19	8.66	5.77	4.09
Low Depression Angle	4.25	5.05	12.39	11.12	7.94

* Low range resolution = 150 m.

TABLE 20
Median Values of Skewness over All Repeat Sector Measurements by Terrain Type for the High Resolution Waveform*

Terrain Type	Median Values of Skewness (dB)				
	Frequency Band				
	VHF	UHF	L-Band	S-Band	X-Band
URBAN	10.59	12.50	13.24	16.64	15.96
MOUNTAINS	5.67	8.13	7.09	9.80	7.46
FOREST/HIGH-RELIEF					
High Depression Angle	8.89	8.58	11.71	14.22	14.85
Low Depression Angle	7.17	7.76	10.70	12.32	9.96
FOREST/LOW-RELIEF					
High Depression Angle	6.85	8.35	8.46	9.60	11.92
Intermediate Depression Angle	6.79	9.58	10.23	11.29	10.60
Low Depression Angle	9.15	7.94	9.71	10.82	11.60
AGRICULTURAL/HIGH-RELIEF	9.43	9.88	13.01	—	15.64
AGRICULTURAL/LOW-RELIEF					
Moderately Low-Relief	9.39	11.66	13.63	13.44	12.97
Very Low-Relief	7.93	10.56	13.41	15.36	15.57
DESERT, MARSH, OR GRASSLAND (Few Discretes)					
High Depression Angle	8.06	9.96	14.02	19.30	7.71
Low Depression Angle	5.82	7.98	22.41	16.25	10.77

* High range resolution = 15 m at L-, S-, and X-bands and = 36 m at VHF and UHF.

TABLE 21
Median Values of Kurtosis over All Repeat Sector Measurements by Terrain Type for the Low Resolution Waveform*

Terrain Type	Median Values of Kurtosis (dB)				
	Frequency Band				
	VHF	UHF	L-Band	S-Band	X-Band
URBAN	14.28	18.10	20.31	25.50	22.97
MOUNTAINS	7.88	10.77	12.31	13.17	13.90
FOREST/HIGH-RELIEF					
High Depression Angle	14.39	15.15	20.23	20.96	21.77
Low Depression Angle	13.40	13.36	17.11	18.49	16.22
FOREST/LOW-RELIEF					
High Depression Angle	13.79	11.22	13.70	15.51	17.72
Intermediate Depression Angle	11.88	16.95	17.25	20.00	18.49
Low Depression Angle	13.78	12.95	15.06	17.29	18.25
AGRICULTURAL/HIGH-RELIEF	15.16	17.01	20.91	25.38	24.01
AGRICULTURAL/LOW-RELIEF					
Moderately Low-Relief	16.99	15.41	19.57	22.93	21.00
Very Low-Relief	14.90	18.24	20.99	21.69	23.31
DESERT, MARSH, OR GRASSLAND (Few Discretes)					
High Depression Angle	11.68	17.02	18.36	13.65	11.09
Low Depression Angle	10.69	11.77	27.77	23.22	17.65

* Low range resolution = 150 m.

TABLE 22
Median Values of Kurtosis over All Repeat Sector Measurements by Terrain Type for the High Resolution Waveform*

Terrain Type	Median Values of Kurtosis (dB)				
	Frequency Band				
	VHF	UHF	L-Band	S-Band	X-Band
URBAN	21.51	25.32	27.26	33.93	32.73
MOUNTAINS	13.85	17.50	16.36	21.38	17.18
FOREST/HIGH-RELIEF					
High Depression Angle	19.05	18.65	25.25	29.74	31.38
Low Depression Angle	15.78	16.80	22.86	26.32	21.43
FOREST/LOW-RELIEF					
High Depression Angle	14.82	17.79	18.99	20.90	25.95
Intermediate Depression Angle	15.22	20.54	22.51	24.72	23.72
Low Depression Angle	19.12	16.61	20.50	23.58	25.60
AGRICULTURAL/HIGH-RELIEF	20.04	20.99	27.28	—	32.88
AGRICULTURAL/LOW-RELIEF					
Moderately Low-Relief	20.12	24.17	28.46	28.63	28.07
Very Low-Relief	17.15	21.77	27.45	31.17	32.12
DESERT, MARSH, OR GRASSLAND (Few Discretes)					
High Depression Angle	17.56	21.07	29.46	40.61	18.40
Low Depression Angle	13.91	18.59	45.53	34.63	24.19

* High range resolution = 15 m at L-, S-, and X-bands and = 36 m at VHF and UHF.

6.4 50-, 70-, AND 90-PERCENTILE LEVELS

Central (medianized) values of 50-, 70-, and 90-percentile levels in the measured low-angle ground clutter amplitude distributions for the low and high range resolution waveforms are given in Tables 23 and 24, respectively. These numbers are medianized over groups of individual repeat sector measurements within each of our 12 general terrain classes (see Table 7) for each RF frequency band. These results were obtained from our repeat sector sort file, including measurements at both vertical and horizontal polarizations and day-to-day repeated measurements. The 50-percentile level is the median level in the distribution. Percentile level is defined in Appendix C.

These percentile levels provide additional information describing the clutter amplitude distributions over and above that provided by the moments. In particular, they provide a simple direct way of envisioning the shape of the histogram, at least at three specific points. To interpret the results in terms of departure from Rayleigh statistics, we need to know that, for Rayleigh statistics, the ratios of 90 to 50 percentile, 70 to 50 percentile, and mean to median are 5.2, 2.4, and 1.6 dB, respectively.

Although indications of the same trends are vaguely discernible in the percentile level numbers of Tables 23 and 24 as we observed earlier in the moments, these percentile level numbers provide less well-defined trends than the moment numbers. It is evident that if we were to work with median clutter strengths instead of means, we would not be able to show trends with terrain type, relief, depression angle, and frequency at all as clear-cut, smooth, and converged as we were able to show with means. The reason for this is that any percentile level, in contrast to a moment, is just a threshold at one particular level of strength indicating relative proportions in numbers of samples above and below the threshold, but unweighted by the actual values of the samples. Thus, the percentile levels are illustrative but less statistically meaningful than the moments.

Nevertheless, there is a great deal of additional specific information bound up in the numbers of Tables 23 and 24. For example, showing these three percentile level numbers together as a triad for each combination of frequency and terrain type illustrates again the extreme range of variability that exists in low-angle ground clutter spatial amplitude distributions. These triads of numbers typically range over 20 dB in Tables 23 and 24. Clearly, clutter cannot be well represented as a constant σ° phenomenon.

Mean clutter strengths in Table 11 are usually much greater than median clutter strengths in Tables 23 and 24, often by as much as 20 dB or so. For Rayleigh statistics, the mean-to-median ratio is 1.6 dB. Our observed large mean-to-median ratios are another indication of large spread in the low-angle clutter amplitude distributions. Often, in Tables 23 and 24, it is the 90-percentile levels that are closest to the means, occasionally the 70-percentile levels. One exceptional situation where the mean is very nearly equal to the median at both low and high range resolution is for the desert, marsh, or grassland terrain class, high depression angle, X-band. We remarked earlier that the X-band mean level of this terrain class was unusual in that it was much higher than at the other frequencies and nearly matched low-relief forest at high depression angle (i.e., at X-band, looking down at low-relief forest is like looking down at desert vegetation or grassland). Another exceptional situation where the mean is close to the median is again for the desert, marsh, or grassland terrain class, this time at low depression angle, at VHF, UHF, and L-band, particularly at high range resolution.

TABLE 23

Median Values of 50-, 70-, and 90-Percentile Levels in Ground Clutter Amplitude Distributions over All Repeat Sector Measurements by Terrain Type for the Phase One Low Range Resolution Waveform*

Terrain Type	Median Values of 50-, 70-, and 90-Percentiles (dB)				
	Frequency Band				
	VHF	UHF	L-Band	S-Band	X-Band
URBAN	–43,–37,–28	–38.5,–32.5,–21.5	–32,–26,–14.5	–44,–32,–17	–41,–32,–15
MOUNTAINS	–14,–9,–3	–18,–13,–8	–22,–18,–12.5	–27,–20,–14	–35,–24,–16
FOREST/HIGH-RELIEF (Terrain Slopes > 2°)					
High Dep. Ang. (>1°)	–16,–12,–7	–22.5,–17,–12	–24.5,–20,–14.5	–30,–24,–18	–27,–22,–16
Low Dep. Ang. (≤ 0.2°)	–29,–25,–21	–29,–22,–13	–28,–24,–18	–33,–26,–20	–33,–26.5,–21
FOREST/LOW-RELIEF (Terrain Slopes < 2°)					
High Dep. Ang. (> 1°)	–21,–16.5,–10.5	–25,–19,–10	–27,–23,–17	–36,–31,–25	–33,–28.5,–23
Intermediate Dep. Ang. (0.4° to 1°)	–37,–29,–23	–42,–33,–25	–42,–31,–25	–48,–37,–28.5	–44,–34.5,–26.5
Low Dep. Ang. (≤ 0.3°)	–52,–49,–44	–55,–48.5,–40	–59,–52,–41	–54,–47,–36.5	–45,–38,–31
AGRICULTURAL/HIGH-RELIEF (Terrain Slopes > 2°)	–44,–39,–30	–41,–36,–28.5	–41,–34.5,–27	–43.5,–37.5,–31.5	–40.5,–36,–26
AGRICULTURAL/LOW-RELIEF					
Moderately Low-Relief (1° < Terrain Slopes < 2°)	–48.5,–40.5,–29.5	–52,–45,–29	–49,–39,–27	–48.5,–40,–30	–38,–32,–25
Very Low-Relief (Terrain Slopes < 1°)	–68,–64,–56	–60,–51,–41	–55,–45,–35	–65,–59,–45	–49,–41,–30
DESERT, MARSH, OR GRASSLAND (Few Discretes)					
High Dep. Ang. (≥ 1°)	–47,–41.5,–34	–58,–50,–39.5	–51.5,–46.5,–36.5	–40,–36.5,–32	–25,–23,–20
Low Dep. Ang. (≤ 0.3°)	–72,–69,–65	–78.5,–75,–70	–75,–71.5,–66.5	–63,–55.5,–47	–47,–43.5,–38

* Low range resolution = 150 m.

TABLE 24

Median Values of 50-, 70-, and 90-Percentile Levels in Ground Clutter Amplitude Distributions over All Repeat Sector Measurements by Terrain Type for the Phase One High Range Resolution Waveform*

Terrain Type	Median Values of 50-, 70-, and 90-Percentiles (dB)				
	Frequency Band				
	VHF	UHF	L-Band	S-Band	X-Band
URBAN	–45,–39,–31.5	–46,–38,–23	–40,–33,–18	–39.5,–34,–24.5	–33,–30,–24
MOUNTAINS	–13,–9,–2	–16,–12,–5.5	–28,–18.5,–12	–40,–27.5,–18.5	–36.5,–25,–16.5
FOREST/HIGH-RELIEF (Terrain Slopes > 2°)					
High Dep. Ang. (>1°)	–15,–11,–5	–26,–20.5,–13	–25.5,–20,–14.5	–34,–28,–21	–29,–23,–16.5
Low Dep. Ang. (≤ 0.2°)	–27,–23,–15.5	–26,–20,–12.5	–29,–24,–18	–38,–30,–22	–37,–29,–21
FOREST/LOW-RELIEF (Terrain Slopes < 2°)					
High Dep. Ang. (> 1°)	–18,–13,–6	–24,–19,–10.5	–28,–23,–17	–39,–33,–27	–35,–29,–23
Intermediate Dep. Ang. (0.4° to 1°)	–35,–29,–22	–42,–32,–23	–43,–31,–24	–49,–39,–29.5	–45,–37,–27
Low Dep. Ang. (≤ 0.3°)	–52,–49,–43	–64,–56,–46	–58,–52.5,–44	–62,–56.5,–43.5	–59,–51,–36
AGRICULTURAL/HIGH-RELIEF (Terrain Slopes > 2°)	–38.5,–34.5,–28	–44,–39,–29.5	–41,–36,–25	—	–44,–37.5,–29
AGRICULTURAL/LOW-RELIEF					
Moderately Low-Relief (1° < Terrain Slopes < 2°)	–47,–41,–31	–53,–46,–33	–51,–43,–30	–55,–46,–33	–45.5,–35.5,–26
Very Low-Relief (Terrain Slopes < 1°)	–59,–56,–51	–62.5,–52,–40.5	–57,–50,–37	–63,–59,–54	–54,–46,–34
DESERT, MARSH, OR GRASSLAND (Few Discretes)					
High Dep. Ang. (≥ 1°)	–49,–45,–38	–59.5,–54.5,–44.5	–48.5,–44.5,–38	–42.5,–39.5,–34	–27.5,–24,–20
Low Dep. Ang. (≤ 0.3°)	–65,–62.5,–59	–74.5,–72.5,–68	–66.5,–62.5,–58	–63.5,–60,–53.5	–49,–45,–39

* High range resolution = 15 m at L-, S-, and X-bands and = 36 m at VHF and UHF.

7. EFFECTS OF WEATHER AND SEASON

In Section 4, general information was provided in Figure 98 and Table 11 showing how the mean strength of ground clutter varies with RF frequency for various terrain types. Although the observed seasonal variations in the measurements were discussed in Section 4, site by site, we did not include any mechanism for taking into account the effects of season and weather in the resultant generalized information, obtained by averaging measurements from similar sites in whatever conditions of season and weather those measurements happened to be made. Are there important trends in our measurements as a result of seasonal or weather-related change? What are the ranges of variability or error bounds in the modeling information presented as a result of effects of season and weather?

We do not see any significant trends with season or weather in our data. Let us reflect on why this is so. Throughout this report, we have emphasized the importance of spatially localized or discrete sources in low-angle clutter statistics. Many of the measurement sites were on low-relief prairie farmland in western Canada. At the beginning of our program, for example, when standing in an Alberta wheat field and seeing nothing but wheat to far horizons, in thinking of clutter modeling we thought in terms of dielectric constant of wheat, moisture content of soil, and fields high in mature wheat versus harvested fields in stubble versus plowed fields and snow-covered fields, all of which led us to expect significant seasonal variations in clutter strength. We did not think very much about vertical discrete objects because, visually, they seemed relatively sparse and unimportant. It turned out, that when we actually made the radar measurements at such sites to ranges of 25 or 50 km or more, the incidence of discrete sources was large and their effect was dominant.

In the early days of radar, general acceptance of the idea that "angels" were caused by birds came slowly because there did not appear to be that many birds; but over hundreds and thousands of square kilometers of radar coverage, there can be enormous numbers of birds to account for angels (i.e., nonzero Doppler echos). Similarly, there are enormous numbers of stationary discrete or localized vertical scattering features dominating zero-Doppler ground clutter statistics. Thus, it is not so much the wheat field itself as the fence around it, the road and telephone line through it, and occasional storage granaries or trees around ponds in it, that act as clutter sources. The dramatic seasonal variations that occur in the physical appearance of the surface of the wheat field have relatively little effect on the returned clutter statistics. The actual vertical sources tend to be relatively unchanged, summer and winter. Thus, in general, we saw little seasonal variation in ground clutter strengths, generally on the order of 3 dB or so, with no noticeable trends.

Tree lines are very common discrete clutter sources. A tree line within a large regional clutter patch will contribute strong clutter cells to the overall patch amplitude distribution, independent of whether the trees happen to be in leaf or bare, or wet or dry. Seasonal and weather effects will only cause minor variations in these strong contributions. Of more significance in the distributions is whether the tree line exists, or more generally, the relative incidence of occurrence of tree lines on landscapes. We have previously provided information showing how clutter amplitude distributions vary with the percent of tree cover, which indicates that the dominant sources causing much of the wide spread typically observed in these distributions for agricultural terrain are isolated trees.

Nevertheless, season and weather do act to introduce variation in ground clutter. What are the ranges of variability or error bounds in prediction caused by these changes? In Sections 7.1 and 7.2 we show the ranges of variability of mean clutter strength with weather and season, respectively, based on our repeat sector data base of measurements. In these results, differences in Phase One repeated measurements in all five frequency bands, both polarizations, and both range resolutions are combined.

7.1 DAY-TO-DAY VARIABILITY

Elsewhere in this report, we have discussed that, in the repeat sector at each site, we repeated the measurements a number of times during the time on site. A major purpose of these repeated measurements was to indicate the variability in ground clutter that occurs due to changes in weather and other environmental factors (see Table A-21). Table C-3 shows a sequence of mean strengths for an L-band experiment repeated 11 times over a 2-1/2 week period at Peace River. (Usually we did not obtain this many repeats.) During the measurement period at each site, we kept our remote weather station activated in the repeat sector and kept our ground truth file (see Table A-3) updated with current information, both as it existed on site and in the repeat sector.

In general, we saw little obvious correlation of changes in clutter with weather. Thus, here we just take into consideration all the day-to-day differences in mean strength between repeated experiments. The difference taken in every case is the absolute difference of a particular measurement from each of the other measurements in the set of repeated measurements at a given frequency, polarization, and resolution at that site.

The histogram of all such day-to-day differences in mean clutter strength from the repeat sector measurements is shown in Figure 107. Note that the ordinate is a logarithmic scale. All day-to-day differences are bound up in this histogram, including minor differences due to calibration variation, and minor differences due to underlying system parameter variation, such as antenna step/scan versus continuous scan in azimuth or high PRF versus low PRF (see Table A-21). Day-to-day calibration consistency as shown by repeatability of returns from a discrete reference target of opportunity at each site is usually well within 1 dB (see Tables A-12 and A-13). Minor differences due to underlying system parameters are often observed to be small (see variations with experiment type in Table C-2). Thus, when large differences occur in the histogram of Figure 7, they are usually caused by real changes in the clutter patch.* As mentioned above, we do not attempt here to actually correlate or attribute these differences to weather in a deterministic causative manner. Dynamic processes of change in landscape are complex. For example, should we count as legitimate the change that was caused by a train crossing the flat Corinne farmland repeat sector during data taking? We believe that most of the changes in the histogram are not due to such singular events and indeed are due to weather. However, it is more correct to associate the histogram with all environmental changes, including man-made and natural, and with all day-to-day system and calibration variations.

---

* Very infrequently, differences might be due to unobserved measurement equipment malfunction (e.g., the RF preamplifier dropping out in midexperiment), although we screened the data and removed obvious malfunction experiments.

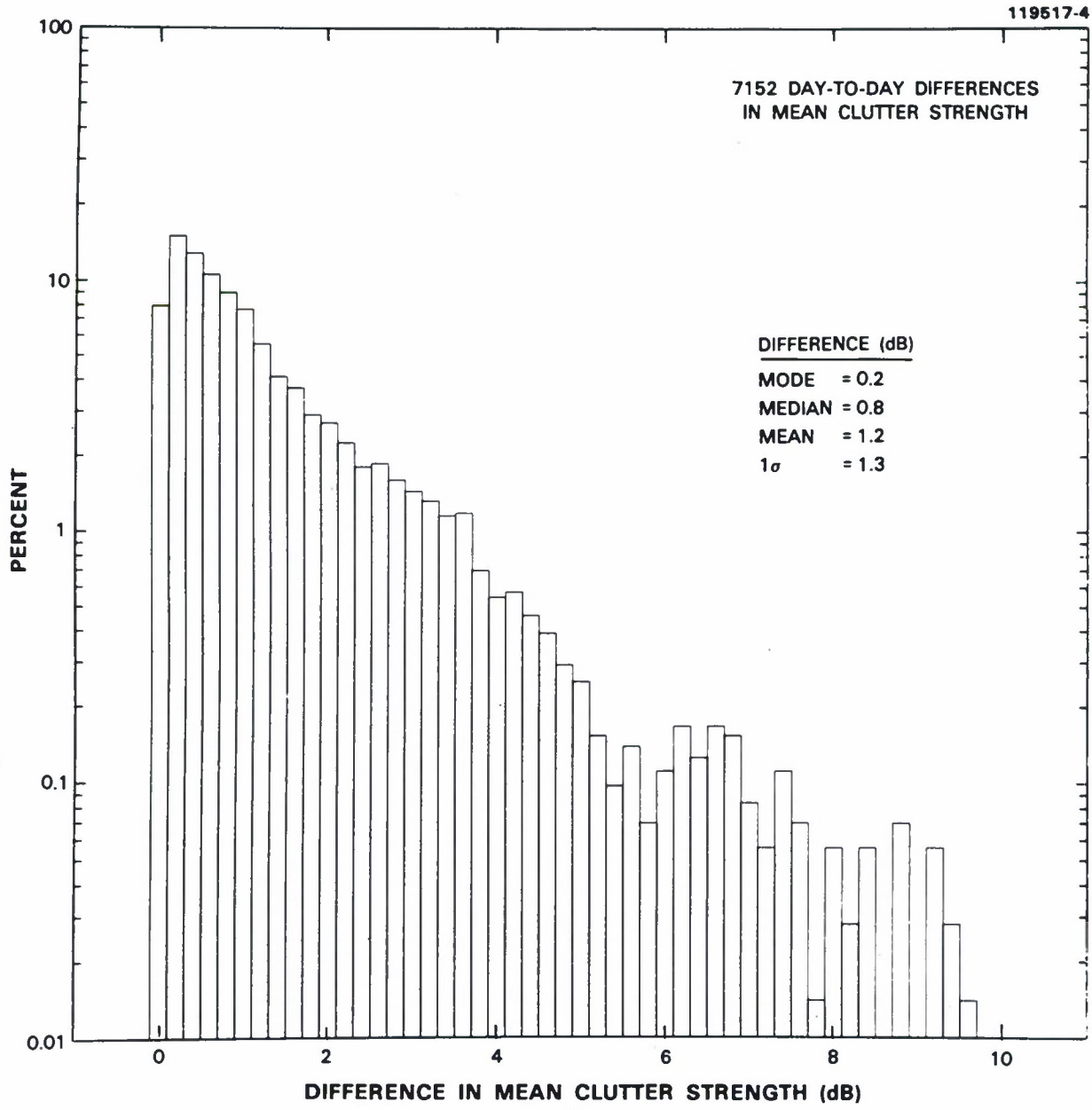

Figure 107. Histogram of diurnal differences in mean ground clutter strength. Phase One repeat sector data. All five RF frequencies, both polarizations, and both pulse lengths. All 49 site visits.

In summary, concerning day-to-day variability in mean clutter strength as observed by Phase One, the results of Figure 107 indicate that the most likely day-to-day difference (i.e., the mode of the distribution) in mean clutter strength in the Phase One repeat sector measurements is 0.2 dB, the average difference is about 1 dB (i.e., median difference = 0.8 dB, mean difference = 1.2 dB), and the one-sigma range of variability beyond the mean is to 2.5 dB (i.e., 85 percent of the day-to-day differences ≤ 2.5 dB). The tail of the distribution of day-to-day differences does show occasional (i.e., at a few one-hundredths of one percent probability of occurrence) day-to-day differences near 10 dB, but some or all of these may be due to measurement equipment malfunctions or singular events like train passings. We may conclude that changes in clutter mean strength due to weather are usually relatively small, certainly compared to the total range of variation of clutter mean strength shown in Figure 98.

7.2 SEVEN REPEATED VISITS

Phase One made seven seasonal revisits to five different sites (e.g., see Table D-1). However, because a repeat sector was not established for the first visit to Katahdin Hill, for this report there are actually six revisits to four sites. Three of these sites, Cochrane, Brazeau, and Gull Lake West, had one revisit each. Beiseker had three revisits. The individual seasonal variations in mean strengths in these measurements were discussed in Section 4. Here, the accumulation of all the differences in mean strength at these sites, as exist between seasonally different pairs of corresponding measurements, each pair at the same site, frequency, polarization, and resolution will be presented.

Figure 108 shows the histogram formed from this accumulation of seasonal differences in mean strength. The difference taken in every case is the absolute difference in decibels between the later and earlier measurements at a particular site at the same frequency, polarization, and resolution. As mentioned above, Beiseker had three revisits. If differences are allowed for all combinations of Beiseker visit numbers, two at a time (viz., six), the Beiseker results would swamp out the results from the other sites. We prefer each Beiseker revisit to count once, allowing the three revisits to Beiseker to count the same together as the three revisits to the Cochrane, Brazeau, and Gull Lake West sites. Thus, for Beiseker, we arbitrarily chose to only include absolute differences of each subsequent visit from the first visit in the histogram of Figure 108.

The results of Figure 108 for seasonal variation of mean clutter strength indicate that the most likely seasonal variation in mean clutter strength in the Phase One repeat sector measurements (i.e., the mode of the distribution) is 1.5 dB, the average variation is about 2 dB (i.e., median difference = 1.8 dB, mean difference = 2.3 dB), and the one-sigma range of variability beyond the mean is to 4.1 dB (i.e., 84 percent of the seasonal differences ≤ 4.1 dB). This value of 4.1 dB is considerably larger than the corresponding value of 2.5 dB in the day-to-day variations, as we would expect. The maximum observed seasonal difference in Figure 108 is 8.07 dB from Gull Lake West at L-band, 150-m pulse, horizontal polarization. The maximum seasonal difference at Beiseker was 7.07 dB, also at L-band, 150-m pulse, but at vertical polarization (see Section 4.1.4.2). Seasonal changes, though, are still quite small compared with the total range of variation of clutter mean strength shown in Figure 98. For Beiseker alone, in the distribution of all 88 combinations of seasonal differences across four visits (e.g., including fourth visit minus third, fourth minus second, etc.) as first discussed in Section 4.1.4.2, the mode, mean, median, and standard

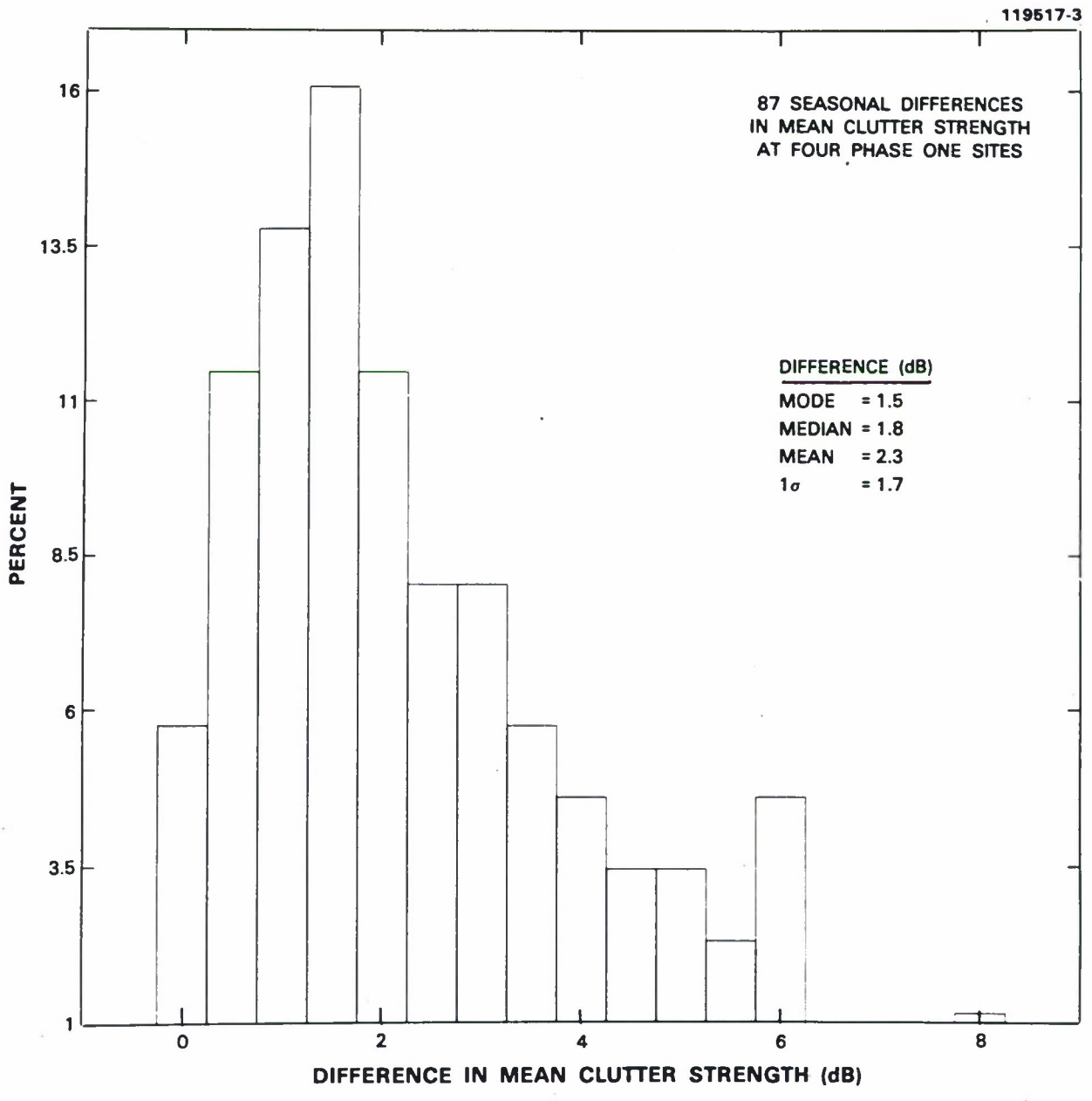

Figure 108. Histogram of seasonal differences in mean ground clutter strength. Phase One repeat sector data. All five RF frequencies, both polarizations, and both pulse lengths. Sites are Cochrane, Brazeau, and Gull Lake West, two seasonal visits each; and Beiseker, four seasonal visits.

deviation are 1.0, 2.0, 1.7, and 1.5 dB, respectively, or only slightly less than the corresponding values of 1.5, 2.3, 1.8, and 1.7 dB, respectively, in the four-site data of Figure 108. This may begin to indicate that seasonal variation is not too different from one site to another, but see the individual site discussions of seasonal differences in Section 4. Of the 12 extreme outliers in the histogram of Figure 108, seven come from Gull Lake West, three come from Cochrane, and two come from Beiseker.

7.3 TEMPORAL AND SPATIAL VARIATION

Figure 109 shows cumulative distributions of both day-to-day and seasonal variations in mean clutter strength as measured by Phase One. These data come from the histograms of Figure 107 and 108, respectively. Thus, the day-to-day variations shown in Figure 109 are based on repeat sector measurements over the two- to three-week stay at every Phase One site. In Figure 109, 71 percent of day-to-day variations, largely due to changes in weather, are less than 1.5 dB. The seasonal variations shown in Figure 109 are based on six repeated visits by the Phase One equipment to selected sites for the purpose of investigating seasonal variability. In Figure 109, 71 percent of seasonal variations are less than 3 dB.

In the above (i.e., Figures 107, 108, and 109), day-to-day and seasonal variability in mean clutter strength over repeat sectors are characterized by forming single-sided distributions of absolute values of differences* between measurements. This is the natural thing to do when there are only two in the cluster of repeated measurements, for example, two seasonal repeats. When there are more than two in the cluster (e.g., four seasonal repeats at Beiseker), this approach provides all combinations of differences (e.g., six differences among the four Beiseker repeats, although we allowed only four) including the large difference between the two outliers. The resultant one-sided histogram of absolute values of differences is primarily characterized by the mean (i.e., average difference), median, and mode (i.e., most likely occurring difference) of the distribution. In particular, the standard deviation in this one-sided distribution is a secondary or relative attribute that gives the range of variation about the mean difference but, unless quoted with the mean difference, by itself does not provide any absolute information on average or typically occurring day-to-day or seasonal differences. These one-sided histograms are a very satisfactory way to show day-to-day and seasonal differences. Even though the number of samples in them grows combinatorially with number of repeated measurements in the cluster (although we restricted this in the seasonal differences at Beiseker), they do include the difference between each measurement and every other measurement in the cluster (i.e., equal weight to every pair), and they do not impose meaningless signs (i.e., positive or negative) to differences.

We may also characterize day-to-day and seasonal variability in mean clutter strength over repeat sectors, not by forming single-sided distributions of absolute values of differences between measurements, but by forming two-sided distributions of differences of individual measurements from central values within groups of measurements of common frequency, polarization, and resolution. These two-sided distributions of differences from central values provide one-sigma ranges of variability directly

---

* Differences in decibels; ratios in power.

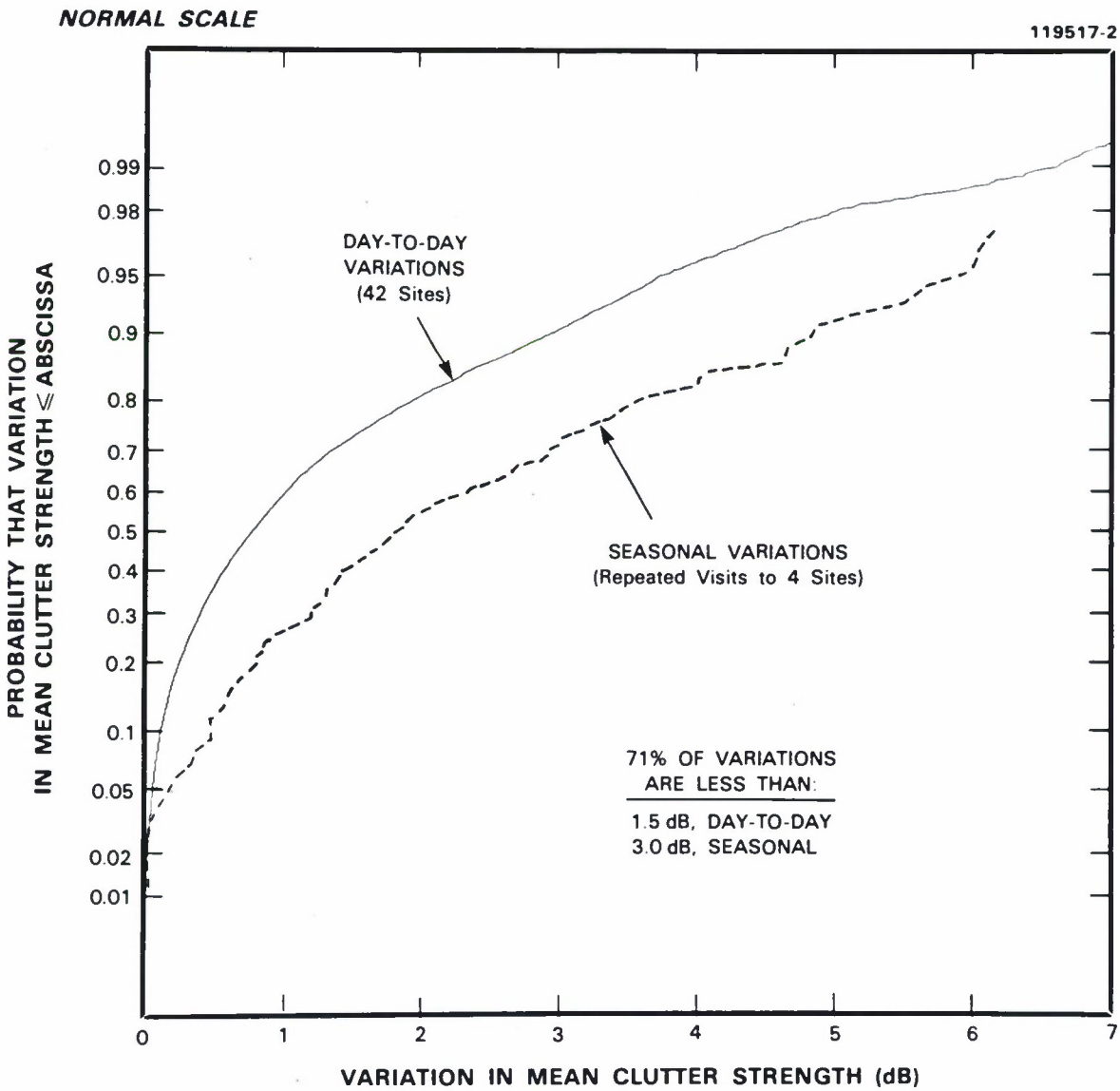

Figure 109. Diurnal and seasonal variability in mean ground clutter strength. Phase One repeat sector data. All five RF frequencies, both polarizations, and both pulse lengths. Cumulative distributions of data histogrammed in Figures 107 and 108.

comparable* with the one-sigma numbers we use to specify spatial variability. That is, in considering spatial variation, we form the distribution of mean strengths from all repeat sector patches of a given terrain class, specify a central value in the distribution, and characterize variability in the distribution by the one-sigma range of variation about the central value. To follow a parallel approach for temporal (i.e., day to day or seasonal) variation where we have clusters of repeated measurements of each repeat sector patch, we first need to normalize the central value of each cluster to zero in order to remove patch-to-patch spatial variation. Thus, for each repeated cluster, we first specify the central value in the cluster, then we determine the differences (both positive and negative) of each measurement in the cluster from the central value, and finally accrue all such temporal differences from all clusters into one aggregate histogram. The resultant histogram of differences is two-sided, approximately symmetric, and approximately normal (i.e., law of large numbers). Recall that it is showing differences from central values of clusters of repeated measurements, not differences between pairs of measurements in the cluster. It is a two-sided or polarized distribution (although the sign is meaningless) centered at (or very near) zero. The mean, median, and mode in this two-sided distribution are all at (or very near) zero. This two-sided distribution is primarily characterized by the standard deviation or one-sigma value of the distribution. To the extent that the distribution is normal, 68 percent of the day-to-day or seasonal differences lie within the one-sigma range of variation.

We now provide such two-sided distributions for day-to-day, seasonal, and patch-to-patch variations in repeat sector clutter patch mean clutter strength, respectively. Day-to-day and seasonal variations constitute long-term temporal variations for a given patch. Patch-to-patch variations constitute spatial variations from one patch to another within a given category of terrain classification (there are 12 in all, see Table 7) and within a given RF frequency band. These three distributions of variability in mean ground clutter strength are shown in Figure 110. In each case, the variation is the difference in mean clutter strength from a central value within a group of measurements repeated in time (i.e., day to day or seasonal) or in space (patch to patch for a specific terrain class). Because these data are all similarly derived to show central differences (as discussed in the preceding paragraph), the three distributions of Figure 110 showing day-to-day, seasonal, and spatial variability are all directly comparable and are all primarily characterized by their one-sigma ranges of variability. As is indicated in Figure 110, these one-sigma ranges of variability for day-to-day, seasonal, and patch-to-patch variations are 1.1, 1.6, and 3.2 dB, respectively.

When all is said and done, we are working with the same set of day-to-day and seasonal repeat sector measurements whether we form one-sided or two-sided distributions of differences. Thus, aside from statistical niceties, we should still get similar numbers to characterize typically occurring day-to-day and seasonal variations in distributions. To observe that this is largely so, consider that the ±1.1-dB and ±1.6-dB one-sigma numbers from the two-sided day-to-day and seasonal distributions, respectively, as

* By comparable, we mean that we may compare the one-sigma numbers with the assurance that we are comparing the same attribute from similarly derived, two-sided, zero-mean distributions (i.e., comparing apples with apples), not that the day-to-day, seasonal, and spatial one-sigma numbers are nearly equal.

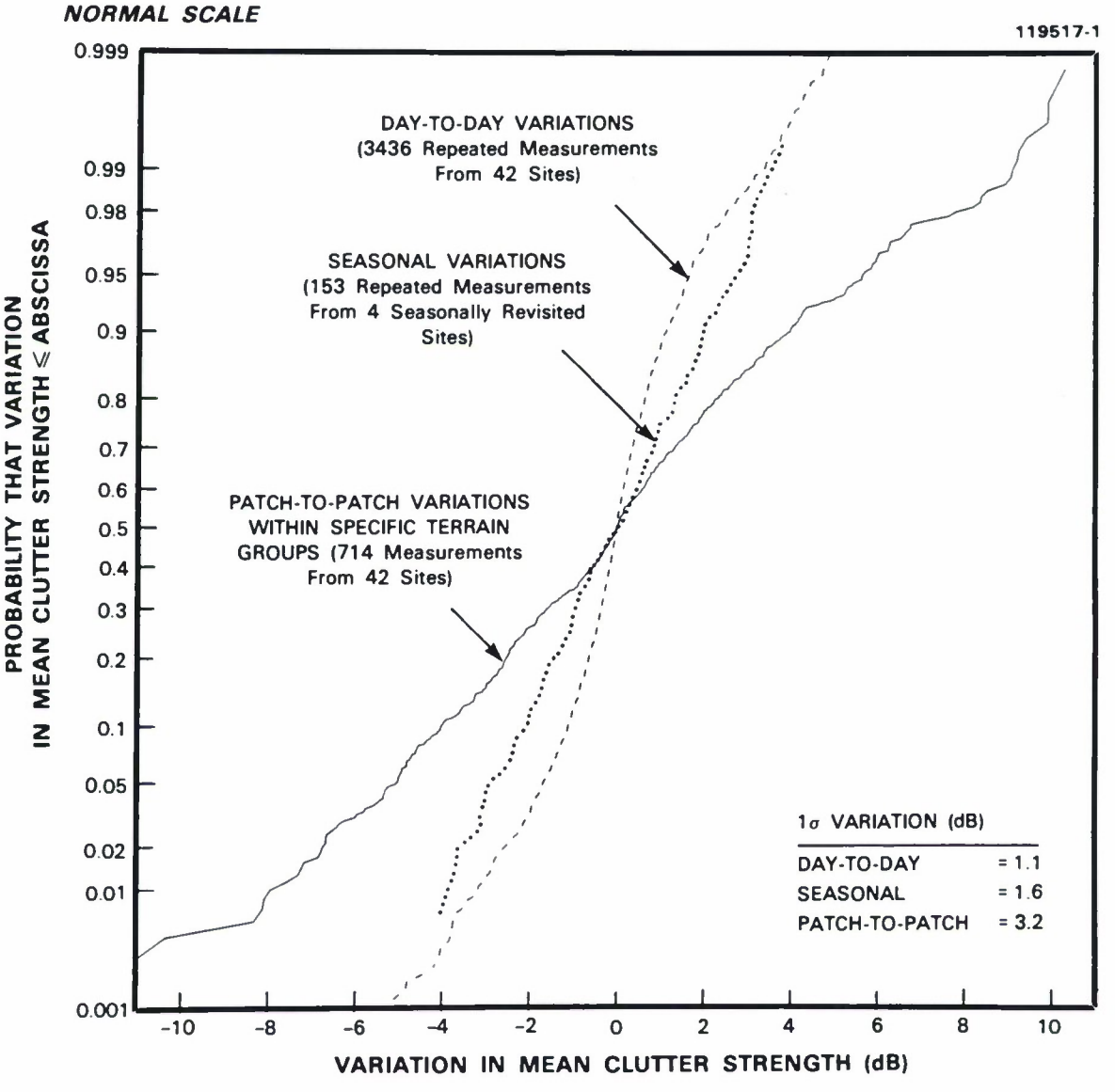

Figure 110. Temporal and spatial variability in mean ground clutter strength. Central differences. Phase One repeat sector data. All five RF frequencies, both polarizations, and both pulse lengths.

shown in Figure 110, which encompass 79 and 65 percent of central difference variations, respectively, when doubled to represent absolute differences between individual measurements encompass 80 and 71 percent of variations, respectively, in the one-sided distributions shown in Figure 109.

Each distribution in Figure 110 will be discussed in turn. First, the seasonal variations in Figure 110 are based on differences in our digest set of best measurements (i.e., Tables D-2 through D-6) for the four seasonally revisited sites. The approximate linearity of this curve indicates that the decibel values of seasonal central differences are approximately normally distributed. To the extent that they are, 68 and 95 percent of them are within one-sigma (i.e., ±1.6 dB) and two-sigma (i.e., ±3.2 dB) ranges of variation, respectively. These percentages are closely approximated by the actual percentages of differences within these ranges of variation, which may be obtained directly from the ordinate in Figure 110, as 65 and 94.5 percent, respectively.

Next, the day-to-day variations in Figure 110 are based on our repeat sector sort file (see Section 6.1) containing all repeated experiments at each site, not just the best (i.e., digest) experiments. In establishing these day-to-day variations, we eliminated from our sort file experiments at different tower heights and other parametric variations that would not be appropriate to attribute to day-to-day variability. In addition, we edited out what we knew to be obviously bad experiments due to equipment malfunction. The resultant distribution of day-to-day central differences is approximately normal over its central 60 percent (from 0.2 to 0.8 cumulative probability). However, the spreads in the tails (approximately 0 to 20 percent cumulative probability on the left side; approximately 80 to 100 percent cumulative probability on the right side) of this distribution are considerably greater than would be provided by linear extrapolation of the central quasi-normal distribution. In fact, it is apparent in Figure 110 that in the extreme tails (i.e., 1 or 2 percent on each side), the day-to-day differences appear to approach asymptotically and nearly coincide with the seasonal differences. That is, whatever the mechanisms at work that cause the largest (although infrequent) seasonal changes, mechanisms are also at work to cause similarly large (but infrequent) changes on a day-to-day or weekly basis.

Finally, as were the seasonal variations, the patch-to-patch variations in Figure 110 are based upon our digest data set of best measurements (Tables D-2 through D-6). These variations are the differences from the central values given in Table 11 of the cluster of measurements in each frequency band in the 12 scatter plots showing mean clutter strength versus frequency by terrain class presented in Section 4. In other words, this distribution characterizes the prediction accuracy that we may associate with the modeled values of mean clutter strength by frequency band and terrain type as given in Table 11. As with the seasonal variations, the distribution of patch-to-patch central differences in Figure 110 is approximately normal over its complete range (i.e., 72 and 94 percent of differences lie within one-sigma and two-sigma ranges, respectively, compared with 68 and 95 percent for the normal distribution). As would be expected, this distribution of spatial variations is considerably broader than the distributions of day-to-day and seasonal variations (i.e., the one-sigma and two-sigma ranges for patch-to-patch spatial differences are ±3.2 dB and ±6.4 dB, respectively).

The temporal and spatial variability of clutter as given by the distributions of Figure 110 is the variability that remains after we have separated the data by terrain type. It is interesting to compare this residual variability with the overall range of variability in the clutter phenomenon without distinguishing terrain type, for example, as is illustrated in Figure 99. It is the 3.2-dB one-sigma patch-to-patch spatial

variability that determines the prediction accuracy of our clutter model. The one-sigma patch-to-patch spatial variability in mean ground clutter strength by frequency band before terrain classification is as follows: 16.6, 13.6, 9.7, 7.1, and 5.8 dB, at VHF, UHF, L-, S-, and X-band, respectively (see Table 12). In contrast, the corresponding one-sigma patch-to-patch spatial variability in mean clutter strength by frequency band after terrain classification is: 3.9, 3.8, 2.9, 2.7, and 2.3 dB at VHF, UHF, L-, S-, and X-band, respectively. These latter five numbers are how the overall 3.2-dB one-sigma spatial variability in Figure 110 splits up by frequency band. In comparing these measures of patch-to-patch spatial variability in mean clutter strength before and after terrain classification, we make the following observations.

- Terrain classification substantially reduces variability in all bands.
- The amount of the reduction is greatest at VHF and decreases with increasing frequency (i.e., amount of reduction = 12.7, 9.8, 6.8, 4.4, and 3.5 dB at VHF, UHF, L-, S-, and X-bands, respectively).
- The variability after terrain classification still decreases somewhat with increasing frequency from 3.9 dB at VHF to 2.3 dB at X-band, but this decrease is very much less than the corresponding decrease before terrain classification.

Thus, it is clear that specifying terrain type, terrain relief, and the depression angle at which the terrain is illuminated, as is done in this report, greatly improves the accuracy to which the mean clutter strength from that terrain can be predicted and that nonterrain-specific approaches to clutter modeling must inherently involve large uncertainties.

8. SUMMARY

How strong is radar ground clutter? How does the strength of the clutter vary with the type of terrain in which the radar is situated? In particular, whatever the terrain, how does the strength of the clutter vary with RF frequency over the range of operational frequencies used in modern radar technology?

These questions have perplexed radar engineers since the advent of radar during World War II. Answers to these questions are important because the performance of ground-sited radar against low-flying targets is often limited by ground clutter interference even when state-of-the-art clutter cancellation processing is employed. Because of this importance, many specific clutter measurements have been performed and reported over the years, but they have not led to a characterization of clutter providing generally accepted answers to the above questions.

Why is this the case? Central to the difficulty in clutter characterization and prediction is the fact that terrain is essentially infinitely variable, and every clutter measurement scenario is different. Hence, ground clutter's most salient attribute is variability. As a result, our questions concerning clutter strength need to be answered statistically. As is amply illustrated by discussions of individual measurements in this report, we can usually understand what goes on in any given measurement; however, every measurement is fraught with terrain and propagation specifics, and we usually cannot generalize on the basis of any one measurement scenario. Thus, the clutter literature, seemingly characterized by inconsistency and contradiction, is really just reflecting the fact that clutter is an extremely variable statistical process. The literature frustrates us with single-point measurements whose broader significance is not understood.

Therefore, we set out on a major new program of ground clutter measurements. The objective of our program was to provide new general understandings and predictability to the ground clutter statistical phenomenon. The way we planned to achieve this was to collect large amounts of data in the belief that averaging over large amounts of data would allow underlying fundamental trends to emerge that are often obscured by specific effects in individual measurements. During the three-year period from 1982 to 1984, we operated our five-frequency Phase One clutter measurement radar system continuously in the field collecting multifrequency clutter data at 42 different sites. Because of our particular interests in characterizing clutter, many of our measurement sites were in western Canada, in terrain of relatively low-relief and at northern latitudes. In addition to this emphasis, however, we also attempted to measure all important terrain types, including mountains, cities, desert, marshland, farmland, and woodland. Each of our Phase One sites and the measurements we obtained there are described in this report. Altogether in this measurement program, we collected 475 Gbytes of pulse-by-pulse calibrated ground clutter data. We intend to maintain these data indefinitely at Lincoln Laboratory.

Ground clutter measurements are difficult to perform accurately. Although our Phase One measurements of necessity were carried forward as field operations, our five radars were of instrumentation level quality and our first priorities throughout the program were the quality of data and accuracy of calibration. As a result, more time was spent in calibrating, monitoring, and maintaining our measurement system than in actually collecting data with it. Our calibration procedures and results are documented in this report.

The results of our Phase One measurement program are summarized in Figure 98 and Table 11. As an easy-to-comprehend summary, Figure 98 and Table 11 represent our best current answers to the most

pressing high-level questions we set out to answer with our Phase One clutter measurement program. The results of Figure 98 and Table 11 were obtained from repeat sector measurements at each site, which are the data we currently have under analysis. The repeat sector at each site was an azimuth sector of concentration in which measurements were repeated a number of times to increase the reliability of the results. Altogether we have 4465 measurements constituting our repeat sector data base.

The results of Figure 98 and Table 11 have a number of advantages that are not obvious at first consideration. First, underlying them is a universally applicable terrain classification system consistently applied across 42 different repeat sectors. This classification system causes the clutter statistics to cluster within class and to separate between classes. That is, this system separates differences in nominally similar terrain (e.g., undulating versus rolling) and measurement scenario (e.g., fractional variation in depression angle) that are enough to cause significant variation (different classes) in the clutter returns. Our terrain classification system, described in this report, is basically formulated at 1:50,000 scale to classify both land-surface form and land cover and quantifies important parameters such as terrain relief, terrain slope, and depression angle.

Second, the data shown in Figure 98 and Table 11 are medianized and hence generalized central values within terrain classes. That is, even at best, terrain is variable within class, and any single measurement in a given terrain class comes from a spectrum of all possible measurements in such terrain. The data shown in Figure 98 and Table 11 are medianized central values over many measurements and thus representative of generally occurring levels of clutter strength in each terrain class.

Third, the data of Figure 98 and Table 11 were all reduced using consistent data reduction procedures. Complicating factors in data reduction, such as electromagnetic propagation (ground clutter is not a free-space measurement), geometric shadowing (a dominant influence in the low-angle regime), radar sensitivity limitation, radar noise contamination, and differing degrees of coherency in clutter returns are explained in this report. Furthermore, the data underlying Figure 98 and Table 11 were accurately calibrated.

Finally, each measurement underlying the medianized data of Figure 98 and Table 11 is itself a centrally selected measurement from a group of identically repeated measurements in which occasional anomalous outliers have been removed. Example sequences of such repeated measurements are provided in this report. Thus, in total, the results of Figure 98 and Table 11 are the product of much effort devoted to concerns with accuracy, generality, and statistical consistency.

We now summarize the results of Figure 98 and Table 11. First, these results indicate 66 dB of variability in mean strength of ground clutter from mountains at VHF to marshland or desert at UHF. However, these results also provide a rational means of sorting through this variability, through specification of terrain type, relief, depression angle, and RF frequency. In gross terms, it is seen that we utilize just five, major, easy-to-distinguish terrain categories, namely, mountains, cities, forest, farmland, and, as an encompassing fifth category, desert, marsh, or grassland with few discrete clutter sources. As we would expect, we observe that mountains and cities produce strong clutter returns, and desert, marsh, and grassland produce weak clutter returns; these new results now quantify how strong and how weak. Results from our preceding Phase Zero pilot program of ground clutter measurements at X-band showed that, at the very low, near grazing incidence angles of ground-based radar, depression angle as it affects shadowing on a sea

of discrete clutter sources is of dominant importance to clutter statistics. Our Phase Zero findings, and in particular the dependence on depression angle, are essentially duplicated in the Phase One X-band results of Figure 98 and Table 11. In addition, we continue to see similarly important dependencies on depression angle at the other frequencies, VHF, UHF, L-, and S-bands, such that fractional variations of depression angle cause major variations in clutter statistics.

However, the purpose of this report is not so much to dwell on the previously emphasized important role of depression angle, which more fundamentally affects statistical dispersions or spreads of clutter amplitude distributions, but to take up the question of frequency dependence in these distributions. The question of frequency dependence requires an empirical approach. The summary data of Figure 98 and Table 11 show that in forest of high-relief and/or at high depression angle, mean ground clutter strengths decrease significantly with increasing frequency; whereas, in very low-relief farmland, mean ground clutter strengths increase significantly with increasing frequency. The frequency dependence of mountain clutter mirrors the behavior of high-relief forest clutter, except that it is stronger; the frequency dependence of desert or marshland clutter mirrors that of very low-relief farmland, except that it is weaker. (An exception occurs where, at high depression angle at X-band, desert clutter is as strong as forest clutter.) For much commonly occurring terrain, either farmland or forest of moderately low-relief leading to intermediate illumination angles, we see little general dependence of mean clutter strength with frequency. In such terrain, mean clutter strengths hover around the -30-dB level, VHF to X-band. In summary, the data of Figure 98 and Table 11 bring statistical order to the problem of predicting mean clutter strengths from spatial macroregions of terrain. They answer the questions of how strong clutter is for various terrain types and for RF frequencies as they vary from VHF to X-band.

Within any spatial macroregion consisting of hundreds or thousands of resolution cells, extreme cell-to-cell fluctuation occurs about the mean value as provided by Figure 98 and Table 11. A proper clutter model will model these statistical fluctuations. Our clutter model, reported elsewhere, does so by modeling the clutter returns as random numbers from Weibull distributions. Each Weibull distribution in the model is characterized by a mean strength and a spread parameter. The mean strength carries the dependence on RF frequency. The spread parameter carries the dependence on radar spatial resolution.

One purpose of this current report is to provide detailed data documentation of the actual multifrequency mean strengths underlying our clutter model. Any model needs to reach towards simplicity and generality. Thus, in our clutter model, we performed some subjective smoothing of trends as we merged complementary results from our Phase Zero and Phase One programs and attempted to remove minor variations that we judged to be statistically insignificant. The results of Figure 98 and Table 11 contain no such subjective smoothing but are exact results as delivered by our repeat sector measurements, medianized within terrain class, and including both vertical and horizontal polarizations and high and low range resolutions. Careful comparison between our model and the repeat sector multifrequency data of Figure 98 and Table 11 will reveal the extent to which the model does not carry all of the detailed variations shown in Figure 98 and Table 11.

This report also provides general information on the effects of polarization, resolution, weather, and season on mean clutter strength. The effects of all of these parameters are generally relatively small, basically because mean clutter strength is dominated by strong discrete clutter sources that are physically complex with respect to polarization and relatively invariant with weather and season. With polarization,

overall we see only a slight trend where vertical polarization provides stronger mean clutter than horizontal by 1.4 dB on the average. However, the one-sigma variability about this average is 2.8 dB, and occasional differences in mean strength with polarization can occur in the 5- to 10-dB range, with either vertical or horizontal being stronger.

Radar resolution fundamentally affects spreads in clutter amplitude distributions, not the means which we emphasize here. Across all the repeat sector measurements of this report, the mean strength measured at high resolution is only 0.81 dB stronger on the average than that measured at low resolution. The one-sigma variability with resolution about this average is 2.2 dB. Variations of mean strength with resolution indicate the existence of small numbers of discrete interfering scatterers within a resolution cell.

Weather and season act to introduce statistical variability in mean clutter strength without apparent trend. On the basis of our repeated measurements at each site, we specify the one-sigma variability due to short-term changes with weather at 1.1 dB, with occasional variations (i.e., 10 percent) greater than 3 dB. On the basis of our seasonal revisits to six sites, we specify the one-sigma variability due to long-term changes with season at 1.6 dB with occasional variations (i.e., 10 percent) greater than 4.8 dB.

The long-term diurnal and seasonal temporal variabilities of mean strength in our repeat sector measurements of 1.1 and 1.6 dB, respectively, may be contrasted with the sector-to-sector spatial variability within groups of common terrain type in the measurements. This spatial variability has a one-sigma range of 3.2 dB. This represents the best current measure of prediction accuracy for our model.

This report emphasizes mean strengths of clutter amplitude distributions measured over spatial macroregions consisting of many contiguous resolution cells. The most basic descriptive measure of any statistical distribution is the mean of the distribution, which is the average of all the samples in the distribution, each sample weighted by just its own strength. The means usually occur high in our measured clutter amplitude distributions, often near the 90-percentile level, driven there by occasional strong returns from discrete sources.* However, because the distributions are not simply behaved does not mean that we should discard the standard techniques of statistical science for bringing them under general description. We mention this seemingly self-evident fact here because means at high percentile levels can occasion a sense that they should be discounted. We mention again that returns from discrete sources over a wide range of strengths comprise the phenomenon we are attempting to describe. The phenomenon is not so simple that, for example, moving to the median somehow rids us of a few classical, water-tower type of contaminating discretes and leaves us with a better central measure of a well-behaved, discrete-free clutter background.

For complete descriptions of our clutter amplitude distributions, in addition to mean levels we also provide general information in this report on higher moments and percentile levels, medianized over a

---

* For this reason, we caution that we certainly do not advocate use of the mean as a constant σ° clutter model. No other single attribute of the distribution serves this purpose either, however, because the constant σ° that provides equivalent system performance as real clutter is system and performance parameter specific.

number of individual repeat sector measurements within the same terrain groups as our means. Concerning higher moments, we provide standard deviation, skewness, and kurtosis. The standard deviation is the basic statistical measure of spread, and from it the Weibull spread parameter of our clutter model is completely determined. Skewness and kurtosis are normalized third and fourth central moments, respectively. These quantities are of particular importance in theoretical investigations, for example, in studies involving K-distributed statistics that attempt to get at the demanding problem of spatial correlation or texture within spatial macroregions. Concerning percentiles, we provide 50-, 70-, and 90-percentile levels in our clutter amplitude distributions in this report. They provide an easy descriptive means of visualizing the distributions, although otherwise they contain less meaningful statistical information in three or four numbers than do the moments.

This report provides mean ground clutter strength versus frequency, VHF through X-band, as measured over repeat sector spatial macroregions of terrain at 42 different sites. These results were obtained under one unified program of measurements utilizing consistent and accurate calibration throughout. As such, they provide much new information on the frequency dependence of radar ground clutter and bring connecting tissue to a disjointed literature. Many of the results, at least in detail, are specific to the site at which they were obtained. In this report, we average out such specificity by combining results from sites of similar terrain class. In this manner, we arrive at generalized characteristics of mean ground clutter strength versus frequency for most important terrain types.

This currently available information on the frequency dependence of low-angle ground clutter is based on a statistical population of just 42 repeat sector clutter patches. When these 42 samples are divided among five major categories of terrain and then further partitioned by relief and depression angle, they do not leave very many samples per category. We are currently analyzing our Phase One multifrequency 360-deg survey data at each site that provide clutter amplitude distributions for many more patches, on the order of 80 patches per site, as opposed to the one patch per site provided by our repeat sector data base. These new results will improve the statistical rigor with which we predict multifrequency clutter characteristics.

REFERENCES

1. J.B. Billingsley and J.F. Larrabee, "Measured spectral extent of L- and X-band radar reflections from wind-blown trees," MIT Lincoln Laboratory, Lexington, Mass., Project Report CMT-57 (6 February 1987). DTIC AD-A179942/8.

2. S. Ayasli, "Propagation effects on radar ground clutter," *Proc. IEEE National Radar Conference*, IEEE Aerospace and Electronic Systems Society and the IEEE Los Angeles Council, Los Angeles, Calif. (12–13 March 1986).

3. H.C. Chan, "Radar sea-clutter at low grazing angles," *Proc. Inst. Electr. Eng.* **137,** 102–112 (1990).

4. S. Ayasli, (private communication, 1990).

5. E. Jakeman, "On the statistics of K-distributed noise," *J. Phys. A* **13,** 31–48 (1980).

6. S. Watts and K.D. Ward, "Spatial correlation in K-distributed sea clutter," *Proc Inst. Electr. Eng.* **134,** 526–531 (1987).

7. S. Ayasli, "SEKE: A computer model for low-altitude radar propagation over irregular terrain," *IEEE Trans. Antenna Propag.* **AP-34,** 1013–1023 (1986).

REPORT DOCUMENTATION PAGE

Form Approved
OMB No. 0704-0188

1. AGENCY USE ONLY (*Leave blank*)	2. REPORT DATE	3. REPORT TYPE AND DATES COVERED
	15 November 1991	Technical Report

4. TITLE AND SUBTITLE

Multifrequency Measurements of Radar Ground Clutter at 42 Sites

5. FUNDING NUMBERS

C — F19628-90-C-0002

6. AUTHOR(S)

J. Barrie Billingsley and John F. Larrabee

7. PERFORMING ORGANIZATION NAME(S) AND ADDRESS(ES)

Lincoln Laboratory, MIT
P.O. Box 73
Lexington, MA 02173-9108

8. PERFORMING ORGANIZATION REPORT NUMBER

TR-916
Volume 1: Principal Results

9. SPONSORING/MONITORING AGENCY NAME(S) AND ADDRESS(ES)

Department of the Air Force
SAF/AQL
The Pentagon
Washington, D.C. 20330

DARPA
1400 Wilson Blvd.
Arlington, VA 22209

10. SPONSORING/MONITORING AGENCY REPORT NUMBER

ESD-TR-91-061

11. SUPPLEMENTARY NOTES

None

12a. DISTRIBUTION/AVAILABILITY STATEMENT

Approved for public release; distribution is unlimited.

12b. DISTRIBUTION CODE

13. ABSTRACT (*Maximum 200 words*)

This report determines how ground clutter strength varies with RF frequency from VHF to X-band in ground-sited radar. This determination is accomplished by providing extensive empirical results from multifrequency clutter measurements conducted at 42 different sites widely dispersed over the North American continent. These results indicate that the frequency dependence of ground clutter strength depends upon terrain type and can vary, for example, from a strongly decreasing function of frequency in forest to a strongly increasing function of frequency in farmland. Five major terrain categories are defined that encompass this dependence, namely, urban, mountains, forest, farmland, and desert. Within each terrain category, results are also shown to be dependent upon the relief or roughness of the terrain and upon the depression angle at which the terrain is illuminated. The depression angle dependence is important, even for the very low angles (typically within a degree of grazing incidence) and small (typically fractional) variations in angle that occur in ground-sited radar. This report presents specific clutter strength results at each of five frequencies (VHF, UHF, L-, S-, and X-band) from each of the 42 sites at which measurements were conducted. The report then combines results from similar sites to obtain the general dependence of clutter strength versus frequency for each terrain category. Clutter strengths are described in terms of moments (including the mean) and percentile levels (including the median) in measured clutter amplitude distributions resulting from cell-by-cell spatial variation over a selected large kilometer-sized macroregion of terrain at each site called the repeat sector. Measurements over the repeat sector at each site were repeated a number of times to increase the reliability of the results. In addition to determining the frequency dependence of ground clutter strength in various terrain types, this report determines dependencies of clutter strength with radar polarization and resolution and specifies long-term temporal variability of clutter strength with weather and season. The report includes descriptions of the clutter measurement equipment and measurement procedures, provides calibration results, and describes the resultant multifrequency ground clutter measurement data bases that are now maintained at Lincoln Laboratory.

14. SUBJECT TERMS				15. NUMBER OF PAGES
radar ground clutter	terrain reflectivity	land clutter	radar clutter	758
clutter measurements	low-angle	backscatter	electromagnetic propagation	16. PRICE CODE
clutter models	multifrequency	multipath		

17. SECURITY CLASSIFICATION OF REPORT	18. SECURITY CLASSIFICATION OF THIS PAGE	19. SECURITY CLASSIFICATION OF ABSTRACT	20. LIMITATION OF ABSTRACT
Unclassified	Unclassified	Unclassified	None